

Conceptual Multidisciplinary Design via a Multiobjective Multifidelity Optimisation Method

Spyridon G. Kontogianis

PhD Thesis



Computational Aerodynamics Group
Cranfield University
Cranfield, UK
May 2018

Cranfield University

School of Aerospace, Transport and Manufacturing

PhD Thesis

**Conceptual Multidisciplinary Design via a Multiobjective
Multifidelity Optimisation Method**

Spyridon G. Kontogiannis

Supervisors: Prof. Mark Savill, Dr. Timoleon Kipouros

May 2018

© Cranfield University, 2018.
All rights reserved. No part of this publication may be reproduced
without the written permission of the copyright holder.

Except where acknowledged in the customary manner, the material presented in this thesis is, to the best of my knowledge, original and has not been submitted in whole or part for a degree in any university.

Spyridon G. Kontogiannis

Abstract

Air travel demand and the associated fuel emissions are expected to keep increasing in the following decades, forcing the aerospace industry to find ways to revolutionise the design process to achieve step-like performance improvements and emission reduction goals. A promising approach towards that goal is multidisciplinary design. To maximise the benefits, interdisciplinary synergies have to be investigated early in the design process. Efficient multidisciplinary optimisation tools are required to reliably identify a set of promising design directions to support engineering decision making towards the new generation of aircraft.

To support these needs, a novel optimisation methodology is proposed aiming in exploiting multidisciplinary trends in the conceptual stage, exploring the design space and providing a pareto set of optimum configurations in the minimum cost possible. This is achieved by a combination of the expected improvement surrogate based optimisation plan, a novel Kriging modification to allow the use of multifidelity tools and a multiobjective suboptimisation process infill formulation implemented within an multidisciplinary design optimisation architecture.

A series of analytical test cases were initially used to develop the methodology and examine its performance under a set of criteria like global optimality, computational efficiency and dimensionality scaling. These were followed by two industrially relevant aerodynamic design cases, the RAE2822 transonic airfoil and the GARTEUR high lift configuration, investigating the effect of the constraint handling methods and the low fidelity tool. The cost reductions and exploration characteristics achieved by the method were quantified in realistic unconstrained, constrained and multiobjective problems.

Finally, an aerostructural optimisation study of the NASA Common Research Model was used as a representative of a complex multidisciplinary design problem. The results demonstrate the framework's capabilities in industrial problems, showing improved results and design space exploration but with lower costs than similarly oriented methods. The effect of the multidisciplinary architecture was also examined.

Αφιερωμένο με όλη μου την αγάπη στους γονείς μου που με στήριζαν πάντα ώστε να φτάσω εώς εδώ, καθώς και στον αδόλεσχο αδερφό μου που ήταν πάντα εκεί για να κριτικάρει τι τα θέλουμε όλα αυτά που κάνω...

Acknowledgements

I would like to thank my supervisors Prof. Savill and Dr. Kipouros for offering this research position and to appreciate Prof. Savill for supporting me in my PhD decisions and in any situation, for sharing his opinions and for being a genuinely good and caring person.

The sincerest of gratitude goes to Vasileios Mazis, Vangelis Skaperdas and everyone from Beta CAE Systems who assisted me with the models of Chapter 7. Your invaluable help was critical and deeply appreciated! My special thanks also go to Dr. Laszlo Konozy for the inspiring conversations, never limited to science and to Dr. Francois Gallard for his helpful and insightful comments.

I consider myself to be very fortunate to have met Prof. Paulos Hatzikonstantinou and I thank him for being an unlimited source of inspiration, wisdom and a perfect all-around role model. I similarly thank Prof. Myron Giannadakis for fuelling and boosting my love for science from early on.

I would like to express my appreciation to Richard Rogers for providing some of the most incredible experiences of my life, trusting me with flying the Pitts Special (twice!) reminding why aeronautics is so cool, in periods where it was nothing but papers and numbers on a screen. That was awesome!

The pages that follow describe only the work done during the past years. However, the PhD is way more than that. It is a long trip, a roller coaster of emotions, moments and experiences that I am grateful to have shared with some wonderful people in various locations. Special thanks to my friend, flatmate and colleague - and now Dr.! - Jean Demange for sharing his joyful company and thoughts (on top of python wizardry!), Luigi Mura who was always "super cool" to offer his help of any form, Alex Georgiades who documented my rise(!?) to the musical scene of Bristol, Jesus Nieto who is just an unbelievable character that defies logic and of course to all my fellow researchers: Kamal Haider, Javon Farao, Andrea Castrichini, Simone Simeone, Joe Loxham and Fabio Crescenti for our more than enjoyable "supercritical meetings"! Also, to Angelos Lakrintis and to Ali Turaihi for willingly offering their company, food, a base and for always helping out.

I want to somehow transfer my appreciation to the Old Duke and to Bristol, that provided the physical and emotional stage for inverse-engineering myself. My thanks should also travel slightly to the north, to Ioannis Kolovos and his surprisingly comfortable couch (and garage), and to the rest of the do-group! (triple-do! you can't beat that without just over a domino of actions). Thanks also to Antonis Messinis for our discussions and for reminding me how I suck at chemistry (I do), to Jordan Perdikidis for accompanying those nice basketball-souvlaki Sundays and to trusty ol' Goober who did his best.

Special acknowledgement to Hassan for feeding me with a "cheeseburger with everything" in these adventurous (yeah, right) late Friday nights after work, usually combined with some nice film noir! Also, to Star Trek and Dukes of Hazzard for providing a breath

of relaxation, and to Giorgis for the food, attitude and good times.

I cannot express but the warmest of thanks to my dear friends: to Vassilis with his enviable positive attitude (how do you do it?), to Dimitris for the support, discussions and our wonderful shared experiences ("The road to Ajabuja..."), to Stefanos for being there to grow with me in every corner of this earth, to Thanos for his company, respect and non-stop willingness to speak and suggest, to Chrysi for sharing her thoughts, advices, b-movies, travelling companionship and everyday support throughout the PhD and to Zoe for all the discussions, suggestions and care. Thank you all for being there and putting up with my quirks.

I also appreciate the support of my guitar, harmonica and baglamadaki and thank them for a transcending soul extension.

I owe a special thanks to my godmother Chara and my uncle Nikos for implicitly or explicitly introducing me to aeronautics and to my brother for igniting the spark without knowing. I am also grateful to my grandparents for paving the way. I am giving the utmost respect to my family for being the foundation of what I am and what I have/can/will achieve. Thank you deeply!

Finally, I would like to thank myself for the support, belief, dedication and persistence. Without me I do not think this PhD work would have been possible.

*... If you can dream—and not make
dreams your master;
If you can think—and not make
thoughts your aim; ...*

Rudyard Kipling

Contents

Abstract		V
Acknowledgements		IX
Nomenclature		XXVII
1 Introduction		1
1.1 Background to this Study		1
1.2 Aims and Objectives		3
1.3 Contribution to Knowledge		3
1.4 Thesis Outline		4
2 Optimisation Methods and Multidisciplinary Design in Aeronautical Engineering		7
2.1 Aircraft Design Process		8
2.1.1 Aircraft Development - A Historical Overview		8
2.2 Current Design Approach and the Need for Multidisciplinary Design		9
2.3 Contemporary Optimisation Elements		12
2.3.1 Geometry Parameterisation		12
2.3.2 Mesh (Re)generation and Deformation		18
2.3.3 Sampling		21
2.3.4 Variable Screening		23
2.3.5 Metamodelling Techniques		24
2.4 Surrogate Based Optimisation		32
2.5 Using Variable Fidelity Analysis Tools		36
2.5.1 Treed Metamodelling		37
2.5.2 Space Mapping		38
2.5.3 Multifidelity Trust Region Optimisation		38
2.5.4 Co-Kriging and Multifidelity Expected Improvement Criterion		38
2.6 Constraints in Optimisation		40
2.6.1 Penalty Methods		40
2.6.2 Lagrangian Methods		42
2.6.3 Sequential Quadratic Programming		42
2.6.4 Managing Constraints in Surrogate Based Optimisation		42
2.7 Multiobjective Optimisation		45
2.7.1 The Concept of Dominance		45
2.7.2 The Weighted Superposition Method		45

2.7.3	Multiobjective Methods in Surrogate Based Optimisation	47
2.8	Optimisation Algorithms	48
2.8.1	Gradient Free Algorithms	49
2.8.2	Gradient Based Algorithms	51
2.9	Multidisciplinary Design Optimisation	55
2.9.1	Generic Problem Formulation	57
2.9.2	Monolithic Architectures	58
2.9.3	Distributed Architectures	59
2.10	Aerostructural Optimisation Requirements and Considerations	62
2.10.1	The Aerostructural Coupling Problem	62
2.10.2	Volume Mesh Deformation due to Structural Deformation	65
2.10.3	Low Fidelity Aerostructural Analysis Tools	66
2.10.4	Structural Weight Estimation Methods	66
3	Optimisation Methodology	69
3.1	Desired Optimisation Attributes	69
3.2	Methodology Requirements	70
3.2.1	Requirements to Tackle Early Design Stage Needs	70
3.2.2	Attributes for Efficient Implementation in Multidisciplinary Problems	71
3.3	Methodology Overview	72
3.3.1	Geometry Parameterisation and Mesh Deformation	73
3.3.2	Surrogate modelling in a Multifidelity Context	73
3.3.3	Surrogate Based Optimisation in a Multifidelity Context	78
3.3.4	Multifidelity Treatment in Kriging Model	79
3.3.5	Multifidelity Infill Sampling Plan	81
3.3.6	Single Objective Suboptimisation Process	83
3.3.7	Multiobjective Suboptimisation Process	83
3.3.8	Constraints Handling Formulations	86
3.4	Implementation on Multidisciplinary Problems	91
3.5	Summary	95
4	Methodology Demonstration in Small Scale Problems	97
4.1	Framework Demonstration	97
4.1.1	1D - Test Case	98
4.1.2	2D - Test Case	99
4.2	Scalability Characteristics	102
4.3	Sellar Multidisciplinary Optimisation Test Function	106
4.3.1	Sellar Problem Mathematical Formulation	108
4.3.2	Sellar Problem Multidisciplinary Optimisation Formulation in this Surrogate Based Optimisation-Multifidelity Context	108
4.3.3	Results	112
4.3.4	A Note on Constraints	114
4.3.5	A Note on the Multidisciplinary Analysis Loop	115
4.4	Summary	117

5	Industrially Related Application in Aerodynamic Shape Optimisation Problems	119
5.1	The Transonic Airfoil Design Problem	119
5.2	RAE2822 Test Case	120
5.2.1	Problem Formulation	121
5.2.2	Geometry Parameterisation	123
5.2.3	Analysis Tools	124
5.3	Results	126
5.3.1	Unconstrained Drag Minimisation	126
5.3.2	Lift-Constrained Drag Minimisation	133
5.3.3	Multiobjective Optimisation	144
5.4	Summary	147
6	Comparison Between Trust Region and Expected Improvement Methods	149
6.1	Surrogate Based Optimisation Methodology	150
6.1.1	Trust Region	150
6.1.2	Hypervolume Indicator	153
6.2	Garteur High-Lift Configuration	155
6.2.1	Problem Formulation and Geometry Parameterisation	155
6.2.2	Aerodynamic Analysis	156
6.3	Results	157
6.3.1	Garteur case	157
6.3.2	RAE2822 case	161
6.4	Summary	164
7	Industrial Multidisciplinary Design Optimisation Application	165
7.1	Wingbox Structure and Structural Considerations	167
7.1.1	Loads and Structural Design Conditions	167
7.1.2	Material Considerations for Typical Wingbox Configurations	167
7.1.3	Structural Elements	169
7.2	Common Research Model	171
7.2.1	Problem Description	171
7.2.2	Parameterisation Strategy	173
7.2.3	Design Constraints	176
7.2.4	Aerodynamic Analysis	177
7.2.5	Multidisciplinary Feasible Architecture Formulation	181
7.2.6	Asymmetric Subspace Optimisation Architecture Formulation	183
7.2.7	Aerostructural loop: Mapping the Aero Loads and Structural Displacements	187
7.3	Multidisciplinary Feasible Architecture Results	188
7.3.1	Sensitivity in Constraint Models	188
7.3.2	Pareto Front Results	190
7.3.3	Physical interpretation	194
7.4	Asymmetric Subspace Optimisation Architecture Results	202
7.4.1	Pareto Front Results	202

7.4.2	Physical Interpretation	206
7.5	Comparison between the Formulations	213
7.6	Summary	218
8	Conclusions and Future Work	219
8.1	Summary	219
8.2	Conclusions	222
8.2.1	Surrogate Modelling for Multifidelity Optimisation	222
8.2.2	Multifidelity Tools in Surrogate Based Optimisation Formulation	223
8.2.3	Multiobjective Formulation	224
8.2.4	Surrogate Based Optimisation Plan	225
8.2.5	Handling Constraints	225
8.2.6	Multidisciplinary Architectures	226
8.2.7	Multidisciplinary Architecture Comparison	227
8.2.8	Summary of conclusions	228
8.3	Future Work	229
8.3.1	Dimensionality Reduction	229
8.3.2	Kriging Training Frequency	229
8.3.3	Concept for Hybrid Algorithm - 1	229
8.3.4	Concept for Hybrid Algorithm - 2	230
8.3.5	Multipoint Optimisation	231
8.3.6	Mesh Deformation	231
8.3.7	Low Fidelity Tool for Aerostructural Optimisation	231
8.3.8	Bi-Level Multidisciplinary Formulation for Aerostructural Optimisation	232
8.3.9	Alternative Cruising Constraints Formulation in Asymmetric Subspace Optimisation	232
8.3.10	Additional Work on the Common Research Model	232

List of Figures

2.1	The conventional aircraft configuration conceived by G.Cayley, featuring a lifting surface and conventional empennage.	9
2.2	O. Lilienthal performed an extensive series of experiments with various glider designs. The results were monitored in a scientific manner and were later used by the Wright brothers.	9
2.3	Typical design process: Multiple disciplines work in parallel using their own tools to perform disciplinary analysis and design.	10
2.4	Sequential versus Multidisciplinary Optimisation.	11
2.5	In the case of aerodynamics driven sequential optimisation, aerodynamic optimality is satisfied and the lift distribution is always elliptic. When information <i>from</i> the structures <i>to</i> the aerodynamic discipline is provided (coupling of the disciplines), the resulting lift distribution optimises the coupled system [3].	12
2.6	Direct comparison of a range maximisation problem. When designed sequentially, the wing does not reach the performance of the multidisciplinary optimised one, despite its superior aerodynamic efficiency [3].	13
2.7	Example of an FFD application in a BWB aircraft. Increased control is obtained in areas of interest via control points refinement. Furthermore, an FFD box can be inserted inside another FFD box [8]	15
2.8	FFD boxes and continuity around a solid object [7]	15
2.9	Original and Deformed grid around a wing [32].	19
2.10	Grid becomes invalid when algebraic warping is used for large rotational deformations [33].	19
2.11	Standard LHS and LHS using a metric. In the second case the location of the point in the bin is predefined [57].	22
2.12	Appropriate choice of screening method is dependent on the number of design variables [74].	24
2.13	Standard RBF and Hermitian RBF [57]. Notice how the addition of extra information (gradient) improves the function approximation.	28
2.14	Support vector regression [57].	29
2.15	Overview of a typical optimisation using surrogate models [103]. The true problem f is solved by creating the approximate model a , into which optimisation is performed. The true function is called again in order to update and improve the validity of the surrogate.	33
2.16	In the expected improvement (EI) criterion, the point which shows the maximum potential improvement is used as the next sampling point [107]. . .	36

2.17	Conventional optimisation approach (top) versus MF (AMMO) approach [106].	39
2.18	Example of a 2D design space with two constraints c_1 , c_2 [3]. Here, constraint number two is active.	41
2.19	Initial surrogate build-up and first infill point for a constrained SBO EI approach [107]. The bold line is the true function, the dashed line is the surrogate prediction and the thin line is the constraint surrogate. The constraint limit is shown in dash-dot line.	44
2.20	A typical Pareto Front consisting of non dominated points. These points can also be identified with a series of a, b combinations and a single objective function.	46
2.21	Multiobjective Expected Improvement criterion [107]. In this case two objectives are being considered.	48
2.22	A typical gradient based optimisation process. An analysis and the computation of the gradient (sensitivity analysis) feeds a method to provide the search direction. Given that, line search is performed and the procedure keeps iterating until conditions are satisfied [3].	52
2.23	Monolithic architectures. MDO uses a single optimisation problem introducing a coupled MDA [57].	57
2.24	Distributed architecture. The problem is decomposed into multiple suboptimisation problems [57].	57
2.25	MDF architecture. Analyses are iteratively until convergence as a part of an MDA. In this example, the Gauss-Seidel loop is used [158].	59
2.26	Diagram for ASO [158].	61
2.27	Diagram for BLISS [158].	61
2.28	Non matching grids. The aerodynamic and structural grids as a general rule do not share the same nodes [170]	63
3.1	A qualitative display of the MF Kriging model requirement in a 1D example. Interpolation is performed through the HF data but LF data are fitted since they are subject to error.	76
3.2	MF infill sampling approach.	82
3.3	Flowchart describing the suggested MF SBO methodology.	87
3.4	Constraint handling methods, acting during the suboptimisation process.	91
3.5	In its simplest form in monolithic MDO formulations, the methodology can act as a black box optimiser acting on variable fidelity industrially defined MDA workflows.	92
3.6	Description of an industrial aerostructural optimisation process. The multidisciplinary analysis involves the convergence of all related disciplines to provide the objective function and constraints. For ASO architecture, structural analysis is substituted by structural sizing.	93
3.7	In MDF, the methodology acts directly on the interface of a (predefined) multidisciplinary analysis. Upon multidisciplinary convergence, objective function and constraints of the appropriate fidelity are provided.	94

3.8	In ASO, the methodology exploits existing industrial analysis and disciplinary optimisation tools. At least one discipline performs an optimisation with respect to its local design variables. Thus, the global variables in the system level are reduced, improving the efficiency of the methodology. . .	95
4.1	Comparison of ordinary Kriging versus MF modKriging. The regression of the LF points improve the accuracy of the approximation.	99
4.2	Comparison of the negative expected improvement as resulting from Kriging and the modified Kriging for various shape parameters.	99
4.3	Modified Branin function contours, acting as high and low fidelity functions. The analytical error of the LF function is also compared against the RBF model prediction. Four HF (square) points are used in the error model generation.	101
4.4	High Fidelity function representation using MF modKriging. Four HF (square) and 16 LF (triangle) points are used.	102
4.5	Convergence history comparison of HF, MF ordinary, MF modified Kriging and Co-Kriging.	103
4.6	Effect of implementing the Error MSE term within the modified Kriging. .	104
4.7	Scalability analysis using Rosenbrock function.	107
4.8	Sellar XDSM flowchart for MDF formulation.	110
4.9	Sellar XDSM flowchart for ASO formulation.	111
4.10	Convergence comparison between MDO formulation and methodology. Results represent the mean convergence behaviour of these non-deterministic methods.	112
4.11	MDA convergence comparison for MDF and ASO architectures.	114
4.12	MDA convergence comparison of Jacobi and Gauss-Seidel method for MDF and ASO architectures.	116
5.1	Drag rise in transonic flows.	120
5.2	RAE 2822 Airfoil. In this test case eight active Control Points are used. .	123
5.3	C-type mesh generated around the RAE2822 airfoil.	124
5.4	Elapsed time based convergence comparison of several methods for the simple airfoil case.	128
5.5	Elapsed time based convergence comparison of several methods when considering that the RAE2822 convergence corresponds to that of a hypothetical MDO problem. This is done by substituting the airfoil analysis cost by the MDO analysis cost assumption made in section 5.3.	129
5.6	Effect of the LF tool, error correction model and Kriging tuning skipping in the elapsed time convergence for the simple airfoil problem.	130
5.7	Effect of the LF tool, error correction model and Kriging tuning skipping in the elapsed time convergence for a potential MDO problem when considering that the RAE2822 convergence corresponds to that of a hypothetical MDO problem. This is done by substituting the airfoil analysis cost by the MDO analysis cost assumption made in section 5.3.	131

5.8	Definition of the partially converged analysis as a LF tool and the effect of using a solution well within the initial convergence oscillations.	131
5.9	Comparison of the resulting geometries and corresponding Cp distributions in the unconstrained case.	132
5.10	Typical airfoil configuration convergence for the unconstrained drag minimisation problem. As we move from the red configuration to the blue one, drag is decreased.	133
5.11	Convergence comparison of the examined optimisation methodologies. Partially converged fluent simulations were used as the low fidelity tool. The lift constraint was tackled with the feasibility method and the surrogate model used to approximate the constraint function was the multifidelity modified Kriging.	134
5.12	Convergence comparison of the examined optimisation methodologies. In this, VGK was used as the low fidelity tool. The lift constraint was tackled with the feasibility method and the surrogate model used to approximate the constraint function was the multifidelity modified Kriging.	135
5.13	Convergence comparison between the two constraint handling approaches. In this, VGK was used as the low fidelity tool. Multifidelity modified Kriging was used to approximate the constraint function.	138
5.14	Convergence comparison between two metamodeling approaches for the estimation of the constraint function. In this, VGK was used as the low fidelity tool. Results from the penalty method are plotted.	140
5.15	Convergence comparison between two low fidelity analysis tool possibilities. Results are based on the feasibility method.	142
5.16	Convergence comparison between two low fidelity analysis tool possibilities. Results are based on the penalty method.	143
5.17	Comparison of the resulting geometries and corresponding Cp distributions in the constrained case.	144
5.18	Comparison of the multiobjective formulations of expected improvement as presented in section 3.4.7.	145
5.19	Pareto front comparison of the CFD based, HF EI, MF EI modKriging and MF EI Co-Kriging methods, and their sensitivity to the LF tool and the error correction model (where applicable).	147
6.1	Multiobjective multifidelity trust region optimisation framework [200] . .	152
6.2	Hypervolume definition from a normalised Pareto Front and a reference point	154
6.3	GARTEUR configuration	155
6.4	Hypervolume indicator convergence and Pareto front after 125 CFD calls for the Garteur case.	159
6.5	Pareto Front for the GARTUER airfoil optimisation case after 14-127 HF calls.	159
6.6	Parallel-coordinate plot for the Garteur case pareto points after 125 CFD calls.	160
6.7	Garteur configurations resulting from all optimisation methodologies. . .	160

6.8	Hypervolume indicator convergence after 125 CFD calls for the RAE case.	162
6.9	Pareto front after 125 CFD calls for the RAE case.	163
6.10	Three representative Pareto front shapes for the MF TR and MF EI methods.	163
7.1	Materials traditionally used in aeronautical applications [237].	169
7.2	Wingbox structural elements [237].	171
7.3	CRM structural configuration. CONM2 masses represent fuel and high lift systems' masses, connected with the structure with RBE3 elements. For clarity, shear webs are omitted.	172
7.4	CRM aerodynamics and structural parameterisation. Thickness is in mm.	175
7.5	C _p distribution grid convergence study for the HF analysis.	179
7.6	Global aerodynamic coefficients grid convergence study for the HF analysis.	179
7.7	High fidelity aerodynamic surface grid. O-type grid layers are used for boundary layer resolution.	180
7.8	Comparison between low fidelity (EULER) and high fidelity (RANS) solution in terms of pressure distribution.	181
7.9	XDSM flowchart for MDF formulation of CRM aerostructural optimisation.	182
7.10	XDSM flowchart for ASO formulation of CRM aerostructural optimisation.	185
7.11	Aerodynamic loads mapping on the CRM datum. Pressure loads are interpolated with RBF functions while the forces generated near non-structural surfaces (LE/TE) are transferred to the beams using RBE3 elements. . . .	188
7.12	The satisfaction of the range constraint can be achieved through a more efficient aerodynamic design, a more efficient structural design or a tradeoff between both.	191
7.13	Pareto front comparison between the HF and the MF methods, using "feasibility" to handle the constraints for the MDF formulation. Balance is required between aerodynamic and structural performance. A very efficient structural design leading to low aerodynamic performance will not improve range. Aerodynamic efficiency is more important in that aspect. Even dominated points can provide higher range than high drag pareto points. . . .	192
7.14	Comparison of the HF and MF pareto front convergence via the hypervolume indicator for the MDF formulation.	193
7.15	Maximum Von Mises stress in the rib-shear webs assembly during high g maneuvers, MDF formulation.	194
7.16	Maximum Von Mises stress in the skins assembly during high g maneuvers, MDF formulation.	195
7.17	Maximum vertical displacements during high g maneuvers, MDF formulation.	196
7.18	Skin thickness distribution, MDF formulation.	197
7.19	Pressure distribution of the datum, minimum drag, minimum weight and compromise design in different locations across the span, MDF formulation.	199
7.20	Wing sections of the datum, minimum drag, minimum weight and compromise design in different locations across the span, MDF formulation. . . .	200
7.21	Pressure distributions - Planform view and sweep angle, MDF formulation.	201

7.22	Pareto front comparison between the HF and the MF methods, using "feasibility" to handle the constraints for the ASO formulation. As in MDF, a tradeoff is required between aerodynamics and structures to achieve range performance.	204
7.23	Comparison of the HF and MF pareto front convergence via the hypervolume indicator for the ASO formulation.	205
7.24	Maximum Von Mises stress in the rib-shear webs assembly during high g maneuvers, ASO formulation.	206
7.25	Maximum Von Mises stress in the skins assembly during high g maneuvers, ASO formulation.	207
7.26	Maximum vertical displacements during high g maneuvers, ASO formulation.	208
7.27	Skin thickness distribution, ASO formulation.	209
7.28	Pressure distribution of the datum, minimum drag, minimum weight and compromise design in different locations across the span, ASO formulation.	212
7.29	Wing sections of the datum, minimum drag, minimum weight and compromise design in different locations across the span, ASO formulation. . . .	213
7.30	Pressure distributions - Planform view and sweep angle, ASO formulation.	214
7.31	Comparison between the pareto front generated using the MDF and the ASO formulation.	216
7.32	Comparison between the convergence of pareto front generated using the MDF and the ASO formulation using the hypervolume indicator.	217
7.33	Comparison between the normalised lift distribution resulting from the MDF and ASO formulations and that of the aerodynamic optimum. . . .	218
8.1	Brief overview of hybrid algorithm 1.	230
8.2	Poster from Airbus PhD Day 2016.	258
8.3	Poster from Airbus PhD Day 2017.	259
8.4	Modal shapes of datum common research model	261
8.5	Modal shapes of datum common research model	262
8.6	Modal shapes of datum common research model	263

List of Tables

5.1	Physical conditions for RAE2822 case	123
5.2	Unconstrained case - Methodologies examined	127
5.3	Constrained case - Methodologies examined	136
5.4	Multiobjective case - Methodologies examined	147
6.1	High-Lift optimisation parameters	155
7.1	Physical conditions for CRM case	172
7.2	CRM V.15 Wing characteristics	172
7.3	Design variables	174
7.4	Constraints	178
7.5	HF analysis numerical model details	180
7.6	Shell Elements Thickness (mm) - MDF Architecture	198
7.7	Shell Elements Thickness (mm) - ASO Architecture	210

Nomenclature

Greek Symbols

μ	Mean calculated in Kriging models
σ^2	Variance calculated in Kriging models
Φ	Gram matrix in Radial Basis Functions models
Ψ	Correlation matrix used in Kriging models
ψ	Correlation vector used in Kriging predictor
α	Angle of attack
α_i	Slack variables in Lagrangian function
α_k	Line step in the search direction provided by a gradient based method
Γ_{aero}	Virtual work of the fluid acting on the aerodynamic surfaces
γ_s	Expansion or shrinkage of trust region radius
Γ_{str}	Virtual work of the structure due to displacements
δ_k	Trust region hyper-radius
Δt	Time step allowing particles to travel in Particle Swarm Optimisation
$\hat{\theta}_l$	Optimum Kriging shape parameter provided by after the training of the model
θ	Shape parameter used in Radial Basis Function and Kriging models
λ	Regularisation parameter used in Radial Basis Function models
λ	Lagrangian multipliers
ρ	Ratio of improvement in trust region method
σ	Von Mises stress
σ_e^2	Variance of the error surrogate model
σ_y	Von Mises yield stress of the material
ϕ	Kernel function in Radial Basis Function models
$\Phi(x)$	Cumulative distribution function
ϕ_{ij}	Element of the gram matrix
$\phi(x)$	Probability density function
ψ_{ij}	Element of the correlation matrix

Latin Symbols

a	Parameters vector in Radial Basis Function models
c₀	Vector of system constraints
c_i	Vector of disciplinary constraints
c_i^c	Vector of disciplinary consistency constraints
D	Design space

\mathbf{d}_k	Search direction calculated by a gradient based method
\mathbf{e}	Vector of error training data
\mathbf{f}_0	Vector of shared objective functions
\mathbf{f}_i	Vector of local objective functions
\mathbf{H}	Transformation matrix correlating structural mesh and aerodynamic surface mesh displacements
\mathbf{K}	Transformation matrix correlating structural grid displacements and aerodynamic volume mesh displacements
\mathbf{L}	Transformation matrix correlating aerodynamic surface mesh and aerodynamic volume mesh displacements
\mathbf{M}_{fs}	Matrix involving the correlation between structural and aerodynamic mesh nodes in the Radial Basis Functions method for the aerolastic mapping problem
m_k	Co-Kriging model predictor used in a trust region formulation
\mathbf{M}_{ss}	Structural gram matrix in the Radial Basis Functions method for the aerolastic mapping problem
\mathbb{O}	Objective space
\mathbf{r}_p	Reference point coordinate used in the calculation of the hypervolume indicator
\mathbb{S}	Structural design space
$\mathbf{S}(u, t, s)$	Coordinates of a deformed point originating at (u, t, s) using Free Form Deformation
\mathbb{T}	Design space included within the trust region hypersphere
\mathbf{u}_{aero}	Aerodynamic surface mesh displacements
$\mathbf{u}_{aero,v}$	Aerodynamic volume mesh displacements
\mathbf{u}_{str}	Structural mesh displacements
\mathbf{x}	Design vector
\mathbf{x}^*	Design point solution of the suboptimisation problem
\mathbf{x}_0	Shared design variables vector
\mathbf{x}_c	Center of the basis function in Radial Basis Function models
\mathbf{x}_{str}	Structural design variables vector
\mathbf{y}	Vector of function training data
c_1	Particle Swarm Optimisation factor representing cognitive learning
c_2	Particle Swarm Optimisation factor representing social learning
C_D	Drag coefficient of a wing planform
C_d	Drag coefficient of an airfoil
C_L	Lift coefficient of a wing planform
C_l	Lift coefficient of an airfoil
C_{Mcg}	Moment coefficient around the center of gravity of the wing
c_r	Contribution rate used in the calculation of the hypervolume indicator
D	Drag
e	Error surrogate model
f	Objective function
f_{HF}	High fidelity objective function
$f_i(u)$	Bernstein polynomials used on Free Form Deformation

f_{LF}	Low fidelity objective function
g	Constraint function
$g_j(t)$	Bernstein polynomials used on Free Form Deformation
$h_k(s)$	Bernstein polynomials used on Free Form Deformation
I_h	Hypervolume indicator
I_{hs}	Surrogate Pareto front hypervolume indicator
\mathcal{L}	Lagrangian function
L	Lift
m_p	Number of Pareto points used in the calculation of the hypervolume indicator
n_p	Number of Pareto front to compare in the calculation of the hypervolume indicator
P	Penalty function
p	Smoothing parameter used in Radial Basis Function and Kriging models
PF'	Reduced Pareto Front
PF_s	Surrogate Pareto Front
p^g	Best solution encountered by the swarm in Particle Swarm Optimisation
p^i	Best solution encountered by particle i in Particle Swarm Optimisation
p_k	Candidate points for improvement in trust region method
\hat{p}_l	Optimum Kriging smoothness parameter provided by after the training of the model
R	Range
r_1	Particle Swarm Optimisation factor of random value inducing the stochastic element in cognitive learning
r_2	Particle Swarm Optimisation factor of random value inducing the stochastic element in social learning
s	Mean squared error of a Gaussian Based model
s_e	Mean squared error of the error surrogate model
SF	Safety factor
SFC	Thrust-specific fuel consumption
u^i	Velocity of an i^{th} particle in Particle Swarm Optimisation
V	Flight speed
w	Particle Swarm Optimisation factor representing the inertia of a particle
W_{fuel}	Fuel weight
W_g	Final aircraft weight
W_i	Initial aircraft weight
W_r	Aircraft non-structural weight
W_{TO}	Aircraft take-off weight
$W_{w, str}$	Wingbox structural weight
x_i^*	The i^{th} design point solution of a multiobjective suboptimisation problem
\hat{y}	Surrogate model predictor
Y	Objective function value of pareto front member
y^+	Wall y-plus used in turbulence modelling
y_{HF}	High fidelity tool output
\bar{y}_i	Disciplinary state variables
\hat{y}_i	Target variables

y_i	Coupling variables
y_i^*	The objective function value of a member of the pareto set
y_{LF}	Low fidelity tool output
y_{min}	Minimum objective function value found
Z_d	Factor relating the low and high fidelity tool outputs
Z_ρ	Factor relating the low and high fidelity tool outputs

Abbreviations

AAO	All At Once
AD	Automatic Differentiation
AMMO	Approximation Model Management Optimisation
ASO	Asymmetric Subspace Optimisation
ATC	Analytical Target Cascading
BEM	Boundary Element Method
BFGS	Broyden-Fletcher-Goldhurb-Shanno
BK	Blind Kriging
BLISS	Bilevel Integrated System Synthesis
BSM	Beam Structural Model
CAD	Computer Aided Design
CAE	Computer Aided Engineering
CFD	Computational Fluid Dynamics
CFL	Courant-Friedrichs-Lewy number
CO	Collaborative Optimisation
CP	Control Point
CRM	Common Research Model
CSM	Computational Structural Mechanics
CSSO	Concurrent Subspace Optimisation
CVT	Constant Volume Tetrahedron
DAO	Distributed Analysis Optimisation
DFP	Davidson-Fletcher-Powell
DK	Detrended Kriging
DoE	Design of Experiments
E-RBF	Extended-Radial Basis Functions
ECO	Enhanced Collaborative Optimisation
EI	Expected Improvement
EPD	Exact Penalty Decomposition
FEA	Finite Element Analysis
FEIC	Feasible Expected Improvement Criterion
FEM	Finite Element Model
FFD	Free Form Deformation
FSI	Fluid Structure Interaction
GA	Genetic Algorithms
GB	Gradient Based
GEK	Gradient Enhanced Kriging

HAR	High Aspect Ratio
HF	High Fidelity
IAC	Industry Affairs Committee
IATA	International Air Transport Association
IDF	Individual Discipline Feasible
IFFD	Iterated Fractional Factorial Designs
IPD	Inexact Penalty Decomposition
ISC	Infill Sampling Criteria
KKT	Karun-Kush-Tacker conditions
KS	Kreisselmeier–Steinhauser
LE	Leading Edge
LF	Low Fidelity
LHS	Latin Hypercube Sampling
LOP	Low Order Polynomials
MDA	Multidisciplinary Analysis
MDF	Multidisciplinary Feasible
MDO	Multidisciplinary Design Optimisation
MDOIS	MDO of Independent Subspaces
MELE	Mixture of Explicitly Localised Experts
MF	Multifidelity
MILE	Mixture of Implicitly Localised Experts
MLE	Maximum Likelihood Estimation
MLS	Moving Least Squares
Mm	Minimax and Maximin
MO	Multiobjective
MOE	Mixture OF Experts
MOPSO	Multiobjective Particle Swarm Optimisation
MOTS	Multiobjective Tabu Search
MPCs	Multiple-Comparison Procedures
MSE	Mean Squared Error
N-M	Nelder-Mead
NNI	Nearest Neighbour Interpolation
OA	Orthogonal Arrays
OAT	One factor at a Time
OF	Objective Function
OML	Outer Mold Line
PF	Probability of Feasibility
PI	Probability of Improvement
PRMOTS	Path Relinking Multiobjective Tabu Search
PSO	Particle Swarm Optimisation
QSD	Quasiseparable Decomposition
RAE	Royal Aircraft Establishment
RANS	Reynolds Averaged Navier Stokes
RBF	Radial Basis Functions
RMSE	Root Mean Squared Error

RSM	Response Surface Models
SA	Spalart-Allmaras turbulence model
SAND	Simultaneous Analysis and Design
SBO	Surrogate Based Optimisation
SLB	Statistical Lower Bound
SO	Single Objective
SQP	Sequential Quadratic Programming
SR1	Symmetric Rank-1
SSPs	Screening and Selection Procedure methods
SVD	Singular Value Decomposition
SVM	Support Vector Machine
SVR	Support Vector Regression
TD	Training Data
TE	Trailing Edge
TFI	Transfinite Interpolation grid deformation method
TGP	TreedGaussianProcess
TR	Trust Region
TS	Tabu Search
UD	Uniform Design
WGC	Weighted Global Criterion
XDSM	EXtended Design Structure Matrix

Introduction

Αρχή ήμισυ παντός...

Πλάτων

1.1 Background to this Study

It is universally accepted that the growth tendency of the airline industry will continue during at least the first half of the 21st century. With different businesses, logistic models and ideas emerging, the exact characteristics of the future commercial aviation market are not entirely understood, as there might be a tendency to shift from the hub towards a point-to-point transport. In an effort to reduce the uncertainty of the future airline industry market, the Industry Affairs Committee (IAC) of the International Air Transport Association (IATA) issued a research study [1] to identify risks and opportunities that the aviation industry may face until 2035.

Whatever the future holds, one thing is certain: more and more passengers will use aircraft for their travel. Consequently, the fuel consumption is also expected to increase in the following decades. This unfortunately results to a significant increase in CO_2 and NO_x emissions, posing environmental threats that need to be addressed vigorously. In this spirit, the European Commission defined the ACARE 2050 [2] vision for the emissions of future commercial transport aircraft. Among others, a target of reducing fuel consumption and CO_2 emissions by 75% is set. To achieve this goal, around 20% to 25% reduction has to be attained through the improvement the airframe.

During the past decades, the aircraft industry has been successful in improving their designs in a series of aspects, including fuel and noise emissions, costs, safety etc. However, in the recent years it has become apparent that improvements follow an asymptotic trend. A

lot of research effort and cost translates only to small improvement in the aforementioned fields. A fresh approach towards aircraft design is necessary to perform the technological leap required to achieve the ACARE 2050 goals.

In order to revolutionise the industrial design procedures, one should act early in the design process and steer towards new innovative configurations. Therefore, conceptual studies should become more extensive as well as reliable to support these ambitious design goals. There is also the need for a more physical understanding of the compromises made by engineers during early tradeoff studies. Engineering tools should provide not only design suggestions but also the maximum amount of reliable information possible so that designers can confidently decide based on how a system design direction will affect other aircraft sub-systems. Once again, the reliable assessment of several engineering concepts at an early stage is critical for the success of the final configuration. The process should therefore use a series of different objectives in which the potential designs should be optimised.

An important factor that should be considered if a performance jump is to be achieved, is interdisciplinary synergies. The aircraft is a complicated system composed by a series of sub-systems affecting each other. The new aircraft development procedures should comprehend how the sub-systems interact with each other and use this interaction to guide the iterative design process. Early design and feasibility studies shall focus on the aircraft as a system, taking into account disciplinary goals driven by a series of multidisciplinary objectives.

Although currently investigated by various research groups and slowly emerging in the industry, truly multidisciplinary studies are still not a standard industrial practice; the various disciplines are still sequentially optimised given a leading discipline, especially in complex problems. To perform such studies — especially since these should be reliable in the conceptual stage — new design and optimisation tools have to be developed according to the above considerations. Such engineering capabilities should also reduce the computational and elapsed time costs associated with these complex multidisciplinary operations. Expensive physical procedures like wind tunnel experiments have to be minimised but of course not withdrawn, since if exploited properly they can support computational tools in their challenging task.

Multidisciplinary optimisation tools have also to be adjusted to the geographical needs of the industry. Companies tend to globally expand, with the design being currently performed under remote areas. An efficient multidisciplinary tool and design process should require the minimum amount of interdisciplinary information exchange to avoid costs related to the communication between groups of different technological expertise. As a part of this aerospace engineering effort towards innovative and efficient configurations, this work aims in the development of a numerical optimisation methodology to support design studies based on the above considerations.

1.2 Aims and Objectives

The aim of this thesis is to develop and evaluate an optimisation methodology that can be used to efficiently and reliably guide the early stage design of an aerospace configuration (e.g. transonic wing) towards a set of objectives. The numerical tool has to take into account multidisciplinary interactions between the sub-system disciplines to achieve a higher performance than the one achieved with the current design methods. To achieve this goal, the following steps have to be taken:

1. Use a surrogate based optimisation plan to reduce the analysis-related computational costs, taking advantage of the low dimensionality of the conceptual design studies.
2. Develop a multifidelity method to further decrease computational costs while still providing high fidelity results that correspond to a preliminary design stage.
3. Evaluate the effect of the low fidelity analysis tool in the convergence and cost attributes of the developed optimisation methodology.
4. Adjust the methodology into a multiobjective formulation so that it can be used for design problems that involve conflicting objectives.
5. Assess and improve the methodology using a series of analytical and aerospace-related test cases.
6. Embed the method within a greater multidisciplinary design and optimisation formulation and demonstrate the capabilities of the complete multidisciplinary optimisation methodology in the aerostructural design of a transonic wing configuration.
7. Compare and assess the use of different multidisciplinary architectures that are suitable for aerostructural optimisation.

1.3 Contribution to Knowledge

The work described in this thesis uses a series of sub-methods or concepts that have been specifically developed as a consequence of the needs of this particular research and to the author's best knowledge they are an addition to the existing methodologies. These include:

- The development of a methodology that applies appropriate ideas from surrogate based optimisation, multifidelity and multiobjective optimisation. The methodology uses these existing concepts as building blocks to compose a novel framework that exploits their most promising attributes with the respect to the targets specified.

- The novel application of the developed method in the context of multidisciplinary optimisation. None of the similar methods has been applied for complex industrial level multidisciplinary design problems, or as a part of a multidisciplinary optimisation architecture. In addition, a comparison study between two different architectures that use this optimisation methodology is conducted.
- The use of a multidisciplinary optimisation in the conceptual design stage through an exploratory optimisation scheme. It is common practice in the literature for multidisciplinary studies to be performed in the detailed design stage. However, if applied in early stages (as in this work), the exploration attributes of the methodology takes fully advantage of the interdisciplinary synergies identified.
- The development of a modified Kriging model that is tailored to the needs of multifidelity optimisation. This is proposed as a novel alternative to the more costly Co-Kriging method which is the standard practice within a multifidelity data environment. A modification on the mean squared error formulation to accommodate for the uncertainty induced by low fidelity analyses is also suggested. Under this modification, Radial Basis Function models used to correct the error associated with the low fidelity data can be also used to calculate the mean squared error of the error model itself. This is necessary if the modified Kriging model is to be used within a multifidelity Expected Improvement surrogate based optimisation formulation. The Radial Basis Function error model correction is proven to be conditionally superior to the Kriging error model correction when used within this modified Kriging model context.
- A simple yet effective infill sampling criterion to decide whether a low or high fidelity analysis should be performed to improve the design space understanding, while considering the computational cost requirements. This takes advantage of the already generated error surrogate model and allows flexibility of use depending on the engineer's needs and the design stage within which is applied.

1.4 Thesis Outline

The thesis is structured as follows:

Chapter 2 discusses in more depth the traditional aircraft design process and the need for shifting to a multidisciplinary approach in order to improve the performance of the new generation of aircraft, hence posing the research problem. It subsequently offers a review of the theory as well as the cutting edge of the literature related to multifidelity, multiobjective, multidisciplinary and surrogate based optimisation.

Chapter 3 initially provides a set of detailed specifications for the optimisation methodology, based on the problem described earlier. The developed methodology is then presented in detail throughout the rest of the chapter.

Chapter 4 uses a series of test cases of successively increasing complexity to demonstrate the optimisation methodology. 1D and 2D cases are being used to visually explain the surrogate model-related modifications as well as to fine-tune optimisation parameters. The extended Rosenbrock function is used to assess the scalability characteristics of the methodology. The analytic Sellar test function includes all the attributes of a multidisciplinary optimisation problem allowing the assessment of the methodology in such an environment. It is also used to perform a comparison between two different multidisciplinary formulations.

Chapter 5 demonstrates the framework in an industrially relevant transonic airfoil design problem using the RAE2822 configuration. An unconstrained, constrained and multiobjective formulation of this problem are presented. The author's methodology is compared against other optimisation approaches and a parametric study is also conducted. In particular, the effect of the error correction metamodel, low fidelity analysis tool, constraint handling method as well as constraint metamodel is evaluated.

Chapter 6 is dedicated to the comparison of the methodology against a similar multiobjective surrogate based optimisation methodology developed within our research group. The assessment of the methods is based on their performance in the GARTEUR high-lift and the RAE2822 transonic airfoil test cases.

Chapter 7 demonstrates the methodology in a complex and expensive multidisciplinary design optimisation problem, for which the framework has originally been developed. The Common Research Model wing configuration has been used, featuring the characteristics of a realistic transonic wing aerostructural design problem. Following the findings of Chapter 4, the methodology is implemented in two different architectures, becoming a self-contained multidisciplinary framework in its own right, and the efficiency of each of the architectures is discussed.

Chapter 8 offers a comprehensive summary of the findings of the work. Reflecting on the literature as well as the performance of the methodology, suggestions for future work in multidisciplinary optimisation are provided.

Optimisation Methods and Multidisciplinary Design in Aeronautical Engineering

...give me sight beyond sight!!!

Lion-O

THIS chapter begins with an overview of a typical aircraft design process in an attempt to clarify the respective needs of the aerospace industry. It is then followed by a presentation of the fundamental theoretical aspects of optimisation, as well as the cutting edge approaches and methods used by researchers in the present day. The literature review was performed, and presented, with a critical eye focusing on the PhD aims, as well what can be used or modified to progress this scientific area. As such, when discussing the theory and the research advances in the field, considerations regarding the applicability of each approach are provided. This acts as an explicit reasoning as to why each approach might be more appropriate over others¹ for this particular work requirements. These support the choice of the methodologies employed by the framework, as well as the foundation behind the development of any new methodologies during this PhD thesis.

This PhD work focused in the development of an increased reliability conceptual to/and preliminary design framework for rapid optimisation of aeronautical related systems (wings etc.). This had also to take into account the interdependence and interaction of the various subsystems within in a Multidisciplinary Design Optimisation (MDO) environment.

Therefore, the existing methodologies which the literature review is focused on and are employed by the computational framework, as well as any developed methodology, follow three principal directions:

- The minimisation of computational costs, without affecting the final design (ideally

¹An overview of the method can implicitly provide such information, however a separate more explicit explanation was considered necessary for increased clarification.

global minimum) or the reliability (fidelity) of its performance.

- It should be embedded in a multidisciplinary framework to account for the coupling of the aerospace related engineering systems (aerodynamics and structures will be considered in this study).
- It should not just provide the optimum design under given conditions but also provide a reliable and extensive insight on the design space so that it can be a guide and contributor to design decision making in an industrial aeronautical environment.

2.1 Aircraft Design Process

2.1.1 Aircraft Development - A Historical Overview

The formal birth of aviation is traced in the beginnings of the 20th century. After the first powered flight — and boosted by World War I — aerospace engineering took off to greater speeds, maneuverability and altitude. From a physics point of view, this translates to a variety of conditions and engineering problems which characterised each aerospace era. In the 19th century, the problem opposing powered heavier than air flight was two fold. Although the fundamentals of fluid mechanics were well established from the work of pre-era mathematicians, the formulation of the equations themselves was not appropriate to provide clear design directions. Hence, experimentation in form of trial and error was the typical way for the pioneers to achieve viable flying solutions. Significant contribution in this direction was provided by sir G.Cayley (who "invented" the conventional aircraft configuration) (see Fig.2.1) and O.Lilienthal (see Fig.2.2) among others. By the end of the 19th century, the "correct" design direction was known. However, a second problem proved to be a barrier: engine power. Aerodynamics design was effective enough to support human weight. However, this dictated heavy structural designs, followed by heavy motors of insufficient power. Only when engines were powerful and light enough did the complete system of aerodynamics, structures and propulsion provide an overall good design to achieve flight. This is a typical example of the interdisciplinary connection in a complex engineering system such as the aircraft. Hence, it was shown from an early stage, that the secret to an efficient design was not only considering each engineering discipline (aerodynamics, structures etc.) alone, but also their interactions with the other disciplines. This allowed a more efficient compromise, a more revealing design process and finally, superior configurations. Technological advances provided more powerful and light engines, as well as lighter and "stronger" structures. The simultaneous advance of aerodynamics through the development of analysis tools propelled the design further. After a few decades, — and with the advent of the jet engine — this disciplinary synergy allowed aircraft to fly in transonic speeds.



Figure 2.1: The conventional aircraft configuration conceived by G.Cayley, featuring a lifting surface and conventional empennage.



Figure 2.2: O. Lilienthal performed an extensive series of experiments with various glider designs. The results were monitored in a scientific manner and were later used by the Wright brothers.

2.2 Current Design Approach and the Need for Multidisciplinary Design

Aerospace engineering involves high correlated disciplines. The typical design procedure requires the assessment, via an analysis method (experimental, theoretical or computational), of a disciplinary performance followed by a redesign driven by the feedback provided by the analysis. In short, this design loop is guided to efficient design directions by experienced engineers who exploit the physical feedback provided by experiments or computational analyses, in a process similar to the one shown in Fig.2.3.

Of course this is just a simplistic depiction of the procedure since in reality the industrial processes are way more complicated than this. The aircraft is a complex system consisting of many different subsystems interacting with each other. Especially when considering aviation safety requirements and certification regulations which make aviation a very slow moving industry, the requirements in human resources are increased. Therefore, for better management, coordination and efficiency of the engineering work, aerospace manufacturers follow a strategy of *distributing* the work into many groups and subgroups. These are associated with disciplinary and subdisciplinary analysis and design work, generating their own expertise and using their own disciplinary analysis tools. Nowadays, given the ease of communication and information transfer, these engineering groups may be distributed even across countries, working isolated and communicating mainly in predefined review meetings which demand interdisciplinary information exchange.

Hence, each discipline involved in an engineering system is designed by the respective engineering group until it reaches the required level of maturity. In the following stages, the design becomes progressively more mature and detailed until it reaches convergence.

In a computational design study or an optimisation environment, engineering experi-

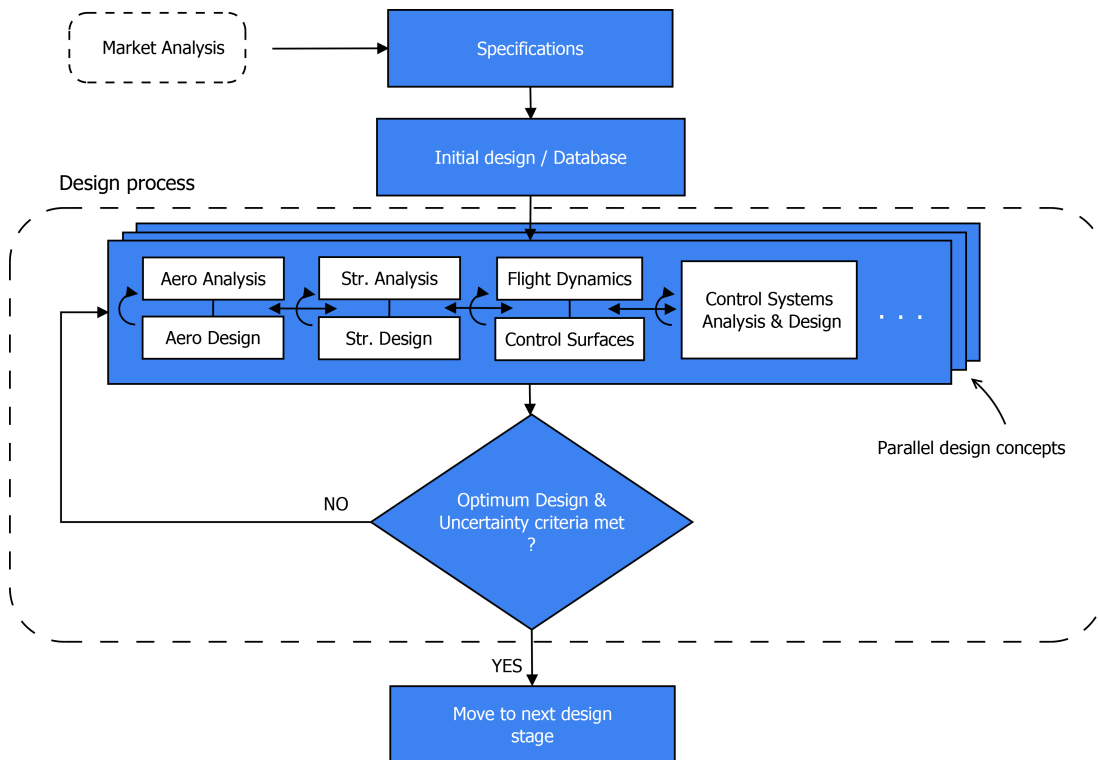


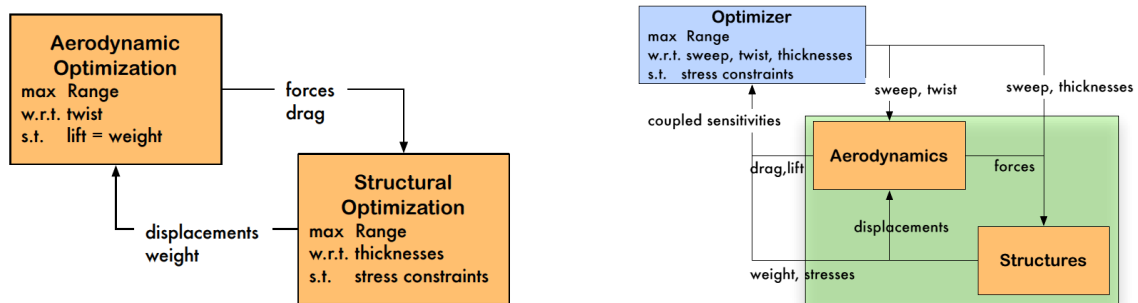
Figure 2.3: Typical design process: Multiple disciplines work in parallel using their own tools to perform disciplinary analysis and design.

ence is assisted by an optimisation framework. An important difference between a traditional and a computational design process, is the understanding and involvement of the physical background of a system's discipline. An experienced engineer, on top of being able to foresee the required design changes to improve disciplinary efficiency through understanding of the physics involved, can also predict how these changes may impact other disciplines. Hence, the engineer may consciously proceed in a direction which will not maximise the efficiency of his discipline, but will maximise the efficiency of the overall engineering system. A typical example of this, is quality and cost. When designing a product to meet the highest quality and performance standards, cost discipline is inevitably driven by performance. Therefore, even when minimizing the cost for a given performance, the cost will still be higher than another product for which performance and cost are concurrently considered. The product then will not be overall in the market as one with the disciplinary tradeoff (for slightly less quality will have significantly lower costs²). Multiple disciplines should not be confused with constraints, for the latter do not provide separate physical information in the design nor the system, rather just criteria as to which design is acceptable and which is not³. The experience of a technical director and the communica-

²This multidisciplinary design concept has a common ground with multiobjective optimisation discussed later.

³In early MDO efforts, or cases where no major computational resources are available, constraints are used as a surrogate to MDO, to produce a more meaningful design. For example, structural calculations may provide a wing thickness. However, in this case aerodynamics and structure disciplines are not optimised concurrently or coupled together. Rather, a simple criterion decides whether a potential aerodynamic design

tion between disciplinary groups of different disciplines is now replaced by an algorithm. Hence, an automatic computation method of interdisciplinary communication should be used, so that it is the the overall efficiency of the system which is optimised and not each single discipline. A typical aeronautical example (considered in the present PhD thesis as well), is a design involving the interaction between aerodynamics and structures. When the subsystems are not coupled (as in sequential approach), aerodynamic design is followed by structural design using aerodynamic loads as an input (see Fig.2.4). This is an iterative procedure dictated by aerodynamics, and as such the final design will have the optimum aerodynamic efficiency (e.g. elliptic lift distribution) and the best structural design possible, constrained by the aerodynamic shape.



(a) A typical sequential design procedure. In each step, after an aerodynamics optimisation, the structures are optimised to match the desire aeordynamic shape. Common design variables have fixed values dictated by aerodynamics [3].

(b) A coupled design procedure. For a specific design point which includes aerodynamic, structural and common variables, aerodynamics and structural analyses are performed simultaneously until this Multidisciplinary Analysis (MDA) converges [3].

Figure 2.4: Sequential versus Multidisciplinary Optimisation.

When two or more disciplines are designed simultaneously, information is exchanged between them, and the final result is the optimised *system*. In this case, it might be that neither discipline has been optimised, however, the coupled system is free to reach its maximum efficiency (see Figs.2.5, 2.6). This is illustrated by an aero-structural design example. In such a system, aerodynamics' variables also have an impact to structures and *vice versa*. Hence, by changing the lift distribution and the wing thickness, a structural analysis (or even sizing) has to be performed, providing new structural displacements, affecting the aerodynamic performance. After a Multidisciplinary Analysis (MDA) cycle is performed, the design point and the respective objective function values are used to feed the optimisation process. In this simple Multidisciplinary Optimisation (MDO) case, the optimisation process does not use a single disciplinary analysis to evaluate the merit function, but an MDA iterative procedure.

should be accepted or not.

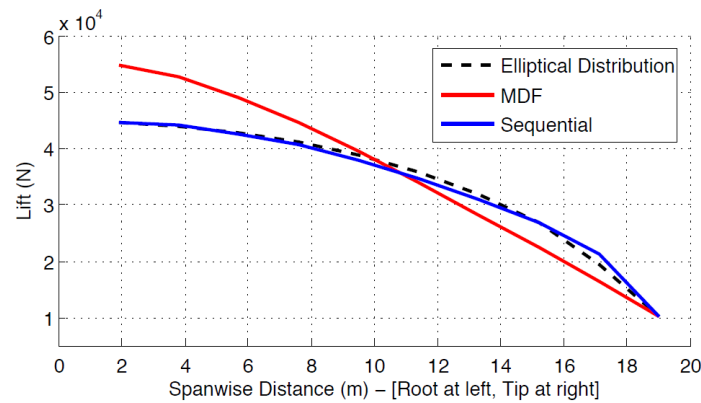


Figure 2.5: In the case of aerodynamics driven sequential optimisation, aerodynamic optimality is satisfied and the lift distribution is always elliptic. When information *from* the structures *to* the aerodynamic discipline is provided (coupling of the disciplines), the resulting lift distribution optimises the coupled system [3].

2.3 Contemporary Optimisation Elements

An optimisation process applied to an industrially realistic aerospace design problem is way more complex than the optimisation of a mathematical function. The fact that in most cases the objective function is not a result of simple analytical calculations, combined with the need to minimise computational costs, led to the development of various techniques which require additional optimisation building elements. This section presents these elements within the process of aerospace design, also providing an overview of the respective state of the art research work. Potential gaps, research limits as well as applications of such methodologies are identified. This review allows the educated selection of the elements that are most appropriate for implementation within the author's unified methodology (Chapter 3). Furthermore, required modifications and extensions of these methods are identified, some of which are included in this unified framework⁴.

2.3.1 Geometry Parameterisation

An aircraft design process, like any physical product design, in order to allow parametric changes of it, requires a robust and strict mathematical way of representing geometry in terms of design variables⁵. In a conventional design procedure, CAD engineers are responsible for manually applying the geometric changes dictated by the aircraft development. Hence, there is a physical interface between design and geometry update. However, in MDO, the very nature of the design optimisation process demands an automated generation of the updated geometry or its changes.

⁴Others are suggested for future research work.

⁵By parameterisation, we refer to the definition of a geometry as a result of given parameters.

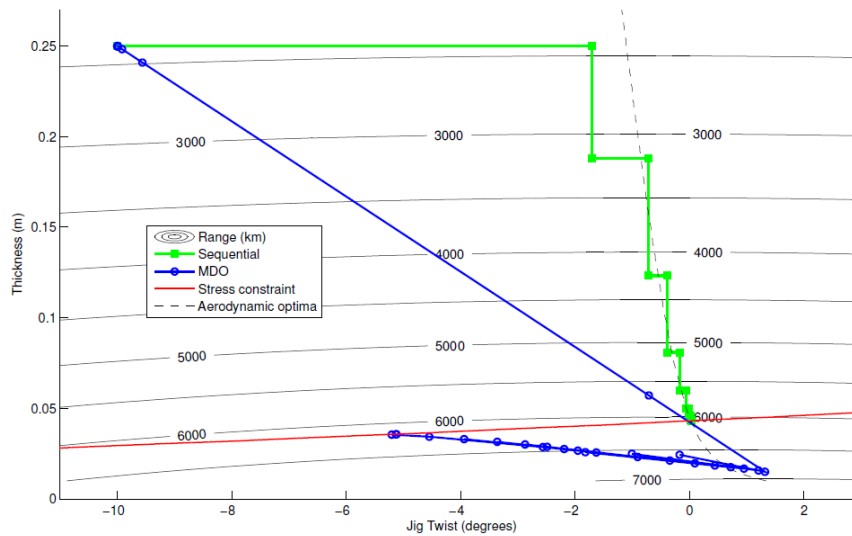


Figure 2.6: Direct comparison of a range maximisation problem. When designed sequentially, the wing does not reach the performance of the multidisciplinary optimised one, despite its superior aerodynamic efficiency [3].

Sobester and Forrester [4] provide general guidelines for setting an efficient geometry parameterisation. Typically, this includes the minimisation of the number of design variables to unambiguously describe a given geometrical parameterisation range, as well as the avoidance of parameters that cause geometrical discontinuities. Following such suggestion, the — unfortunately contradicting — attributes that an optimisation framework should possess [4] are conciseness, robustness and flexibility.

Geometry parameterisation techniques are grouped into categories depending on their attributes. These include discrete methods, polynomial methods, analytical methods, CAD-based methods and Free Form Deformation methods. In typical engineering practice, polynomial methods are of wide use. In this, objects like OML (Outer Mold Line) are composed by simple elements like curves, which are then parameterised by mathematical operations (known as the 2 and $\frac{1}{2}$ dimensionality concept). Namely, parameterised curves and shapes are then "extruded" along other parameterised curves, to produce the final 3D geometry.

In an ascending order of complexity, the family of polynomial methods for curve and surface parameterisation [4, 5] includes *Bernstein*, *Bézier* and *Rational Bézier Curves*, *Bézier Splines*, *B-Splines* and *Knots and Nonuniform B-Splines*, *Nonuniform Rational B-Splines* (NURBS) as well as *Ferguson's Splines* [6]. Parameterisation of curves is used extensively for the development of airfoil sections, fuselage sections as well as guiding curves for the aforementioned sections. For completeness purposes, the *PARSEC* method is also mentioned. It uses mathematical expressions to directly represent an airfoil. This approach is limited to 2D cases (airfoils) and as such it cannot be used in this research work which requires a more generalized technique.

In 3D geometry problems like wing design, OML surfaces parameterisation techniques

are of main interest. Following the 2 and $\frac{1}{2}$ dimensionality concept, which uses an already designed curve, different ways of translation along guiding curves are possible to generate a surface. These include [4] *Lofted Surfaces, Translated Surfaces, COONS surfaces, Bézier surfaces, B-Splines Surfaces, NURBS Surfaces*.

The above methods focus on ways to use control point positions to *generate and parameterise* geometries. There is another class of methods that use an *already defined* geometry (the datum geometry) with the design variables parameterising its *changes*. The *Hicks - Henne Bump function* method falls in this category, parameterising the changes in the form of bumps superimposed in the datum geometry curve. This is an easy to apply method with the advantage of maintaining a smooth geometry when the datum geometry is smooth as well. However, it lacks flexibility and its form is not intuitive to allow its use in complex geometries.

Another popular method is the *Free Form Deformation* [7] (FFD) by T.W. Sederberg. A grid of control points defines an FFD box, which includes the geometry of interest as shown in Fig.???. The control points perturb the geometry using Bézier curves and Bernstein polynomials. Each control point movement defines a design variable and allows the direct calculation of the new geometrical coordinates using the following expression for a 2D shape (surface) in 3D space:

$$\mathbf{S}(u, t, s) = \sum_{i=0}^m \sum_{j=0}^n \sum_{k=0}^p a_{ijk} f_i(u) g_j(t) h_k(s) \quad (2.3.1)$$

In this, $S(u, t, s)$ represents the coordinates of a deformed point originating at (u, t, s) , and m, n, p define the grid of control points in the x, y, z direction. Instead of the Bernstein polynomials $f_i(u), g_j(t), h_k(s)$, several modifications using other forms can be done.

One of the advantages of the method is that it can deform locally while permitting a variable degree of continuity with the undeformed regions. Flexibility is attained even with a low number of design variables when control points are distributed depending on the local flexibility needs. It is a highly intuitive method in terms of the effect that each control point movement has on the geometry. For gradient based optimisation methods, this approach can also provide sensitivities of the surface mesh to the design variables [9], [10]. The fact that it maintains the grid topology, makes the FFD compatible with mesh deformation tools⁶ and can be used as one as well (more on grid deformation methods in the following section). An additional advantage over the rest of the methods is the direct definition of sections of the geometry that are desired to be unchanged, simply by letting the respective sections out of the FFD box. Changes are then performed only in the part of the geometry inside the FFD box. A disadvantage is the difficulty to predict the optimum positions,

⁶This approach can be used in any geometric entity like computational grids which require "parameterisation" as well.

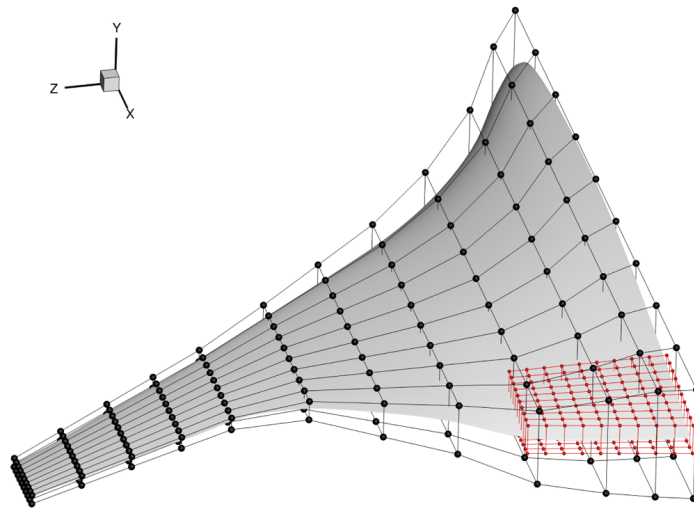


Figure 2.7: Example of an FFD application in a BWB aircraft. Increased control is obtained in areas of interest via control points refinement. Furthermore, an FFD box can be inserted inside another FFD box [8]

number of control points and bounds of design variables to cover the desired design space. However, this is an inherent negative characteristics of parameterisation techniques.

The method was developed in 1986 as a solution to the problem of "defining solid geometric models of objects bounded by free-form surfaces [7]". In his paper, Sederberg also included a method to provide smooth connectivity of k^{th} degree of continuity between the geometry of the respective various planes of the FFD box (see Fig.2.8). This is done by freezing the k cells adjacent to the control point of interest.

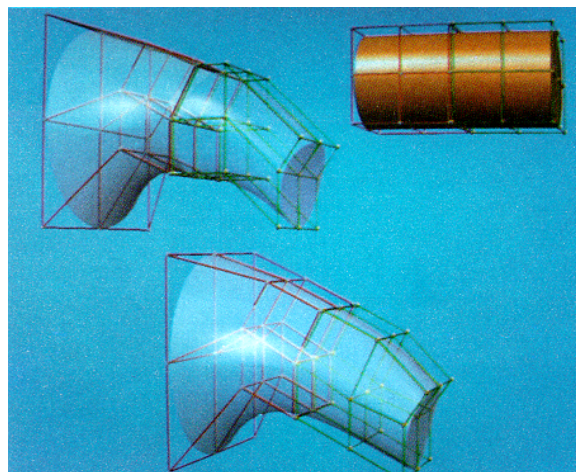


Figure 2.8: FFD boxes and continuity around a solid object [7]

Four years afterwards, S.Coquillart [11] extended the method. He highlighted the need for a refinement technique for small bumps, pointing out the hierarchical B-Splines refinement approach with three chunks in each FFD sub-cube. He stressed that a parallelepipedically shaped FFD box does not provide flexible deformation for complex shapes, proposing

the modified "EFFD" method that allows the FFD box to take any arbitrary shape as well as composite lattices.

In 1992, Hsu, Hughes and Kaufmann [12] noted that some shapes are not generated in an intuitive way. Within an optimisation context, this could be a problem since it relates to the bounds of each variable (control point) so that a novel geometry can be attained. In their proposal the FFD equations are solved inversely. With the new position of a surface point is defined, the required control points' positions are updated. Such an approach leads to an undetermined system (since infinite combinations of control point movements can set the point to the exact location), but the accepted solution is the one related to the minimum least square error. Of course, such a method cannot be used in this interactive way inside the framework of an automatic optimisation loop⁷. However, this inverse characteristic could be used to determine the bounds of the design variables given the desired deformed geometrical extremes.

H.J. Lamousin and W.N. Waggenspack, Jr. [13] also recognised that FFD lattices should not be uniform proposing a new procedure. This is an extension of the EFFD approach into more general shapes based on NURBS. Their approach requires from the user to select a set of points, topology (say mesh elements) to model the embedding object.

Samareh [14] applied FFD for Aerodynamic Shape Optimisation (ASO). He outlined various methods of geometry parameterisation and their attributes, focusing on CAD methods Feature Based Solid Modelling (FBSM tools) and the FFD approach. The incompatibility of CAD approaches with gradient based optimisers is noted, as in FBSM it is difficult to compute grid point sensitivities to design vectors. On the other hand, FFD was found to be appropriate for the conceptual/preliminary design stage with a defined topology and for not excessive changes required.

Another popular method is the *Class Shape Transformation* (CST) proposed by B.M. Kulfan [15, 16] and J.E Bussoletti of Boeing Commercial airplane group. It is a method specifically developed for aerospace applications (e.g. airfoils, wings, cowlings, fairings etc.) with the distinctive characteristic of distinguishing the shape of interest in thematic parts. For example, an airfoil is divided in an upper and lower section, leading edge (LE) section, aft section and trailing edge (TE) thickness; and described using different class functions and respectively grouped design variables, superimposed to create the complete expression of the upper and lower section. This method and its improvement [17] are highly flexible within its aerospace application region, as it can transcend families of airfoils or have increased control inside an airfoil family. Depending on the application however, (as in the present work), novel geometries might also be of interest, raising a doubt regarding its potential in such cases.

As a final note on aerospace design parameterisation, standardized geometrical concepts and variables like span, surface area, twist, sweep etc., can be used as a design vari-

⁷In fact, it can potentially be used in the emerging field of interactive optimisation

able. However, although intuitive and widely used in specific areas of the industry, these methods severely limit the scope of the designs. In order to unconstrainedly explore the design space for new and potentially novel configurations, one should deviate from the secure but restricting use of these concepts and use surface geometric representation in a purer form, as the one described in this section.

For a brief but informative overview of the geometry parameterisation methods, the interested reader is referenced to the review paper of Samareh [18]. In this work, shape parameterisation techniques especially for MDO purposes are being discussed and the special needs of Multidisciplinary Shape Optimisation (MSO) and Computational Structural Mechanics (CSM) are pointed out. The introduction of more disciplines (e.g. structures) creates extra numerical setup requirements to the optimisation procedure. An example of this is the case where the OML geometry is connected to the inner structural geometry of a wing and so do the grids (further details are provided in the next section). For a more thorough presentation as well as comparisons on the assets and the results produced by the various methods, [19–23] are suggested.

Taking into account the above, and considering the complex 3D design cases associated with MDO, it is evident that our attention should be focused in the FFD or CST method. The Hicks-Henne bump function method is not appropriate since the FFD and CST methods are more intuitive and flexible while providing the necessary smoothness. FFD's deviation from the standard concepts of aerodynamic design (contrasting to CST), allows novel design exploration. Novel geometry exploration is therefore assisted by the generality of the approach and in a sense it is suitable for both local and global exploration.

During this thesis, the FFD method was used for the geometric parameterisation. Another important attribute of the method is its applicability in computational grids. As discussed in the next section, for complex 3D aerodynamic models, the parameterisation of the geometry alone is not sufficient since it would demand the costly regeneration of the computational mesh. FFD can parameterise the changes of both the geometry and the grid, and this is the way it is being used throughout the computationally expensive cases of the present work (e.g. Chapter 7). FFD is an extensively used concept that has shown its appropriateness for a conventional transport aircraft as well as a supersonic platform [24] design. Ronzheimer [25] has used it for simple airfoil cases, unconventional geometries (VELA), as well as MDO wing geometries (CFD/CSM) displaying its potential to handle aerodynamics and structure deformations simultaneously. The concept of the initial geometry being parameterised based on deformation rather than on geometric building blocks, is sensible since it resembles the design procedure. Concurrently, as Samareh [18] points out, it reduces the number of required shape design variables and provides good flexibility without lacking in conciseness. The changes due to a control point movement also have a "design meaning" since they directly provide qualitative information on what changes are more beneficial for the design.

2.3.2 Mesh (Re)generation and Deformation

In aerodynamics simulations (CFD) where numerical methods are required to solve a discretised set of equations, a computational grid is generated around the geometry⁸. During the optimisation process a geometry is analysed (assessed), followed by the description of a new geometry which in turn should be analysed again and so on. This pattern requires the consecutive use of computational grids around the updated geometry to conduct the disciplinary analyses. The simplest approach in order to tackle this requirement is simply to regenerate the grid for every new geometry. However, this is not always an efficient strategy since generating a grid is computationally expensive especially in complex 3D geometries [27], as well as being a potential source of inconsistency due to topology and connectivity changes.

Grids are categorized into structured and unstructured types, and similarly, grid deformation methods for structured and unstructured grids have been developed [18].

Structured Grids

For structured grids, interpolation has been extensively used. Gaitonde's [28] framework involves a transfinite interpolation (TFI) for which the effect that type blending functions have on the quality of the grid is displayed. Soni's [29] blending function based on arc length, proved to be robust and effective for regeneration or deformation of grids. Jones and Samareh [30] extended Soni's approach for cases where multiblock grids have to be regenerated or deformed. Hartwich [31] used a slave-master concept to semi-automate the grid generation process and a Gaussian distribution function to preserve the integrity of the grids.

Moigne [32] used a flexible grid approach for an adjoint-based optimisation framework where the inner cells are deformed along the grid lines that start from the geometry and end to the boundary (see Fig.2.9). Attenuation is used to diffuse the nodes' displacement across the grid lines. This is calculated based on the "arc length position of the nodes across the grid line" and is necessary to establish zero node displacements in the boundaries.

More recently, Kenway and Martins [33] used the linear elasticity method within a wing optimisation study. In fact, a blend of a linear elasticity method and an algebraic method was used to deform the grid in the best possible quality. Every mesh edge was replaced with a spring constant, inversely proportional to its length. In the algebraic warping, the initial original distribution of interior points was used, which although fast, was not robust especially for rotational deformations (see Fig.2.10). Also, this created problems in blocked mesh since perturbations were attenuated only inside the block. To avoid poor quality,

⁸Here, the focus is not on the mathematics and practices of this scientific art. For an overview of the theory behind mesh generation see [26]

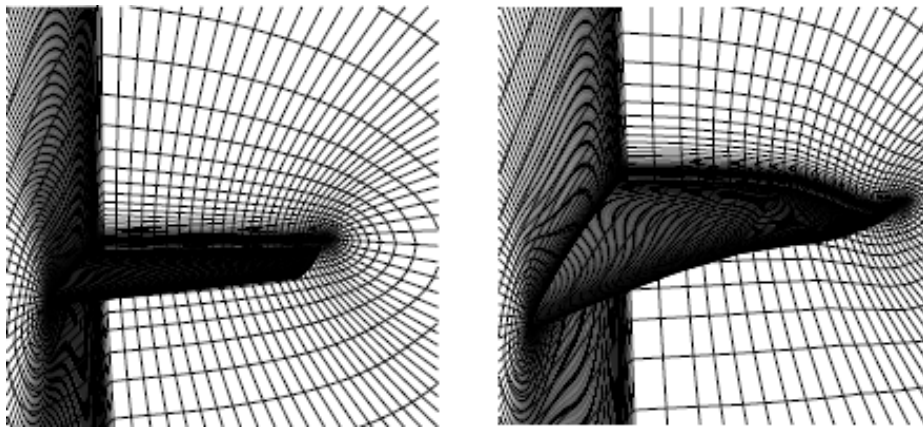


Figure 2.9: Original and Deformed grid around a wing [32].

the farfield boundaries had to be extended (which may be difficult or costly in complex geometries).

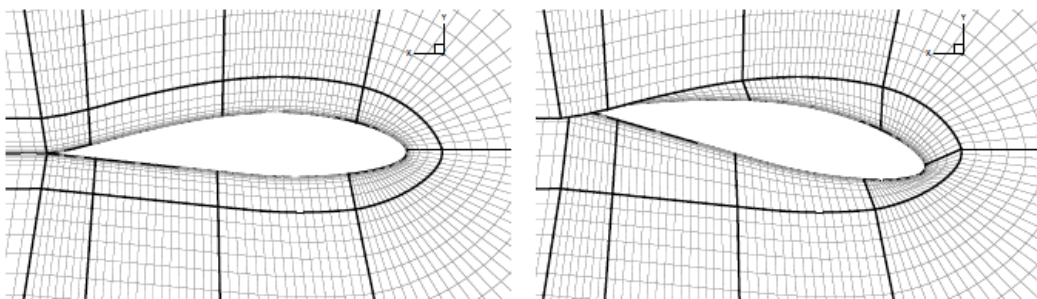


Figure 2.10: Grid becomes invalid when algebraic warping is used for large rotational deformations [33].

The linear elasticity approach can lead to a good quality deformed grids even for large deformations, however it comes with a high computational cost. With a hybrid scheme, a linear elasticity-based scheme is employed for coarse grids, handling the low-frequency perturbations while algebraic warping is used for small, high-frequency perturbations. This allows high quality grids with reduced computational expenses.

Unstructured Grids

Before proceeding further to these methods, let us first point out that the FFD parameterisation method discussed in the previous section can be also used to deform grids in a way similar to its application on geometries. Furthermore, it is insensitive to grid topology and can be used for both structured and unstructured methods with the same formulation.

For unstructured grids, a large number of concepts have been proposed, mostly based on physics-inspired concepts like the spring analogy, linear elasticity, stiffness tension models, even methods based on heat conduction.

To avoid a costly regeneration of 3D grids, Botkin [34] performed a local regridding for specific edges and faces depending on the design variables that change their value. Farhat and Lin [35], used a moving reference frame that was attached to selected nodes, in order to perform transient and aeroelastic problems⁹ (more on the aeroelastic problems' requirements in a following section). Another approach uses the concept of linear springs [36, 37] to model the nodes movement providing a pseudo-stiffness to the grid. The method was displayed in an aerolastic application for the standard AGARD wing 445.6. Although a promising idea, in fine meshes this can result in significant grid deformations after a few flow and grid iterations, often causing convergence issues. This was due to nodes being moved and placed very close after the grid deformation iterations. As a result, high levels of skewness — or even negative volumes — would exist causing numerical instabilities. Cell size has to be minimized dictating a significant decrease of time step (through CFL condition).

Degand et al. followed a different approach, paralleling grid deformation to torsional spring deformations [38]. This skips the invalid deformations due to crossovers of points through cell edges and the method was later extended to 3D [39]. Although slightly more complicated (triangle faces were used inside the tetra cell), nodes avoided crossover with tetra faces. A similar method for 2D as well as 3D cases was developed by Murayama et al. [40].

Similarly, Xia [41] applied a stiffness tension model that uses the cell volume to avoid the generation of negative volumes, an approach which proved to be efficient and robust. Nielsen [42] improved the robustness of the spring analogy methods by proposing a method based on modified linear elasticity theory. Later, in 2009 Dwight [43] developed his own version of the linear elasticity method with both cases tested showing robustness potential.

Like Degand et al, Crumpton and Giles [44] followed the physical phenomena analogy to model grid deformation. Instead of springs, they used the heat conduction equation. Information regarding cell volume "stiffness" was provided in the form of the k conduction coefficient.

Liu et al. [45] employed the Delaunay graph mapping technique. This proved to be less computationally expensive and more effective than the spring analogy approaches method.

Following a different path, Beckert and Wendland [46] employed the concept of meta-modelling to appropriately deform unstructured meshes. Specifically, they used RBF for Fluid Structure Interaction (FSI) problems, as the method can be extended to tackle the volume deformation requirements arising from aerostructural optimisation (see section 2.10.2). A de Boer et al. [47] also used an RBF-based deformation technique which was not computationally expensive while not requiring grid connectivity information as well. Fundamental information on RBF models is provided in a following section within surrogate modelling context.

⁹Aeroelastic computations have essentially the same grid needs with MDO optimisation that concerns aerodynamics and structures.

2.3.3 Sampling

As a means of reducing the computational expenses associated with costly analyses, a family of optimisation or data learning methodologies construct analytical functions (meta-models) which model the outcome of the analyses for a given design. To create an initial model of the function of interest, we first need to compute this function in a set of points in the design space, called *Training Data* (TD). Sampling¹⁰, is the statistical discipline of determining the locations of points in the design space that are most appropriate for the initial construction of the surrogate model. The quality of the model generated is directly dependent on the training data. Hence, the goal of the sampling process is to provide the basis for an optimum quality surrogate, while keeping the required number of analyses at minimum.

Due to the deterministic character of computational experiments, sampling for optimisation differs from traditional design of experiments [48]. A typical example of this difference is avoiding to sample in the design space boundaries. A problem arises from the use of computational experiments within an optimisation problem is the treatment of constraints. The difficulty here is caused by our inability to know the non-feasible design space areas a-priori. As it will be seen in Chapter 3 however, this does not really obstruct the optimisation process, since training data in infeasible regions provide feedback as to where these regions are on the design space.

Sampling plans often use a criterion to assess how well the distribution of points is performed. Optimising this criterion results to a set of initial data distributed in a way to provide the maximum amount of information out of a given number of sampling points. Over the years, many sampling methods have been developed, or adjusted from classical Design of Experiments (DoE). Some of the most popular include *Monte Carlo*, *Sobol* [49], *Latin Hypercube Sampling* (LHS), *Orthogonal Arrays* and *Minimum discrepancy methods*

Fang et al. [50] provide a review of Uniform methods comparing LHS with the uniform design (UD) approach. In LHS, the points are randomly located in the vicinity of the bin while in UD, the training data are deterministically located (in the center). The points can be also defined in the nodes, as showed on the right part of Fig.2.11. Both methods are equivalent in a discrete design space. The *Orthogonal Arrays* (OA) method can be considered as a generalisation of the LHS methods. In [51], Tang combines the LHS methods with the advantages of OA.

Sampling can either be a one-shot or a stagewise process, known as Bayesian learning process. In the former, all training data result from a single Sampling process in the start of the optimisation. The trained surrogate model is then used to locate the optimum design. In a stagewise (or adaptive) sampling process, well defined criteria are used to introduce new training points in stages. In this manner, information is enriched by the feedback acquired

¹⁰The word "Sampling" is more commonly found in computational literature than Design of Computational Experiments.

during the optimisation process.

Liem et al. [52] argue that an adaptive sampling plan is more effective to adequately approximate the design space, especially in cases where the number of required training data is not known. Following a Bayesian method, they identified sample points using Halton [53, 54] sampling, based on exploration criteria. In [55], Nair et al. used adaptive sampling in conjunction with LHS. Following the initial training of the metamodel using small numbers of TD, LHS was used to provide a longer set of TD. For each point, the posterior prediction variance based on the initial surrogate was calculated.

The potential of adaptive sampling plans is displayed in [56] where a Bayesian approach is used with Infill Sampling Criteria (ISC) to detect the new TD. Although more complex and costly since it requires an optimisation (suboptimisation process) for every new input value, it is shown that it is overall more efficient than a single stage sampling plan.

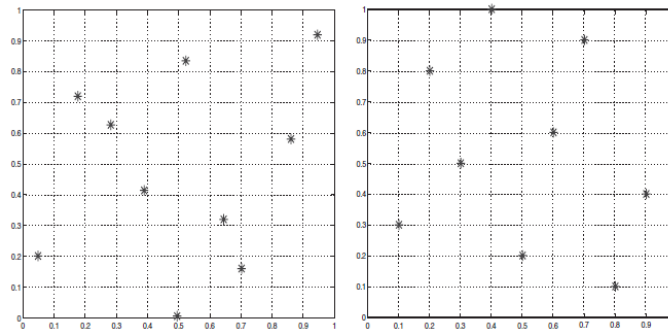


Figure 2.11: Standard LHS and LHS using a metric. In the second case the location of the point in the bin is predefined [57].

It can be concluded that the requirements of an efficient sampling process to train a metamodel through the whole design space (global surrogate), include uniformity, space filling characteristics and low computational cost¹¹ (low number of training data points).

Introduced by McKay, Beckman and Conover [58] as a new way to produce uniform training data, LHS has shown to be very efficient in disciplines that desire global data learning elements. To increase uniformity, metrics were introduced spawning several adaptations. One of the most popular metrics comes from Johnson [59] which uses the concept of Minimax and Maximin designs (Mm). In this approach the minimum distance between points is maximised. Later, Morris and Mitchell [60] proposed a new metric for LHS plans arguing that the classic maximin (Mm) metric of Johnson is not robust in special cases.

Currin et al. [61] assessed the LHS method in a Bayesian framework using the cross validation and maximum likelihood approach (see section 2.3.5) confirming its uniformity characteristics.

¹¹In terms of space filling and uniformity characteristics, the full factorial approach is optimum solution, however, the associated cost makes this approach extremely costly.

Since training data feed the surrogate models, it is interesting to examine how sampling plans interact with different metamodelling techniques. Such an investigation for various sampling methods and surrogate models was performed by Simpson and Lin [62]. The interaction between the sampling method and the number of training data was also examined.

The efficiency of the surrogate models is increased when adaptive sampling is employed. Therefore, although important for the initial stages of the optimisation, ultimately the initial sampling is not critical for its success.

2.3.4 Variable Screening

A large number of design variables allows a wider and more flexible optimisation problem. However, the process is negatively affected by what is generally referred to as a *curse of dimensionality*. High dimensionality leads to an increase in computational expenses occurring from increased sampling analyses requirements, surrogate model training costs and the optimisation exploration procedure (with the notable exception of adjoint based gradient algorithm optimisers). It also increases the multimodality of the problem, implicitly deteriorating the metamodel's efficiency. Therefore, reducing the dimensionality has a significantly positive impact on the optimisation framework. The groups of methods aiming in this is referred to as screening. Effective screening however is challenging in a complex and multimodal design space as the effect of the design variables might not be obvious. Screening methods differ in the assumptions used regarding the input-output relation and number of design variables as shown in Fig.2.12. The screening method should be effective in identifying dominant variables as well as being robust to metamodel techniques and design space characteristics.

The most common screening methods proposed, include *Group screening* [73], *One factor at a time designs* [74] (OAT), *Fractional factorial design, Elementary Effects* [64, 65], *Iterated Fractional Factorial Designs* (IFFD) [66], *Edge design* [67], *Sequential Bifurcation* [68] and its extensions [69, 70], *Screening via analysis of variance and visualisation* [71]. A method using partial derivatives has also been introduced [64] to identify the importance of the variables. In 2006, Schonlay and Welch [71] presented their approach which is based on Gaussian approximation to model the input-output relationship of the function. Goldsman and Nelson [72] and Kleijnen [73] provide an overview of the Screening and Selection Procedure methods (SSPs) and the Multiple-Comparison Procedures (MCPs).

Building on the concept of screening, that is the progressive identification of the dominant design variables and the subsequent drop of the inactive ones, a review on the works of Constanine et al., J. Alonso, F. Palacios, T.W. Lukaczyk on the topic of Active Subspaces was conducted. This interesting concept is well presented in [75] and an extension of it is proposed in [76]. Its distinctive feature is that it does not depend on providing information on the importance of each separate design direction as other screening approaches do to reduce the dimensionality. Design space dimensionality is reduced by identifying lin-

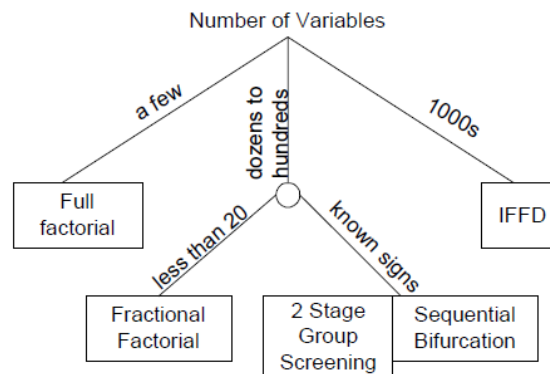


Figure 2.12: Appropriate choice of screening method is dependent on the number of design variables [74].

ear combinations of more than one basis vectors in the design space (active subspaces), in which the objective function shows significant variations, thus resulting to new non basis vector — linearly dependent on the fundamental design directions. Therefore, the basis axes do not correspond to a single design variable anymore. They form a new basis of reduced dimensionality, at which each basis vector corresponds to a linear combination of the initial basis. The initial design variables values are therefore "changing together". A recent application of this method can be found in [77].

2.3.5 Metamodelling Techniques

The use of models of reduced complexity and surrogate modelling in engineering optimisation dates back at least to 1974 and the work of Schmit et al [78] in structural optimisation. As discussed earlier, with the sampling complete, the data can be used to train the metamodel [63], This is essentially nothing but performing an interpolation or regression through the training data to allow a cheap estimation of the objective function and the constraints for any point in the design space.

Based on their collaboration with the initial sampling and potential bayesian surrogate update process, metamodels can be categorized into *global* or *local*, according to the region of validity on the design space. A global model is generated using a space filling sampling technique, covering the whole design space with reasonable accuracy. In the local approach, training data are generated in the vicinity of the datum geometry with the accuracy of the model there being higher but to a limited region extend and improving only across the optimisation direction path through infill data.

Note how this distinction refers to the DoE-Surrogate-Update plan and not the model alone. The choice of a global or local approach of course depends on the aims of the designer as well as the chosen optimiser. The metamodel training costs is another factor that affects the choice of metamodelling plan especially in the case where frequent updates

are performed.

In turn, the metamodelling plan involves the choice of interpolating or fitting the data. When surrogate models are used in conjunction with physical experiments and traditional DoE methods, random error and noise (due to experimental uncertainties) is introduced in the sampling data. However, the majority of computational analyses (as the ones used in optimisation) are deterministic. Hence, even when error is present (e.g. physical modelling error), this is consistent in all analyses performed during the optimisation process, which within this scope are considered to be accurate. Therefore, surrogate based calculations should reproduce the data and as such, interpolation methods are better suited for optimisation purposes.

The surrogates can also be divided into black box and physics based approximations. The former do not require any physics related information, only the set of data. They are easier to use, exhibiting a broader scope of application knowledge of the governing equations of the analysis problems.

The most common surrogate modelling approaches used in engineering problems are *Response Surface Models* (RSM) and *Polynomial Regression, Radial Basis Functions* (RBF), *Support Vector Regression* (SVR) and *Kriging*. RSM and RBF methods fall in the category of generalized linear metamodelling, since they use a linear summation of functions.

The factors that dictate the choice of the surrogate are its flexibility to capture the desired function, computational cost, ability to provide information regarding important parameters¹² or any other extra information.

Flexibility usually comes with the price of computational cost but it may overall be advantageous over a model which although cheaper, fails to capture the important aspects of the desired function.

Although RSM has perhaps been the most extensively used [79] approach in engineering, nowadays its use is limited since it lacks the flexibility of other methods. Also, if high order polynomials are used to increase its flexibility, it becomes unstable. It is also important to state that this method, being a regression, may experience problems in modelling deterministic functions, as mentioned by Sacks [48].

Moving Least Squares

The Moving Least Squares (MLS) method could be considered as an extension of a polynomial regression or interpolation. The novelty of this concept is that it allows the definition of various levels of importance in the training data, for the calculation of the polynomial coefficients. Hence, each sampling point has a weighting factor (e.g. if $w_i = 0$ then the i^{th}

¹²It can be essentially used as a screening method as well.

point has zero effect on the surrogate model generation [80].

Radial Basis Functions

The main characteristic of this method is the basis function (kernel) which is expressed as function of the euclidean distance between the design points,

$$\phi = \phi(\|\mathbf{x} - \mathbf{x}_c\|) \quad (2.3.2)$$

where \mathbf{x}_c is the center of the basis function around which the radially symmetric function is imposed. Hence, \mathbf{x}_c are the sampled positions in the design space. For N training data points, the surrogate function has the form,

$$\hat{y} = \sum_{i=1}^N \alpha_i \phi(\|\mathbf{x} - \mathbf{x}_c\|) \quad (2.3.3)$$

RBF methods can be distinguished based on the kernel function used, which among others involve,

- Linear: $\phi = \|\mathbf{x} - \mathbf{x}_c\|$
- Cubic: $\phi = \|\mathbf{x} - \mathbf{x}_c\|^3$
- Gaussian: $\phi = \exp(-\theta\|\mathbf{x} - \mathbf{x}_c\|^2)$
- Multiquadric: $\phi = \sqrt{1 + \theta\|\mathbf{x} - \mathbf{x}_c\|^2}$
- C4-Matern: $\phi = \exp(-\|\mathbf{x} - \mathbf{x}_c\|) \cdot (3 + 3\theta\|\mathbf{x} - \mathbf{x}_c\| + (\theta\|\mathbf{x} - \mathbf{x}_c\|)^2)$

The training of the RBF model refers to the evaluation of the α parameters. This is done using the training data x_j and the interpolating condition,

$$y_j = \hat{y}_j = \sum_{i=1}^N \alpha_i \phi(\|\mathbf{x}_j - \mathbf{x}_i\|) \quad (2.3.4)$$

The coefficients are calculated by solving the determined $N \times N$ system. In a matrix form this is expressed as,

$$\mathbf{\Phi} \mathbf{a} = \mathbf{y} \quad (2.3.5)$$

where Φ is called the Gram matrix.

The appropriate choice of kernels is crucial for the quality of the design space representation. For example, in [81], it is shown that multiquadric kernels produce the most accurate results on the examined problems. The condition of Eq.2.3.4 generates a symmetric Gram matrix. In order for the parameters to be determined, Gram matrix should be nonsingular and the kernel function positive definite, a condition satisfied in most cases when the Gaussian or Multiquadric kernels are used. In this case, Cholesky decomposition is the fastest way to solve Eq.2.3.5. If nonsingularity is not guaranteed, the superimposition of a polynomial term can reform the linear system so that Eq.2.3.5 can be solved.

Some of the kernel functions — like the Gaussian and Multiquadric —, feature the *shape parameter* θ . This controls the method's generalisation and smoothness by defining the domain of influence of each kernel. This parameter can be defined based on the experience of the user, the desired region of the kernel effect or can even result from an optimisation as in the work of Wang [82]. Other approaches use the *Cross validation* method¹³ (leave - k - out) as a metric to drive the θ optimisation. The use of optimisation and cross validation significantly increase the computational cost.

Although Eq.2.3.4 dictates an interpolation through the training data, the method can also perform a regression if the dataset is noisy. In this case, Eq.2.3.5 is transformed into,

$$(\Phi + \lambda \mathbf{I})\mathbf{a} = \mathbf{y} \quad (2.3.6)$$

where the regularisation parameter λ controls the distance between the "real" value and the one provided by the surrogate. RBF is a cheap method, however it is still affected by dimensionality as well as the size of the training data set.

The accuracy of the method can be improved if the interpolating condition of Eq.2.3.4 is augmented with data defining the slope of the function (that is, the "trend" of the function in the vicinity of the data), as in the Hermitian RBF (see Fig.2.13). For N training data and P design variables Eq.2.3.4 becomes,

$$y_j = \hat{y}_j = \sum_{i=1}^N a_i \phi(\|\mathbf{x}_j - \mathbf{x}_i\|) + \sum_{i=1}^N \sum_{j=1}^P a_i a_j \frac{\partial \phi(\|\mathbf{x}_j - \mathbf{x}_i\|)}{\partial x_j} \quad (2.3.7)$$

Now the system unknowns are $N(P + 1)$ requiring the inclusion of the gradient conditions to become determined.

$$\nabla y_i = \nabla \hat{y} \quad (2.3.8)$$

Of course, the computational cost for generating this model is increased due to cost relating to the gradient computation. If an efficient method for computing the objective

¹³This is defined in section 2.3.5

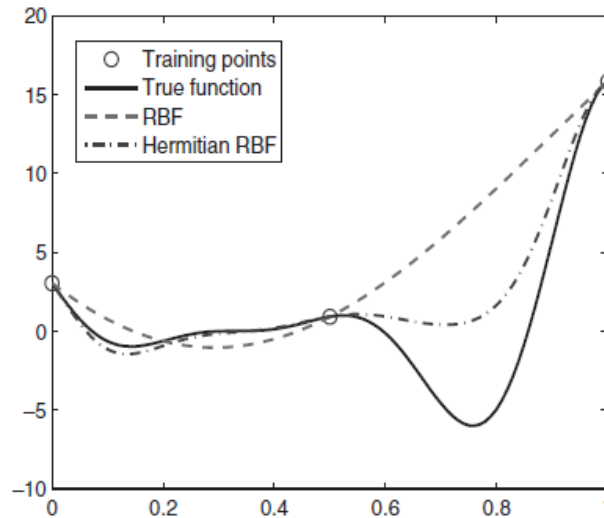


Figure 2.13: Standard RBF and Hermitian RBF [57]. Notice how the addition of extra information (gradient) improves the function approximation.

function sensitivity is available (like Automatic Differentiation or Adjoint analysis), then this cost penalty is minimised. In a similar manner 2^{nd} order derivative information can be provided. However, a Hessian matrix is usually very costly to calculate and as such, it is more efficient to invest the computational budget in function evaluations instead. Gradient information can be introduced to other metamodeling techniques as well. Examples include the Gradient Enhanced Kriging (GEK) and the polynomial regression method shown by van Keulen [83].

Mullur and Messac [84] reasoned that since the RBF method is uniquely defined by an algebraic system solution, its flexibility and freedom is reduced, not allowing the designer to impose his own requirements. In their Extended-RBF method (E-RBF), they superimposed a summation of non-radial basis functions in Eq.2.3.3, using the difference in coordinate distance instead of the euclidean distance. Extra parameters are introduced, making the algebraic undetermined. In this case, an optimisation process is required to estimate the parameters.

Finally, an important consideration when using RBF is the issue of the numerical stability of the RBF model, as a function of the shape parameter. The works of M. Mongillo [85] and B. Fornberg et al. [86] provide excellent companions for such a study. A direct impact of these numerical examinations is the implementation of the Matérn functions in the RBF models as well as a concise shape parameter formulation to match their approach¹⁴.

¹⁴In fact, their findings were observed in my own work, as well as the lowest shape parameter values that would not induce instabilities.

Support Vector Regression

The Support Vector Regression (SVR) is a special case of the Support Vector Machine (SVM) technique by Vapnik [87]. It is an interesting method that performs regression which can be adjusted and used accordingly. The unique feature is that it allows the definition of a range in which the sampling data are trusted without affecting the SVR prediction (see Fig.2.14). This is particularly useful when a random error element or computational noise are present (i.e. oscillatory convergence and problems in data accuracy in general). The points that lie between the surrogate hypersurface and the predefined range are ignored and only the training data laying outside this range are used (the support vectors). For more information on the method, the reader is referenced to [87] and [88].

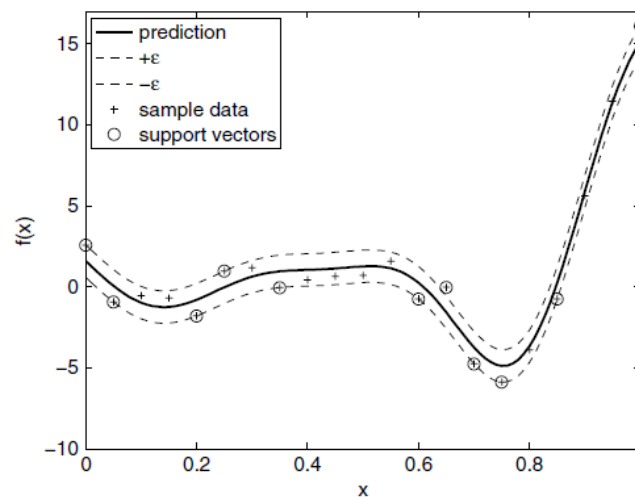


Figure 2.14: Support vector regression [57].

Kriging

The (Ordinary) Kriging method (also referred to as Gaussian Process Interpolation/Regression), is a more complex and flexible approach than the standard RBF. Its engineering use originates from a paper by Sacks [48] and it has been quite popular since, as it provides a higher accuracy as well as an estimation of the error of the model itself. Its founding idea is that training data are a "realisation of a stochastic process" [57] and that the model generated, is the one most likely to have produced the training data results. It uses a Gaussian assumption to estimate the correlation between training data based on their euclidean distance, similarly to Gaussian kernel-based RBF. Contrary to standard RBF however, Kriging requires an optimisation to fine-tune the smoothness and shape parameters (referred to as hyperparameters), a process that increases the cost of the method. The value of the shape parameter θ (defined as in the RBF kernels) provides information on the correlation between training data points for each dimension and as such, on high "active" the respective design variable is. Therefore, the θ value can potentially be exploited for screening method as well.

In the case of a noisy design space (due to discretisation error or oscillatory convergence), a modification similar to regressive RBF can be formulated, by using a regression constant λ ¹⁵.

Following the development and use of Kriging in engineering problems, several modifications have been proposed. The *Universal Kriging* [89] is similar to the Ordinary Kriging but no longer treats the mean value parameter as constant across the design space. This allows to capture trends in the data with higher accuracy. In practice though, knowledge of these trends are not usually known a priori. To improve over the drawbacks of Universal Kriging, the *Blind Kriging* (BK) was proposed by Joseph [90] as a direct modification over the former. Another variant is the *Detrended Kriging* (DK). This is a linear regression model which is combined with Ordinary Kriging.

Martin and Simpson [91] compare Ordinary Kriging, Universal Kriging and Detrended Kriging in cases (ranging from 1D to 5D), using *Maximum Likelihood Estimation* (MLE) and *Cross Validation* as metrics to trim the hyperparameters. In the high dimensionality case, the Ordinary Kriging was proven to be the most efficient.

Simpson et al. [92] present the difficulties of using Kriging in global MDO by using the aerospike nozzle of the venture star X-33 shuttle, which is described by three design variables, and a 25 points orthogonal array sampling plan.

Kriging is perhaps the most expensive metamodelling technique due to its hyperparameters tuning requirements. Toal, Bressloff and Keane [93] examined the effect of five Kriging tuning in redesigning a RAE2822 pressure distribution from a NACA0015 airfoil, also showing Kriging's complexity and its dependence with problem dimensionality. The latter proved to be of major importance when choosing the optimum tuning strategy. Increasing the number of design variables allows for a potentially better design but over a critical number of dimensions, the problem gets too complex to be efficiently explored with the given computational budget.

Jin et al. [94] performed an extensive metamodelling comparison using five different criteria and fourteen test cases categorized based on dimensionality, linearity as well as noisy and smooth behaviour. It was evident that in overall performance, RBF and Kriging were superior to the other models. RBF showed optimum accuracy and robustness characteristics with the problem scaling having little impact on the model. For large sampling cases, Kriging performed slightly better than RBF, with RBF however being more robust.

¹⁵This might be critical for the success of the optimisation algorithm because when smoothing the design space the optimiser is less likely to stuck in a noise induced local minimum.

Physics Based Approximations: Scaling and Reduced Basis Methods

All methods discussed until this point did not assume or require any physical information, using the data as black box results. If the disciplinary analysis source code is available, one can access any physics related information. In such cases, the models generated can either use physics information to predict the objective function or directly approximate the physics involved. However, the necessity of source code access and the fact that each approximation method is tailored only to a specific analysis code limits the operational range of this approach. A simple way to exploit physical information is to use the concept of *scaling* [95], that can be improved by the inclusion of 1st and even 2nd order information.

Another physics based approximation approach includes the family of the Reduced Basis Methods for linear and nonlinear problems. Here, the generated surrogate model approximates the field variables (i.e. pressure) instead of the objective function. This approach can be very computationally efficient, also showing global characteristics due to the satisfaction of the governing equations. Many formulations have been developed and typical applications relative to this PhD thesis include structures [96] and aerodynamics [97].

Partitioning of Surrogate models: Mixture of Experts

The potential gains of using multiple surrogates within the same single design space is explored by the concept of *partitioning* and *Mixture of Experts* [98] (MOE). The basis behind these methods is that by splitting the design space into subspaces, each associated with the respective metamodel, a more robust and detailed description of the design space can be attained compared to a single global model. Masoudnia and Ebrahimpour [99] provide an overview of the basics of the method. The two main ideas are *Combination*, where a formulation incorporates information from all surrogate models, and *Selection*, where assessment criteria are used to select the most appropriate metamodel for each subspace region. In the latter approach, N subspaces are stochastically partitioned, trained by different metamodels. The major requirements are: the choice of the surrogates, the *Gating function* that splits the data appropriately, and a *Probabilistic model* to combine the experts and gating functions. The methods for combining the outputs of the experts can be *Non-Trainable* or *Trainable*.

The categorisation of the various MOE methods is based on the partitioning strategy. Depending on the model training algorithm, the method is split into *Mixture of Implicitly Localised Experts* (MILE) and *Mixture of Explicitly Localised Experts* (MELE) [99].

In [52], Liam, Mader and Martins propose the partition of design space in multiple subspaces that use GEK, Universal Kriging and RBF techniques. The partitioning they are using employs clustering algorithms from [100], performing local expert training in each subregion. The method is applied for a mission optimisation based on a Boeing 777

wing. The mixture of two GEK models was more accurate than the respective mixture of Kriging, while the global approach and the exploration sampling for GEK and Kriging could not converge.

Metamodelling Assessment Methods

Martin and Simpson [91] define two characteristics that a surrogate model should possess: ability to reproduce the data and to approximate. Quantifying model efficiency is beneficial for its improvement, through its parameters tuning and most appropriate method selection. In analytical test cases this is examined by direct comparison with the true function in the form of Maximum Error and Root Mean Squared Error (RMSE) etc. However, in real design problems this cannot be performed due to the cost of calculating the objective function. The appropriate assessment methods depends on the surrogate approach. For example, methods like RMSE are based on the deviation between the function value and the surrogate prediction in the training data points. This is an efficient approach for regression metamodelling but it cannot be used when interpolation is performed, since by definition the function values and the surrogate values are identical in the training data. In these cases the cross validation/leave- k -out method may be an effective choice. Given N training data points, q equal subsets are generated, each involving $N - k$ data (k random points are removed). The model is then the surrogate generated and the resulting values in the positions of the k data points are calculated, allowing the quantification of its accuracy. A special case of cross validation is when $k = 1$. In this case, the method is called "leave-one-out".

The efficiency of metamodelling assessment methods for various potential metamodelling, was studied by Meckesheimer et al. [101]. They examine how well various assessment techniques perform on Kriging, RBF and Low-Order polynomials (LOP). The leave-one-out method was found to be more effective for RBF and LOP, also showing lower computational cost.

2.4 Surrogate Based Optimisation

Following its training, the metamodel is used to guide the optimisation process. However, after the initial sampling, the surrogate model is not accurate enough to support an optimisation procedure towards the true optimum¹⁶. Hence, it needs to be updated and improved while simultaneously guiding the process. Surrogate Based Optimisation (SBO) methods, use adaptive bayesian sampling techniques to accomplish this goal [102]. The process of sampling a new point is referred to as infill process. The infill sampling defines how to update the metamodel and which infill design point should be used. Analysis is then per-

¹⁶Unless an excessive number of sampling points is used. But this is never the case in real industrial plans.

formed on this point, sampling is performed and the surrogate is updated as shown in the example of Fig.2.15. Through an SBO methodology our goal is to: improve the meta-model accuracy — and consequently our confidence to the point found as optimum —, while simultaneously guide the optimisation process.

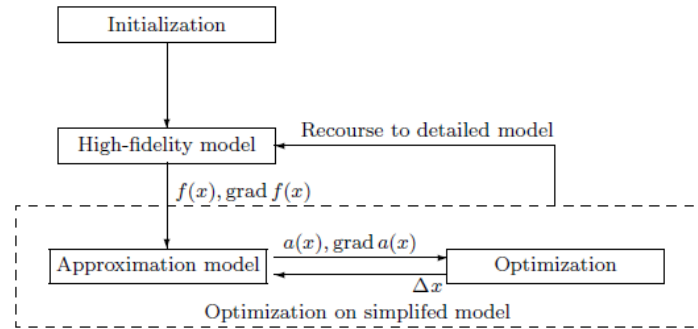


Figure 2.15: Overview of a typical optimisation using surrogate models [103]. The true problem f is solved by creating the approximate model a , into which optimisation is performed. The true function is called again in order to update and improve the validity of the surrogate.

Overall, the methods to manage surrogate models for optimisation purposes can be categorized as follows:

- **Exploitation Methods:** These approaches take advantage of the metamodels to locally improve their accuracy. The improvement of the models is only performed along the path of the optimisation process. Hence, these approaches lead to a local minimum.
- **Exploration Methods:** Here, computational effort is put to improve the global accuracy of the metamodel. With the surrogate considered globally accurate, the optimiser is used to explore the design space and provide global optimality.
- **Balanced Exploitation/Exploration:** A balance between the two aforementioned approaches is sought.

Jones [104] provides a great review of seven different methods of using surrogate models within an optimisation process. The methods are categorized based on the type of the metamodel (interpolation/regression), the approach (one/two stage) and the ability to reach the global optimum region. Popular approaches include the *Trust Region* (TR), *Statistical Lower Bound* (SLB), *Expected Improvement* (EI), *Probability of Improvement* (PI) and *Goal Seeking* methods. Out of these, a quick review of the TR and EI methods is provided, as they are more relevant and representative of the concept for local and global optimisation respectively, as well as more promising within the scope and goals of the present work.

Trust Region Approach

The Trust Region method applied within an infill strategy originates from nonlinear programming [105]. Here, the surrogate model is generated only within a limited region (around the current design point) in which it is trusted to be accurate. The original TR method provided a strictly defined estimator of how well a quadratic Taylor series approximates the function of interest. In SBO context, more complex approximation techniques such as RBF or Kriging are used without discarding nevertheless, the main concept of the method. The surrogate model predictor s is minimised within a bounded region defined by the euclidean distance $\|\mathbf{a}\|$, around the current suboptimisation starting point \mathbf{x} .

$$\min_{\mathbf{x} \in \mathbb{D}} y(\mathbf{x} + \mathbf{t}) \quad (2.4.1)$$

which is bounded by,

$$\|\mathbf{s}\| \leq \delta_k \quad (2.4.2)$$

In this, δ_k refers to the trust region hyper-radius and so for the current iteration k , the model is trusted only within this area. After each infill sampling analysis, the trust region δ_k is increased if the model was accurate, shrunk if the model was inaccurate or remain unchanged in any other case. The assessment of the model is based on the difference between its prediction and the function value. The increase or decrease of the trust region, as well as the condition under which a prediction is considered to be accurate or not, is defined by coefficients set by the user. Therefore, the method is adjusted based on experience and can be tailored to the task at hand. Suggestions and more information on the method are provided by Alexandrov [103]. For a short discussion on a formulation that tackles both unconstrained and constrained problems see [57]. An implementation of the Trust Region method for variable fidelity tools, was done by Alexandrov et al. [106] and is presented in a following section.

Probability of Improvement and Expected Improvement Approach

The Kriging metamodel technique is based on a Gaussian correlation assumption between the training data, and allows the estimation of its mean squared error. By combining the function prediction with the mean squared error prediction, a series of infill sampling criteria are developed [88]. The simplest is the concept of the Statistical Lower Bound which involves the suboptimisation process,

$$\min_{\mathbf{x} \in \mathbb{D}} \hat{y}(\mathbf{x}) - k s(\mathbf{x}) \quad (2.4.3)$$

where \hat{y} is the Kriging predictor, k is a defined constant and s is the error associated

with the model. Such an approach does not lead to dense iterates and is not guaranteed to sufficiently explore the design space to lead towards the global optimum region. A way to improve this and simultaneously balance between exploration and exploitation, is provided by the Probability of Improvement. In this method, information on the uncertainty of the Kriging model is again inserted through the MSE estimation. A formulation for the probability of a potential design point in the design space to be improved [107] is developed¹⁷. The infill process is performed for the design point in which the probability of the current minimum value to be improved is maximised. In this case, dense iterations may be performed. If an improvement cannot be found following the search, then the method has the inherent attribute of exploring other regions, thus searching more globally. This is provided by the uncertainty information that steers the method to reduce it in undersampled regions. The drawback of this method is that when bad or sparse sampling is used, the method may fail. The hyperparameter values are not representative of the design space, resulting to unreliable function and error estimation, especially for deceptive functions.

Taking the PI formulation a step further, the actual expected function improvement can be estimated and thus the Expected Improvement is of interest. Under this infill criterion, the infill design point would be the one showing the potential of improving the current minimum the most (see Fig.2.16). This approach is very similar to the PI method, and their shared characteristics which are briefly stated below:

- There is no requirement for input definition regarding a desired improvement.
- The global optimum area is located without excessive exploration. However, after its determination, consecutive local searches around the current best increase make the method inefficient. In this stage, one should switch to a local method.

¹⁷More information and a complete mathematical formulation of this is presented in Chapter 3.

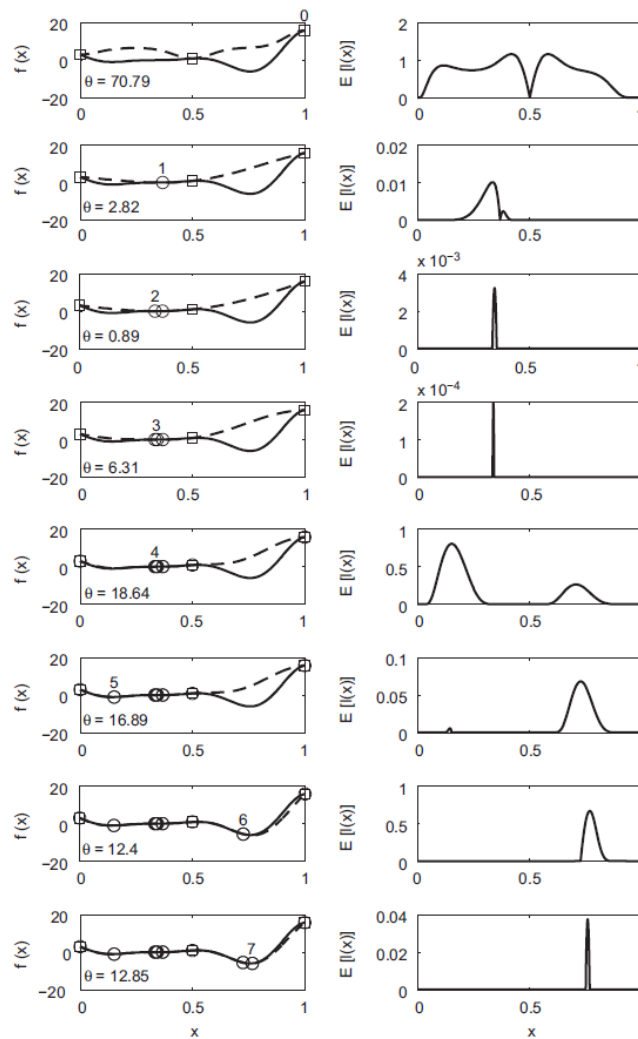


Figure 2.16: In the expected improvement (EI) criterion, the point which shows the maximum potential improvement is used as the next sampling point [107].

2.5 Using Variable Fidelity Analysis Tools

Within an optimisation process, disciplinary analysis can be performed by various numerical tools of corresponding fidelity levels [108–110]. The difference in fidelity may be the result of:

- Physical modelling approach
- Different order of discretisation in the respective numerical schemes (numerical order or grid resolution)
- Different levels of convergence [111]

The decrease in the solution accuracy is usually (but not always) followed by a reduction of computational cost¹⁸. Therefore, with the existence of MF tools, it is of our interest to examine how we can exploit them within an optimisation framework in order to reduce the high computational expenses associated with high fidelity (HF) tools. The goal is to efficiently incorporate physical information so that we achieve convergence similar to a HF optimisation, but with less computational cost.

In the MF context, it is assumed that the expensive HF result is accurate, and the cheap low fidelity (LF) method is associated to an error. Typically, the relation between the two is expressed as,

$$y_{HF} = Z_{\rho}y_{LF} + Z_d \quad (2.5.1)$$

where y_{HF} and y_{LF} are the high and low fidelity tool outputs respectively and Z_{ρ} and Z_d are factors. When $Z_{\rho} = 1$, Z_d simply expresses the error of the cheap tool for a given design point. In the case where $Z_d = 0$, Z_{ρ} expresses the ratio between the HF and LF values. The first case is probably more extensively used within the MF methods, with the LF tool error expressed as,

$$Z_d = y_{HF} - y_{LF} \quad (2.5.2)$$

In this approach, an error correction surrogate model is used to correct a LF evaluation to approximate the true function. For the training of the error model, both HF and LF data are required to define the error data set. When the error is a smooth function, good accuracy is achieved without the need for too many training data. As a result, using and correcting an LF tool is more efficient than using an HF tool and surrogate¹⁹. This data fusion method is computationally efficient especially if the LF tool is significantly cheaper than the HF one.

2.5.1 Treed Metamodelling

Nelson and Alonso [112] proposed a flexible way of using metamodels (Kriging) and MF tools. They suggest that is beneficial to use both LF and HF tools in the sampling process depending on their design space validity. In their work, HF tools are used in areas of the design space where high fidelity is required and LF analysis is used in cases where HF and LF would show similar results. A design space partitioning to allow global optimum convergence by data enrichment in the search direction is proposed. This method, called

¹⁸This occasionally creates the misunderstanding that a LF tool is one which is cheap. Although usually this is the case, the term "low fidelity" refers to the reliability of the tool, that is the confidence that we have in the results. In fact, there may be cases where a fast tool is actually of a higher reliability, so this should be termed as high fidelity. In most cases however, HF results are associated with higher computational expenses.

¹⁹In cases where the error is not a smooth function, the correction process can be expensive and inaccurate and an MF approach is not recommended.

TreedGaussianProcess (TGP), also allows a parallel training of the design subspaces. A challenge in their partitioning strategy is the lack of information required to form local Kriging models, in order to avoid discontinuities at boundaries. Their partitioned surrogates are initially updated by local infill in locations of possible extrema and as the optimisation process proceeds a more space filling infill method is used (uniform sampling, LHS, Monte Carlo etc.). The advantage of their approach is parallelisation which has a significant impact especially in higher dimensionality problems.

2.5.2 Space Mapping

Space Mapping [113] is an MF technique that follows a different approach. It does not use the predescribed data fusion technique and surrogate modelling. Instead, the LF results are being distorted so its minimum and maximum values are aligned with the respective HF results. For a more extensive review of the method see [114]. For the way of determining the space mapping function see [115]. Based on the Space Mapping approach, Bakr et al. [116] modified the method to use it in a Trust Region framework. Here, the corrected LF tool is used as a surrogate for the HF function. Another modification of the method is the global space mapping. For more information see Bandler et al. [117].

2.5.3 Multifidelity Trust Region Optimisation

In [106], Alexandrov et al. use multiple fidelity tools to guarantee that the optimum point would coincide with the one located by a pure HF optimisation process. They use a 1st order approximation and their model management optimisation (AMMO) framework illustrated in Fig.2.17. A trust region approach employs a locally accurate surrogate model, based on both LF and HF simulations.

Their linear approximation has essentially the form of a 1st order scaling method that can be summarized as a Trust Region-based use of the scaling metamodelling approach. They ensure that although the LF model does not provide the true optimum, it still provides the proper search direction. This is achieved by consistency between their 1st order surrogate model and the HF function, that is, the local trends of LF are similar to HF. The efficiency of AMMO, like in any MF methodology, depends on the ability of the LF model to predict the trends of the HF tool.

2.5.4 Co-Kriging and Multifidelity Expected Improvement Criterion

The Co-Kriging method refers to the modification of Kriging to incorporate training data of multiple fidelity. Following its training, which is more costly than Kriging due to extra hy-

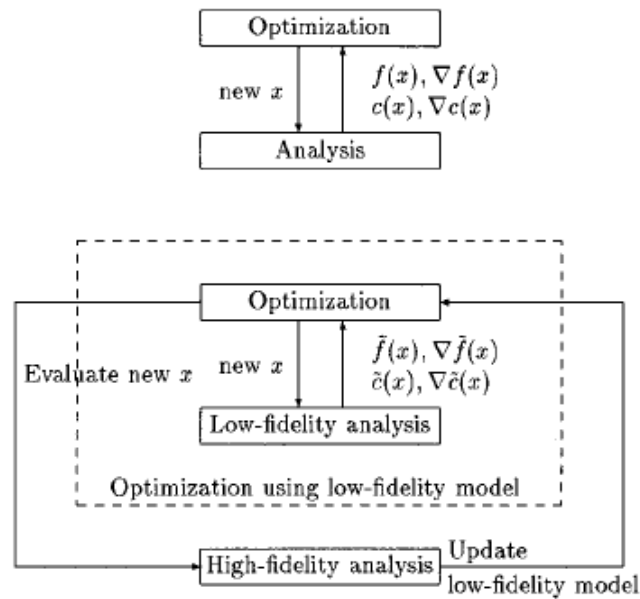


Figure 2.17: Conventional optimisation approach (top) versus MF (AMMO) approach [106].

perparameters optimisation associated with the LF tool correction, Co-Kriging can be used in a way similar to Kriging within an SBO context as reviewed by Jones [104]. An example of a Co-Kriging application is shown by Forrester [118] using the Expected Improvement approach as an infill criterion. Since the MF data involved noise, a regression Co-Kriging was used, with 2 levels of filtering (two regularisation λ diagonal constants). It is shown that using multiple levels of fidelity increased the accuracy of the optimisation results while significantly reducing computational costs. It was suggested that in case where the HF tool is too expensive, more computational expenses should be invested in the infill sampling rather than the initial sampling. Gradients can also be used to improve the accuracy around the training data [119].

Different levels of analysis convergence can also act like variable fidelity tools, as examined by Forrester et al. [111] for a NASA aerofoil test case. In this, partially converged CFD simulations are used as a LF tool and the "number of simulations and the level of convergence necessary to perform accurate optimisation" is examined. Overall it was shown that using more partially converged simulations produce a higher accuracy surrogate than using fewer fully converged simulations. The true (HF) function is approximated using the concept from Eq.2.5.1. Infill analyses use only HF simulations based on the EI criterion. A robust and accurate assessment of their surrogate model was conducted a posteriori, by comparing the surrogate predicted values with the ones obtained by the true function. The correlation coefficient r^2 by Edwards [120], spanning from 0 (no correlation) to 1 (exact match of data), was used.

Dev Rajnarayan, Alex Haas and Ilan Kroo [121] have used the Expected Improvement method within a multifidelity environment and an additive surrogate model formulation similar to the one used in this PhD work (see Chapter 3). Their application was however

limited to a single discipline and single objective aerodynamic design problem.

2.6 Constraints in Optimisation

In industrial applications, the design space is usually constrained (see an example of this in Fig.2.18). In that case, we aim at minimizing the objective function given that a design quantity should be equal (equality constraints) or higher (inequality constraints) than a specific value²⁰. The problem is expressed as,

$$\begin{aligned} & \min_{\mathbf{x} \in \mathbb{D}} f(\mathbf{x}) \\ & \text{subject to } H_j = h_j(\mathbf{x}) - h_{target} = 0, j = 1, \dots, n \\ & \quad G_i = g_i(\mathbf{x}) - g_{limit} \geq 0, i = 1, \dots, m \end{aligned} \quad (2.6.1)$$

The satisfaction of equality constraints has more mathematical than engineering value. In engineering design, equality constraints may never be satisfied with a slight infeasibility being tolerated. In such a case, the equality constraint is transformed into an inequality one as $\|h_j(\mathbf{x}) - h_{target}\| \leq \epsilon$, where ϵ is a predefined tolerance.

Like the objective function, the constraint function values are not known prior to the disciplinary analysis (in fact in most cases, the objective function and the constraint functions values result from the very same disciplinary analysis). In the special case where it is known that a constraint quantity is highly dependent on a specific design variable, feasible values of this variable can be initially estimated. On a second stage, optimisation with this design variable being inactive can be performed.

Several ideas have been examined in the literature, with the main methods found in engineering problems including *Penalty methods*, *Lagrange multipliers* as well as some concepts being used within SBO. Other methods which are not discussed here include the Feasible direction method and Chromosome repair method [122, 123].

2.6.1 Penalty Methods

The penalty methods is a simple concept aiming to diverge an optimisation algorithm away from infeasible regions. When any of the constraints is violated, a high value (penalty) is added to the objective value which is returned to the optimiser. The most basic approach is perhaps the *One pass* external function method, where high value is simply added to the

²⁰A typical aerodynamics optimisation case is to minimize C_D given $C_L \geq C_{Lvalue}$.

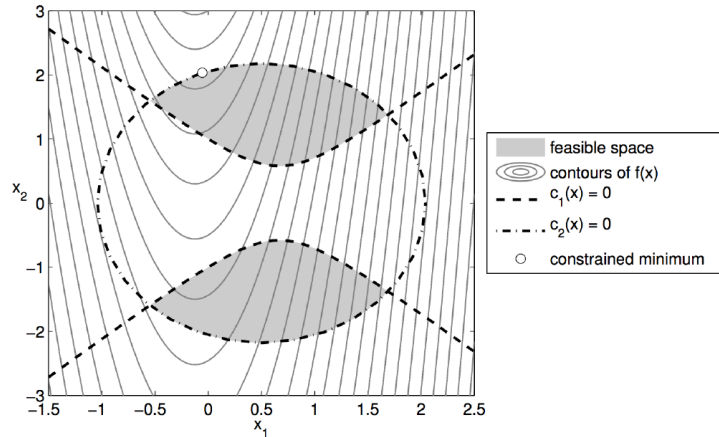


Figure 2.18: Example of a 2D design space with two constraints c_1, c_2 [3]. Here, constraint number two is active.

Objective Function (OF) value when the constraint is violated. The disadvantages of this method however, is that it does not provide any further information to assist optimisation, while introducing a function discontinuity which can pose significant difficulties for gradient based optimisation methods. To overcome such drawbacks, several variations have been developed. A follow-up idea is to assess the level of infeasibility and define the penalty value depending on it. Furthermore, in an optimisation including several constraints, the number of violated constraints can also be introduced in the penalty formulation. Combining both of the above concepts, the value returned to the optimiser will take the form,

$$f_{con}(\mathbf{x}) = f(\mathbf{x}) + \sum_{j=1}^n P_j \|H_j(\mathbf{x})\| + \sum_{i=1}^m P_i \|G_{v,i}(\mathbf{x})\| \quad (2.6.2)$$

where H_j and $G_{v,i}$ are the equality and inequality constraints' violation, while P_j, P_i are the respective scale function which can be either constant or a function of the infeasibility.

In the *interior penalty methods*, a penalty may be even applied to feasible design points which are very close to the constraint boundary in order to reduce the discontinuities near the constraint boundaries while providing information regarding the infeasible region. Based on the penalty function used, it can be a *logarithmic barrier* or *inverse barrier penalty* method. The significant disadvantage of this approach is that the optimum point located might be offset from the actual optimum.

The penalty value applied may not only be dependent on the design space position but also on the optimisation stage in which it is applied. In the case of *Sequential Unconstrained Minimisation Techniques*, the penalty takes a low value in the initial stage of the optimisation when more space exploration is desired. In the final stages, where more local search is performed, the penalties have higher values [124].

2.6.2 Lagrangian Methods

In the Lagrangian approach, the objective function is directly perturbed before its evaluation. The expressions of the constraint functions are implemented in the OF as,

$$L(\mathbf{x}, \lambda_h, \lambda_g, \mathbf{s}) = f(\mathbf{x}) - \sum_{j=1}^n \lambda_j H_j(\mathbf{x}) - \sum_{i=1}^m \lambda_i [G_i(\mathbf{x}) - \alpha_i^2] \quad (2.6.3)$$

where \mathcal{L} is the Lagrangian function. Following the same notation as Eq.2.6.1, H_j and G_j are the constraint functions, λ are the Lagrange multipliers, while α_i are *slack variables*, which in this case turn the inequality to equality constraints as, $G_i - \alpha_i^2 = 0$. To define the new OF, the two set of multipliers are evaluated using the Karun-Kush-Tacker (KKT) conditions which are the necessary conditions for a stationary point²¹. Since the KKT conditions require the derivative of the function, the Lagrangian method is best suited for gradient based optimisation algorithms in which the OF sensitivities will have already be computed.

This approach can be combined with the penalty methods simply by adding a penalty in the Lagrangian expression. For more information on the Lagrangian approach see Nocedal and Wright [125]. Alexandrov et al. [106] used a Lagrangian approach in their Multi Fidelity Optimisation method presented earlier.

2.6.3 Sequential Quadratic Programming

Sequential Quadratic Programming [126] [127] (SQP) is perhaps the most common method for tackling constraints in a gradient based optimisation algorithm. The idea behind SQP is to model the Lagrangian function as a quadratic function with linear constraints²².

2.6.4 Managing Constraints in Surrogate Based Optimisation

Constraint handling in SBO typically uses generic methods like the penalty methods or more specialised ones by extending the SBO methodologies [128]. In an SBO framework, as with the objective functions, the constraint functions are modelled using surrogates. If possible, the feasibility of the design point should be checked before performing a costly sampling analysis. Ideally, if the exact constraint function is cheap to evaluate, then no

²¹A stationary point is a point in the design space for which the first order derivative of the OF is zero. For a point to be a local minimum, the sufficient conditions include second order derivative requirements as well.

²²Usually this approximation is used in a Trust Region approach where the quadratic approximation is only valid in the trust radius.

surrogate has to be used at this stage. In case its cost is equivalent to the objective function computation — or in the common case were the constraint values result from the same disciplinary analysis as the objective function — then a more complex approach has to be used to cheaply examine if the design point is feasible.

When a global SBO approach like PI or EI is used, the minimum is simply replaced by the minimum feasible value. The use of Kriging or Co-Kriging models, allows the estimation of the probability of the constraints not being violated. Under this concept, the new infill point is the one that simultaneously satisfies both the infill criteria (e.g. TR minimum, PI, EI) and the constraints' feasibility prediction. Since PI and EI infill are using probabilistic criteria based on the Kriging error estimator, the probability of a design point obeying the constraints can be explicitly included in the infill plan. The accuracy of this probability estimation is assessed with the error estimator of the respective constraint surrogate. Hence, a design point showing high expected improvement based on an accurate OF surrogate but with an inaccurate constraint surrogate, might be non-feasible. The probability of a design point being feasible is expressed as a probability of improvement over the constraint limit. By combining this expression with the OF probability of improvement, an expression of the probability of a feasible design point improving the OF is calculated. In the same manner, the probability of obeying the constraints is fused with the expected improvement criterion. Both cases can be considered as a two stage balanced exploration/exploitation scheme for a constrained problem. This approach is illustrated in Fig.2.19.

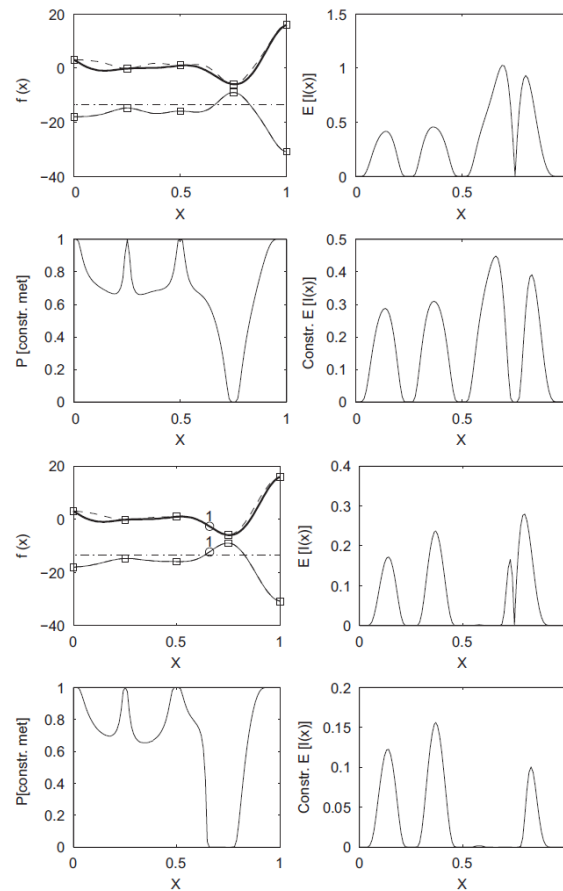


Figure 2.19: Initial surrogate build-up and first infill point for a constrained SBO EI approach [107]. The bold line is the true function, the dashed line is the surrogate prediction and the thin line is the constraint surrogate. The constraint limit is shown in dash-dot line.

Since the statistical condition of improving the OF—*given* the feasibility condition—is expressed as a product of two probabilities, the infill criterion might not be very straightforward. Consider a case where a point has a high potential of improving the function (or a potential of high improvement) but a low probability of feasibility. On the other hand, consider a case of a point with a very low potential of improving the function (or a potential of low improvement) but a high probability of feasibility. These two may lead to similar infill criterion value. The final choice can be considered arbitrary or in a sense defined by the objectives of the designers. More information on this formulation is available on Chapter 3. The resulting behaviour of this criterion is discussed in more detail in Chapter 5.

2.7 Multiobjective Optimisation

In typical industrial applications, a single objective is not sufficient for quantifying the performance of a system. There are usually more than one criteria associated with its performance, that are typically conflicting. As such, efficient engineering design aims in developing configurations with good tradeoff characteristics and in getting knowledge of the performance of the system in different objectives. Especially in cases where a design direction for efficient tradeoff is not obvious, information regarding the performance on different criteria is critical for supporting the decision making and guiding the design.

2.7.1 The Concept of Dominance

With a product being assessed by many figures of merit, in most cases a design cannot be objectively declared as superior over another. In such design problems, the concept of dominance is employed which forms the foundation of most Multiobjective (MO) optimisation algorithms [129]. Provided N objective functions, a design point is *dominant* over another when it simply performs better in all N objectives. When a design is superior over another in one objective but lacks in another, the two designs are considered equal and are called non dominated. Therefore, a non dominated point is a design point which is superior over the rest of the designs in at least one objective. Several Multiobjective optimisation algorithms (such as Evolutionary Algorithms or other population based algorithms), initiate the optimisation process by multiple datum geometries and use the concept of dominance to assess whether the new sampled point is "better" than the current *optimum set*. MO optimisation cases do not provide a single optimum design point, but a locus of non dominated points called the *Pareto Front*.

2.7.2 The Weighted Superposition Method

The concept of dominance is used by MO optimisation frameworks. However, we can also transform the MO problem into a single objective one (SO) so that single objective optimiser can be used. Since each point in the pareto front is better than any other pareto point in one of the objectives, it is implied that this point is the optimum in a problem defined by a single objective function, composed by the weighted superposition of the multiple objectives [130, 131]. For example, in a typical aerodynamics optimisation problem in which case the objectives are the aerodynamic coefficients, the use of weighting coefficients w_1 and w_2 can compose the single objective as,

$$I = w_1 C_L + w_2 C_D \quad (2.7.1)$$

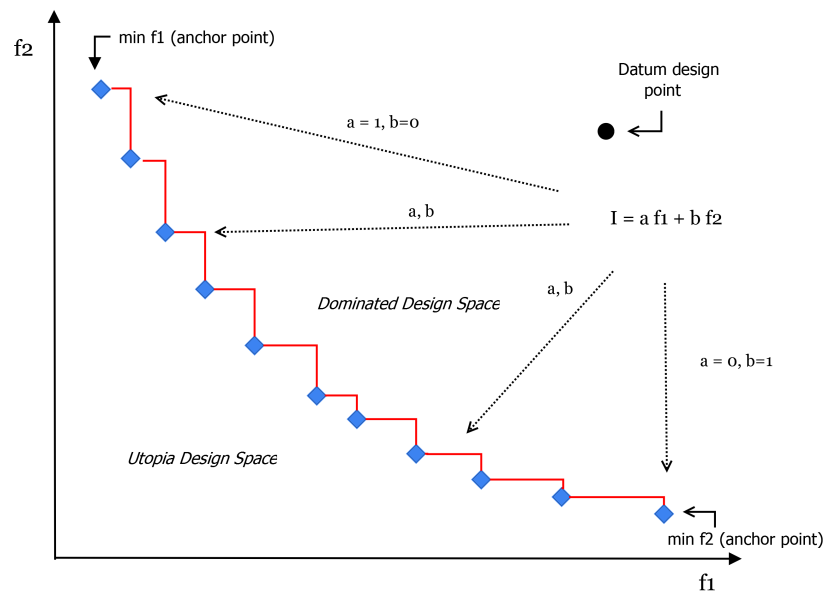


Figure 2.20: A typical Pareto Front consisting of non dominated points. These points can also be identified with a series of a, b combinations and a single objective function.

It can be observed that the Pareto front is essentially the locus of the optimum points resulting from problems expressed by I functions and therefore can be reconstructed by a set of different w_1, w_2 optimisation studies (see Fig.2.20). This inverse approach to the Multiobjective optimisation problem involves the a priori definition of the desired w_1, w_2 coefficients whose ratio represents the design direction. The single objective optimiser will then find the single optimum based on this design philosophy. This approach is efficient when the design orientation is provided (namely, already identified by the engineers following the initial design stages). However, this is not the case in the early design phase, when extensive design and objective space exploration is desired to extend the maximum information from tradeoff studies. In this case, a costly multi objective optimisation forming a Pareto front is required. Also, as reported in [107], a drawback of the weighted OF approach is its inability to locate the true minimum when the Pareto front is convex. It could be summarized that MO methods are best suited for conceptual design or novel design explorations, where engineering tradeoff feedback is required, whereas the weighted OF approach is appropriate for final design finetuning studies.

Work towards a multiobjective Pareto tradeoff analysis in multidisciplinary problems has been performed by Mastroddi and Gemma [132] using aerodynamic efficiency, weight and range as objective functions. The problem was not solved by an explicit MO optimiser, but on normalized parametric studies Weighted Global Criterion (WGC) using SNOPT gradient based optimiser.

The weighting superposition method in multiobjective problems can be also used in optimisation cases involving multiple design conditions²³. Nemeč et al. [133] performed

²³Under a superposition method, an objective can be considered as a design condition and vice versa. In

a MO and multipoint optimisation for the high lift section NLR7301 and RAE2822, using the weighted coefficient concept for C_L , C_D so that they are close to a priori set targets. C_D was used in the O.F. only when $C_D > C_{Dtarget}$.

Multipoint optimisation can be also formulated as an MF optimisation problem, as in the work by Toal and Keane [134]. In this, weighted superposition results of all design conditions are considered as high fidelity whereas low fidelity data are the result of a single condition.

2.7.3 Multiobjective Methods in Surrogate Based Optimisation

When the optimisation framework is not based on surrogate modelling, the process is straightforward since the methodology that produces the pareto front is already defined in the optimiser algorithm. However, in an SBO framework specific formulation arrangements are required to form a pareto front.

For the N objectives, N metamodels are generated based on the training data set. In this standard MO SBO formulation of the PI criterion, it is not the point of the maximum probability of improvement that is sought. The infill point is the one with the maximum probability of being a new member of the pareto set or an improvement on any existing member of the set (see an example that feature two objective functions and two metamodels in Fig.2.21). The probability that a design point will dominate a single member i of the front over all N objectives Y is calculated as,

$$P(Y_1 < Y_1^i \cap Y_2 < Y_2^i \cap \dots \cap Y_N < Y_N^i) \quad (2.7.2)$$

This standard method does not require the computation of multiple infill points during every sampling iteration. When a single design point is evaluated, the method inherently tries to improve the pareto front. However, this infill criterion may not be able to provide sufficiently wide design space exploration resulting to a not equally populated pareto front. More information about this formulation is presented in the next chapter, where also a simple alternative to address the problem of the objective space exploration is proposed.

fact, multipoint problem can be formulated and solved as multiobjective problem using either the superposition method or the pareto dominance concept.

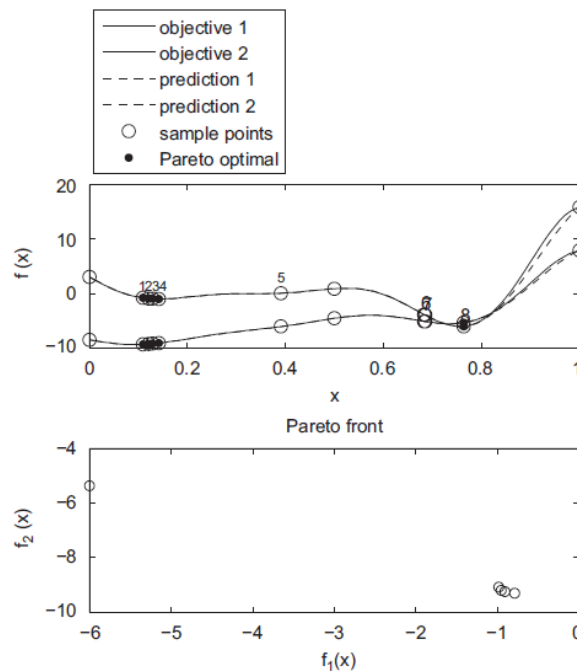


Figure 2.21: Multiobjective Expected Improvement criterion [107]. In this case two objectives are being considered.

2.8 Optimisation Algorithms

The optimisation algorithms can be considered as the heart of any optimisation process. In the straightforward case involving only a single method of analysis and no surrogate modelling, the optimiser—given a design point—provides the next design point for analysis. In more complicated procedures which involve analysis tools of variable fidelity as well as surrogate modelling, the use of the optimiser is not straightforward, nevertheless it remains the core of the process. In the SBO case, the optimiser is used to solve the suboptimisation problem; to find the infill point based on the employed SBO plan. The function and efficiency of the optimiser is critical for the behaviour and success of an optimisation framework, and it should be selected according to the optimisation requirements.

The optimisers can be categorized based on features such:

- *Deterministic, heuristic or stochastic.* An optimiser is deterministic when for a given input (datum point), the output is always the same every time the process is repeated. The heuristic methods follow this one-to-one relationship between inputs and outputs but make use of a specific pattern to proceed from the current optimum to the next point. Stochastic methods involve an element of randomness in the optimisation process. If performed many times from the same datum, the final result and the path followed will not be identical.
- *Gradient based or Gradient free.* Gradient based algorithms require the sensitivity

of the objective function over the design variables in order to calculate the search direction in the design space. These fall in the deterministic category. Gradient free methods only require the computation the function evaluation (and not its gradient) and can be either heuristic or stochastic.

- *Global or Local optimisers.* Global optimisers perform an exploration of the design space aiming the location of the global optimum area. Local optimisers search directly for an improvement near the current point, usually exploiting gradient information, and as such may stuck in a strong or weak local optimum.
- *Single or Multiobjective*

2.8.1 Gradient Free Algorithms

Gradient free algorithms are easier to implement and under specific conditions they may guarantee global optimality. However, since they are provided with a probabilistic search direction as well as aiming in more extensive design space exploration, they are more computationally expensive. Their ultimate goal is to guarantee global convergence with the minimum function calls.

Genetic Algorithms

Genetic Algorithms (GA) fall in the category of Evolutionary Algorithms [135, 136], which like many of the gradient free optimisers, use a physical selection procedure inspired by everyday life, nature laws etc. Genetic algorithms in particular are based on the theory of evolution of living organisms using three basic components; *Survival of the fittest*, *Reproduction process* for the propagations of the genetic traits, *Mutation*.

GA use an initial population assessing the various designs "simultaneously". After each iteration the population is changed according to the promising design directions. An advantage of such methods is their stochastic element (through mutation) which helps avoid local optima even for deceiving functions, while it can be used for continuous, discrete or integer design variables. However, the requirement of large number of population members combined with the slow convergence and the multiple operations when defining the new population, make these methods highly expensive when used to call functions like CFD analyses. It can handle both single as well as multi objective problems, with the latter being a more sensible application as global exploration favours tradeoff studies. GA use the concept of dominance to construct a ranking of the population members.

Antoine [137] employed a GA framework to perform an environmental MO optimisation involving the minimisation of cost, fuel, NO_x and CO_2 . Typical population ranking

was used as a means for tackling the MO nature of the problem while constraints were satisfied using penalty methods.

Particle Swarm Optimisation

Particle Swarm Optimisation [138] (PSO) is a stochastic method that can be adjusted to local or global characteristics. It uses the concept of a swarm behaviour and intelligence. Agents (usually referred as "birds") move in the design space searching for the optimum. Each iteration provides a new design point for each agent, hence a "movement" from an old point to a new one. The movement is adjusted by cognitivism (self-experience) and social cognition (social interaction) parameters. The cognitivism is essentially a weighting factor defining the importance of the optimum design encountered by specific agent affecting the next design point sought by the same agent. Social cognition is provided again by a factor adjusting the impact of the optimum that any agent of the swarm has encountered. The movement of an agent i in search of the next design point is expressed by,

$$x_{k+1}^i = x_k^i + \left(wu_k^i + c_1r_1 \frac{(p_k^i - x_k^i)}{\Delta t} + c_2r_2 \frac{(p_k^g - x_k^i)}{\Delta t} \right) \quad (2.8.1)$$

where, w is a factor representing inertia, c_1 and c_2 are the factors representing the cognitive and social learning and r_1 and r_2 are the respective random numbers inducing the stochastic element. Δt is a factor that eventually controls how far in the design space any agent will be able to move given its velocity u_k^i . p_k^i represents the best solution that agent i has encountered while p_k^g is the best solution found so far by the swarm.

This is a method that it is easy to develop, implement, adjust or modify and it can perform a wide design space exploration. Although the basic method is unconstrained, constraints can be easily implemented with the Lagrangian or the penalty function methods. PSO can be extended to MO problems, using the concept of dominance. A typical example is the Multi Objective Particle Swarm Optimisation (MOPSO) algorithm [139] that selects the leader of the swarm using the concept of pareto dominance, classifying it as a Pareto Dominance MOPSO type — see [140] for an overview of other approaches.

Nelder-Mead method

The Nelder-Mead method [141] (also known as the Non-linear Simplex method) is a heuristic approach which uses a sequence of geometrical operations to estimate the optimum of a function. It has the potential to identify the global minimum region in low dimensional design cases (typically less than fifteen). In higher dimensionality problems it becomes inefficient, especially when used to call costly analysis problems. It can be classified between local and global methods due to its limited exploration attributes originating from its

pattern based process not involving statistic elements.

TABU Search

TABU Search [142, 143] is not a standalone algorithm like the ones previously presented. It refers to a "macroscopic" method that guides a heuristic pattern so that the design space can be explored beyond local optimum. The heuristic approach typically used by this framework is the Hooke and Jeeves [144] method, performing a pattern pattern (called *the move*) which explores the neighbourhood of a design point referred to as $N(x)$. In TABU Search, moves are performed in a modified neighbourhood $N^*(x)$ and only moves that reduce the OF are permitted [145]. The modified neighbourhood is the result of an adaptive selective memory structure (short and long memory structure). Three flexible, distinctive and of different life span memories create the tabu list: *Short term*, *Intermediate term* and *Long term* memory. An attribute memory approach is also used in which the memory structures are fed not by the solution but by the solution properties (attributes). Attribute memory includes, *Recency* and *Frequency* memory. To move to promising regions, the actions of *intensification* and *diversification* are used controlling the local/global behaviour.

The Single Objective TABU Search of Tilley and Connor [146] was extended to a Multiobjective TABU Search algorithm (MOTS) by Jaeggi et al. [147]. A modification was also proposed, called PRMOTS (Path Relinking Multiobjective Tabu Search) featuring a variable selection scheme aiming in reducing the dimensionality by dropping inactive design variables. In both MOTS and PRMOTS constraints are tackled with penalty functions. MOTS was used by Trapani [148] for the aerodynamic optimisation of a multielement Garter airfoil configuration to maximise lift and minimise drag. MOTS was compared against the well established NSGA-II code dominating the respective NSGA-II results, also showing a wider pareto front.

2.8.2 Gradient Based Algorithms

Gradient based algorithms are very efficient in terms of required iterations, since the gradient provides additional "physical" information to guide the optimisation process. Such methods however cannot provide the exploration required in the early stages of the design. Nevertheless, they provide an efficient approach for local fine-tuning in detailed design stages.

For a given design, the OF (primal) is evaluated, followed by a sensitivity analysis of the OF over the design variables depending on the characteristics of the problem. This is a vast research area all by itself, including various methods and submethods. Some of these are very briefly discussed in the following section. Using the sensitivity (gradient), a search direction \mathbf{d}_k is calculated so that the current design vector can be updated towards

this direction as in the following relation,

$$\mathbf{x}_{k+1} = \mathbf{x}_k + \alpha_k \mathbf{d}_k \quad (2.8.2)$$

Gradient based algorithms are categorised based on the method used to calculate the search direction using the sensitivity information. The final stage of the process is to calculate how far along this direction should the next design be — provided by α_k .

This iterative procedure (shown in Fig.2.22) is ceased when the optimality criteria (Karuhn-Kush-Tucker conditions for constrained problems) are met. These include the 1st order optimality conditions which state that the gradient of the function f is zero²⁴,

$$\frac{\partial f}{\partial x_i} = 0, \text{ for every design variable } i \quad (2.8.3)$$

In order to characterize a design point as a local optimum, the 2nd order (curvature conditions) should be satisfied. That is, the Hessian matrix \mathbf{H} (square and symmetric matrix) of the 2nd order partial derivatives should be positive definite.

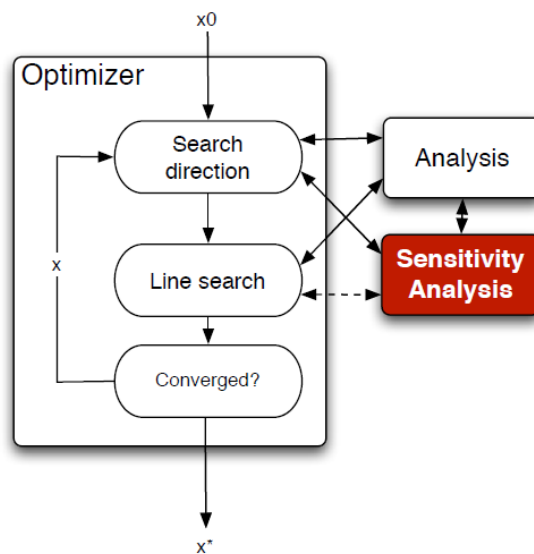


Figure 2.22: A typical gradient based optimisation process. An analysis and the computation of the gradient (sensitivity analysis) feeds a method to provide the search direction. Given that, line search is performed and the procedure keeps iterating until conditions are satisfied [3].

²⁴This is a sufficient condition for a point to be stationary.

Sensitivity Analysis

Methods which provide the gradient of a function on a design point, that is the dependence of an output to a n -dimensional input, fall in the scope of sensitivity analysis. Here, the interest is in calculating the vector,

$$\nabla f(\mathbf{x}) = \sum_{i=1}^n \frac{\partial f}{\partial x_i} \mathbf{e}_i \quad (2.8.4)$$

and the sensitivity of the active constraints in a similar fashion. The research focus is on computing the derivatives as efficiently as possible while keeping high levels of accuracy. There are four main approaches in sensitivity analysis [149]: *Finite Difference*, *Complex-Step Derivative*, *Automatic Differentiation* and *Direct/Adjoint Methods*

Finite Difference is perhaps the easiest approach, based on a Taylor series expansion to approximate the partial derivatives. This requires the calculation of the function variation over all n variables and the total cost is $n + 1$ times the calculation of f . In this method, the step size is an important issue. The truncation error needs to be minimised, but if the step size becomes too small, cancellation errors become dominant. In this case, further reduction of the step size leads to an increase of the approximation error. The complex-step method [150] is a step towards the solution of this problem, where the change in the OF value is expressed in complex number terms.

Automatic Differentiation [125](AD) is an approach that can reach analytical computation accuracy as it uses the chain rule of derivation when this is implemented in the code. It can be used either in *forward* or *backward* mode depending on the direction of propagation of the derivatives of the chain rule. It involves a decomposition of the operations performed when a gradient of a function is analytically computed. Although AD is superior to expensive finite difference methods, its use is limited to studies where the analysis source code available.

Martins et al. [150], provide an overview of the complex step approach and its connection to AD. It was shown how problems of complex step method can be solved with the AD concept (complex step is equivalent to the forward mode of AD - but with an easier implementation).

A simple forward mode AD without need for extensive modifications was introduced by Lyu et al. [151] to allow for aerodynamic simulations involving turbulence modelling. In their verification test case — an ONERA M6 test case with six design variables and 21 constraints — the aerodynamic gradients differ by 10^{-9} and the spatial gradients differ by 10^{-4} to the complex step obtained sensitivities.

Direct/Adjoint methods [152] belong in the analytic sensitivity category and when avail-

able, they can be the most accurate of all methods. A limiting factor however is their dependency on the disciplinary analysis governing equations. The mathematical formulation of the adjoint-based sensitivity method can become very complex involving quantities like the surface and volume mesh sensitivity with respect to the surface mesh as well as the flow adjoint, depending on the sensitivity of the flow solution to the volume mesh. Each of these terms require specific techniques to be evaluated. Such a presentation extends the scope and purpose of this chapter and it is not included.

Nevertheless, it can be said that the choice of a direct or adjoint method to calculate the sensitivity of the function over the design variables, depends on the number of functions compared to the number of design variables. As typically the design variables are more than the objective function considered (they are actually way more), the adjoint formulation is more efficient. In fact, the big advantage of the adjoint based optimisation is that the cost of the sensitivity analysis is independent of dimensionality. This is what makes it appealing in the final stages of a design when detailed design studies are performed, including hundreds or thousands of design variables²⁵.

Mader et al. [153] propose ADjoint, a combination of AD and adjoint, in an effort to avoid their drawbacks. ADjoint is consistent, can handle complex problems and can be used for many sets of governing equations without significant changes. It also reduces memory requirements. Results from ADjoint are validated against results from the complex step approach.

The typical cost of solving the adjoint equations is comparable to solving a complete RANS CFD simulations. Adjoint methods are also classified to *continuous* or *discrete* depending on the order of their differentiation and discretisation process. The discrete adjoint method is more common and well established in the aerodynamics design community. An extensive overview of sensitivity analysis is provided in [152], followed by suggestions on dealing with Hessian approximation for aeronautical cases.

Gradient Based Optimisers - Calculating Search Direction

Given the gradient \mathbf{g} of the OF at a design point \mathbf{x}_k in iteration k , the search direction is calculated. The simplest way to calculate the search direction is the *Steepest Descent* method where the search direction is simply the negative normalised gradient as,

$$\mathbf{d}_k = -\frac{\mathbf{g}(\mathbf{x}_k)}{\|\mathbf{g}(\mathbf{x}_k)\|} \quad (2.8.5)$$

This method converges linearly, performing a normal zig-zag path towards the optimum. A simple improvement over this method is the *Conjugate Gradient* that uses data from

²⁵Obviously increasing the number of variables would have an effect in other stages of the optimisation process. It would increase the design space, the cost of creating a surrogate (in case of a hybrid surrogate/-gradient based optimisation), as well as increasing the multimodality of the design space.

previous search directions to accelerate the convergence²⁶. The property of conjugacy ($\mathbf{d}_i^T \mathbf{A} \mathbf{d}_j = 0$ for $i \neq j$) is used. This directs the optimisation to be aligned with the axes of the ellipsis (when matrix \mathbf{A} is positive definite). The method is also known as *Fletcher-Reeves* for non linear functions.

Newton methods introduce 2^{nd} order information near the design point, in the form of Hessian matrix and as such they provide a quadratic approximation near the current design point. Of course, this approximation is only accurate near the design point.

Being higher order methods and introducing more information on the design trends, they are more effective, requiring fewer iterations to converge. However, the method is negatively affected by potential ill-conditioning problems of the Hessian matrix as well as the very high costs of its computation.

To detour this problem, *quasi-Newton* methods have been developed. These provide ways to approximate the Hessian matrix [125], and are categorized based in their approach. Common methods include the *Davidson-Fletcher-Powell (DFP)* method, the *Broyden-Fletcher-Goldhurb-Shanno (BFGS)* method and the *Symmetric Rank-1 Update (SRI)* method. Perhaps the most effective and commonly used method is the BFGS method.

Line Search

Given a search direction \mathbf{d}_k , an appropriate step length α_k should be used so that Eq.2.8.2 can be applied to locate the next design point. A very small step length might not provide sufficient decrease while a too large one might lead to overshoot and produce a very slight decrease (if any). This is the case where the local minimum is overpassed and the derivative of the function in the search direction is no longer negative.

A suboptimisation problem is required to determine the optimum step length α_k by minimizing $f(\mathbf{x}_k + \alpha_k \mathbf{d}_k)$. Methods that solve this optimisation problems are called *exact* and are very costly. *Inexact* methods like *Backtracking* use guess steps which can guarantee that neither short nor long steps will be used. To secure a proper step value, several criteria can be used, including the *Sufficient Decrease criterion*, *Curvature criterion*, *Wolfe* and *Strong Wolfe conditions* as well as the *Goldstein conditions* [125].

2.9 Multidisciplinary Design Optimisation

The beginning of this chapter briefly displayed the need for switching from a sequential to multidisciplinary design approach. This section provides a more elaborate discussion on

²⁶For the first iteration, steepest descent is used.

the way multidisciplinary design and optimisation problems can be formulated.

A methodology that defines how the various disciplinary analyses or optimisation problems should interact in order to exchange information required for the MDO, is called *architecture* (also referred to as *formulation*). The architectures are split into two main categories:

- *Monolithic* architectures
- *Distributed* architectures

Monolithic architectures use a single optimisation stage, which during each iteration call what essentially is some kind of MDA process and returns the functions of interest. This approach includes the simplest and perhaps easiest to implement concepts. However, a significant requirement for their use is the existence of an easy and direct way to exchange information between the various disciplines to satisfy their consistency requirements. Furthermore, the implementation demands good load balancing as well as limited disciplinary information exchange in order to be efficient. This requirement makes such an option impractical for the aeronautical industry which has highly distributed structure in a global scale. Major aeronautical industries (AIRBUS, Boeing etc.) have independent departments — scattered around the world — each specializing into a disciplinary design. Hence, an approach that allows the groups to work independently while minimizing the quantity and frequency of exchanged information is preferred. In such cases, distributed architectures are more convenient as they use a system-level optimiser that guides the subsystem (disciplinary) optimisers. Hence, the disciplinary analyses and optimisation processes can be performed independently with less frequent exchange of disciplinary information required. Distributed architectures can be classified in:

- Non-hierarchic: Data are exchanged with no well defined hierarchy and feedback between the disciplines.
- Hierarchical: Well defined hierarchy between data exchange and no feedback is available between the disciplines.
- Hybrid

An overview of these approaches for a typical aerostructural problem is shown in Figs.2.23, 2.24.

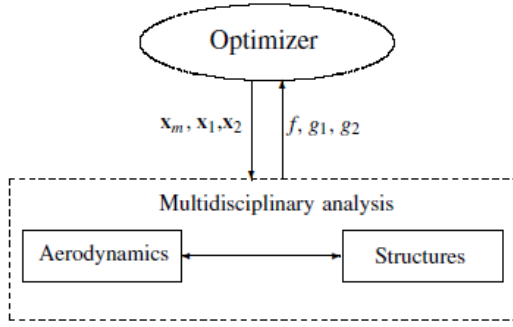


Figure 2.23: Monolithic architectures. MDO uses a single optimisation problem introducing a coupled MDA [57].

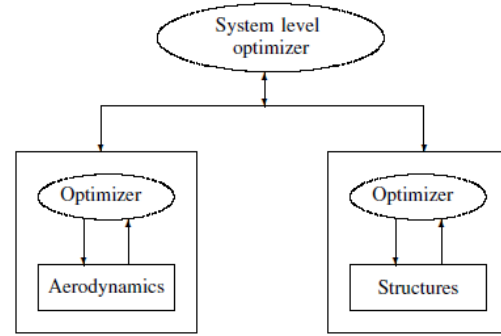


Figure 2.24: Distributed architecture. The problem is decomposed into multiple suboptimisation problems [57].

2.9.1 Generic Problem Formulation

With multiple disciplines present, the design variables \mathbf{x} vector can be split into subvectors, each containing the local variables of the i^{th} discipline (\mathbf{x}_i) as well as the vector of the shared variables \mathbf{x}_0 . The state variables of each discipline is represented by \bar{y}_i . The exchange of information between the i^{th} discipline and the other disciplines is done by the coupling (or response) variables y_i , which is a subset of \bar{y}_i since not all outputs of a disciplines are useful to others. Also a mechanism to transform y_i to useful format is required. A typical example of that is the transfer of pressure or lift force information from the surface CFD mesh cells to the CSM ones. To allow parallel computations, these state variables may be copied into target variables \hat{y}_i . Of course, although processed in parallel, y_i and \hat{y}_i should have the same values. Hence, consistency constraints $c_i^c = \hat{y}_i - y_i$ should hold.

Mathematically, the MDO problem is formulated as:

$$\begin{aligned}
 & \min_{\mathbf{x} \in D} \quad \mathbf{f}_0(\mathbf{x}, \mathbf{y}) + \sum_{i=1}^N f_i(\mathbf{x}_0, \mathbf{x}_i, \mathbf{y}_i) \\
 & \text{w.r.t.} \quad \mathbf{x}, \hat{\mathbf{y}}, \mathbf{y}, \bar{\mathbf{y}} \\
 & \text{subject to} \quad \mathbf{c}_0(\mathbf{x}, \mathbf{y}) \geq \mathbf{0} \\
 & \quad \mathbf{c}_i(\mathbf{x}_0, \mathbf{x}_i, \mathbf{y}_i) \geq \mathbf{0}, \text{ for } i=1, \dots, N \\
 & \quad \mathbf{c}_i^c = \hat{\mathbf{y}}_i - \mathbf{y}_i = \mathbf{0}, \text{ for } i=1, \dots, N \\
 & \quad R_i(\mathbf{x}_0, \mathbf{x}_i, \mathbf{y}_{j \neq i}^t, \bar{\mathbf{y}}_i, \mathbf{y}_i) = \mathbf{0}, \text{ for } i=1, \dots, N
 \end{aligned} \tag{2.9.1}$$

where \mathbf{f}_0 is a shared objective (or a vector of shared objectives in the case of MO optimisation), and \mathbf{f}_i are local objective functions. \mathbf{c}_0 , \mathbf{c}_i and \mathbf{c}_i^c are the system, disciplinary

and consistency constraints respectively (presented in vector form). \mathbf{R}_i are the disciplinary analysis residuals.

2.9.2 Monolithic Architectures

The most common monolithic architectures found in the aerospace related literature include:

- *All at once* [154] (AAO). It solves the general formulation of the problem but is rarely used due to its complexity.
- *Simultaneous Analysis and Design* [155] (SAND). Here, the consistency constraints c_i^c are dropped.
- *Individual Discipline Feasible* (IDF). The IDF architecture²⁷ is defined by dropping the disciplinary analysis constraints present in the AAO scheme. In the event of a sudden stop in the procedure, the last resulting design would not satisfy multidisciplinary feasibility.
- *Multidisciplinary Feasible* (MDF). The disciplinary analysis constraints as well as the consistency constraints are removed [154]. This is perhaps the simplest approach and it involves an MDA in which the disciplines are sequentially solved (typically using a non-linear Gauss-Seidel loop [156]) (see Fig.2.25). Variations can be developed depending on the order of execution of the disciplines affecting the convergence rate, and the iterative MDA process stops once disciplinary feasibility has been achieved. Fig.2.25 shows the optimisation sequence of this architecture in an *XDSM* [157] format, a currently accepted way to consistently present MDO architectures.

²⁷It can be also seen as Distributed Analysis Optimisation (DAO) in the literature.

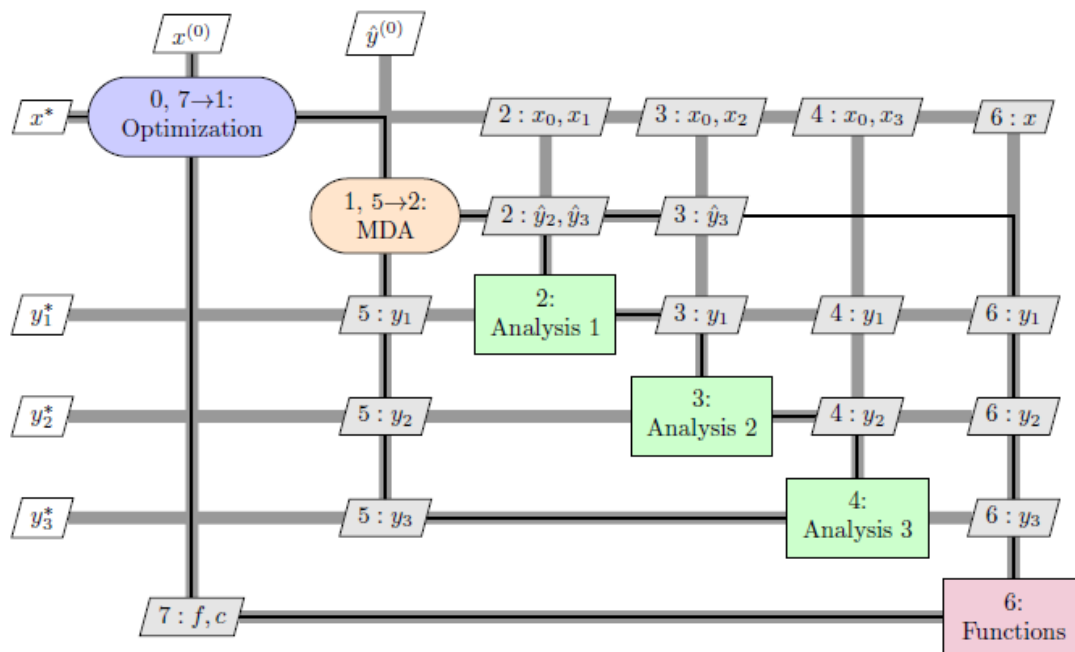


Figure 2.25: MDF architecture. Analyses are iteratively until convergence as a part of an MDA. In this example, the Gauss-Seidel loop is used [158].

2.9.3 Distributed Architectures

Distributed architectures are developed based on a monolithic analogue, either IDF or MDF. IDF-based distributed architectures are classified in either penalty or multilevel based. Hybrid architectures, exhibiting characteristics of both MDF and IDF formulations, can also be developed.

- *Concurrent Subspace Optimisation (CSSO)*. CSSO [159] decomposes the MDO into a number of disciplinary suboptimisation problems which have disentangled variables. The system level uses a series of coefficients for each discipline to extract information regarding the design variables. Surrogate modelling has also been implemented [160] while modifications have been proposed for MO problems [161].
- *Bilevel Integrated System Synthesis (BLISS)*. In BLISS [162], local design variables are used in a disciplinary level while the shared design variables are used in the system level. An MDA is required to force interdisciplinary feasibility (see Fig.2.27). It is typically applied with gradient based optimisers, with BLISS/A and BLISS/B having been proposed depending on the sensitivity analysis method used. Surrogate modelling can also be employed in the computation of sensitivity.
- *BLISS-2000*. This is an improvement over the original BLISS, proposed by Sobieski [163] and it does not require an MDA to restore design feasibility. In the optimum

design point, coupling variable targets provide the consistency. Information provided between the various disciplines is based on surrogate models. The effect of each discipline is controlled by weighting coefficients acting on the state variables. This method is more flexible and efficient as it allows the parallel execution of the various disciplines surrogate models.

- *MDO of Independent Subspaces* (MDOIS). This architecture is designed for cases where no shared objectives f_0 , shared constraints c_0 or shared design variables are present. Disciplines are only connected through the coupled state variables. An MDA is performed after the subproblems convergence, to guide them to a new design. Its non-realistic assumptions make it inappropriate for use in current complex aeronautical problems.
- *Asymmetric Subspace Optimisation* (ASO). ASO [164] is efficient in cases where the computational costs of the various disciplines are not well scaled (such an aerodynamic analysis versus a structural analysis). There is a reduction on the optimisation and MDA costs by defining a disciplinary optimisation of the cheap discipline within the MDA (see Fig.2.26). The system-level design variables are reduced and there is a better *load balancing* within the ASO/MDA loop.
- *Collaborative Optimisation* (CO). CO belongs to the distributed IDF and multilevel family of architectures. It is appropriate in cases where there is small coupling bandwidth (low number of shared variables) [165]. Here, independent disciplinary optimisation problems are formulated. The system optimiser minimises the OF, while the disciplinary optimiser minimises interdisciplinarity inconsistency. It has been applied in many aeronautical related problems but it is characterized by poor performance.
- *Enhanced Collaborative Optimisation* (ECO). This is a modification of the CO formulation. The objectives of the system level and disciplinary subproblem optimisation are reversed. In the disciplinary subproblem, the system objective is minimized.
- *Quasiseparable Decomposition* (QSD). QSD [166] is suitable for the generic case of problems where objectives and constraints are only a function of the shared design variables and the shared coupling variables. This is a bilevel method for which the solutions of the disciplinary subproblems form constraints of the system problem.
- *Analytical Target Cascading* (ATC). ATC was originally developed as a design method by minimising the difference between the design and the target. It was reformulated [167] so it could be used as an MDO architecture. The OF includes an addition of disciplinary penalty relaxation functions and a penalty relaxation of the global design constraints. Constraints are typically tackled by weighted penalty functions, with the modifications focusing mostly on the choice of the penalty function. It has been extensively used in the automotive sector while there are some aerospace applications as well.
- *Inexact Penalty Decomposition/Exact Penalty Decomposition* (IPD/EPD). IPD/EPD can be applied to problems where no shared OF and constraints are present. Therefore, a

disciplinary subproblem is solved subject to disciplinary constraints. The disciplinary OF is augmented by penalty functions, penalising the inconsistency between the discipline and the system information. The choice of penalty functions, defines whether the formulation is classified as IPD or EPD and has an impact on the method's efficiency and convergence rate.

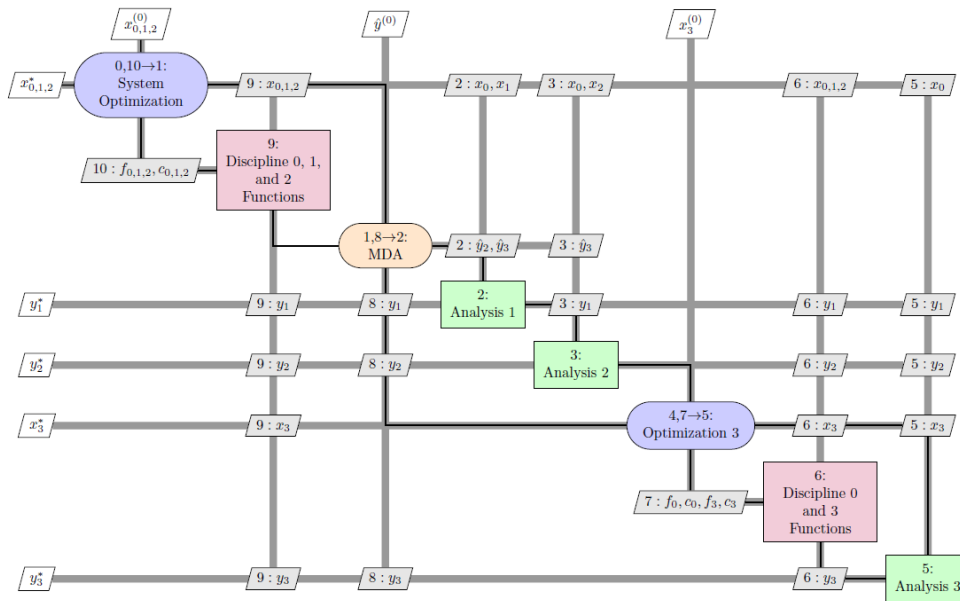


Figure 2.26: Diagram for ASO [158].

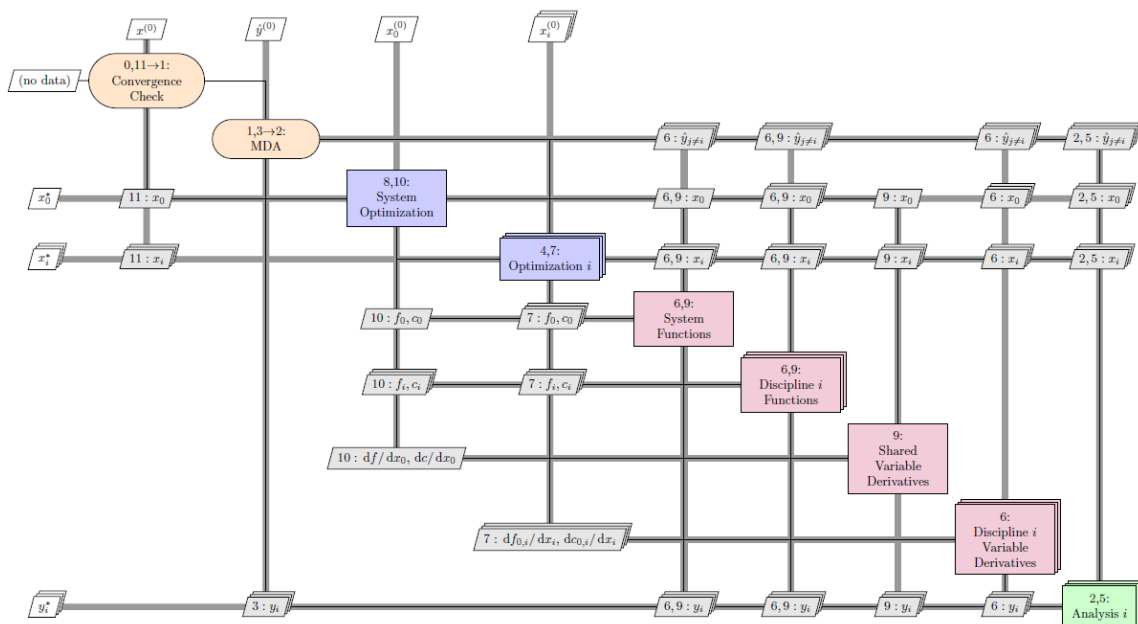


Figure 2.27: Diagram for BLISS [158].

For a detailed up-to-date review of the MDO architectures, see [158]. Also, [168, 169] provide information on MO MDO formulations, as well as an efficiency-based comparison between some of the most popular architectures to the aerospace industry.

2.10 Aerostructural Optimisation Requirements and Considerations

This section presents some requirements that arise specifically in aerostructural optimisation cases and they directly or indirectly originate from the aerostructural MDA loop. They include the coupling of the aerodynamics and structures through the transfer of aerodynamic loads and structural displacements as well as the estimation of the structural weight, required to enforce meaningful final wing designs.

2.10.1 The Aerostructural Coupling Problem

Monolithic and MDF-based distributed MDO architectures, require a multidisciplinary analysis that when converged, provides the global quantities that are used as objective functions or constraints of the MDO problem. In aerospace MDO applications, this typically involves the C_D and the weight, as the most common MDA is an aerostructural analysis. The static aerostructural analysis associated with this type of design problems is essentially a specific case of a fluid-structure interaction (FSI) problem. Such types of MDA require the exchange of information between the involved disciplines, during the analysis process. The two major solving methods for such problems are:

- Monolithic (Fully Coupled) approach
- Partitioned (Loosely Coupled) approach

In the *Fully Coupled* approach, the physical problem is solved by a single analysis code able to handle both the structural and the fluid simulation. Typically, in this computational setup there exists a single grid for both the structural and the fluid discipline. Exchange of boundary condition information (fluid-generated forces and structural displacements) is done automatically within a single solver in these conformal grids, so the analysis in each time — or pseudo time — step is performed in a synchronized manner. In the *Loosely Coupled* approach, the multidisciplinary analysis is split into two distinctive analysis codes. Each one involves its own computational domain and the grid in the disciplinary interface is typically non-conformal. Therefore, a surface exists in which the nodes of the fluid grid do not coincide with the nodes of the structural grid as shown in Fig.2.28. This demands the development of an additional algorithm whose main purpose is to properly distribute the

quantities of interest between the aerodynamic and structural grid. This approach has been more popular the recent years due to the development of many disciplinary analysis codes and software as well as specialized mesh generation tools. The loads/deformation mapping procedure requires the satisfaction of at least the following two physical conditions:

- Conservation of energy over the interface
- Conservation of forces

Further important considerations include the numerical accuracy, the conservation of numerical order of the associated solvers and of course efficiency.

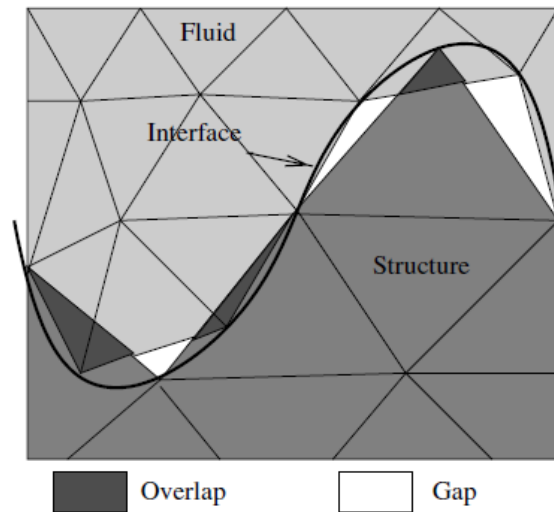


Figure 2.28: Non matching grids. The aerodynamic and structural grids as a general rule do not share the same nodes [170]

Energy preservation is achieved through the virtual work of the fluid acting on the aerodynamic surface Γ_{aero} , which should be equal to the virtual work of the structure (due to displacements) Γ_{str} . This condition results to a fundamental equation regarding the deformation projection of the structural grid on the aerodynamic surface grid,

$$\mathbf{u}_{aero} = \mathbf{H}\mathbf{u}_{str} \quad (2.10.1)$$

This correlates directly the displacements on the aerodynamic mesh \mathbf{u}_{aero} (due to structural deformation) to the displacements of the structural mesh \mathbf{u}_{str} obtained by the structural analysis solver. The matrix \mathbf{H} is the transformation matrix, and the methods are categorized depending on how this matrix is constructed. The aerodynamic forces are projected to the structural surface grid in a similar manner.

Focusing more on this partitioned approach, many methods have been developed to approximate the forces and deformation between the two grid types. A de Boer et al. [170] provided a brief overview of some of the methods used to estimate the transformation matrix.

An obvious and straightforward approach is simply to discard the whole concept of approximating the forces/deformations with interpolation models, and use only the values in the existing grid nodes. In this method, called *Nearest Neighbour Interpolation* (NNI) [171], the quantities of interest on the desired grid node have the value of the closest mesh node of the other discipline. The only advantage of such an approach is its simplicity, but when the grids are not close to matching (as is almost always the case), the transfer between the forces and deformation leads to significant errors.

A more complicated approach is constructed by describing \mathbf{H} with the use of appropriate basis and weighting functions and the Galerkin method. This ultimately leads to the expression of \mathbf{H} as a product of two matrices [172–174]. Depending on the way these matrices are generated, this process splits into *Gauss interpolation* and *Intersection method*. A method that has been extensively used since its introduction is the method of Brown [175] based on rigid links.

Another approach that has been recently popular among researchers due to its simplicity and accuracy, is using RBF functions for generating the interpolation models [176–178]. In an aeroelastic deformation case, the transformation matrix results from the product of the matrix containing all the correlation vectors between the aerodynamic nodes (for which we seek the displacement) and the structural nodes \mathbf{M}_{fs} , with inverse of the structural Gram matrix \mathbf{M}_{ss}^{-1} . In a matrix formulation, this reads:

$$\mathbf{H} = \mathbf{M}_{fs}\mathbf{M}_{ss}^{-1} \quad (2.10.2)$$

It might be important to note that the selection of the kernel function significantly influences the final result. Popular kernel functions have already been reported, however some might not always be appropriate. In this application, one would require a function that provides some local control, so that the forces or displacements taken into account for the approximation in a specific node are limited to the close neighbour nodes. This means that the function values should be inversely proportional to the radius. Therefore, choices like linear or cubic kernels are completely inappropriate within this context. There are two more important benefits associated with such an RBF methodology. Under these conditions, the grid points are essentially "sets of point clouds" and no grid connectivity information is necessary. Therefore they can be used within any type of grids. A further advantage is that rigid body motion²⁸ can be recovered by including a p-order polynomial in the radial basis

²⁸A typical example of such a motion is one corresponding to a full aircraft configuration gust response, in which the fuselage is free to move in 3D space. Such an application is out of the scope of the present PhD work.

function. This augments the sizes of the required matrix but the computational expenses are not significant.

A comparison of the methods, performed above by A. de Boer [170] reveals that the order of accuracy is 1 for the NNI method and 2 for all the rest apart from the RBF based, which has an order of accuracy of 2.5. As expected, the error of the method depends on how fine the non-conformal grids are, but the general trend is that RBF presents more accurate forces/deformation mapping without an increase of the computation time.

Further approaches for tackling this mapping problem are briefly reviewed in [179]. The Constant Volume Tetrahedron (CVT) method proposed by Goura [180] is also another promising and completely different approach. The Boundary Element Method [181] (BEM) is another unique approach, in which the gap between the structure mesh (e.g. surface of the skin of a wingbox) and the aerodynamic surface mesh, is considered to act like an elastic material.

Finally, another flexible method has been developed recently by Samareh [182]. Like the ones discussed previously, the method uses a matrix formulation that conserves energy and moment, while being independent of the mesh topology. In a similar manner to A. de Boer's results, the accuracy depends a lot on the mesh discretisation refinement.

For a more general overview of various approaches to tackle the interface problem, the reader is referred to the review paper of Guru P. Guruswamy [183].

2.10.2 Volume Mesh Deformation due to Structural Deformation

Following the structural analysis, the deformed structure should provide the updated aerodynamic OML shape — deformed due to its aerodynamic loads — through interpolation of the non-conformal mesh nodes as discussed above. However, once the new wing surface mesh is defined, the volume mesh has to be deformed to adapt to the deformation of the surface boundary .

To satisfy this requirement, Rendall and Allen [179] take advantage of the promising characteristics of their RBF based approach and extend it to create a unified methodology for FSI. In this, apart from using the RBF for the loads/deformation mapping, they foresee its potential in grid deformation (as briefly stated in section 2.3.2). In a manner similar to displacement interpolation, a displacement of aerodynamic surface node due to aerodynamic shape parameterisation also leads to the need of deforming the volume mesh accordingly — that is performing interpolation to calculate the volume grid node displacement. Therefore, the RBF methodology for deforming the volume mesh due to shape parameterisation is essentially the same as the one due to structurally originating aerodynamic shape deformation. It is only its application that changes²⁹. The displacement $\mathbf{u}_{\text{aero}_v}$ of the

²⁹Conceptually as a process, and as a required element of multidisciplinary optimisation, surface and

aerodynamic volume node is described by:

$$\mathbf{u}_{\text{aero}_v} = \mathbf{L}\mathbf{u}_{\text{aero}} = \mathbf{L}\mathbf{H}\mathbf{u}_{\text{str}} = \mathbf{K}\mathbf{u}_{\text{str}} \quad (2.10.3)$$

Here, \mathbf{L} is a transformation matrix providing the volume mesh node displacements vector $\mathbf{u}_{\text{aero}_v}$, given the aerodynamic surface nodes displacements vector \mathbf{u}_{aero} . \mathbf{H} is the transformation matrix, transforming the structural node displacements \mathbf{u}_{str} into aerodynamic surface node displacements as in Eq.2.10.1. The total transformation matrix \mathbf{K} is the result of the product between \mathbf{L} and \mathbf{H} and it relates the volume mesh deformation directly to the structural grid displacements.

The last section of this chapter deals with the overview of LF tools and the classification of weight estimation methods for aerostructural applications. Further information regarding typical setup of structural and aerostructural cases can be found in [184–189].

2.10.3 Low Fidelity Aerostructural Analysis Tools

A well known LF tool for aerostructural analysis is ASWING by Mark Drela [190]. This is a development over his initial work found in [191], with the ability to simulate the performance and response of the full aircraft configuration. Therefore, apart from performing static aeroelastic analysis, it can also predict other dynamic phenomena like flutter and gust response. It is appropriate for preliminary design and has been successfully tested when used in the development of Daedalus human powered aircraft.

Recently, an LF aerostructural analysis tool was proposed by Lambert et al. [192]. Its main characteristic is its structure which can accommodate any LF aerodynamic solver to calculate the aero loads. These loads are then projected to a Beam Structural Model (BSM) solved in Nastran. Its main application falls in the emerging High Aspect Ratio (HAR) designs. As such, it uses a non-linear structural analysis so that it accounts for the large tip displacements associated with HAR wings.

2.10.4 Structural Weight Estimation Methods

The objective function derived from the structural part of the MDA is the weight of the structure required to withstand the aerodynamically defined loads, typically in a 2.5g maneuver. The weight of the wing structure should be calculated during each design point analysis, and therefore a LF and a HF weight estimation tool (if a MF methodology is

volume mesh deformation to adapt to structural deformation are still distinguished from the mesh deformation required by the design parameterisation.

used) needs to be adjusted with the respective structural design. Ideally, the weight estimation process should be sensitive to the structural and coupled design variables. In an opposite case, the optimiser will identify a subset of inactive design variables. Apart from leading to non meaningful designs, this will create numerical instabilities in the case of SBO.

Traditionally, weight estimation for the conceptual design stage uses statistical data which correlate the weight of the wing or the aircraft with significant aircraft characteristics (wingspan, number of passengers etc.) — known as *Class I* methods. However, for a use in conceptual and conceptual to preliminary aerostructural optimisation or trade-off studies, models need to be more accurate and sensitive to an already defined (within some maturity) structure design. Such methods comprise the *Class II* and *Class III* categories. Here, aspects of the design are taken into account, and in detailed estimations of Class III, FEM models are used for increased accuracy. A historic review of the various methods developed is available in [193]. As Elham points out, a Class II *and* 1/2 is defined, and the respective methods use both analytical and empirical approaches leading to a wide range of attained accuracy. Elham [194] proposes EMWET, a weight estimation methodology that uses an analytical approach — based on typical strength of materials theory — for the wingbox and an empirical method for the rib weight. This LF tool is designed for use in rapid MDO, as a LF weight estimation tool [195].

In his PhD thesis, Dababneh [193] provides an overview of mass estimation methods and directly connects the given aero loads to the weight of the structure using a Nastran structural sizing application. To account for the variable fidelity effect, the methodology is applied to four different wingbox models of increasing fidelity.

Optimisation Methodology

Let's get dangerous!!!

Drake Mallard

IN the present chapter, the needs raised by multidisciplinary design are described and then a detailed and systematic overview of the developed optimisation methodology to satisfy those needs is provided. It involves some basic ideas and mathematical formulations which are currently being used as standalone tools from the optimisation community. These function as the building blocks of this framework and are presented first. They are accompanied by the author's ideas and modifications to adapt the framework to our pre-specified design needs. Finally, the unified optimisation methodology developed by the author is presented.

3.1 Desired Optimisation Attributes

The previous chapter provided an overview of a typical aircraft design process as well as the various optimisation methods currently under development from research groups and their use for the design of aeronautic configurations. Evidently, regardless of the various attributes any optimisation tool may possess, if it is to be used in the industry it should be as fast as possible. Of course, as one can argue, this is quite a vague requirement as optimisation computational expenses depend on the method, which in turn depends on the design need that the tool aims in covering. However, what can be said with confidence is that for each application, an optimisation tool should be fast *to allow the engineers to perform many design studies in a reasonable wall clock time to extract information required for the design process*. This is particularly true in the conceptual design stage, when the design space is more extensive and requires efficient exploration studies to suggest potential design solutions. Therefore, the formulation and the inherent attributes of the optimisation approach might change the way the tool is used, as well as the duration of the industrial studies. A

MO method provides a set of optimum designs and requires fewer number of job executions to provide sufficient design information. The repetition of the optimisation study in this case aims in providing additional pareto front points as well as new designs dominating earlier pareto points. A single MO job is more computationally expensive than any respective SO process, with the latter however requiring more repetitions to provide similar amount of information. In an early development phase, extracting as much design information as possible is crucial, with the goal being to rapidly and reliably assess multiple design possibilities. Hence, *an explorative gradient free MO formulation is more appropriate in the scope of this design stage*. Multidisciplinary design involves disciplinary interactions and design change propagation [196] by definition. As such, it should be considered in the early design stage where disciplinary synergies can be identified and exploited. The interdisciplinary interactions increase the extent and complexity of the design stage; there are more potential design directions that have to be examined by the engineers in the conceptual stage. Therefore, the need for fast MO optimisation in multidisciplinary design problems is even higher.

Having established the importance of a MO formulation and computational efficiency, it should be stressed that the use of low fidelity analysis is only one of the ways to get results fast, but certainly not the best. Short wall clock times are the result of the use of low cost analysis models, but this is a deceptive benefit as it comes with the expense of design reliability. The reduction of the analysis fidelity raises the issue of performance uncertainty. This is by no means acceptable in conceptual multidisciplinary design procedures as it usually means a lack of understanding and configurations that in the long run are far from optimum. Hence, there is the *need to keep optimisation costs low while maintaining a high level of reliability, to avoid additional costs associated with redesign and fixes during the preliminary and detailed design stage*.

3.2 Methodology Requirements

3.2.1 Requirements to Tackle Early Design Stage Needs

Following these needs, an efficient optimisation framework for early design stages should possess the following attributes:

1. Design space exploration and ability to identify the dominant design directions that lead to global optimality.
2. Multiobjective formulation that can identify the optimum tradeoff between the objectives, providing a pareto set.
3. Reliability. The design directions provided in the form of the pareto set, should be of a high level of fidelity that corresponds to later design stages.

4. Low computational costs — despite the above specifications — to allow its effective use within the conceptual design processes.
5. User friendly. The framework should act as a complete standalone optimisation black box that can accommodate any kind of heavy analysis design problems. It would therefore be an efficient alternative to costly standalone MO gradient free optimisers.

It is widely understood and accepted in the optimisation research community that a methodology cannot achieve its goals without being inefficient in other aspects. In this sense, a method that covers the requirements above displays the following limitations:

1. Although providing design directions for global optimality and the global optimum area should be expected, the actual global optimum point cannot be located by an exploration scheme.
2. A fine-tuning optimisation framework that is efficient in local search is required to locate the actual global optimum point, after the global optimum region has been identified. This "optimisation pattern" is in total agreement with the successive design freedom reduction observed during the design process (conceptual design followed by more detailed design with a narrower design space).
3. As with any exploratory optimisation study, its cost will be higher than a local one. This is due to the need for dense infill sampling as well as the inherent attribute of exploration schemes to allow for — some — stochastic moving in the design space even after initially locating promising design directions.

3.2.2 Attributes for Efficient Implementation in Multidisciplinary Problems

In multidisciplinary design problems, the methodology developed is being used within the standard MDO architectures. This is a novel optimisation direction as typically MDO problems involve gradient based algorithms which require a low number iterations to reach convergence to a local optimum. In the presence of few objectives and constraints but many design variables as in detailed design, adjoint-based optimisers are indeed very efficient — when sufficient convergence of the primal and adjoint equations can be achieved [197]. However, this framework is specifically designed to satisfy the early stage needs outlined above. Consequently, it should reduce the costs associated with the coupled MDO design space exploration while providing design directions of high reliability to accelerate the transition cycle between the conceptual and preliminary design stage. Within an MDO architecture its use is appropriate and efficient as an MDO process guide through the system level. The elements composing the method have been specifically selected in such a way so that the framework can make use of any analysis tool or type, which essentially acts as a black box analysis, called by a black box optimisation tool.

This feature makes the framework flexible, allowing its easy implementation even in industrial environments characterized by geographically remote design groups that use their own internally developed software. Distributed MDO architectures are more appealing in these cases, since the optimisation process is split within the design entities. The optimisation methodology has been specifically developed to maximise its efficiency in such MDO applications. In distributed architectures, the system level still calls heavy analysis problems — combination of MDA and disciplinary optimisation problems —, but the associated dimensionality is reduced. This increases the efficiency of surrogate modelling methods [88] making them useful even in such complex optimisation problems.

That is a novel approach on MDO that utilises concepts aiming in:

- Reduction of the analysis-related costs
- Shortening design cycle periods
- Reliability in the design directions
- Satisfaction of the design exploration needs

In addition, a truly multiobjective formulation which is novel in MDO, is of great interest for the industry and especially in the conceptual stages, as it provides more design information and complete tradeoff studies. Following this need, this methodology was developed to tackle multiobjective problems as well.

3.3 Methodology Overview

With the requirements of the methodology clearly identified, one can develop the necessary formulation. This is done by a well defined "assembly" of some of the methods presented in the previous chapter, which are considered appropriate based on the specifications.

To satisfy the requirements outlined earlier, the proposed methodology features a combination of the following optimisation approaches.

- Use of surrogate models to predict the trends of the objective and constraint functions. The advantage of using metamodels is that the cost of generating and exploring a surrogate is lower than using function calls. This potential gain however is limited on the special case of relatively low dimensionality problems with small number of training data points. A conceptual design optimisation study falls within this category since, what is sought at this stage is the dominant design variables and trends. Detailed fine tuning cases cannot be handled efficiently by the use of surrogates.

- A method [104] that can make efficient use of the surrogate models providing design space exploration and global optimality without investing excessive computational resources.
- An optimiser that is efficient in solving the suboptimisation problem introduced by the use of a surrogate based optimisation plan. It should be able to perform MO global search.
- Use of analysis models of variable fidelity. Fast low fidelity tools should be used to accelerate the iterative sampling process, but the design directions should be reliable. Only configurations examined with high fidelity analysis tools are considered reliable.

The proposed methodology constitutes the core of the optimisation framework to be used within an MDO environment/formulation. In a loosely coupled plan, this translates to performing multidisciplinary analyses once a new infill design point has been identified by the method.

3.3.1 Geometry Parameterisation and Mesh Deformation

The geometry parameterisation is performed using the FFD method. As discussed in section 2.3.1, it was evident that FFD can cover the 2D and 3D geometry parameterisation needs regardless of the geometry for which it will be applied to (conventional or novel). It is a fast and robust method that provides a high level of flexibility without the need for an excessive number of control points. This approach is very popular in free source or commercial preprocessing software, which makes it easily accessible in industrial environment as well. An important aspect is that the same method can also be implemented for the CFD mesh deformation required for each new design. In fact, it works as a CAD free method which is actually what an aerodynamic optimisation algorithm requires. A direct parameterisation of the aerodynamic surface mesh (OML) is sufficient, with no further needs for geometry parameterisation. As such, seeking a dedicated mesh deformation algorithm — like the ones presented in the previous chapter — is avoided. The mesh deformation required to map the structural displacements in the deformation of the aerodynamic surface raises other requirements and a different method is being used. More on this on section 7.2.7.

3.3.2 Surrogate modelling in a Multifidelity Context

First, let us define the optimisation problem in its generalised unconstrained form. Our goal is to minimise a function (or a set of functions) of interest $\mathbf{f} \in \mathbb{O}$, as defined in equation

(3.3.1).

$$\min_{\mathbf{x} \in \mathbb{D}} \mathbf{f}(\mathbf{x}). \quad (3.3.1)$$

Here, \mathbf{x} is a design point, a vector of dimension n and \mathbb{D} is a subset of \mathbb{R}^n , where $n \geq 1$. \mathbb{O} is a subset of \mathbb{R}^l , where $l \geq 1$ is the objective space size.

The above problem — already defined in a form that can be solved by a black box gradient free optimiser — can be transformed into a different formulation with the implementation of surrogate models and MF analysis methods, as described in the sections that follow.

For simplicity, consider a single objective space $l = 1$ so that vector of functions \mathbf{f} essentially becomes a scalar function f . Suppose the existence of a set of analysis tools of variable fidelity used to calculate f , whose results by convention are thereafter represented by y . State of the art MF approaches suggest that the results from LF and HF tools, y_{LF} and y_{HF} respectively, can be superimposed according to the relationship below [107],

$$y_{HF}(\mathbf{x}) = y_{LF}(\mathbf{x}) + e(\mathbf{x}) \quad (3.3.2)$$

This relation implies that the HF result is considered to be "the truth", with the LF results being associated with an error and not providing further information [198]. A typical application of this decomposition within an SBO framework [104] is the Trust Region [199–201] (TR) approach. It involves the generation of a locally accurate error surrogate to correct the LF analysis value according to Eq.3.3.2. However, such an optimisation methodology is not appropriate for our needs for two main reasons. It does not provide the exploration characteristics required in a conceptual design stage. Furthermore, it demands a high number of LF analyses since the LF tool is directly called by the optimiser during the suboptimisation stage. Such an approach, even for low cost LF tools, becomes prohibitively expensive within an MO MDO study. To minimize the suboptimisation costs, the LF results have to be replaced by surrogate model predictions. Metamodels and their occasional training is cheaper for a reasonable number of training data points. Then, during the suboptimisation process, the optimiser calls a surrogate model predictor which is of course way cheaper than a LF analysis. Therefore, in order to secure that the metamodels predict the HF results, MF information should be directly implemented in the surrogate generated using Eq.3.3.2.

Ideally, one would implement this in an RBF model, which would be very cheap to construct. However, it is an important requirement that the SBO plan can provide sufficient design space exploration. Exploratory methods like PI or EI require information regarding the uncertainty of the metamodel itself, in a form of a mean squared error, which can be estimated when a Gaussian correlation is assumed. Therefore, a Kriging model has to be used as basis of the method¹.

¹Mathematically speaking, RBF can still be used to support a PI/EI SBO plan when a Gaussian kernel is

A popular metamodel that can exploit the available MF data — and can also do so within an explorative SBO plan — is Co-Kriging [118]. Unlike Kriging, it uses both LF and HF point correlation to compose a unified MF covariance matrix. Unfortunately, such an approach includes the tuning of extra hyperparameters, increasing the likelihood estimation cost quadratically to the order of the matrix. Therefore, it is considered that Co-Kriging covariance matrix operations make the metamodel generation too expensive for real industrial MDO applications at which we aim.²

Instead, to reduce computational expenses while still approximating the HF function and aiming for global HF optimality, a novel MF modified Kriging based model (MF mod-Kriging) has been developed. The computationally efficient RBF model cannot provide global exploration within an SBO framework [88]. The following paragraphs present the modification of the ordinary Kriging model so that it can be used like Co-Kriging when MF information is available, but without its increased associated training costs.

As stated earlier, only HF results are considered to be accurate within the numerical framework³. Most simulations use LF tools and do not provide additional information [198] to the search, but are only used to efficiently guide it. However, LF results are associated with a non constant error. Therefore, for our Kriging modification to be efficient based on the aforementioned accuracy requirements, it needs to perform as an interpolation through HF points and as a regression through LF ones, as shown in the qualitative 1D example of Fig.3.1. The regression has to be dependent on the predicted error of each LF data point. This error is either estimated by a simple RBF [107] or a Kriging model using Eq.3.3.2, given a sampling of both LF and HF observations in common points. For this, the space filling Latin Hypercube Sampling (LHS) method with a Morris-Mitchell maximin approach [59, 60] is used.

The sampling requires m points analysed only using the LF tool at \mathbf{x}_{LF} , and n new points analysed with both the LF and HF tool at \mathbf{x}_{HF} , where typically — but not necessarily — $n < m$. As such, we define the complete objective value vector \mathbf{y} , and the Error vector \mathbf{e}

used as this also assumes a Gaussian correlation between the training data. However, the use of a constant shape parameter associated with RBF, makes the metamodeling predictions and its MSE prediction less accurate in a challenging multimodal MDO related design. In the error space nevertheless, RBF can be used with greater confidence if this space is smoother.

²The validity of this assumption is examined in following chapters by comparing this approach with a Co-Kriging based one.

³That is, only HF results are considered reliable for the engineer in the sense described in section 3.2.

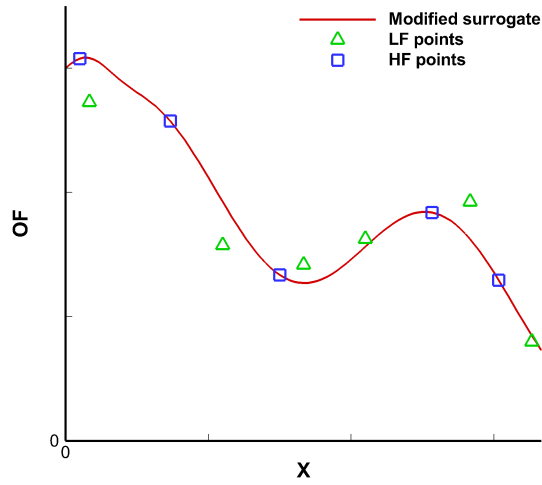


Figure 3.1: A qualitative display of the MF Kriging model requirement in a 1D example. Interpolation is performed through the HF data but LF data are fitted since they are subject to error.

consisting of n data, derived by Eq.3.3.2

$$\mathbf{y} = \begin{pmatrix} y_{LF}^{(1)}(\mathbf{x}_{LF}^{(1)}) \\ y_{LF}^{(2)}(\mathbf{x}_{LF}^{(2)}) \\ \vdots \\ y_{LF}^{(m)}(\mathbf{x}_{LF}^{(m)}) \\ y_{LF}^{(m+1)}(\mathbf{x}_{HF}^{(1)}) \\ y_{LF}^{(m+2)}(\mathbf{x}_{HF}^{(2)}) \\ \vdots \\ y_{LF}^{(m+n)}(\mathbf{x}_{HF}^{(n)}) \\ y_{HF}^{(m+n+1)}(\mathbf{x}_{HF}^{(1)}) \\ y_{HF}^{(m+n+2)}(\mathbf{x}_{HF}^{(2)}) \\ \vdots \\ y_{HF}^{(m+n+n)}(\mathbf{x}_{HF}^{(n)}) \end{pmatrix}, \mathbf{e} = \begin{pmatrix} e^{(1)}(\mathbf{x}_{HF}^{(1)}) \\ e^{(2)}(\mathbf{x}_{HF}^{(2)}) \\ \vdots \\ e^{(n)}(\mathbf{x}_{HF}^{(n)}) \end{pmatrix} \quad (3.3.3)$$

Given the training vector \mathbf{e} including the error observations, the cheapest way to estimate the LF tool error is by using an RBF model. For this, in matrix form we have,

$$\Phi \mathbf{a} = \mathbf{e} \quad (3.3.4)$$

When Gaussian kernel functions are used, the Gram matrix Φ consists of elements of

the form,

$$\phi_{ij} = \exp\left(-\theta\|\mathbf{x}_j - \mathbf{x}_i\|\right)^p \quad (3.3.5)$$

where the smoothness parameter p is set to $p = 2$. Alternatively, to the author's experience Matérn functions provide an accurate and robust choice [85]. The parameters vector α is determined by performing a Cholesky decomposition and back-substitution⁴.

Given the vector solution \mathbf{a} , the error RBF model is trained. The error associated with the use of the LF tool can be now estimated in any design point of the design space. Later in this chapter it is shown how this error estimation metamodel is important in MF modK-ricing.

To demonstrate this, initially suppose an ordinary Kriging, with the correlation matrix,

$$\Psi = \begin{pmatrix} \text{Corr}[y(\mathbf{x}_1), y(\mathbf{x}_1)] & \text{Corr}[y(\mathbf{x}_1), y(\mathbf{x}_2)] & \cdots & \text{Corr}[y(\mathbf{x}_1), y(\mathbf{x}_n)] \\ \text{Corr}[y(\mathbf{x}_2), y(\mathbf{x}_1)] & \cdots & \cdots & \text{Corr}[y(\mathbf{x}_2), y(\mathbf{x}_n)] \\ \vdots & \vdots & \ddots & \vdots \\ \text{Corr}[y(\mathbf{x}_n), y(\mathbf{x}_1)] & \text{Corr}[y(\mathbf{x}_n), y(\mathbf{x}_2)] & \cdots & \text{Corr}[y(\mathbf{x}_n), y(\mathbf{x}_n)] \end{pmatrix} \quad (3.3.6)$$

The elements of this matrix estimate the correlation of the data points by modelling the function as a Gaussian process:

$$\text{Corr}[y(\mathbf{x}_i), y(\mathbf{x}_j)] = \exp\left(-\sum_{l=1}^d \theta_l \|x_{j,l} - x_{i,l}\|^{p_l}\right) \quad (3.3.7)$$

Here, d is the number of the design variables and θ_l and p_l are the shape and smoothing parameters respectively, that need to be defined.

We generate the Kriging predictor by optimising the set of μ , σ^2 , θ_l , p_l parameters. The mean μ and variance σ^2 are easily optimised in a deterministic manner. Finding the optimum shape and smooth parameter ($\hat{\theta}_l$ and \hat{p}_l) however, requires a stochastic optimisation process aiming at maximizing the Likelihood Estimation function⁵ λ given by,

⁴The appropriate method of solving the system actually depends on the properties of the symmetric Gram matrix. Most kernel functions create a positive definite Gram matrix which is most efficiently solved by a Cholesky decomposition. If the matrix is not positive definite, the generic LU decomposition method applies. In the case of ill-conditioned matrices resulting by poor spacing between the training data, SVD decomposition can be used.

⁵Intuitively this means that the optimum parameters are the ones that most likely have produced the sampling data.

$$\lambda = -\frac{n}{2} \log(\hat{\sigma}^2) - \frac{1}{2} \log |\Psi| \quad (3.3.8)$$

Therefore, the hyperparameters optimisation problem is defined by,

$$\hat{\theta}_l, \hat{p}_l = \arg \min_{\theta, p} \lambda$$

Finally, the Kriging predictor takes the form,

$$\hat{y}(\mathbf{x}) = \hat{\mu} + \boldsymbol{\psi}^T \boldsymbol{\Psi}^{-1}(\mathbf{y} - \mathbf{1}) \quad (3.3.9)$$

where $\boldsymbol{\psi}$ is the correlation vector associated with the point to be predicted.

3.3.3 Surrogate Based Optimisation in a Multifidelity Context

The Kriging predictor is not used directly since we apply the Kriging model to provide the next sampling point under the EI [104] plan. This approach can lead to global optimality without prohibitively costly design space exploration. A balance is attained as the search is based both on the most promising design points (according to the predictor y) as well as the uncertainty generated from unexplored regions. To quantify this uncertainty, information is required regarding the metamodel's Mean Squared Error (MSE), given by,

$$\hat{s}^2(\mathbf{x}) = \sigma^2 \left[1 - \boldsymbol{\psi}^T \boldsymbol{\Psi}^{-1} \boldsymbol{\psi} + \frac{1 - \mathbf{1}^T \boldsymbol{\Psi}^{-1} \boldsymbol{\psi}}{\mathbf{1}^T \boldsymbol{\Psi}^{-1} \mathbf{1}} \right] \quad (3.3.10)$$

MSE is zero in training data points and it increases between them due to value uncertainty. The above formulation is used to construct an estimator of the probability of improvement as well as the expected improvement of the objective function in any design space point, given the current minimum value y_{\min} . In any point where $\hat{s}(\mathbf{x}) \neq 0$, the probability of improvement is expressed as,

$$PI = \Phi \left(\frac{y_{\min} - \hat{y}(\mathbf{x})}{\hat{s}(\mathbf{x})} \right) \quad (3.3.11)$$

and the expected improvement is expressed as,

$$EI = (y_{\min} - \hat{y}(\mathbf{x})) \Phi\left(\frac{y_{\min} - \hat{y}(\mathbf{x})}{\hat{\sigma}(\mathbf{x})}\right) + \hat{\sigma}(\mathbf{x})\phi\left(\frac{y_{\min} - \hat{y}(\mathbf{x})}{\hat{\sigma}(\mathbf{x})}\right) \quad (3.3.12)$$

where Φ is the cumulative distribution function

$$\Phi(x) = \frac{1}{2} + \frac{1}{2}erf\left(x/\sqrt{2}\right) \quad (3.3.13)$$

and ϕ is the probability density function. In Eq.3.3.11,3.3.13, erf is the error function expressed as,

$$erf(x) = \frac{1}{\sqrt{\pi}} \int_{-x}^x \exp -t^2/2 \quad (3.3.14)$$

The infill point $x^* \in \mathbb{D}$ is then the solution of the suboptimisation problem,

$$\mathbf{x}^* = \arg\left(\max_{\mathbf{x} \in \mathbb{D}} EI\right) \quad (3.3.15)$$

3.3.4 Multifidelity Treatment in Kriging Model

So far, the ordinary Kriging has been presented as commonly found in literature and extensively used by various research groups. However, this cannot accommodate data resulting from MF analyses. The MF Kriging modification developed proposes a simple way to superimpose LF and HF information within the model. Additionally, this MF information is introduced in the Kriging predictor (Eq.3.3.9) and MSE (Eq.3.3.10), therefore transforming the EI method into an MF EI method.

During this work, a way for a Kriging model to incorporate MF data was examined. This was done by simply adding the error prediction defined earlier, for each LF point in the correlation matrix diagonal. This approach makes the diagonal error term functioning as a regularisation parameter in similar way to a constant parameter being added in the diagonal to fit noisy signals. Physically, this means that we consider the inaccuracy of the LF model to be inducing noise in the objective function space. Research and applications using this approach proved its efficiency and success in improving the objective function approximation. However, it was observed that in high error values (in relation to the diagonal correlation matrix term), the method becomes numerically unstable. The MSE quantity cannot be calculated and subsequently, the method cannot be used robustly in a EI SBO context. This forced the development of an alternative modification where the MF information is not inserted in the correlation matrix.

In this MF modKriging method, the correlation matrix is defined using only the LF training data of our MF vector \mathbf{y} , so that:

$$\Psi = \begin{pmatrix} \text{Corr}[y_{LF}(\mathbf{x}_1), y_{LF}(\mathbf{x}_1)] & \cdots & \text{Corr}[y_{LF}(\mathbf{x}_1), y_{LF}(\mathbf{x}_{m+n})] \\ \text{Corr}[y_{LF}(\mathbf{x}_2), y_{LF}(\mathbf{x}_1)] & \cdots & \text{Corr}[y_{LF}(\mathbf{x}_2), y_{LF}(\mathbf{x}_{m+n})] \\ \vdots & \ddots & \vdots \\ \text{Corr}[y_{LF}(\mathbf{x}_{m+n}), y_{LF}(\mathbf{x}_1)] & \cdots & \text{Corr}[y_{LF}(\mathbf{x}_{m+n}), y_{LF}(\mathbf{x}_{m+n})] \end{pmatrix} \quad (3.3.16)$$

The Kriging predictor \hat{y} now takes the following form:

$$\hat{y}(\mathbf{x}) = \hat{\mu} + \psi^T \Psi^{-1}(\mathbf{y} - \mathbf{1}) + e(\mathbf{x}) \quad (3.3.17)$$

where $\hat{\mu}$ is the Kriging optimised mean value calculated as,

$$\hat{\mu} = \frac{\mathbf{1}^T \Psi^{-1} \mathbf{y}}{\mathbf{1}^T \Psi^{-1} \mathbf{1}} \quad (3.3.18)$$

The HF information is recovered by $e(\mathbf{x})$, which is the surrogate prediction of the LF tool error, defined by Eq.3.3.2. Therefore, Kriging predictor now interpolates the HF points and fits the LF ones depending on their predicted error. However, since the EI estimation is dependent on MSE as well, complete HF information recovery in the EI space demands the alteration of the MSE equation as:

$$\hat{s}^2(\mathbf{x}) = \sigma^2 \left[1 - \psi^T \Psi^{-1} \psi + \frac{1 - \mathbf{1}^T \Psi^{-1} \psi}{\mathbf{1}^T \Psi^{-1} \mathbf{1}} \right] + s_e \quad (3.3.19)$$

where the model variation σ^2 is given by,

$$\sigma^2 = \frac{(\mathbf{y} - \mathbf{1}\mu)^T \Psi^{-1} (\mathbf{y} - \mathbf{1}\mu)}{n} \quad (3.3.20)$$

with n being the number of sampling data points. In Eq.3.3.19, the s_e term is the MSE of the error metamodel, essentially expressing the uncertainty that arises when using the LF tool correction metamodel itself. The MSE quantity is typically provided by Kriging models through Gaussian based correlation matrix operations, as above. Therefore, s_e is formulated in a straightforward way if a Kriging model is used for the LF error prediction. However, as originally defined in the requirements, the optimisation framework should have the minimum computational costs. As such, we often use RBF for the LF error prediction. In this case, by using a Gaussian kernel we can relate the Gram matrix to the Correlation matrix used in Kriging models. By comparing Eq.3.3.5 and Eq.3.3.7 we observe that Gram matrix is identical to the Correlation matrix in the special case that: (i) we define the training data points to be correlated with each other in the same way for all design coordinates (isotropic model), and (ii) this correlation coincides with the correla-

tion defined in the Gaussian RBF kernel through the constant shape parameters θ and p . Namely, for a case where $\theta = \theta_1 = \theta_2, \dots, \theta_d$ and $p = 2$, the following holds,

$$\mathbf{\Psi} = \mathbf{\Phi} \quad (3.3.21)$$

This essentially implies that the RBF model used to express the error of the LF tool has the aforementioned, defined correlation characteristics. Therefore, we can use it to predict a distribution of the MSE, with exactly the same "assumptions" used in any RBF interpolation model (that is, isotropic shape parameter). As such, s_e can now be calculated as,

$$s_e = \sigma^2 \left[1 - \psi^T \mathbf{\Psi}^{-1} \psi + \frac{1 - \mathbf{1}^T \mathbf{\Psi}^{-1} \psi}{\mathbf{1}^T \mathbf{\Psi}^{-1} \mathbf{1}} \right] = \sigma_e \left[1 - \phi^T \mathbf{\Phi}^{-1} \phi + \frac{1 - \mathbf{1}^T \mathbf{\Phi}^{-1} \phi}{\mathbf{1}^T \mathbf{\Phi}^{-1} \mathbf{1}} \right] \quad (3.3.22)$$

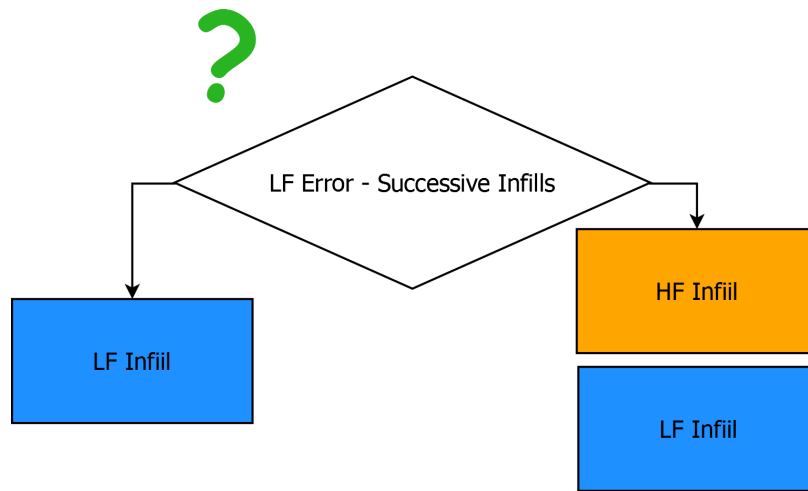
where the variance of the error model σ_e^2 can be calculated using eqs.3.3.10,3.3.20, by setting $\mathbf{\Psi} = \mathbf{\Phi}$ and $\psi = \phi$.

In the generic case where a Kriging model has $\theta_1 \neq \theta_2, \dots, \theta_d$, its predicted MSE distribution will divert from the one similarly predicted by RBF. Nevertheless, such a prediction disagreement is of exactly the same nature as the disagreement between an RBF and a trained Kriging model value predictor.

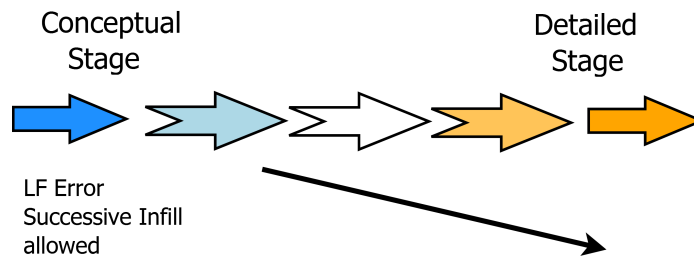
The importance of using Eq.3.3.19 and Eq.3.3.22 lies in the fact that they restore a zero MSE value to the HF data points and a finite value to the LF ones. Apart from fitting LF data according to their predicted errors and interpolating HF data, the method can now distinguish between the uncertainty characteristics of the LF/HF points in terms of MSE, and eventually EI (which is our value of interest). The loss of LF/HF data correlation (as exploited in Co-Kriging) is compensated by the reduction of the overall model training costs.

3.3.5 Multifidelity Infill Sampling Plan

Evidently, this use of MF data to modify the metamodel representation deviates from other popular methods like trust region and space mapping [103, 202]. Furthermore, contrary to typical EI practice, our infill points are not always sampled using the HF tool. The decomposition of Eq.3.3.2 that uses a global error model provides an alternative a more efficient infill sampling plan possibility. A straightforward plan is developed, which allows the engineer to adapt the method to his needs and to the stage of the design process to which the optimisation tool is used. The solution of the suboptimisation problem leads to a potential



(a) Infill tool fidelity criterion.



(b) Versatility of the criterion, to adapt to the desired design stage.

Figure 3.2: MF infill sampling approach.

LF or HF infill analysis. If the error predicted on the infill point is lower than an error threshold defined by the engineer, then the LF tool is considered to be "accurate enough" in this area of the design space and LF analysis is performed. Hence, computational expenses are avoided for points for which the LF tool is reliable enough for the purpose of the respective design stage. The LF analysis would provide sufficient information since LF and HF tools would show no significant difference. Nevertheless, when a predefined number of successive LF infill samplings is surpassed, both HF and LF infill sampling analysis is performed. It is critical to ensure that the error estimation surrogate is updated frequently enough to allow for reliable predictions in all interesting areas. Failure in updating the error surrogate would lead to an excessive number of LF infill samplings, as the predicted error may be very low in unexplored areas⁶. Furthermore, bad error prediction significantly deteriorates the reliability of the y predictor, tricking EI into exploring fictionally promising points⁷.

This flexible infill sampling methodology makes the tool appropriate for an industrial

⁶This is true in RBF models with kernel functions that approach zero in an asymptotic manner, like a Gaussian kernel. It does not hold in linear or cubic kernel cases.

⁷A poor error model can deceive the EI plan, leading to inefficient exploration or convergence to LF optimality.

environment. Since the error and iteration limits can be explicitly defined, the engineer is allowed to use the tool either for conceptual or detailed design. High error threshold and iterations limits lead to a quick optimum tradeoff study in a conceptual design stage. The inverse would be preferable in later design stage studies. This approach is illustrated in Fig.3.2.

3.3.6 Single Objective Suboptimisation Process

When the methodology is applied to single objective problems, the suboptimisation process simply refers to finding the point in the design space with the maximum predicted expected improvement — as in Eq.3.3.15. That is,

$$\mathbf{x}^* = \arg \left(\max_{\mathbf{x} \in \mathbb{D}} EI \right)$$

Any explorative global optimiser can be used at this stage, as the EI space is multimodal. Therefore, to avoid sampling a local optimum related point extensive search is required. Typical options for this include any stochastic algorithm like PSO, MIDACO etc. During the course of this work, the efficiency of various optimisers had been assessed, including ALPSO, NSGA2, MIDACO, ALHSO and Nelder-Mead non linear simplex algorithms. Out of these ALPSO and Nelder-Mead were found superior in terms of cost and result. However, it has to be noted that the cost and efficiency of a gradient free algorithm is not critical. One of the benefits of the presented methodology is that these — costly — global algorithms now act on the simple algebraic EI expression and not on an expensive analysis. Therefore, any gradient free optimiser can be used without cost penalties. As it will be shown in more detail in following section, the imposition of the constraints takes place during this stage as well. Again, this is beneficial because the constraint functions are similarly and cheaply calculated and the feasible design space is efficiently identified during the suboptimisation process.

3.3.7 Multiobjective Suboptimisation Process

The multiobjective suboptimisation process is a very similar procedure in a sense that we are seeking a point or a set of points to be promising in terms of EI. However, there at least two ways with which we can tackle this problem:

- By considering the probability of new design dominating at least a single member of the pareto front, as overviewed in Forrester [88].

- A simple and efficient approach that we propose, which favours the widening of the pareto front, a critical characteristic for early stage MDO as outlined in our requirements.

Expected Improvement for Improving the Current Pareto Front

In this approach, an expression for the probability P of a new sampling point improving I the current pareto front is being used. For example, given two objective function values y_1 and y_2 , and m members of the pareto front $y_1^*, y_2^* \dots, y_m^*$, this is provided by:

$$\begin{aligned}
 P[Y_1(x) < \mathbf{y}_1^* \cap Y_2(x) < \mathbf{y}_2^*] = & \Phi\left(\frac{y_1^{*(i)} - \hat{y}_1(x)}{s_1(x)}\right) \\
 & + \sum_{i=1}^{m-1} \left\{ \Phi\left(\frac{y_1^{*(i+1)} - \hat{y}_1(x)}{s_1(x)}\right) - \Phi\left(\frac{y_1^{*(i)} - \hat{y}_1(x)}{s_1(x)}\right) \right\} \\
 & \times \Phi\left(\frac{y_2^{*(i+1)} - \hat{y}_2(x)}{s_2(x)}\right) \\
 & + \left\{ 1 - \Phi\left(\frac{y_1^{*(m)} - \hat{y}_1(x)}{s_1(x)}\right) \right\} \Phi\left(\frac{y_2^{*(m)} - \hat{y}_2(x)}{s_2(x)}\right)
 \end{aligned} \tag{3.3.23}$$

with Φ being the cumulative distribution function.

The expected improvement is now calculated as,

$$E[I(\mathbf{x}^*)] = P[I(\mathbf{x}^*)] \sqrt{\left(\bar{Y}_1(x) - y_1^*(\mathbf{x}^*)\right)^2 + \left(\bar{Y}_2(x) - y_2^*(\mathbf{x}^*)\right)^2} \tag{3.3.24}$$

Y_1 and Y_2 are expressed by,

$$\bar{Y}_1(x) = \left[\begin{array}{l} \hat{y}_1(x) \Phi \left(\frac{y_1^{*(i)} - \hat{y}_1(x)}{s_1(x)} \right) - s_1(x) \phi \left(\frac{y_1^{*(i)} - \hat{y}_1(x)}{s_1(x)} \right) \\ + \sum_{i=1}^{m-1} \left\{ \left[\hat{y}_1(x) \Phi \left(\frac{y_1^{*(i+1)} - \hat{y}_1(x)}{s_1(x)} \right) - s_1(x) - \phi \left(\frac{y_1^{*(i+1)} - \hat{y}_1(x)}{s_1(x)} \right) \right] \right. \\ \left. - \left[\hat{y}_1(x) \Phi \left(\frac{y_1^{*(i)} - \hat{y}_1(x)}{s_1(x)} \right) - s_1(x) - \phi \left(\frac{y_1^{*(i)} - \hat{y}_1(x)}{s_1(x)} \right) \right] \right\} \\ \times \Phi \left(\frac{y_2^{*(i+1)} - \hat{y}_2(x)}{s_2(x)} \right) \\ + \left[\hat{y}_1(x) \Phi \left(\frac{y_1^{*(m)} - \hat{y}_1(x)}{s_1(x)} \right) - s_1(x) - \phi \left(\frac{y_1^{*(m)} - \hat{y}_1(x)}{s_1(x)} \right) \right] \\ \times \Phi \left(\frac{y_2^{*(m)} - \hat{y}_2(x)}{s_2(x)} \right) \end{array} \right] / P[I(\mathbf{x}^*)] \quad (3.3.25)$$

where ϕ is the probability density function.

As in the single objective process, the new infill point is provided by,

$$\mathbf{x}^* = \arg \left(\max_{\mathbf{x} \in \mathbb{D}} EI \right)$$

This method is used as a basis for comparison with our simple approach presented in the following section. The different infill approaches are assessed in terms of pareto front quality and computational efficiency.

Pareto Expected Improvement Parallel Infill Approach

In our implementation, for an MO problem involving p objectives the suboptimisation problem is explicitly expressed by,

$$\mathbf{x}_1^*, \mathbf{x}_2^* \dots \mathbf{x}_k^* = \arg \left(\max_{\mathbf{x} \in D} EI_1 \text{ vs } \max_{\mathbf{x} \in D} EI_2 \text{ vs } \dots \max_{\mathbf{x} \in D} EI_p \right) \quad (3.3.26)$$

Therefore, a pareto front of this cheap MO optimisation problem, provides k infill points which can be then sampled in parallel. This more than compensates for any potential expenses due to the MO search. Such an explicit MO suboptimisation process approach is not typically found in MO SBO methods [107], however in our experience it is this explicit

formulation that guarantees a wide pareto front. On top of this, allowing parallel infill analyses, it improves the surrogate model's accuracy in the cost of a single analysis .

Multiobjective Particle Swarm Optimisation

The MO EI maximisation problem is solved using our own implementation of Multiobjective Particle Swarm Optimisation (MOPSO) code developed specifically for the needs of this thesis. It is a Multiobjective (MO) version [139] of the PSO algorithm which when applied in the suboptimisation process, provides the dominant points based on the maximum EI of each objective. The leader of the swarm is selected using the concept of pareto dominance classifying it as a pareto dominance MOPSO type (see [140] for an overview of other approaches). In our implementation, a selection method is added to the ones already proposed in [139], able to provide a point to promote diversity and guarantee a wide and uniformly distributed EI pareto front. The optimiser was validated using Fonseca and Fleming function to ensure pareto uniformity and global optimality.

3.3.8 Constraints Handling Formulations

The complete optimisation methodology described in the precedent sections is summarized in Fig.3.3. This displays a typical single or multiobjective optimisation problem that utilises single or multifidelity analysis tools and surrogate modelling.

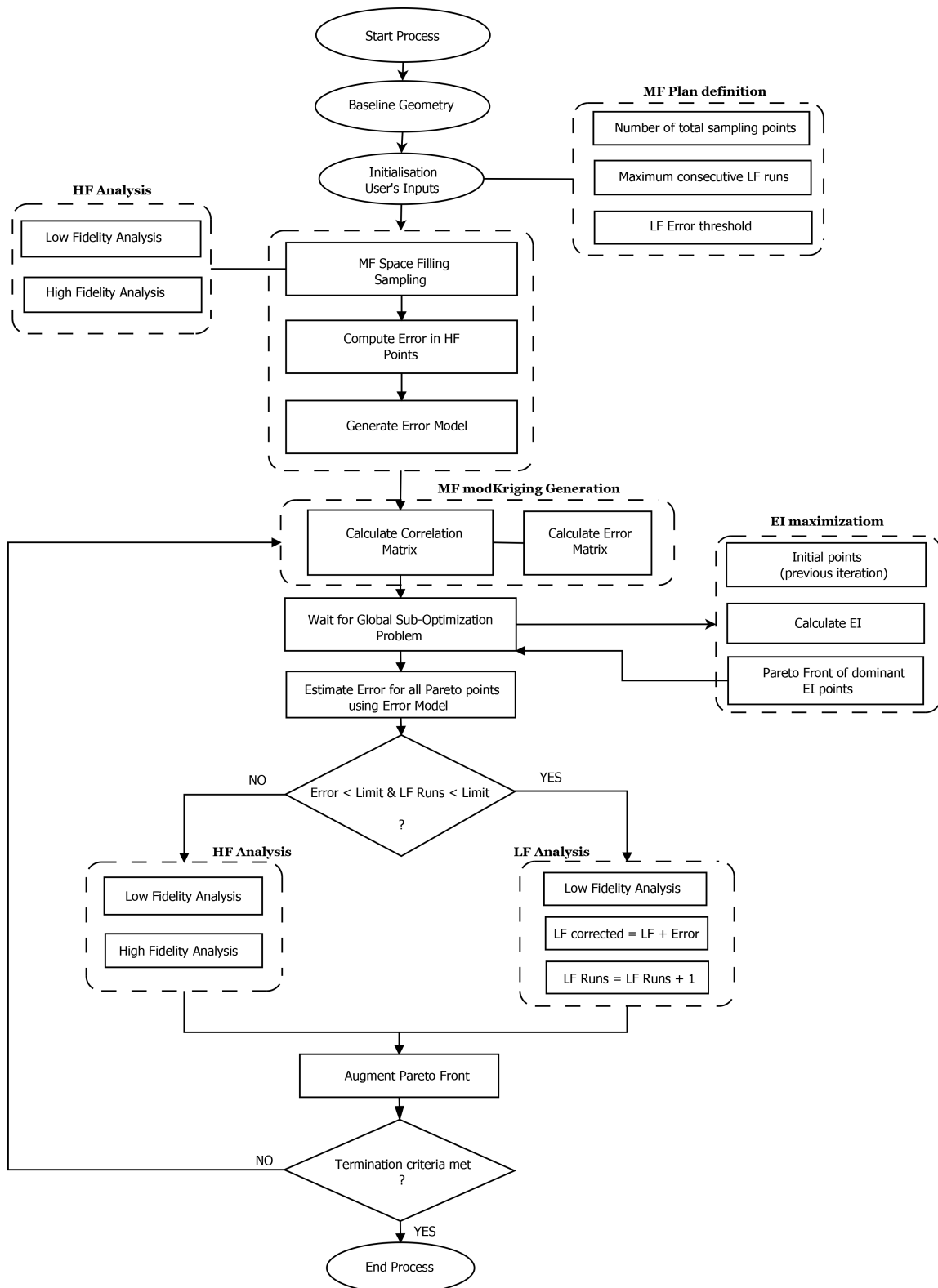


Figure 3.3: Flowchart describing the suggested MF SBO methodology.

Of course, in realistic design applications an optimisation problem will rarely — if ever — be free of constraints. Although the inclusion of constraints in such a problem is not distinctive in Fig.3.3, constrained problems can be tackled by the exact same methodology. This is true because constraint functions are treated in the surrogate generation level and suboptimisation process similarly to the objective function(s).

Suppose a typical constrained optimisation problem as described below:

$$\begin{aligned}
 & \min_{\mathbf{x} \in \mathbb{D}} f(\mathbf{x}) \\
 & \text{subject to } g_1(\mathbf{x}) \geq g_{1,min} \\
 & \quad g_2(\mathbf{x}) \geq g_{2,min} \\
 & \quad \vdots \\
 & \quad g_n(\mathbf{x}) \geq g_{n,min}
 \end{aligned} \tag{3.3.27}$$

Within the proposed surrogate based optimisation method, metamodels are generated for the constraint functions in a way similar to that of the objective function(s). This is a computationally efficient and elegant approach especially in the typical aerospace design case where the constraints are provided by the same analysis tool that calculate the objective function. In this case, a set of data is generated from every design candidate, followed by metamodel generation for the objective function and the constraints.

The constraint value predictions are exploited within the suboptimisation process, in order to steer its solution towards a feasible promising infill point. In this process, there are two main ways in which information from the constraints' models can predict the new point:

- Penalty methods
- Probability of feasibility

Penalty Methods

This approach falls in the general category of penalty methods but specifically applied within an SBO environment. In this, a penalty is applied to points for which any of the constraints' surrogate models' estimations violates the respective constraint.

A penalty can be applied in various forms [107], but experience has showed that simply penalizing the point by setting its EI prediction to zero, is effective. This way, the suboptimisation process is steered to design vectors that are feasible according to the current

metamodel predictions. This is a very simple to implement, yet powerful method. Its ability to work using any metamodel (for instance, cheap RBF instead of Kriging), makes it very attractive for the applications for which the whole optimisation methodology is developed.

On the downside, this method is strongly dependent on the initial constraint surrogate accuracy. Suppose a simple RBF constraint model which is not accurate due to limited (or badly distributed) training data points: the SBO plan will gradually sample points to the area currently believed to contain the optimum. In this case, unexplored areas will be under-sampled leading to inaccurate constraint estimations with no mechanism enforcing a sampling in the unexplored region. This condition will sustain itself: during the suboptimisation process points that should not be penalized might be penalized (or the opposite) and a potentially promising yet unexplored design space region will not be visited. Therefore, the local knowledge of the constraint function in this area will not be improved. This potentially increases the initial sampling requirements, which then translates to cost.

Probability of Feasibility

The second method requires a Kriging surrogate for the constraints, which as presented in this chapter allows the calculation of probability of improvement (PI) within the suboptimisation process. In Eq.3.3.11, one can substitute the constraint i limit $g_i(\mathbf{x})$ instead of the current minimum value y_{min} . This creates the probability of feasibility (PF) [107] for the constraint function i . This essentially refers to the probability that any examined design has to satisfy the constraint i . Therefore, by including the probability of feasibility of all the constraints, as well as the expected improvement of the objective function, the infill plan is altered, to create the Feasible Expected Improvement Criterion (FEIC). In the general case of n constraints, the suboptimisation problem becomes,

$$\mathbf{x}^* = \arg \left(\max_{\mathbf{x} \in \mathbb{D}} (PF_1 x PF_2 x \cdots x PF_n x EI) \right) \quad (3.3.28)$$

Hereafter, to avoid any abbreviation-related confusion, this method is simply referred to as "Feasibility".

The infill point is the one maximizing this combined criterion and the improvement is steered towards regions that are predicted to be feasible and promising. The drawback discussed in the penalty method approach is not present in the feasibility method. This is because in addition to EI , PF_i uses also information from the MSE of the model itself. This is a mechanism that counterbalances the attraction of the promising regions and enforces the sampling of unexplored regions, in which the constraint function is not sufficiently accurate. The result is a constraint metamodel that not only favours global search, but being more accurate also leads to higher success in infill sampling designs in terms of feasibility, during the optimisation process. This approach has shown to be robust and effective, how-

ever there is additional cost associated to the mandatory generation of a Kriging model for the constraint.

A Discussion on the Behaviour of the Methods

For industrial applications that require computationally expensive analyses, a knowledge of the behaviour of each approach and its effect on the optimisation convergence, is essential for the success of each design problem. Usually, such problems are dominated by constraints—which are typically active at the minimum—, increasing the importance of a good understanding on the way convergence and feasibility is achieved. This is especially the case in optimisation studies with limited budget where both final result but also feasibility during the optimisation convergence is desired. Therefore, there is a need to assess and compare these constraint handling approaches, a task presented in Chapter 5 within the scope of a typical airfoil design problem. The following paragraphs provide a brief description of their performance attributes, based on the their fundamental characteristics and the methods are displayed in Fig.3.4.

Regarding the Penalty method, it can be said, that it is more dependent on the sampling success and less robust than the Feasibility method. The suboptimisation process is steered towards points on the limit of the constraint (in active constrained problems), which due to the surrogate model's inaccuracy may prove to be infeasible when analysed. Whether or not the constraint is indeed satisfied, depends on the accuracy of the surrogate model. Especially in high dimensionality problems and when cheap RBF models are used, the accuracy is not sufficient to ensure a high rate of infill feasibility success. However, when more training points populate the promising area, the improvement of the constraint models' accuracy translates to more successful infill sampling. In the penalty method the suboptimisation process still depends solely on the EI as a search criterion and as such the point sampled is more influenced by the EI prediction.

In the feasibility method however, PF_i and EI have equal influence on the suboptimisation. As such, a point very likely to satisfy the constraints (high PF_i terms) but moderate EI , might provide a higher product in Eq.3.3.15, than a point featuring high EI but moderate PI_i terms. When using the probability of a point being feasible as one of the subprocess metrics to maximise, the latter is steered towards infill points well within the feasible predicted design space. As a result, feasibility method tends to be more conservative, providing infill points with higher success rate in terms of constraint feasibility than penalty method does during the optimisation.

While penalty method is more aggressive and less successful in terms of feasibility rates, when sampling points are indeed feasible they tend to exhibit better objective function values since the method leads to active constraint regions. Therefore, especially in problems where the constraints are active at the optimum, the penalty method is expected to provide better final results but in a later stage in the optimisation process. The feasibility

method on the other hand is suitable in providing feasible improvements earlier. However, it tends to reach a plateau quickly, since the infill points are too conservative for any objective function improvement to occur, especially in active constrained problems.

The topology of the constraint functions is also a significant factor on deciding which method to use. A flat or linear function cannot be approximated by Kriging — due to numerical instability reasons— and as such the Feasibility method fails for such problems. Such a problem is encountered in the Sellar test case presented in in Chapter 4.

Based on the above information, an interactive approach to optimisation is suggested. In the initial stages of optimisation feasibility should be used, only to be switched to the penalty method when a plateau is reached.

As a final note, in the cases where the constraint values result from MF tools, the constraint metamodel should be able to accommodate MF data. Therefore, the MF modRBF⁸ or MF modKriging presented in this chapter should be used instead of RBF or ordinary Kriging.

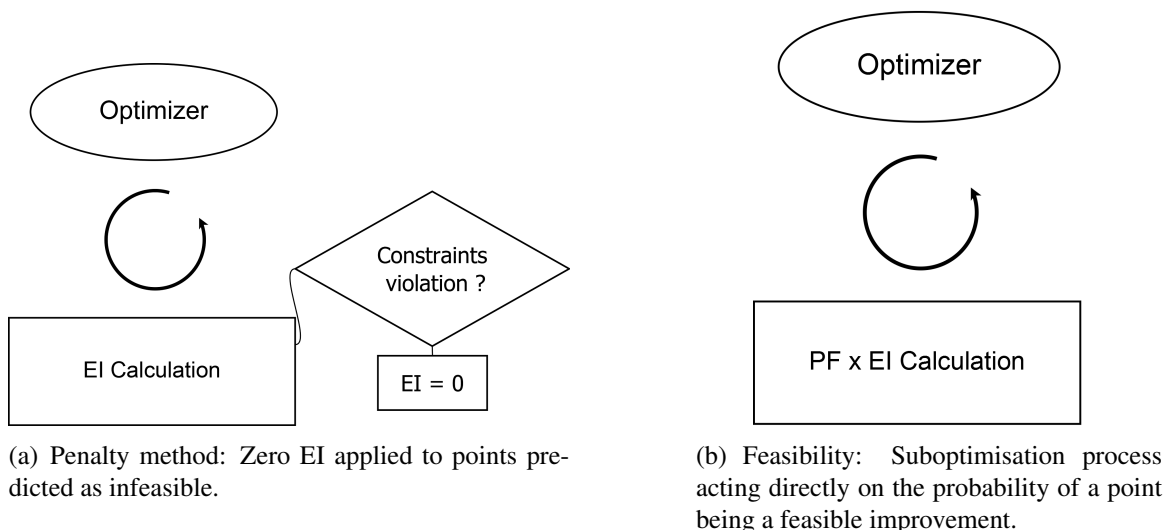


Figure 3.4: Constraint handling methods, acting during the suboptimisation process.

3.4 Implementation on Multidisciplinary Problems

The paragraphs preceding this section refer to the details of the development of a self containing black box type optimisation methodology. As mentioned earlier, the method is flexibly structured to accommodate any type of problem (SO or MO, SF or MF), while

⁸The RBF model can be easily modified to an additive MF modRBF, similarly to the way MF modKriging was modified. In Eq.3.3.17, the Kriging predictor is simply replaced by the RBF predictor.

combining various cost-efficient methodologies related to global exploration and optimisation, as required in preliminary design studies. In addition, it is adaptable to any design stage, engineering workflow or formulation, especially involving industrial inhouse analysis and optimisation software. In this sense, its main role is in the system level optimiser of a distributed architecture based MDO but can also act simply as an optimiser of a monolithic formulation, calling multidisciplinary analyses of variable fidelity (see Fig.3.5).

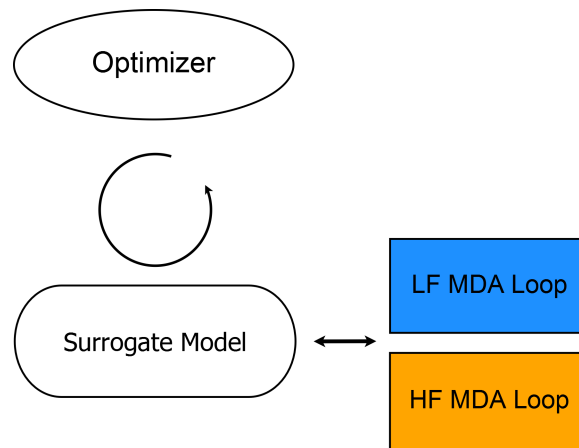


Figure 3.5: In its simplest form in monolithic MDO formulations, the methodology can act as a black box optimiser acting on variable fidelity industrially defined MDA workflows.

Nevertheless, it is well established that the efficiency of the method is affected by the selected MDO architecture. Apart from its distinctive character, each architecture's performance is dependent on the optimisation framework used in the system level. Hence, following current research on MDO architectures for various applications, is interesting to examine how these architectures adapt to this system level optimiser approach.

In this sense, this research thesis focuses in the performance assessment of standard architectures — now making their way into aerospace design — that employ the optimisation method developed.

The examined architectures are:

- Monolithic: MDF
- Distributed: ASO

ASO is essentially a hybrid between typical distributed architectures and MDF, and is developed from a simple modification of MDF. It is a formulation well suited for aerostructural problems [164], like the ones this thesis aims at, due to their inherent poor load balancing.

A typical — industrial scale — aerostructural problem is described in Fig.3.6.

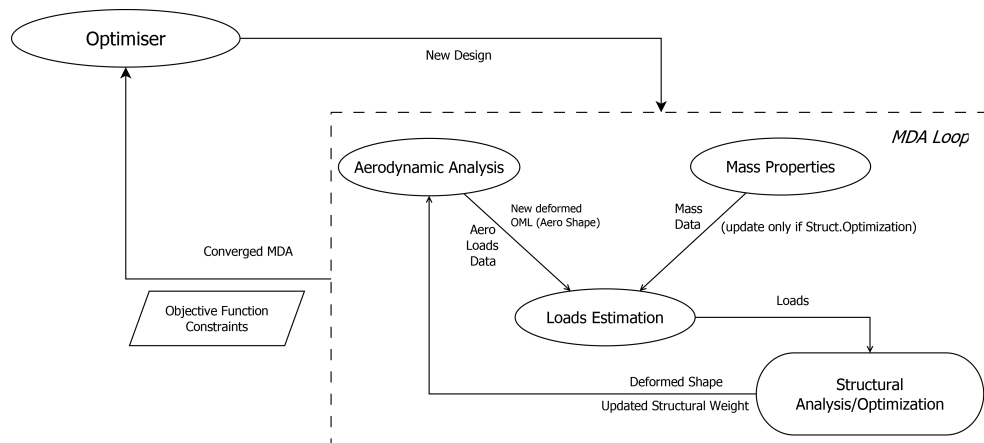


Figure 3.6: Description of an industrial aerostructural optimisation process. The multidisciplinary analysis involves the convergence of all related disciplines to provide the objective function and constraints. For ASO architecture, structural analysis is substituted by structural sizing.

Monolithic Architectures

In the monolithic category, only MDF is examined due to good performance as well as its simplicity and adaptability to any optimisation framework. This choice — popular among other researchers and engineers — also lies in the fact that contrary to IDF, a multidisciplinary feasible solution is always attained. This is an important attribute of an optimisation framework for any industrial design workflow.

In this case, the methodology works as the single optimiser calling a black box function which is simply the expensive MDA process. It is an efficient approach since the goal of the optimiser was to minimise the number of HF MDA calls. The main source of computational cost comes from converging the MDA (a mandatory cost if physically feasible solutions are desired in every iteration). In high dimensionality, training the Kriging model(s) becomes a significant cost as well.

A detailed flowchart of the methodology applied in a typical MDO problem based on MDF, is shown in Fig.3.7.

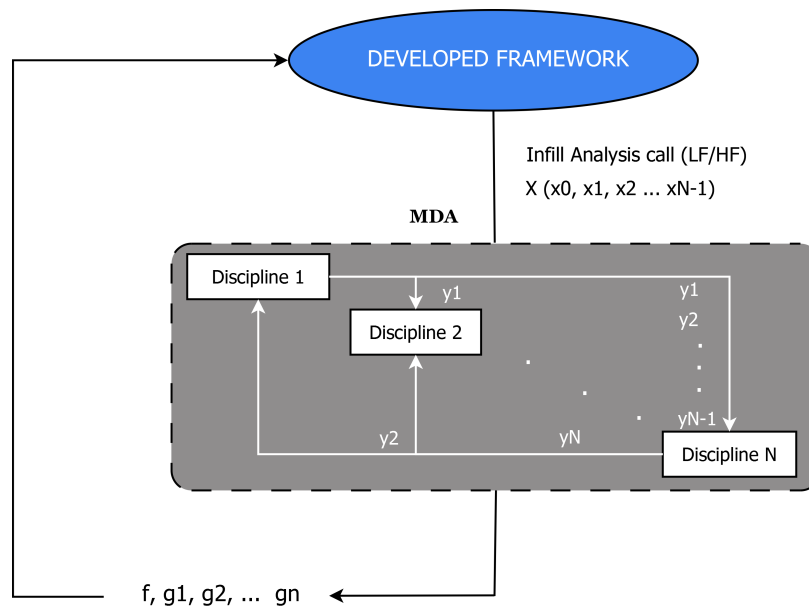


Figure 3.7: In MDF, the methodology acts directly on the interface of a (predefined) multidisciplinary analysis. Upon multidisciplinary convergence, objective function and constraints of the appropriate fidelity are provided.

Distributed Architectures

The optimisation methodology was originally developed mainly for being applied within a distributed architecture environment. The adaptability of the methodology communicating with interfaces of predefined analysis and optimisation tools is exploited in such an architecture, which by definition uses such inhouse software. Apart from this "methodology characteristics match", combining a distributed architecture with a global surrogate based optimiser like the one presented, shares another significant advantage as well: the reduce of dimensionality. Architectures like ASO and Bi-Level reduce the dimensionality of the system level optimiser, as the local (disciplinary) design variables are used only in disciplinary optimisation processes, which are defined as black boxes in existing industrial procedures. Therefore, the optimiser (working in system level) not only interacts with the interfaces these processes but its dimensionality is also reduced. This is crucial for expensive and challenging design problems for which the surrogate based procedure should be as efficient as possible. The inherent fact that inhouse disciplinary analysis and optimisation tools are used in such architectures, makes the whole design methodology more flexible and attractive for industrial applications which invest a lot of human and financial resources in the development of these processes. The implementation of the developed optimisation methodology within ASO is illustrated in Fig.3.8.

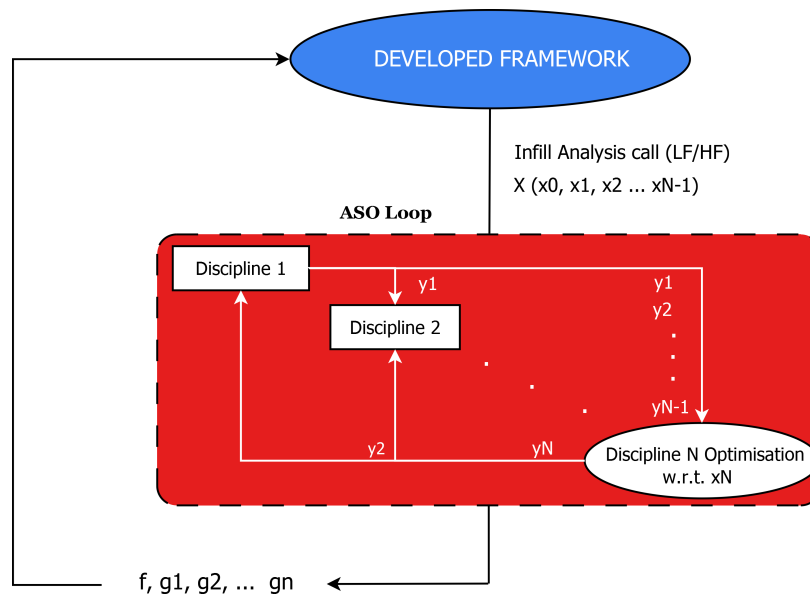


Figure 3.8: In ASO, the methodology exploits existing industrial analysis and disciplinary optimisation tools. At least one discipline performs an optimisation with respect to its local design variables. Thus, the global variables in the system level are reduced, improving the efficiency of the methodology.

3.5 Summary

This chapter presented the methodology developed to tackle the problem of accelerating early design stages by efficiently exploiting HF information. The methodology was designed to support decision making in the conceptual to preliminary phase, through the provision of reliable design directions in the form of a pareto front. More specifically, it aims in exploring the design possibilities of multidisciplinary optimisation problems like aerostructural design without the costs which prohibit such applications in the conceptual stage. The framework uses multifidelity tools within an expected improvement surrogate based optimisation plan to accelerate the process. A novel modification of the ordinary Kriging metamodel was introduced, improving the design space as well as as the expected improvement space in the presence of multifidelity data to avoid the Co-Kriging costs. It also exploits the error correction metamodel to introduce a simple yet effective infill sampling condition, decreasing the costs of the required infill analyses. An alternative to the standard multiobjective expected improvement suboptimisation problem was also proposed, to facilitate parallel infill analyses and widen the objective space exploration.

Methodology Demonstration in Small Scale Problems

If you're not confused, you're not paying attention.

Tom Peters

SUCCESSING the presentation of the methodology, this chapter aims in displaying its application in various test cases. As a first demonstration, analytical cases were selected. Their purpose is threefold: They are cases associated with low computational costs and such as they are suited for the process of troubleshooting and finetuning a research methodology. The analytical minimum is known, while results are available from other researchers. Therefore, the method's behaviour can be easily assessed. Finally, low dimensionality problems (1D, 2D) allow for the necessary visualisation of the design space, so that the modification made on the surrogate model can be understood.

4.1 Framework Demonstration

The presented methodology is assessed and fine-tuned on a 1D and 2D test case commonly used in the literature. The 1D case demonstrates the modified surrogate's discussed attributes in a clearly visualized manner. The 2D case uses the Branin function to illustrate the ability of MF modKriging in providing global optimality under the selected SBO plan even in a sparse sampling.

4.1.1 1D - Test Case

The simple 1D problem is described by the following analytical function, which acts as the HF function we want to approximate.

$$f(x) = (6x - 2)^2 \sin(12x - 4) \quad (4.1.1)$$

This allows to visualize the effect of the error model (and its shape parameter) near the LF points. We also showcase how EI distribution changes when MF modified Kriging is used. Figs.4.1,4.2, clearly show that ordinary Kriging is not suitable when MF tools are available and the proposed modification leads to a more accurate representation of the design space as well as a more "efficient" EI distribution. When ordinary Kriging is used, the LF points and HF points are both interpolated since no MF information is provided. In our modified version however, the HF points are interpolated and LF points are fitted, providing a better estimation of the design space. The effect of the shape parameter is also apparent. For too low θ values, the kernel function tends to be very wide. In these cases, the error information is highly diffused and may decrease the predictor accuracy. However, in high dimensionality problems, this is rarely the case. The points are not quite dense and even very low shape parameters cannot "diffuse" the error to such an extent so as to decrease the predictor accuracy, unless the HF sampling is not "space filling" enough¹. Moreover, an appropriate θ value can be a priori determined (or when Kriging is used for the error correction it is automatically calculated).

To emphasize the error model effect, the LF and HF points were deliberately selected in an "unlucky" manner, also assuming a challenging non-monotone error distribution. In low x regions, the LF tool underestimates the true values but the opposite happens in high regions. Despite that, the surrogate exploits the error information successfully.

Fig.4.2 describes the improved EI as a function of the shape parameter. MF modKriging increases the dominance of the global optimum versus the local ones in this multimodal EI space. This accelerates the convergence of a global stochastic optimiser like the one employed in this framework. We explain that by acknowledging the effect of the error MSE in the EI space: the objective value predictions affect MSE, however MSE also uses information inherent to the correlation matrix (θ_{LF}, ρ_{LF}) which is not altered in MF modKriging (as the matrix here does not include LF/HF correlation information). Therefore, information regarding the uncertainty of LF points could only be provided through the additional error MSE term as discussed in the previous section. As such, when the error MSE term is used in Eq.3.3.10, the MSE of a LF point is no longer zero, as in reality the LF analysis is associated with an error. This corrects the EI space, so that LF points have now a finite EI value as shown in Fig.4.2.

¹Using LHS sampling in this work does not allow such a condition.

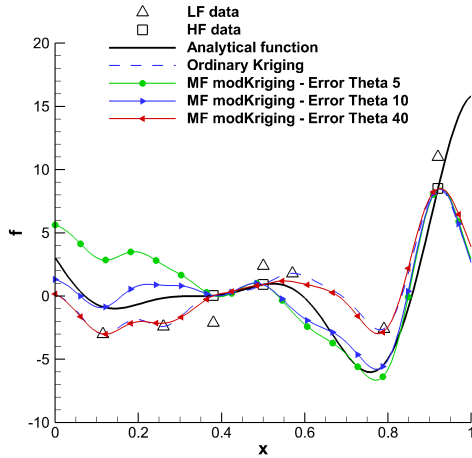


Figure 4.1: Comparison of ordinary Kriging versus MF modKriging. The regression of the LF points improve the accuracy of the approximation.

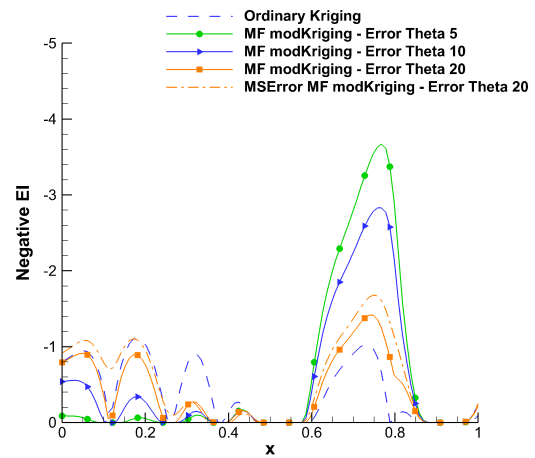


Figure 4.2: Comparison of the negative expected improvement as resulting from Kriging and the modified Kriging for various shape parameters.

4.1.2 2D - Test Case

Problem Formulation

The performance of the MF modified Kriging model within an optimisation process is assessed using the multimodal 2D Branin [88] function described by:

$$f(x_1, x_2) = 2 \left(\left(\frac{x_2 - 5.1x_1^2}{4\pi^2} + 5\frac{x_1}{\pi} - 6 \right)^2 + 10 \left(1 - \frac{1}{8\pi} \right) \cos(x_1) + 10 \right), x_1 \in [-5, 10], x_2 \in [0, 15] \quad (4.1.2)$$

We are using the above test function as a LF tool analysis. The function features 3 global minima, an attribute which makes it appropriate for testing the convergence properties of the method. Its value is doubled so that it scales with the modified Branin function below, used as a HF tool analysis:

$$f(x_1, x_2) = \left(x_2 - \frac{5.1x_1^2}{4\pi^2} + 5\frac{x_1}{\pi} - 6 \right)^2 + 10 \left(1 - \frac{1}{8\pi} \right) \cos(x_1) + 5x_1 + 1, x_1 \in [-5, 10], x_2 \in [0, 15] \quad (4.1.3)$$

This function has a wider global optimum area, allowing a direct comparison of how the design space topology affects the optimisation convergence.

The LF analysis introduces multimodality which serves to showcase how the MF modified Kriging properly exploits LF data while avoiding getting stuck in a local minimum or an LF global minimum instead of the HF one. To demonstrate the methodology's behaviour in high dimensionality problems with sparse sampling, a total of 5 HF and 16 LF

points were used in our sampling.

Kriging Modification Effect on Design Space Prediction

Capturing the LF tool error trends is critical for the success of any MF methodology, including the currently presented one. To ensure this, we compare the true error of the low fidelity function (analytical error) to an RBF prediction of the error using five Training Data. Fig.4.3.d displays that even a such simple and cheap model with sparse data suffices in predicting a smooth and accurate error distribution. By comparing Fig.4.3.a and Fig.4.4, a close match between our metamodel trend predictions and the HF analytical function is also observed. Therefore, LF information was effectively exploited, providing the MF modKriging model with a correct representation of the LF tool error. Furthermore, the latter is the reason behind a HF function approximation that is free of any LF associated minima.

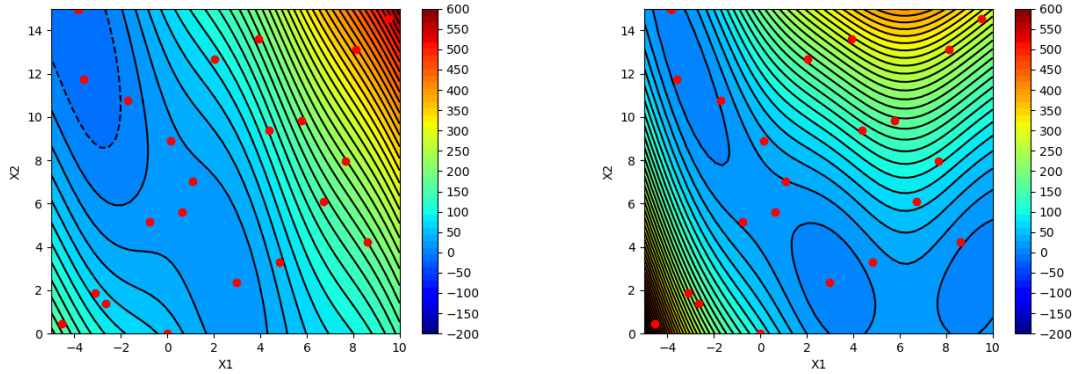
Fine Tuning the Parameters of the Methodology

Multiple optimisation studies were performed to assess the methodology and the use of the error MSE term within the EI calculation as well as to fine-tune the subprocess and hyperparameters tuning optimiser details. Each case was executed a minimum of 5 times to ensure reliability since factors like "sampling luck" had to be cancelled out. For clarity, fewer results are shown.

Tuning the Kriging hyperparameters requires a gradient free [93] optimiser to locate the global maximum of the likelihood function and the respective costs are not prohibitive to provide a reasonably accurate Kriging representation. In a highly dimensional problem with many training data points extensive exploration should be avoided however, as training becomes a significant cost of the SBO. Out of four pyOpt [203] optimisers examined and the SciPy implementation of the Nelder-Mead Non-Linear Simplex algorithm (N-M), N-M and MIDACO proved to be the most robust and efficient. Since N-M was slightly cheaper, it was selected for tuning MF modKriging.

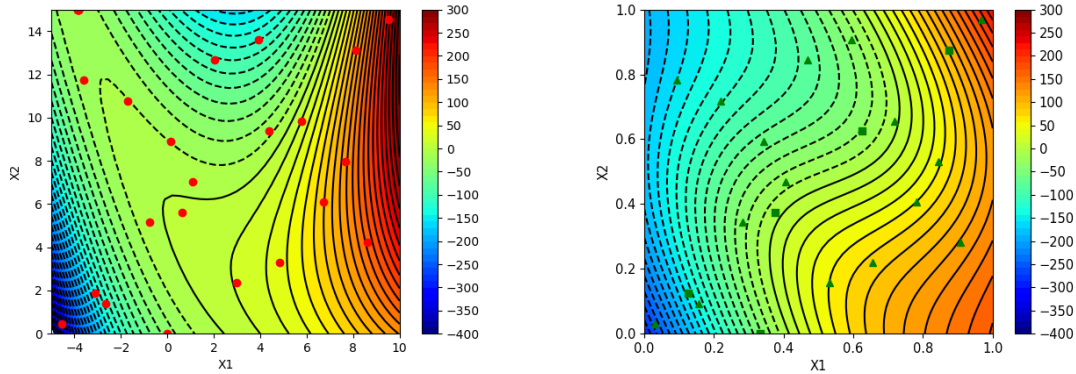
The suboptimisation process requires a global optimiser since the EI evaluation cost is negligible and the maximum EI point is sought in a multimodal space. It was found that the ALPSO and MIDACO algorithms were the most effective exploration algorithms leading to the best infill design points sharing similar computational expenses. For the remaining of this work, ALPSO is used.

Within the MF modified Kriging, HF information (which in industry is considered to be information from a later design stage) is introduced earlier in the design stage through the error model. This leads to a more efficient infill sampling process, and a faster convergence,



(a) HF function - Unimodal Modified Branin function.

(b) LF Braning function



(c) Analytical error distribution between the HF and LF Branin function.

(d) Error representation with a C4 Matérn based RBF model using 5 TD and $\theta = 1.0$.

Figure 4.3: Modified Branin function contours, acting as high and low fidelity functions. The analytical error of the LF function is also compared against the RBF model prediction. Four HF (square) points are used in the error model generation.

confirmed by the findings of Fig.4.5. Regardless of the initial objective function value (which depends on the "luck" of the initial sampling), the modified Kriging provides more robust infill sampling. MF modKriging using 5 HF/16 LF training points was more efficient than the MF method using ordinary Kriging with 21 HF training points. Referencing again Fig.4.2, the optimiser knows more about the design space, has less uncertainty in some of its areas, reduces the respective MSE, which in turn makes the EI distribution more accurate. In most cases, as the one shown, the MF methodology equipped by MF modKriging could reach almost HF optimality in fewer infill iterations. Co-Kriging is similarly effective, having fewer but more drastic reductions in the OF. However, this simple 2D case is not appropriate to reliably compare it with MF modKriging since the major source of both methods' cost lies in the tuning of the hyperparameters in higher dimensionality problems. More insight is provided in the next test case. The MF infill plan described previously leads to wider plateaus in convergence history as only a HF infill is accepted as a reliable

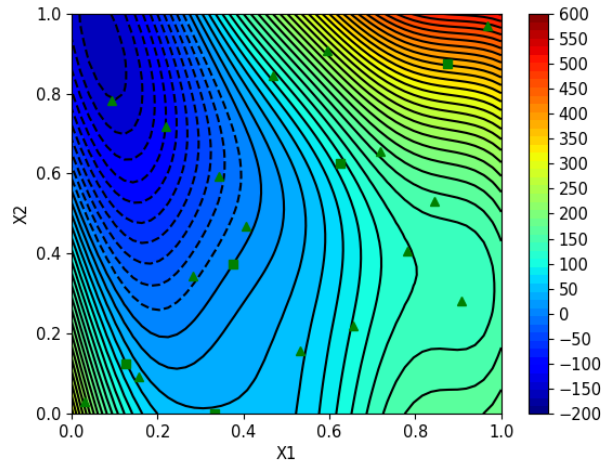


Figure 4.4: High Fidelity function representation using MF modKriging. Four HF (square) and 16 LF (triangle) points are used.

improvement. Despite that, since the number of HF infill points is reduced, the total elapsed time is decreased even if the infill iterations required for optimality are increased.

The effect of the error MSE term is displayed in Fig.4.6 as well. Evidently, introducing the "artificial" MSE term is not critical for the convergence of the method. However, if introduced it provides extra information regarding the uncertainty of the LF error correction model, leading to faster convergence.

4.2 Scalability Characteristics

A multidisciplinary problem can rapidly scale up to very high dimensional design spaces, depending on the number of design variables required to describe a discipline, and of course the number of disciplines. Since the methodology developed is based on surrogate modelling, it is very sensitive to the dimensionality of the problem. The curse of dimensionality primarily translated as increased initial sampling costs and Kriging training costs, as well as high suboptimisation costs, raises a barrier making the method inefficient when a number of design variables has been exceeded. This is because the computational cost (in terms of elapsed time) to train and search the metamodel can become equivalent or even higher than a HF analysis. Additionally, increasing the dimensionality deteriorates the final results for a given computational budget². Furthermore, in a conceptual stage it is important to use only a dominant subset of the potential design variables. In this work, since the methodology aims in multidisciplinary applications among others, it is critical to examine how it

²As shown, even when increasing the computational budget, the results still deteriorate, especially for a non-exploitative optimisation scheme.

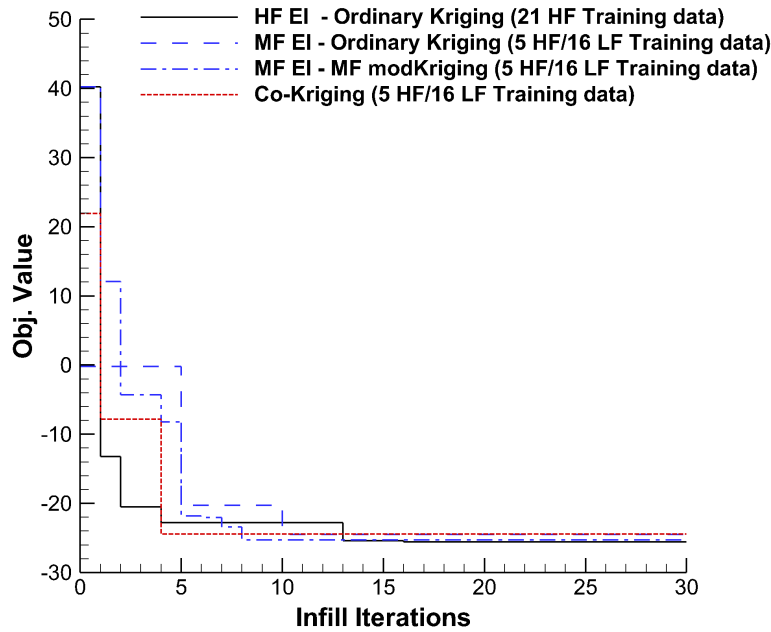


Figure 4.5: Convergence history comparison of HF, MF ordinary, MF modified Kriging and Co-Kriging.

behaves with the dimensionality scale up. We can therefore assess what can be realistically achieved by the method while maintaining its efficiency in its application range.

We conduct this scalability analysis by using the Rosenbrock function [204] which is a reasonable choice, since:

- In its original 2-Dimensional form, it provides a challenging problem with the optimum located in a narrow flat valley.
- In its extended form, it can be used to examine the scalability characteristics of the optimisation framework. This is especially important for a surrogate based optimisation methodology, which is very sensitive to the dimensionality of the problem.

The extended Rosenbrock function, here used as the HF function, is described by:

$$f_{HF} = \sum_{i=0}^{n-1} 100(x_{i+1} - x_i^2)^2 + (1 - x_i)^2 \quad (4.2.1)$$

It features a global minimum of $f_{HF} = 0$ in $x_i = 1$

Since the methodology requires multifidelity analyses, we need to define a LF "version"

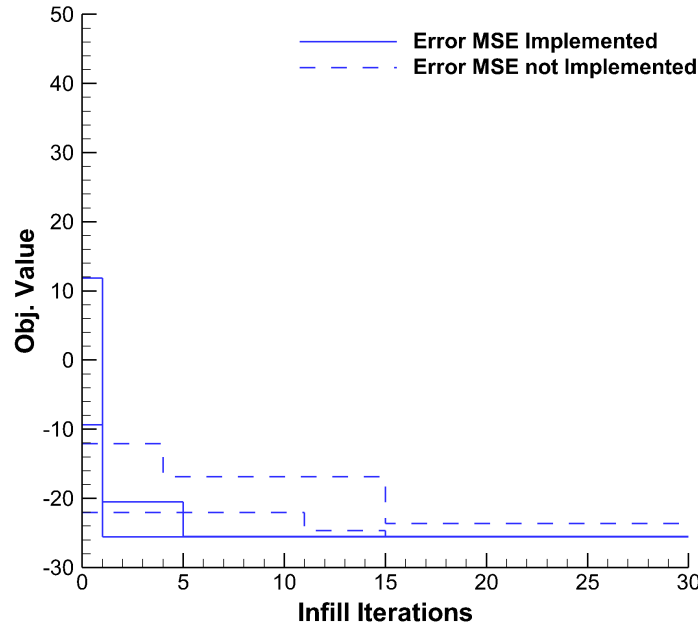


Figure 4.6: Effect of implementing the Error MSE term within the modified Kriging.

of this function. This should not change the main characteristics and trends of the original one but be inaccurate in terms of value. This is achieved with the use of scaling coefficients, inserting an error within the bounds typically observed between aerospace numerical tools.

$$f_{LF} = \sum_{i=0}^{n-1} 105(1.05x_{i+1} - 0.98x_i^2) * (0.95x_{i+1} - 1.03x_i^2) + 0.93(1 - x_i) * 1.08(1 - x_i) \quad (4.2.2)$$

The challenges of the Rosenbrock function are twofold:

- It features a flat and narrow valley leading to the global optimum. The reduced objective functions values and the small function gradients makes it difficult for optimisation methods to descend to the optimum point.
- In high dimensions, the property of unimodality vanishes [205], as local minimum appear.

The framework's scalability attribute is assessed by successively increasing the dimensionality of the extended Rosenbrock function, varying N from $N = 2$ to $N = 64$. The quantification of the method's scalability is based on the optimum value identified, the HF calls required as well as the euclidean distance from the true optimum. Since this SBO approach is non-deterministic, the standard deviation of the required computational costs is also taken into account. Due to the non-deterministic elements of the method as well as its explorative behaviour, the accurate identification is not guaranteed, especially in high

dimensions. Therefore, the method is assessed based on the number of HF calls required to reach a specific reduction ratio, given the maximum value of each dimensional case. For the needs of this analysis, two levels of reduction ratios are set as "good enough", $f_{opt}/f_{max} = 2 \times 10^{-3}$ and $f_{opt}/f_{max} = 5 \times 10^{-4}$. Although the distance from the optimum is calculated in addition to the required number of HF calls, the former cannot be similarly considered as a figure of merit since (as shown) is not representative of the quality of the final result.

The methodology is compared against ALPSO optimiser, the HF Expected Improvement (EI) approach and a Co-Kriging based MF EI process. The effect of the error correction model (RBF or Kriging) is also assessed [206]. Each problem is solved five times to minimise the effects of the stochastic elements of the method. For each case, the number of HF points in the initial sampling is equal to the dimensionality, with the LF points used being triple than the HF ones. The sampling cost is included in the analysis.

From Fig.4.7.a it is evident that when the dimensionality is increased more than 8-D, a very low function cannot be obtained. In fact, especially when Co-Kriging is used as the MF surrogate, the method fails in cases more complicated than 2-D. The rest of the methods depict an almost linear increase of the required HF calls, with the HF EI approach requiring more computational resources in the 4-D than in the 2-D case. ALPSO can ultimately locate the optimum in all problems, but its cost is prohibitive even for low to middle fidelity MDO purposes.

The increase of the dimensionality leads to an increase of the maximum deviation of the required cost observed by our multiple runs. This is a direct result of the methods searching until the minimum is successfully located.

When a lower improvement is considered sufficient for our exploration needs, as in Fig. 4.7.c, then the interest is focused in finding the design trends. In this case, all methods except for MF EI Co-Kriging, can locate a satisfying improvement. Here, a few interesting observations can be made. Low dimensionality problems require a cost that may be similar or even a bit higher than the one of middle dimensionality cases. This unexpected trend results from the methods exploiting the initial sampling after a low number of infill samplings. When converged though, they reduce the OF to a value significantly lower than the limit set—which is not the case in higher dimensions. High dimensionality is associated with a linear cost increase. The reason behind this consistent convergence behaviour, is that the respective sampling can provide sufficient information about the trends of the function. Therefore, with the function being smooth and having a flat hypersurface, one infill sampling is enough to lead to the satisfying improvement of $f_{opt}/f_{max} = 2 \times 10^{-3}$. Following this improvement however, and despite the fact that all following infill samplings are robust in providing low values, a reduction ratio of 5×10^{-4} cannot be achieved. The inherent exploration attribute of the EI method, although necessary for MF conceptual studies, dictates a continuous search through the high dimensional design space³. As such following a few in-

³Of course such an exploration will never be complete, since dense exploration in high dimensions is

fill samplings, an exploitation oriented method would be more efficient, taking advantage of the trends near the optimum point. Nevertheless, if the interest is to identify design trends with a reduced uncertainty early in the design stage, then this approach consistently satisfies this requirement. Furthermore, this linear cost increase trend makes it easy to predict the total costs of the problem, which in turn suggests a feasible and efficient parameterisation strategy. For instance, given a typical computational budget for an early stage tradeoff study, the above analysis suggests that out particular multidisciplinary problem should not exceed 40 design variables.

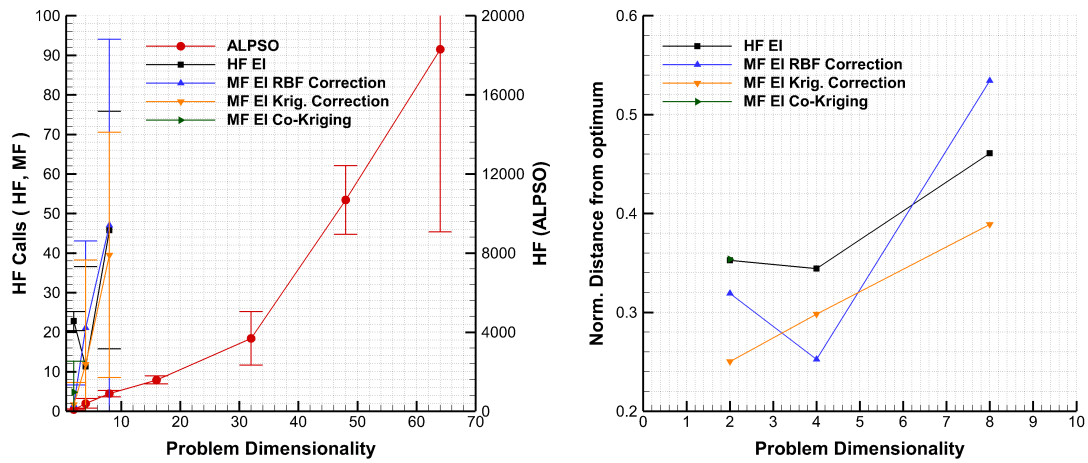
The average distance in terms of normalized euclidean metric for each case is shown in Figs.4.7.b, d. As a general trend, with the increase of the dimensionality the distance between the resulting points and the optimum is also increased. This is not observed in very low dimensionality. There is no direct correlation between the HF calls required, the minimum value found and the distance from the global optimum. A small euclidean norm does not imply a similarly low value, as this correlation depends on the topology of the design space. Therefore, in such complex non-linear (and potentially multimodal [205]) design spaces, this norm cannot be used as reliable performance metric in future studies.

4.3 Sellar Multidisciplinary Optimisation Test Function

As an initial investigation of how an SBO-MF method is adapted and how it would behave for a multidisciplinary problem, a simple analytical case is required. This allows a quick implementation of the method, adapting our black box framework (acting as a system level optimiser) to the problem interface, developed for demonstrating the case [206]. A collection of different MDO test functions were used by Tedford and Martins [207] as an effort to compare and benchmark different MDO formulations.

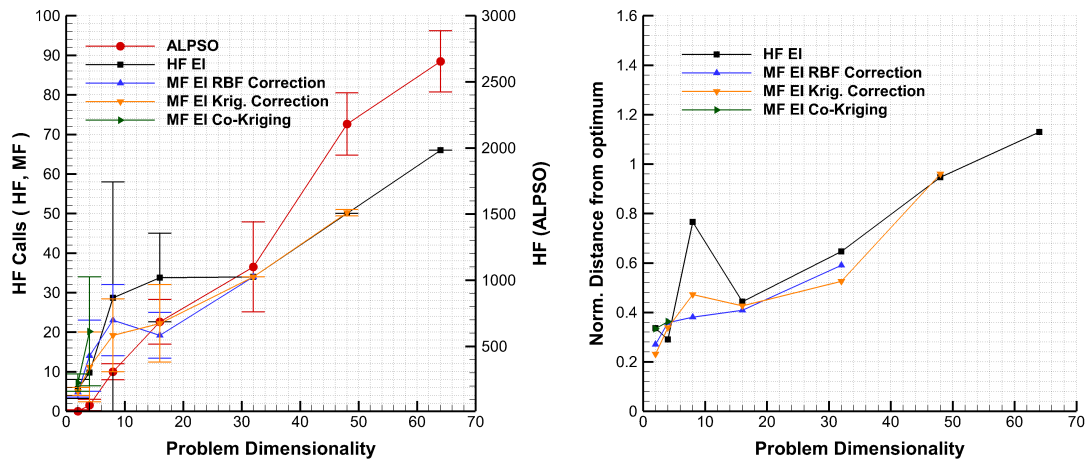
From these test problems, the Sellar [160] function was chosen. It features the characteristics of a true multidisciplinary problem, involving global and local design variables, state variables and constraints. This makes it perfect for the development and assessment of different MDO formulations and their implementations in a new optimisation methodology.

infeasible due to the curse of dimensionality.



(a) Cost increase to reach $f_{opt}/f_{max} = 5 \times 10^{-4}$.

(b) Normalized distance from true optimum for point where $f_{opt}/f_{max} = 5 \times 10^{-4}$.



(c) Cost increase to reach $f_{opt}/f_{max} = 2 \times 10^{-3}$.

(d) Normalized distance from true optimum for point where $f_{opt}/f_{max} = 2 \times 10^{-3}$.

Figure 4.7: Scalability analysis using Rosenbrock function.

4.3.1 Sellar Problem Mathematical Formulation

The Sellar problem used in this work is described by:

$$\begin{aligned}
 & \min_{\mathbf{x} \in \mathbb{D}} x_1^2 + z_2 + y_1 + e^{-y_2} \\
 & \text{with respect to } z_1, z_2, x_1 \\
 & \text{subject to } g_1(y_1) = y_1/3.16 - 1 \geq 0 \\
 & \quad g_2(y_2) = 1 - y_2/24 \geq 0 \\
 & \quad -10 \leq z_1 \leq 10 \\
 & \quad 0 \leq z_2 \leq 10 \\
 & \quad 0 \leq x_1 \leq 10 \\
 & \text{Discipline 1 } y_1 = z_1^2 + z_2 + x_1 - 0.2y_2 \\
 & \text{Discipline 2 } y_2 = \sqrt{y_1} + z_1 + z_2
 \end{aligned} \tag{4.3.1}$$

The LF variation of this problem is generated by slightly altering the discipline sub-problems, by introducing scaling coefficients. Therefore, the LF disciplinary problems become:

$$\begin{aligned}
 & \text{Discipline 1 } y_1 = 0.95z_1^2 + 1.02z_2 + 0.91x_1 - 1.15 * 0.2y_2 \\
 & \text{Discipline 2 } y_2 = 1.15 \sqrt{y_1} + 0.95z_1 + 1.02z_2
 \end{aligned} \tag{4.3.2}$$

In this problem, the global design variables are z_1 and z_2 , with the local variable being x_1 , affecting only discipline 1.

The difference between the Sellar problem used⁴ and the original one lies in the objective function. In this version, it is the local variable x_1 used in the nonlinear design variable term of the objective function. In the original problem from Sellar [160], the global variable z_1 was used for the respective term. The various formulations should be treated with caution, as different authors also use different notation. Here, the OpenMDAO notation is used. In the problem formulation that we tackle, the global minimum value is $f = 3.18339$ and in the optimum point the constraint associated with discipline 1 is active.

4.3.2 Sellar Problem Multidisciplinary Optimisation Formulation in this Surrogate Based Optimisation-Multifidelity Context

The Sellar function is used as a template to examine how disciplinary interaction affects -or not- the behaviour of the methodology. The latter is developed and implemented in a

⁴It can be found in the OpenMDAO site, <http://openmdao.org/releases/0.13.0/docs/tutorials/mdao/intro.html>.

flexible way so that any HPC workflow (single disciplinary or multidisciplinary) can be attached to it. This is essential especially for big multinational industrial environments, in which distributed MDO architectures are appropriate. As such, industrial disciplinary tools are completely autonomous and any design framework should be able to treat them as a black box. To examine how the optimisation methodology is affected by the multidisciplinary formulation of the problem, MDF and ASO architectures are implemented and compared in terms of computational costs. These processes are extensively described by Figs. 4.8,4.9 using the concept of XDSM diagrams, developed specifically for MDO problems.

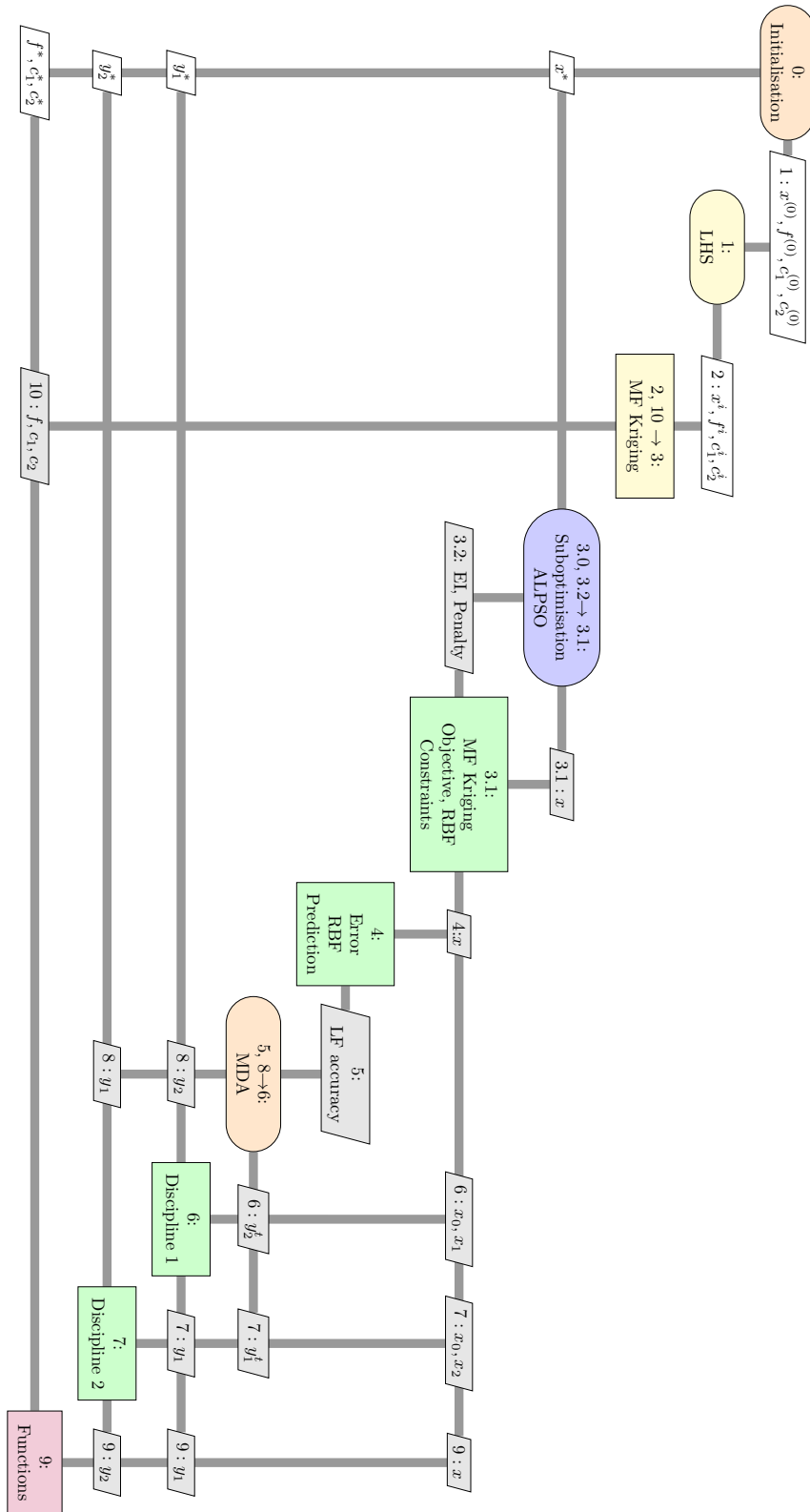


Figure 4.8: Sellar XDSM flowchart for MDF formulation.

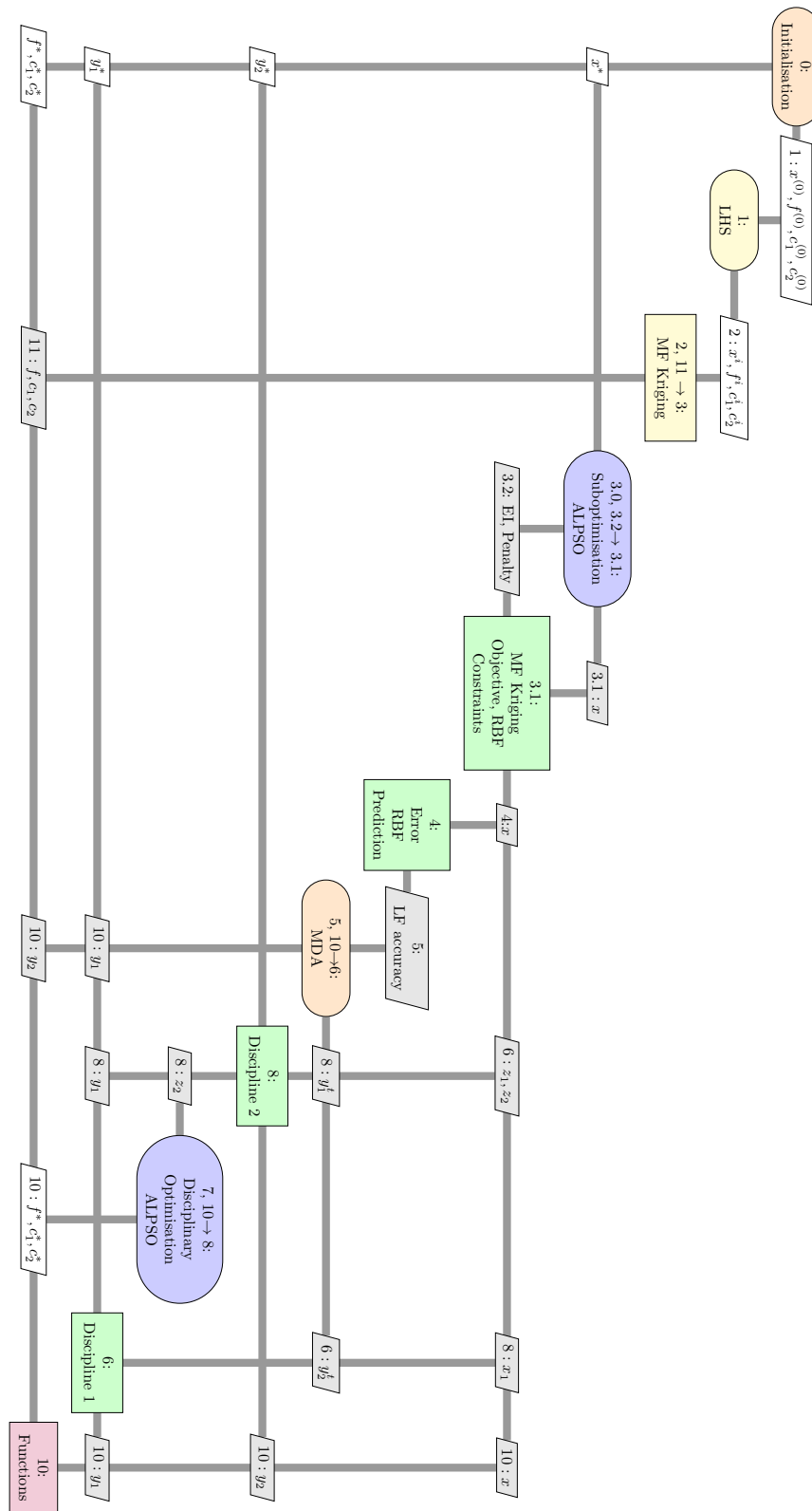


Figure 4.9: Sellar XDSM flowchart for ASO formulation.

The process begins by an LHS sampling followed by the training of the Kriging model. The suboptimisation procedure provides the next infill point; the one that maximises the expected improvement. The infill analysis which follows (treated as a black box in the industry) is the element which diversifies the two formulations. In MDF, disciplines 1 and 2 are iteratively solved within a simple MDA whereas in ASO the disciplinary analysis 1 is substituted by an optimisation with respect to x . This process is sometimes referred to in this work as ASO loop (instead of MDA loop).

4.3.3 Results

Our interest is to examine the convergence behaviour for both the objective function as well as the constraints, including an evaluation of the respective computational costs. For a complete study, we compare our MF EI methods against two other approaches: a gradient free optimiser (ALPSO) and the HF EI approach. All of the methods act on the system level. In the case of the ASO formulation, ALPSO and SLSQP has been employed for the disciplinary optimisation in order to examine the effect of this subprocess to the efficiency of the formulation.

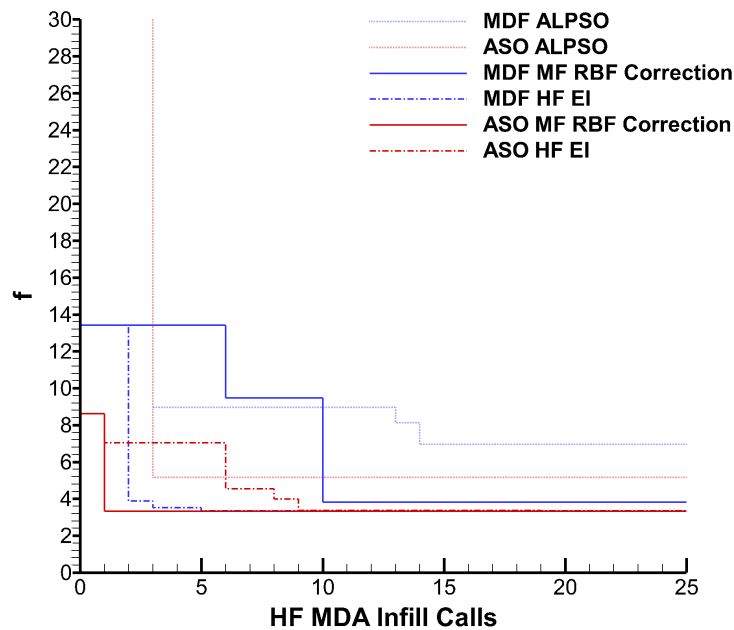


Figure 4.10: Convergence comparison between MDO formulation and methodology. Results represent the mean convergence behaviour of these non-deterministic methods.

From Fig.4.10, it is evident that ALPSO optimiser requires more computational resources to locate the minimum, which in the case of MDF cannot be located at all. When

the SBO methodology is applied, no more than ten HF MDA calls are required to reach a satisfactory convergence, regardless of the approach or the MDO formulation. In the case of MDF, the HF EI is more efficient compared to the MF approach, which still locates the optimum area. The opposite is true when ASO is being used, as the MF approach requires almost half of the HF MDA called by HF EI. Regarding the MDO formulation, ASO is consistently superior over MDF. However, it should be stressed that the above speaks only half the truth. When comparing different MDO formulations, the number of required HF MDA calls is representative of the true computational cost only in the case that the rest of disciplinary calls — or as in the case of ASO, optimisation — are of negligible cost. This is not always the case, but when this criterion is met, ASO is indeed more efficient than MDF as it improves disciplinary analysis load balance [164] as well as reducing the dimensionality of the system level optimisation problem. However, in cases where the discipline optimised in the inner disciplinary optimisation (in this case discipline 1) is not significantly cheaper to analyse than the other disciplines, ASO stops being efficient. In the present case, if discipline 1 represents a cheap discipline so that the inner disciplinary optimisation has a computational cost similar to discipline 2 analysis, ASO would be superior to MDF. This is the case in an aerostructural optimisation; a structural analysis is far cheaper than an aerodynamic analysis, with the respective disciplinary optimisation cost being in the order of magnitude of an aerodynamic analysis. Of course, the cost of the optimiser in the disciplinary process is also of great importance, affecting the total number of disciplinary calls. ALPSO — being a global method — requires at least an order of magnitude more disciplinary iterations than SLSQP. In the context of aerostructural optimisation, this would make an ALPSO based disciplinary optimisation inefficient for the ASO formulation. Therefore, it leads to no surprise that local gradient based optimisers are more appropriate for this role, as they require fewer iterations while being robust in dimensionality increase in the case of adjoint based methods.

Since this problem is a constrained one, including constraints for each of the disciplines, it is very important to examine in detail how each of the two different mdo formulations tackles constraints to converge to a feasible solution.

- In the case of the MDF architecture, a single optimisation process exists: the MF EI methodology, acting in the system level. Therefore, the constraints are imposed through the expected improvement suboptimisation process either using penalty or feasibility method, as discussed in Chapter 3. The system level therefore provides the next infill point which is a point most promising of improving the objective and satisfying the constraints at the same time.
- In the case of the ASO architecture, the optimisation process is split in the system and the disciplinary level as displayed in Fig.4.9. The system level suggests only a part of the new design, the one affected by the global design variables (in this case z_1 and z_2). The rest is defined from the convergence of the disciplinary process. Similarly, the system level (acting on the reduced dimensionality design space) can only force the satisfaction of the constraint associated with the discipline involving only global variables (in this case discipline 2). The feasibility of constraint 1 depends

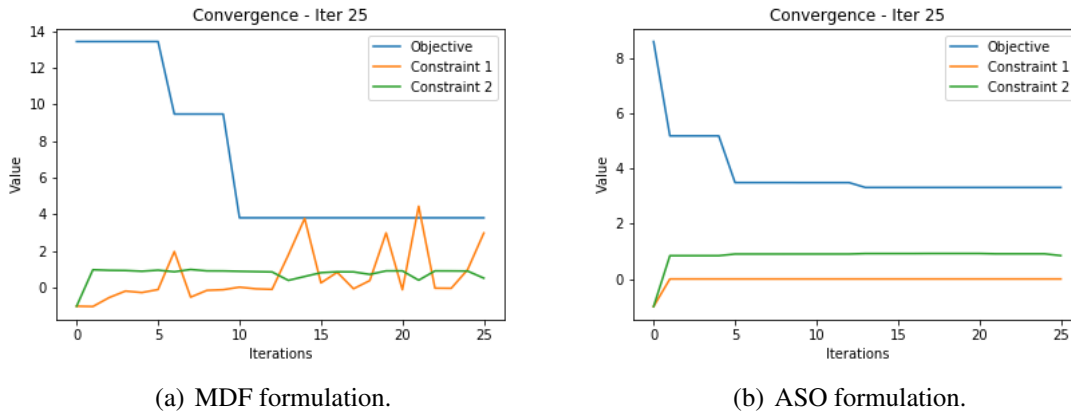


Figure 4.11: MDA convergence comparison for MDF and ASO architectures.

on discipline 1, which is optimised with respect to the local variable x during the disciplinary process.

To sum this up, in MDF the system level enforces both constraints while in ASO it is the disciplinary process who takes care of enforcing constraint 1. Since constraint 1 is active in the optimum point of this problem, the behaviour of the constraint handling method has a significant effect to the overall performance of the problem. The convergence of the constraints is presented in Figs.4.11 and discussed for the two architectures.

4.3.4 A Note on Constraints

MDF formulation typically requires a number of iterations before the challenging constraint 1 is satisfied. This is due to the initially inaccurate RBF models and the aggressive nature of the penalty method, as discussed in Chapter 3⁵. After satisfying this, the RBF models are accurate enough to provide feasible infill points. Following the convergence of the objective function, oscillations are present in the constraints' values. Since the EI method has provided a significant improvement of the objective function (due to its mild exploitation attributes), an exploration is initiated to the rest of the design space for further potential solutions. In the ASO case constraint 1 is satisfied directly from the first iteration. This is because it is explicitly calculated in the disciplinary level in every MDA iteration. Therefore, the disciplinary variable x is chosen so that it optimises the discipline 1 given that in each loop the design point satisfies the constraint 1. The constraint 1 value is constant to 0 in every iteration showing that constraint 1 is indeed active in the optimum. With the x variable defined and "frozen" by the disciplinary optimisation, EI method provides more limited exploration as proven by the almost constant value of constraint 2.

It is noted that in this problem, the feasibility method was not examined since it re-

⁵This behaviour is also observed and discussed more elaborately in the next chapter.

quires training a Kriging process to approximate each of the constraint function. Since the constraints are linear, Kriging becomes unstable and fails due to matrix singularities. The RBF based penalty method is employed instead.

4.3.5 A Note on the Multidisciplinary Analysis Loop

In Figs.4.8,4.9, the two different sampling procedures were overviewed. As mentioned, MDA is an inherently iterative procedure and its treatment separates the MDF and ASO. In ASO, discipline 1 is not analysed but optimised with respect to the local variable x . Nevertheless, the rest of the iterative process is unchanged. Two of the most common mathematical approaches to iteratively solve a coupled system of functions⁶ are the Jacobi and the nonlinear Gauss-Seidel method. Their application in MDO problems has been analysed by Kennedy and Martins [156] and the reader is referred to their work for details of these two solution methods. In short, in Jacobi the updates of the state variables follow this progression:

$$\begin{aligned} y_1^{n+1} &= f(y_2^n) \\ y_2^{n+1} &= f(y_1^n) \end{aligned} \quad (4.3.3)$$

Here, disciplines 1 and 2 can be solved concurrently since they depend on the previous iteration n solution of the coupling discipline.

In Gauss-Seidel, the solution of the coupled system takes the form,

$$\begin{aligned} y_1^{n+1} &= f(y_2^n) \\ y_2^{n+1} &= f(y_1^{n+1}) \end{aligned} \quad (4.3.4)$$

In this approach, the solution takes advantage of the existence of the solution of discipline in the $n + 1$ step. Updated information is inserted in the system accelerating the process. However, this approach demands a sequential iterative procedure. In the case of ASO, the y_1^{n+1} analysis is simply an optimisation given the corresponding state variable of discipline 2, y_2^n .

The Sellar function is being used as a test case to gain feedback before proceeding to a heavy aerostructural optimisation. Therefore, in Fig.4.12 the performance of these two MDA solution techniques is compared for both MDF and ASO architectures.

It is evident that despite the sequential nature of the Gauss-Seidel method, it is more computationally efficient since the updated information drastically accelerates the convergence. Therefore, it is the system solver method being used in the aerostructural optimisation case presented in Chapter 7. What is equally interesting, is the effect of the architecture

⁶Or for that matter, disciplinary analyses as in MDO.

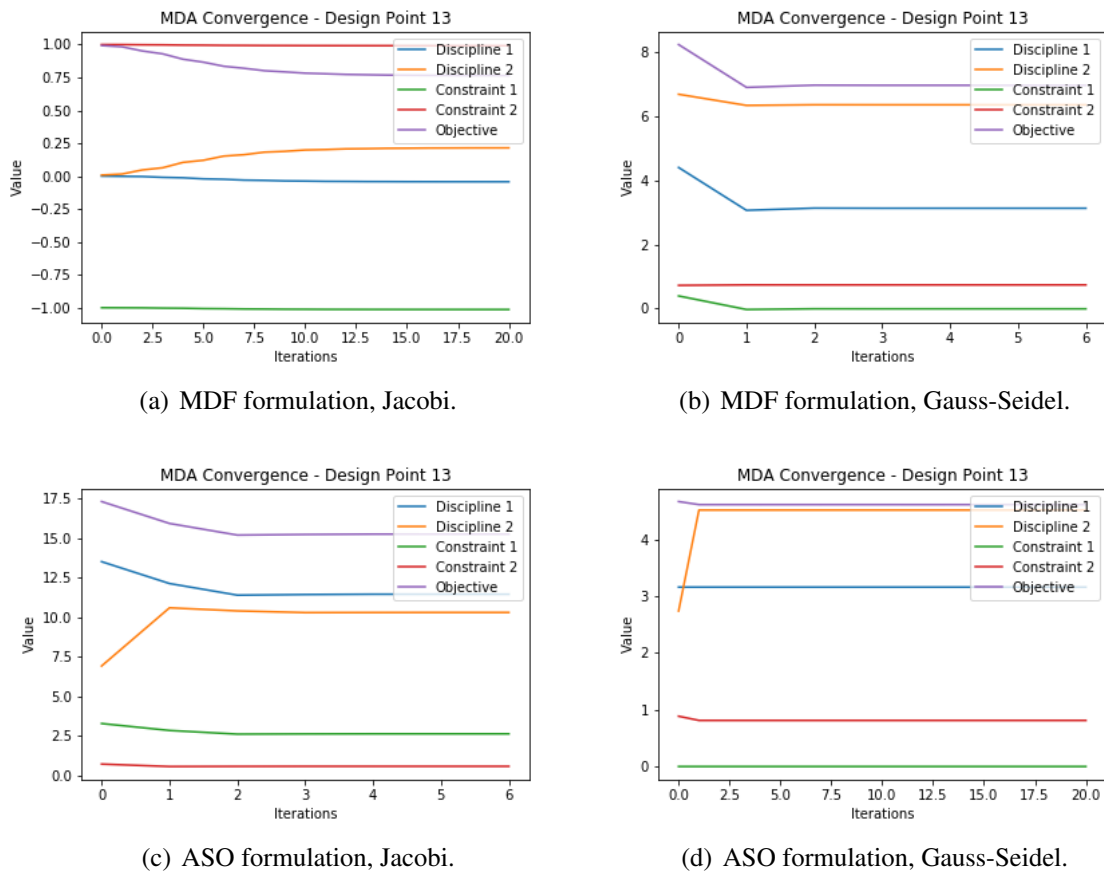


Figure 4.12: MDA convergence comparison of Jacobi and Gauss-Seidel method for MDF and ASO architectures.

to the convergence of the MDA/ASO loop. The disciplinary optimisation has a positive impact on the convergence of the coupled analysis. However, this cannot be considered as true for any multidisciplinary problem since it depends on the effect of the local variable on the discipline as well as the dependency between the disciplines.

4.4 Summary

This chapter served as a preliminary test for the methodology that was presented in Chapter 3. In this, the method is applied in simple analytical problems of known solution. A 1D and 2D cases were used as a first step, to examine the process and fine-tune some of its parameters. This low dimensionality allowed the comprehensive visualisation of design space so that its surrogate prediction could be compared against the real analytical function. It was shown that the method is successful in depicting the key characteristics of the design space, making efficient use of the error information. The local optimum associated with the low fidelity Branin function was avoided and the method consistently converged to the real high fidelity global minimum. The ultimate goal of the methodology is multidisciplinary optimisation and specifically aerostructural problems. To avoid formulating an aerostructural problem of excessively high dimensionality, the methodology was assessed using the extended Rosenbrock function which can be scaled up to arbitrary dimensionality. It was observed that the multifidelity method proposed (based on the proposed Kriging modification) was more robust than a multifidelity one based on the standard Co-Kriging model. For an in-depth and efficient design space exploration to be ensured, no more than 30-40 design variables should be used. As a first multidisciplinary design optimisation application, the analytical Sellar function was employed to examine how efficiently the methodology guides such a coupled problem. Another goal was to compare how the multidisciplinary feasible and asymmetric subspace optimisation architectures perform when used in conjunction with this framework. The methodology was designed to be especially efficient within an asymmetric subspace architecture acting as the system level optimiser, to take advantage of the system level dimensionality reduction associated with this multidisciplinary architecture. This was confirmed by the Sellar function studies as the method performance was superior when used with an asymmetric subspace optimisation architecture than when used with multidisciplinary feasible.

Industrially Related Application in Aerodynamic Shape Optimisation Problems

Once you're in it you're in it. Because you commit yourself to such a level where there's no compromise. You give everything you have. Absolutely everything. And sometimes you find even more...

Ayrton Senna

THE methodology has been so far demonstrated in simple problems and therefore, what naturally follows is its application in industrially relevant problems. As a first step, an aerodynamic design problem was selected involving a common airfoil test case. This gives the opportunity to examine all the possible variations and formulations of the optimisation framework without the need for excessive computational requirements, while still providing valuable feedback from a fairly complex and real life design problem. The problem itself can be also formulated accordingly so that the performance in unconstrained, constrained and multiobjective optimisation cases can be assessed.

5.1 The Transonic Airfoil Design Problem

Following the development of the jet engine and its implementation in transport aircraft, operational speeds increased significantly. Conventional transport aircraft aimed in flying in the maximum possible speed to minimise the flight duration. However, flying in the transonic flow regime is associated with aerodynamic design problems that had to be addressed. At speeds higher than a *Critical Mach Number*, the local acceleration of the flow in the conventional wing design of the time caused strong normal shocks in the upper

surface. As a result, drag increases massively beyond the Drag Divergence Mach Number (see Fig.5.1). Therefore, drag was significantly high and could not allow further aircraft acceleration¹. The drag associated with these Mach numbers had to be decreased by a reduction of the shock strength. This was achieved by a radical new airfoil design called the *supercritical airfoil*. In these configurations, the maximum thickness of the airfoil is moved considerably further from the leading edge (LE) than in a conventional airfoil. This provided a more progressive and smooth flow acceleration along the chord, significantly reducing the strength of the shock. Another design approach used to tackle the drag rise problem was the wing sweep. Essentially, this had the same net effect on the flow around the airfoil. Qualitatively, it can be seen either as means to reduce the chord direction flow component or a way to reduce the t/c thickness of the wing. These were novel design concepts originating from a deep understanding of the underlying flow physics and had a massive impact to other disciplines such as structures and control.

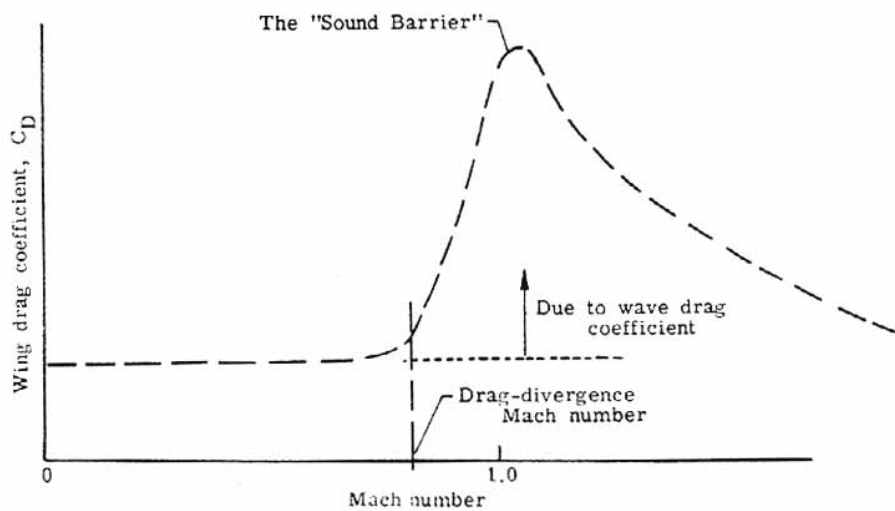


Figure 5.1: Drag rise in transonic flows.

5.2 RAE2822 Test Case

Following this transonic design challenge, and to demonstrate the methodology's potential in tackling similar airfoil design problems, the popular RAE2822 airfoil has been used as a test case. The aim of this work is initially to assess the methodology in a single-disciplinary problem, focusing mainly on its design space exploration capabilities and of course its computational efficiency.

¹In fact drag force was so high that the wing structure would require design modifications to withstand the forces acted in these Mach regions.

5.2.1 Problem Formulation

The test case is formulated as a typical industrial transonic airfoil design problem and the physical conditions correspond to actual aircraft operating conditions. These are shown in Table 5.1.

The problem is set up in a way to allow the demonstration of both a SO and an explicit MO formulation of the proposed methodology, using Lift and Drag as functions of interest, in a coefficient form as follows:

$$f_1 = -C_l, f_2 = C_d \quad (5.2.1)$$

Unconstrained Drag Minimisation

Here, the high fidelity function f_2 is defined in a d -dimensional design space $R^d \mapsto R^1$ where the design variables take values $x \in D \subset R^d$ so that the problem is formulated as,

$$\min_{x \in D} C_d$$

This simple problem serves as a demonstrator of the methodology's fast and global exploration attributes with the results being assessed in terms of the final optimum point OF value and the corresponding computational cost. Since surrogate training does not come to a negligible cost, the total elapsed time is used as a metric instead of the required HF iterations number. The method is compared against a direct HF analysis optimisation driven by an ALPSO optimiser, a HF EI SBO method (performing only HF analyses), an EI SBO method that uses ordinary Kriging— interpolating both LF and HF data — and a Co-Kriging based EI SBO approach.

Lift Constrained Drag Minimisation

The SO formulation of the aerodynamic optimisation problem is extended by including lift constraints, as shown below:

$$\begin{aligned} & \min_{x \in D} C_d \\ & \text{subject to } C_l \geq 0.5 \end{aligned}$$

This is a more realistic design application, testing the method within standard industrial

procedures. Such a case is important as it allows the assessment and comparison of the constraint handling approaches implemented in the methodology. The effect that the constraint handling methods have to the methodology's convergence behaviour might be critical for industrial applications. Usually, these design problems are dominated by constraints, and their computational cost demands a good understanding on the way convergence and feasibility is achieved. This is especially the case in optimisation studies with limited budget where both final result but also feasibility during the optimisation convergence is desired.

In this sense, the two methods presented in section 3.3.8 have been implemented to handle the constraints within the suboptimisation process. In the first approach, a penalty of $EI = 0$ is applied to points for which the surrogate model's C_l estimation violates the constraints. This is sufficient to guide the suboptimisation process to feasible regions according to the current metamodel. For the second approach, the probability of C_l being less than the limit is calculated using the probability of improvement formulation of Eq.3.3.11 (probability of feasibility (PF) [107]). Therefore, the suboptimisation process uses the generic form of Eq.3.3.15, which when applied to this single constraint problem, solves Eq.5.2.2.

$$\mathbf{x}^* = \arg \max_{\mathbf{x} \in \mathbb{D}} PF \times EI \quad (5.2.2)$$

where the probability of feasibility for an inequality constraint problem of $g(\mathbf{x}) \leq g_c$ is expressed as,

$$PF(\mathbf{x}) = \frac{1}{2} \left(1 + \operatorname{erf} \left(\frac{g_c - g(\mathbf{x})}{\hat{\sigma}(\mathbf{x}) \sqrt{2}} \right) \right) \quad (5.2.3)$$

Multiobjective Optimisation

The problem of designing for cruising conditions is typically defined as a lift constrained optimisation problem of drag minimisation. However, an MO formulation can be also of great benefit within an industrial environment. First of all, the presented methodology constitutes the core of a numerical framework to be extended to MDO problems. In MDO, multiple disciplines are associated with multiple — conflicting — objectives. Therefore, we optimise under these conflicting objectives in a cheaper formulation. Furthermore, an MO formulation provides significantly more information than a constrained SO. Several potential optimum configurations are readily available in the engineer's disposal while the pareto front can also feed later-stage local tradeoff studies. Both constitute an element very important for decision making.

5.2.2 Geometry Parameterisation

For this airfoil design problem, Free Form Deformation (FFD) shape parameterisation [7] was used. The control points displacement define the deformation of the surface in the X,Y direction. The bound values are of course dependent on the design requirements and they cannot be strictly and uniquely defined. That is why in this implementation the engineer can explicitly select the bounds desired. To simulate complexity of industrial applications, eight active control points were used creating a 16D design space as shown in Fig.5.2.

Table 5.1: Physical conditions for RAE2822 case

Condition	Value	Units
Angle of Attack	2.31	deg
Mach Number	0.729	-
Reynolds number	6.5×10^6	
Pressure	108987	Pa
Temperature	255.55	K

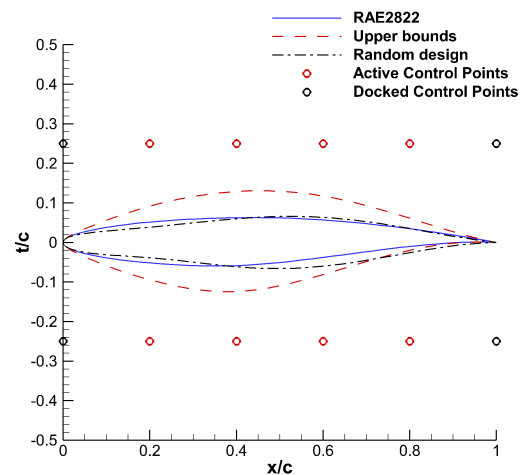


Figure 5.2: RAE 2822 Airfoil. In this test case eight active Control Points are used.

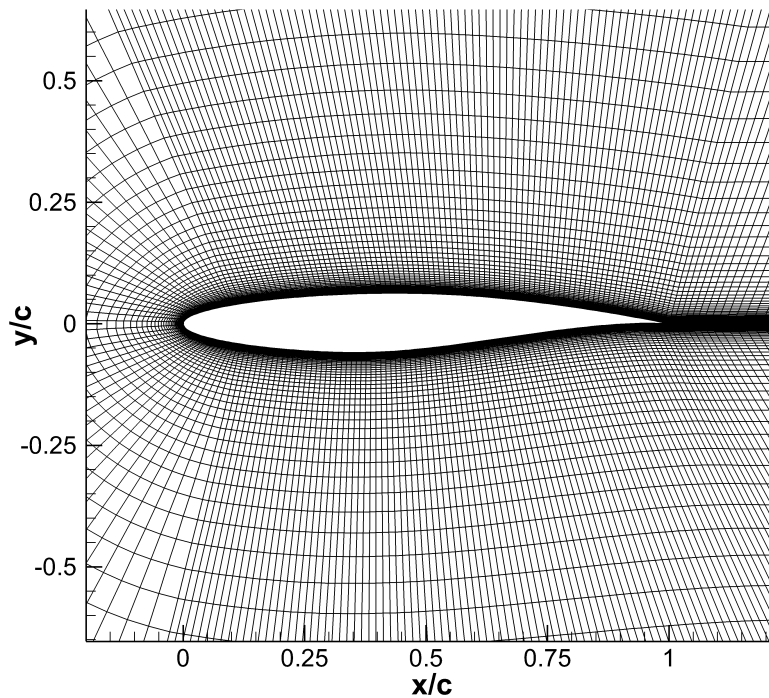


Figure 5.3: C-type mesh generated around the RAE2822 airfoil.

5.2.3 Analysis Tools

The brief introduction of section 5.1 on the challenges of transonic airfoil design, clearly showed the impact that an airfoil's thickness distribution has on its performance. Therefore, the analysis tools should be sensitive to the airfoil thickness, otherwise the mechanism dominating wave drag would be absent. In the latter case, the process would be falsely guided to designs which when assessed with a more reliable tool would prove to be completely inefficient for transonic flight².

High Fidelity Tool

HF analyses are performed using the commercial solver ANSYS Fluent [208], providing the global aerodynamic coefficients. We use a structured C-type grid (see Fig. 5.3) and fully resolve the boundary layer with a y^+ value in the order of 1. A grid validation [209] study ensured that an intermediate grid featuring 38000 cells was appropriate. Special

²This problem is mostly associated with the thickness sensitivity of the LF tool, as HF analyses usually employ RANS CFD simulations.

care was also taken to ensure the grid robustness to geometry changes that arise across the optimisation process. Here, we used grid regeneration instead of deformation since it does not pose significant computational cost. An implicit density based Roe-FDS solver with a 2nd order upwind discretisation scheme was used and Sutherland's model for the dynamic viscosity was employed. Turbulence effects, are modelled using $k-\omega$ SST [210] as to the author's experience it provides the optimum results in attached slender body aerodynamic flows. The maximum number of iterations performed for convergence was set to 3000. To ensure robustness, in cases where limited cycle oscillations are present in the solution, the final result was averaged using values from the last 50 iterations.

Low Fidelity Tool

Since the accuracy and the cost of the LF tool is very important for the success of any MF method, three different LF analyses were used to examine their impact on convergence. An accurate, robust but expensive LF tool was provided by a partially converged [111] ANSYS Fluent simulation, stopped after 800 iterations and using the same numerical setup as the HF tool. Despite its accuracy, the inconsistency of the results — inherent to the concept of partially converged simulations — imposes a challenging multimodal error space. To take this to the extreme, we use another LF tool of decreased accuracy, by stopping the analysis earlier in the convergence (500 iterations). This LF tool imposes an even more challenging error distribution as it is neither accurate nor smooth. The final examined LF tool is VGK [211], a viscous corrected solver based on the method of Garabedian and Korn [212]. It is accurate in cases for which it has been calibrated. However, it is not as robust as the previous two tools for optimisation applications, since it can be only used in attached boundary layer cases. This, combined with the reduced cost, provides feedback on how the convergence history is affected by a cheap tool which is appropriate only to a limited region of the design space. More discussion on this is provided in the following paragraph.

A Note on the Limit and Effect of the Low Fidelity Tool

The choice and use of the LF tool in a multifidelity framework will be seen as a factor of significant impact on the final results. The ability to show similar design trends with HF analysis tool is only one of the requirements. What is equally important in order for a LF tool to be useful, is to share the same design space range applicability with the HF tool and to be robust. It should be able to provide reasonable results (of HF-like trends too) anywhere in the design space — where the HF is also used — without diverging. This is not always possible since LF tools are in many cases developed using data corresponding only to a specific physical conditions domain, making the tool highly inaccurate in other conditions. Their proper use is then especially challenging in frameworks that intend to explore the design space, as the described one. The significant difference of the possible designs lead to different physical conditions around the airfoil (shock waves, flow separation etc.)

which the LF tool is not designed to tackle. As such, it can either provide completely misleading information, or not provide any information at all. The above are confirmed by the results that follow, in which VGK is used as a LF tool in a wide range of geometries that lead to physical conditions which are out of its applicability (strong shocks). These conditions are usually associated with poor performance of such geometries, and hence the LF tool might actually be accurate and robust in the area near the pareto optimum points³. However, the loss of information interacts with the exploration scheme reducing its efficiency. A simple turnaround to this problem is the application of penalty values in poor or non-robust design space regions. The effective solution though is the use of appropriate and more reliable LF tools — which supports decision to assess two different LF methods in the present work.

5.3 Results

As stated earlier, the nature of this SBO method, demands its assessment to be in terms of total elapsed time. To further demonstrate the capabilities of the method to handle expensive cases efficiently, we additionally impose equivalent costs to the analyses described above. As such, we set an HF analysis elapsed time cost of 4hrs and a LF one of 20mins. It is stressed that only HF improvements are considered "accurate", accepted and presented in the convergence history. LF improvements are not presented despite being "accurate enough" in some of the points, with the LF results being used only for surrogate model augmentation.

5.3.1 Unconstrained Drag Minimisation

Figs.5.4,5.5 summarize the findings of the unconstrained aerodynamics shape optimisation study. In this, our proposed method is compared against alternative approaches. For the sake of this comparison, the partially converged Fluent simulation (800 iterations) was used as a LF tool in the MF methods.

It is evident that when ALPSO calls the CFD analyses directly, the convergence is slow and reaches a plateau significantly higher than the minimum C_d value that can be attained. This is not a result of low particle number as both 30 and 100 swarm populations were tried with similar results. It can be explained in particle velocity terms. A less aggressive setup with lower particle velocities would not get stuck to a local minimum. However, this would increase the cost of the already inefficient — compared to the other methods — optimisation process. The same ALPSO setup was successfully used during the suboptimisation

³It should be noted that a wide/narrow pareto front does not necessarily correspond to a wide/narrow design space exploration. The former refers to the objective space whose characteristics should not be confused with the ones of the latter.

Table 5.2: Unconstrained case - Methodologies examined

Nr.	OF Model	LF tool	LF correction
1	-	-	-
2	Kriging	-	-
3	Kriging	Fluent	-
4	modKriging	Fluent	Kriging
5	modKriging	VGK	Kriging
6	Co-Kriging	Fluent	-
7	Co-Kriging	VGK	-
8	modKriging	Fluent	RBF
9	modKriging	VGK	RBF
10	modKriging*	VGK	Kriging

*Training only after HF samplings

process of the HF EI, MF ordinaryKriging EI and MF modKriging EI approaches. In the MF cases, the effect of the initial sampling was examined [213] and two sampling plans were used: one with only 16 HF points and with 16 HF and 32 LF points. The HF EI case used a sampling of 48 HF points. All SBO cases were able to explore the design space more effectively, as they did not stuck to a local optimum like the direct ALPSO approach and showed significantly better C_d minimum values. The HF SBO method was effective in ultimately finding a good optimum value. However, the computational cost associated with the HF initial sampling, made it inefficient compared to the MF methods. The ordinary Kriging, in conjunction with MF data within an EI SBO plan, could not guide the optimisation process to a similarly good final value. This result is in complete qualitative agreement with the findings of the simple 2D case. In this sense, our proposed MF modKriging EI method is more efficient than MF ordinaryKriging. The modification demonstrated in the previous chapters improved the design space approximation and EI distribution according to our predictions, leading to a faster and more robust convergence. It is observed that in every case ran, MF modKriging EI could find an optimum within a 5% deviation from the HF EI optimum, but with less than 50% of the required elapsed time. In this simple design test case, Co-Kriging proved to be the most efficient method. Despite the fewer improvements during the optimisation process, Co-Kriging provided more efficient infill samplings since it takes into account the correlation between LF and HF data.

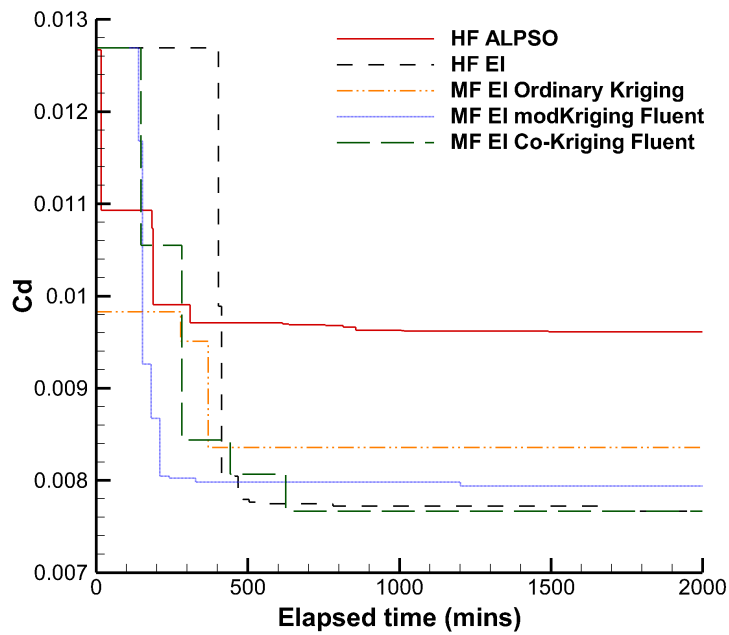


Figure 5.4: Elapsed time based convergence comparison of several methods for the simple airfoil case.

The above observations become even more apparent when the cost of the HF and LF tool increases, as shown in Fig.5.5. Here, the MF methods offer a distinct advantage over the HF ALPSO, HF EI and MF ordinaryKriging approaches, which following the initial sampling, display slow convergence. This is a direct consequence of the infill HF cost against the LF one, which is efficiently exploited by MF modKriging and Co-Kriging. Since MF surrogate models are corrected and HF information is embedded within them, the number of HF infill calls required is reduced, more infill samplings now use LF analyses, decreasing the total computational costs. This is valid especially in cases where the LF tool is accurate enough to follow the trends of the HF objective. In cases where the LF tool is very inaccurate, the cost related to training the error correction might make the method inefficient as more HF training points might be required.

The effect of the LF tool, the error correction model as well as the frequency of the Kriging training is illustrated in Figs.5.6,5.7. Regarding the error correction model, it was observed that Kriging was more efficient in correcting the surrogate predictions, a fact more profound in the early stages of the optimisation and especially when VGK is used as a LF tool. The reason behind this effect is that as the number of TD increases, the training of the model becomes more expensive in terms of elapsed time. In later stages of the optimisation however, the high number of existing TD does not demand the use of the accurate but expensive Kriging model. Instead, the simple but fast RBF model is sufficient. In a similar fashion, avoiding Kriging training in the early stages of the process does not show any benefit. In fact, convergence is delayed. Early in the process, any new infill point provide valuable information that changes the design space estimation a lot compared to infill points

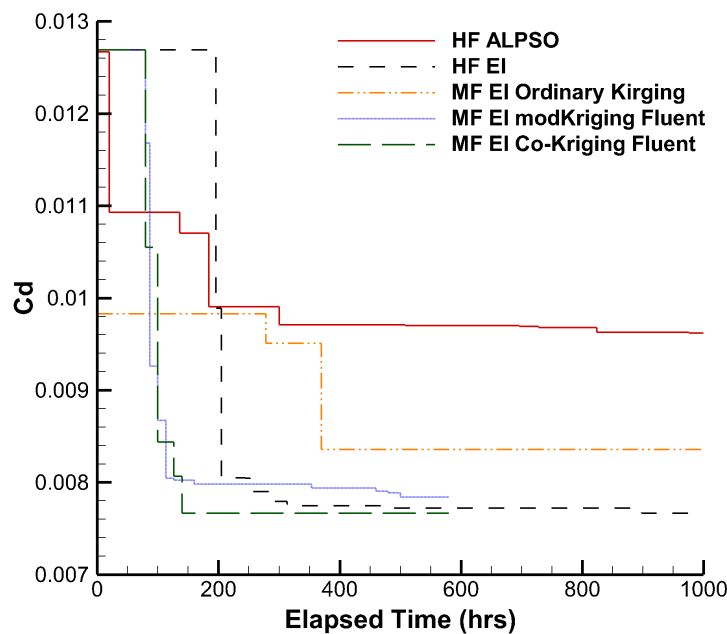


Figure 5.5: Elapsed time based convergence comparison of several methods when considering that the RAE2822 convergence corresponds to that of a hypothetical MDO problem. This is done by substituting the airfoil analysis cost by the MDO analysis cost assumption made in section 5.3.

in later stages, which do not have the same impact. Therefore, the need for Kriging training is higher in the initial stages in order to guide towards convergence. Furthermore, the cost associated with the hyperparameters tuning is higher when more TD are available and as such, skipping Kriging training in later stages of the optimisation process would be more efficient.

As a general trend observed in this particular problem, VGK serves as a more efficient LF tool than Fluent. VGK provides the correct OF trends, steering the optimisation quickly towards the optimum region. Moreover, with the exception of the Co-Kriging case, one can notice that a better final result is reached using VGK as a LF tool instead of Fluent. This reduced physics tool can still steer the process towards the global HF optimum, as the design space where the optimum is located, is well within the validity range of the tool. Fig.5.10 shows the typical progress of the optimisation convergence. It is evident that in this unconstrained case, the major mechanism behind drag reduction is the thickness reduction which attenuates the strength of the shock on the upper surface of the airfoil (see Fig.5.9). As stated earlier, in physical conditions that include weak shocks and limited flow separation VGK is robust, providing accurate and consistent results. This thickness reduction is accompanied by a slight increase of the aft reflex which reduces the lift generated by the airfoil. This decreases the strength of the shock waves even more, therefore assisting wave drag reduction. It is expected that when the LF tool is not accurate (as is the case of the partially converged Fluent analysis termed as "BAD LF Tool" in Fig.5.8(a)), or/and

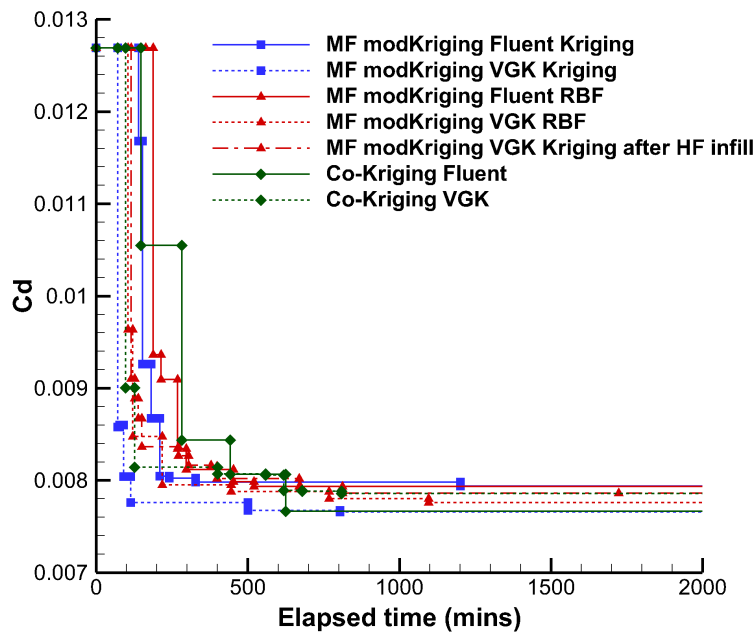


Figure 5.6: Effect of the LF tool, error correction model and Kriging tuning skipping in the elapsed time convergence for the simple airfoil problem.

with OF trends are challenging, the convergence rate is reduced. This hypothesis is investigated by comparing the convergence history of the proposed MF modKriging method when using both Fluent LF tools. Indeed, when this randomness is induced in the error space, the benefits of an MF approach as discussed above are not present anymore. Apart from the extra HF infill points required during the process, it is quite interesting to notice that even Kriging as an error corrector model was not efficient in approximating this challenging error space, with the results being poor compared to the MF methodology that uses a proper LF tool.

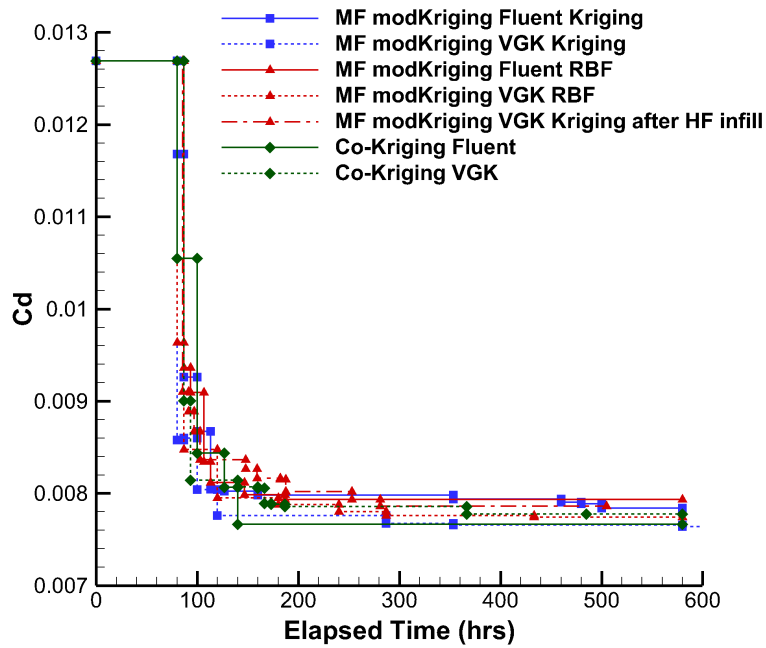
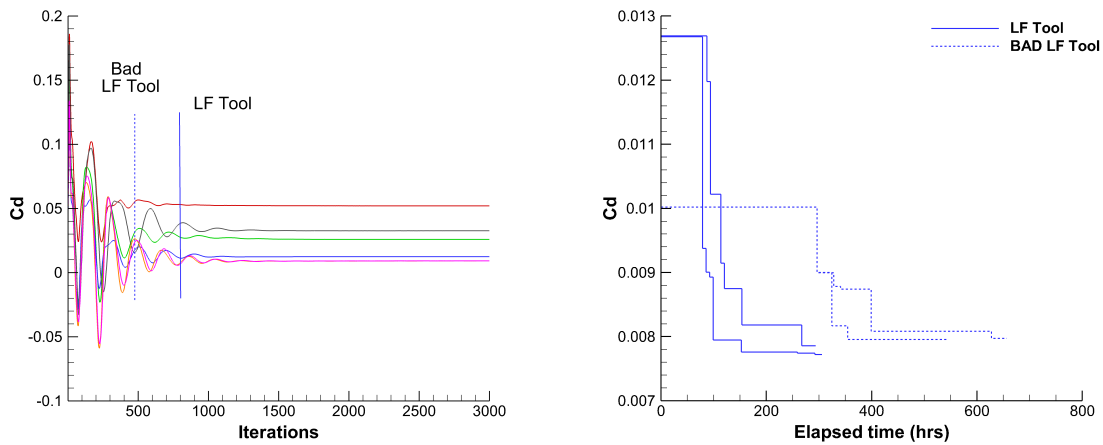


Figure 5.7: Effect of the LF tool, error correction model and Kriging tuning skipping in the elapsed time convergence for a potential MDO problem when considering that the RAE2822 convergence corresponds to that of a hypothetical MDO problem. This is done by substituting the airfoil analysis cost by the MDO analysis cost assumption made in section 5.3.



(a) Typical C_d CFD convergence for various random airfoil configurations. (b) A bad LF tool leads to poor convergence and requires more TD.

Figure 5.8: Definition of the partially converged analysis as a LF tool and the effect of using a solution well within the initial convergence oscillations.

In terms of optimum shapes, shown in Fig5.9, it is evident that the case calling HF CFD

directly does not make full use of this unconstrained case possibilities. It is stuck in a local optimum associated with supercritical airfoil design (similar to the datum), decreasing C_d mainly by a slight shock intensity reduction. On the other hand, all SBO approaches were able to find a better physical mechanism to improve the airfoil's efficiency. Since no lift or pitching moment constraints were present, the SBO methods exploited the FFD parameterisation by generating a thinner reflexed airfoil with no camber and lift, featuring significantly lower wave drag. This demonstrates the ability of the EI approach to successfully explore the design space in order to provide physical mechanism-related feedback to the engineer. All SBO cases converged to very similar designs, being essentially differentiated by the value of the lower middle Control Point (CP) design variable. This difference is most prominent in the Co-Kriging approach which provided the best final result among all methods.

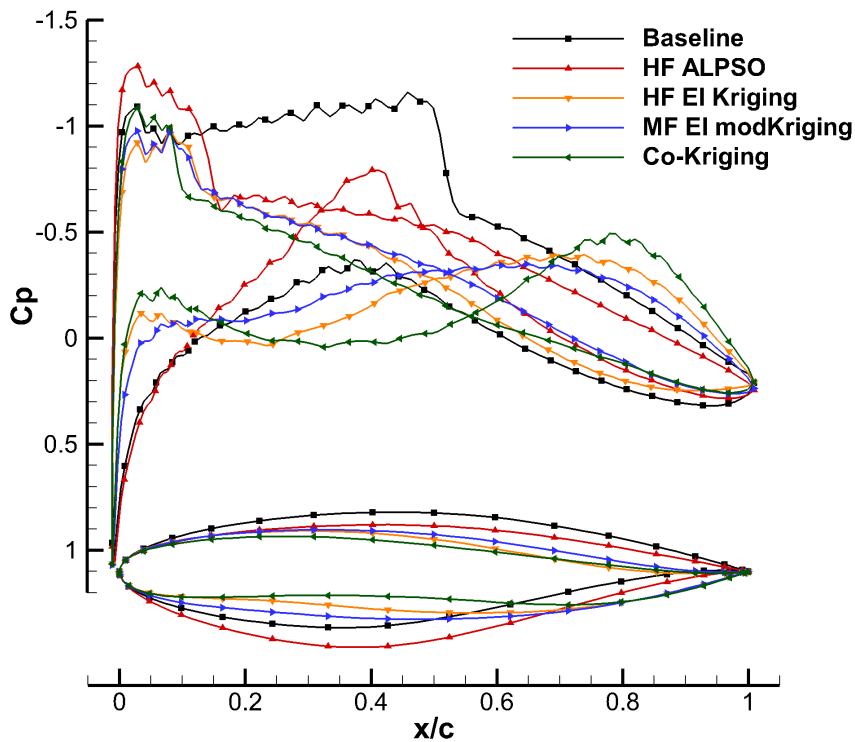


Figure 5.9: Comparison of the resulting geometries and corresponding C_p distributions in the unconstrained case.

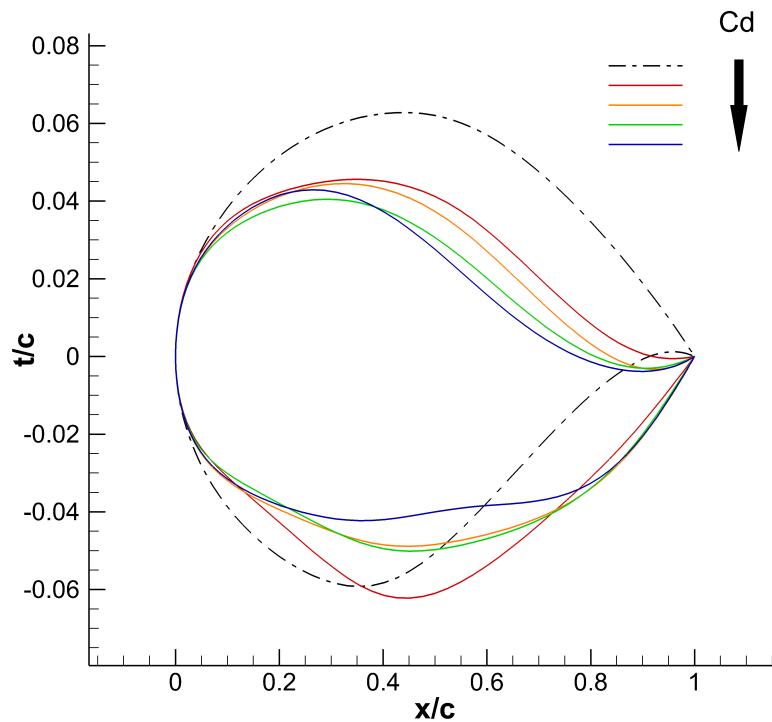
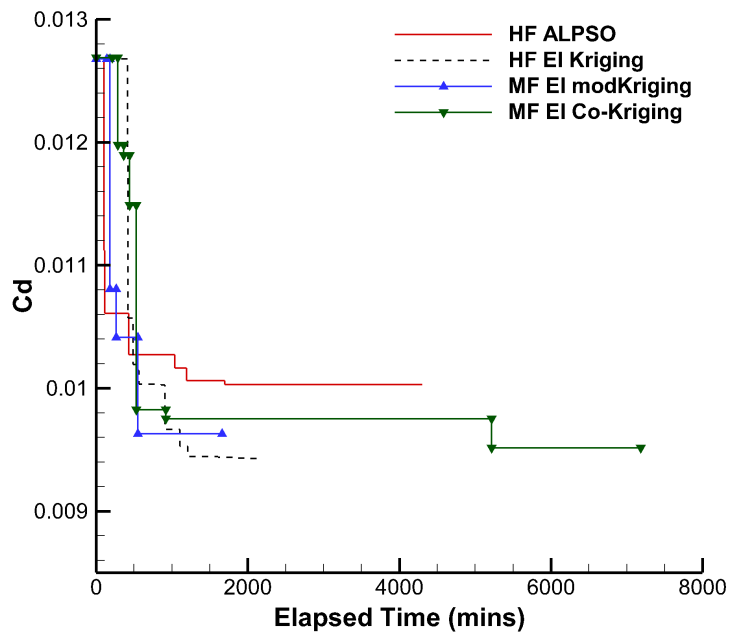


Figure 5.10: Typical airfoil configuration convergence for the unconstrained drag minimisation problem. As we move from the red configuration to the blue one, drag is decreased.

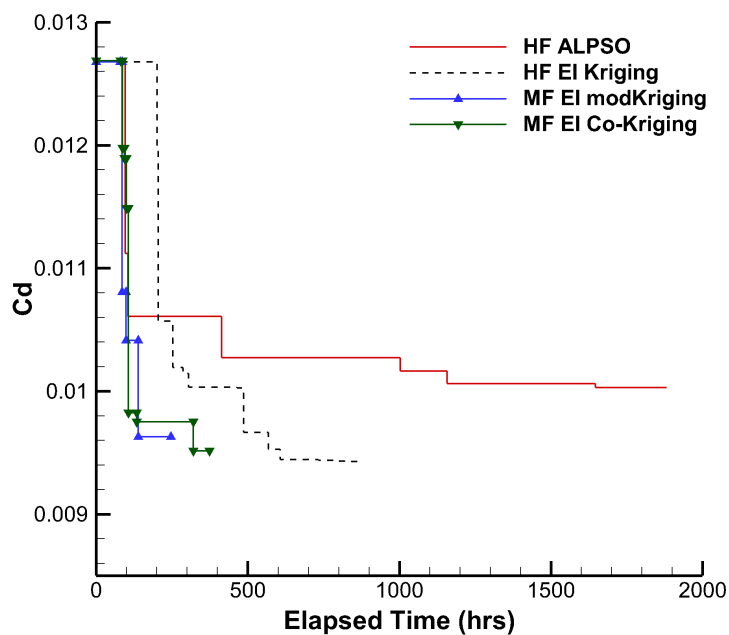
5.3.2 Lift-Constrained Drag Minimisation

Similarly to the unconstrained case, we compare the SBO approaches to the ALPSO-based optimisation (calling only HF analyses) and the HF EI based one. Since it is important to assess the effectiveness of the constraint handling plans for future constrained MDO applications, the SBO cases examine both the Penalty and the PF EI (Feasibility) formulation. The ALPSO cases are explicitly driven by hard penalties and as in the unconstrained cases, the optimiser was stuck in a local optimum.

As shown in Figs.5.11,5.12, our proposed MF method showed great overall potential for expensive problems as it can provide a quick and reliable improvement suggestions to design engineers. In terms of final C_d values, the HF EI approach is slightly superior as it shows approximately 5% improvement over the MF EI result. However, for real industrial problems with cost comparable to multidisciplinary problems, this improvement translates into up to 3 times the computational cost. Furthermore, since the MF EI cases never reached the cost of the HF EI optimisation, additional and more extended runs are allowed to be performed to examine their behaviour in similar elapsed time costs.

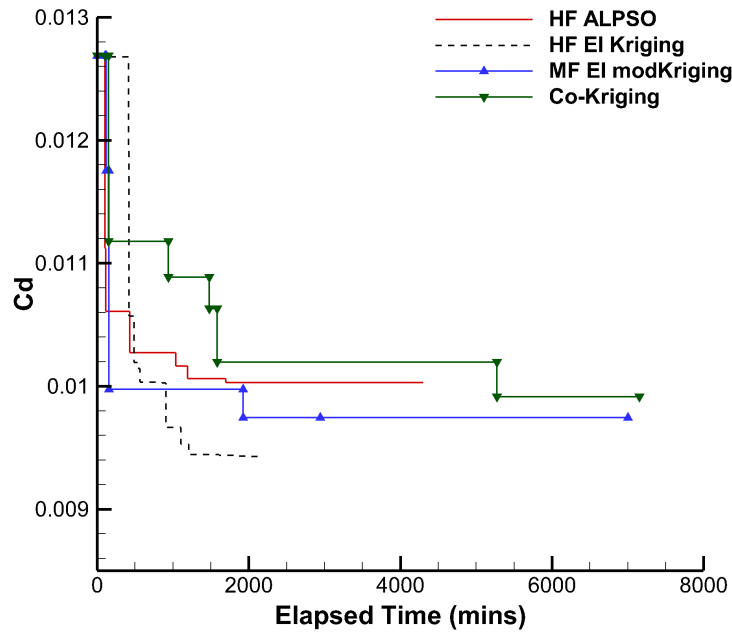


(a) Convergence of the airfoil design problem.

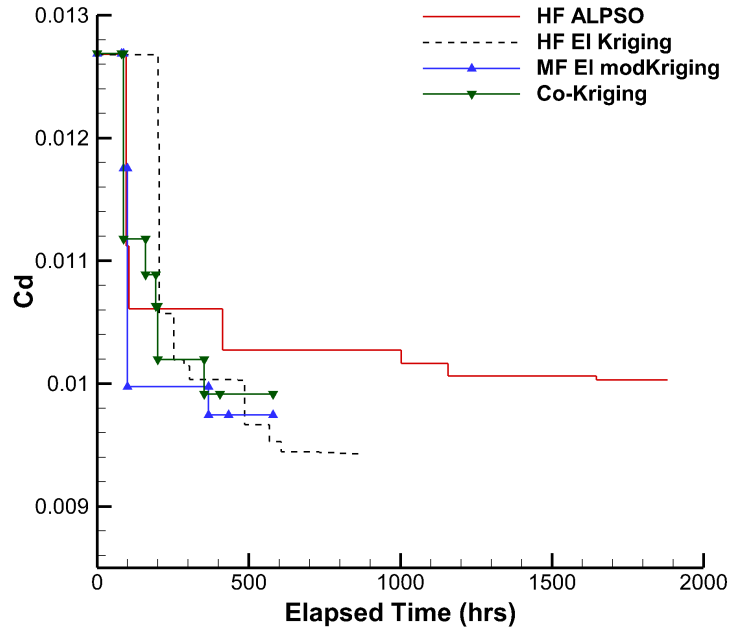


(b) Convergence of the airfoil design problem assuming costs similar to multidisciplinary optimisation.

Figure 5.11: Convergence comparison of the examined optimisation methodologies. Partially converged fluent simulations were used as the low fidelity tool. The lift constraint was tackled with the feasibility method and the surrogate model used to approximate the constraint function was the multifidelity modified Kriging.



(a) Convergence of the airfoil design problem.



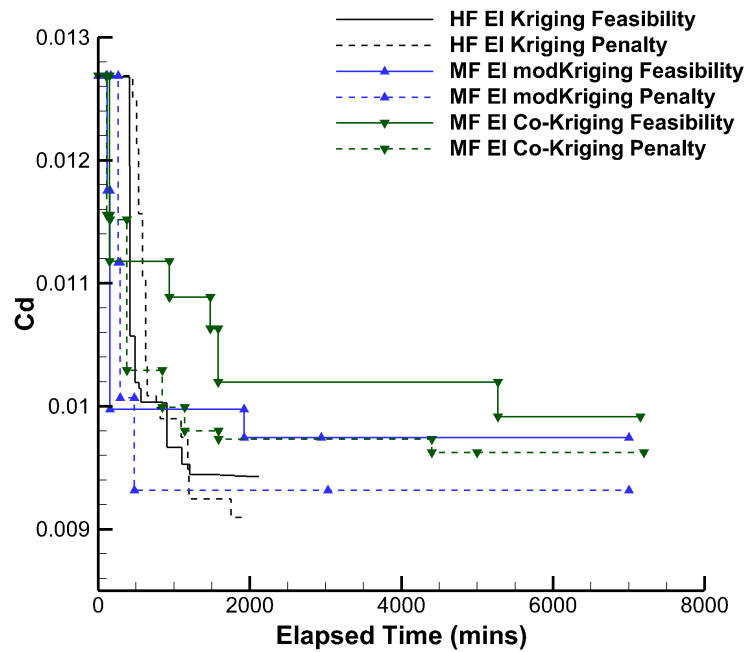
(b) Convergence of the airfoil design problem assuming costs similar to multidisciplinary optimisation.

Figure 5.12: Convergence comparison of the examined optimisation methodologies. In this, VGK was used as the low fidelity tool. The lift constraint was tackled with the feasibility method and the surrogate model used to approximate the constraint function was the multifidelity modified Kriging.

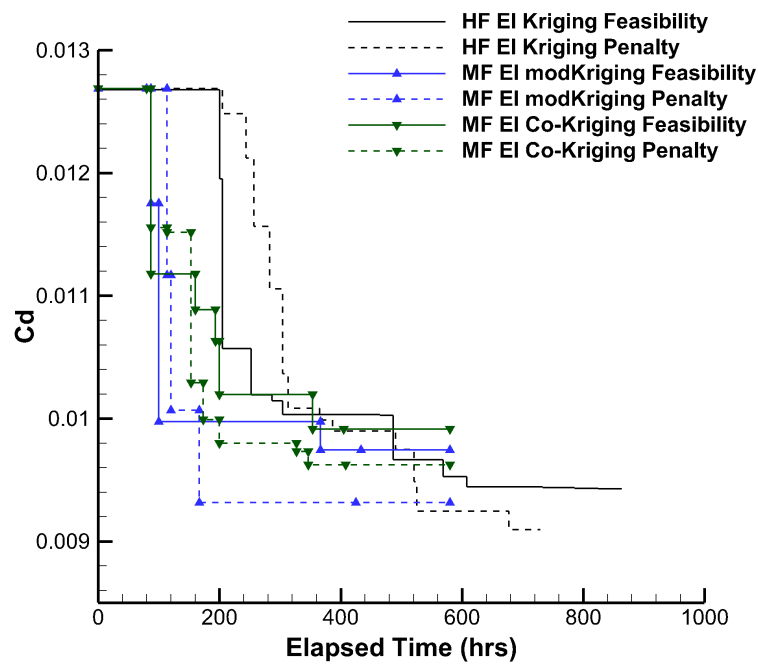
Table 5.3: Constrained case - Methodologies examined

Nr.	OF Model	LF tool	LF correction	Constr.	Constr. Model
1	-	-	-	-	-
2	Kriging	-	-	Feasibility	Kriging
3	Kriging	-	-	Penalty	Kriging
4	modKriging	Fluent	Kriging	Feasibility	modKriging
5	modKriging	Fluent	Kriging	Penalty	modKriging
6	modKriging	VGK	Kriging	Feasibility	modKriging
7	modKriging	VGK	Kriging	Penalty	modKriging
8	modKriging	VGK	RBF	Feasibility	modKriging
9	modKriging	VGK	RBF	Penalty	modKriging
10	modKriging	VGK	Kriging	Penalty	modRBF
11	Co-Kriging	Fluent	-	Feasibility	modKriging
12	Co-Kriging	Fluent	-	Penalty	modKriging
13	Co-Kriging	VGK	-	Feasibility	modKriging
14	Co-Kriging	VGK	-	Penalty	modKriging
15	Co-Kriging	VGK	-	Penalty	modRBF

For both the HF and all the MF cases, it was observed that penalty methods consistently resulted to marginally feasible infill designs. As such, a higher percentage of infill points was infeasible compared to the feasibility method which behaved differently. Starting from higher C_l values (and higher feasible points percentage), the feasibility method gradually approached the constraints boundary while lowering the objective function values. Nevertheless, the penalty approach consistently provided better final configurations in all the cases examined as shown in Fig.5.13. Regardless of the constraint handling approach, the superiority of the proposed method is especially apparent in the case where the analysis cost is high. This is a direct consequence of the fewer HF infill points required. However, the fact that makes the method more appealing than the Co-Kriging based one, is that for this case which requires two surrogate models (for the OF and the constraint), the training costs are significantly reduced. This is a result of the fewer hypertuning parameters in our Kriging method (in contrast to Co-Kriging, no correlation parameter is used). However, most elapsed time savings arise from the inherent ability of our method to avoid a Kriging model for the error correction and use RBF instead. This replacement comes with no significant loss of information since the RBF is used appropriately, to restore the error MSE information required by EI, as discussed earlier.



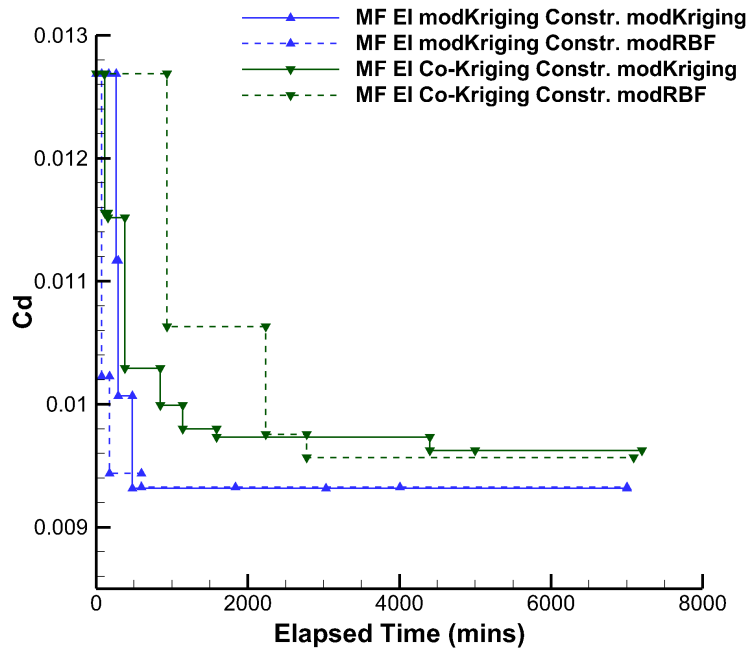
(a) Convergence of the airfoil design problem.



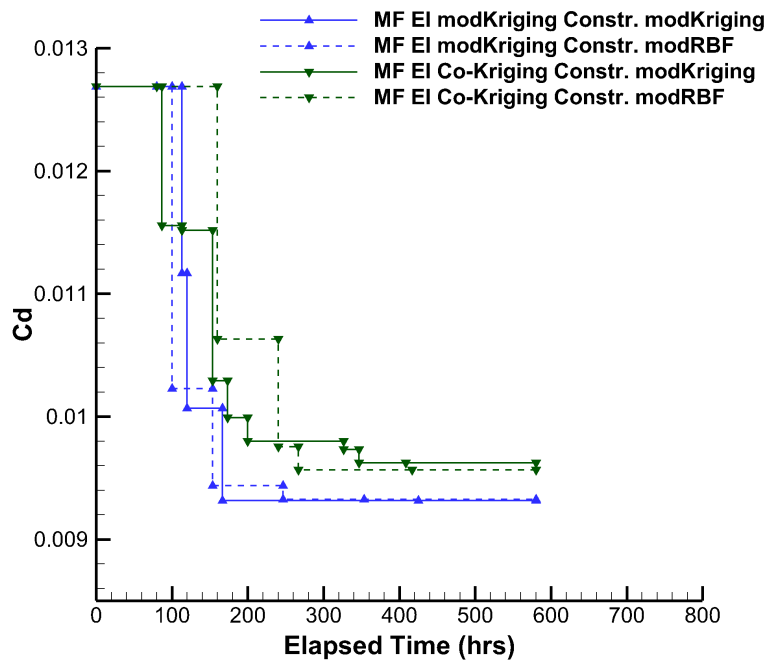
(b) Convergence of the airfoil design problem assuming costs similar to multidisciplinary optimisation.

Figure 5.13: Convergence comparison between the two constraint handling approaches. In this, VGK was used as the low fidelity tool. Multifidelity modified Kriging was used to approximate the constraint function.

In addition to this, there is also the potential for further cost reduction that can be attained by using RBF as the constraint surrogate model in the penalty method cases, as evident in Fig.5.14. Although this reduction is present in both our method and the Co-Kriging based one when penalty method is being used, the effect of the constraint model replacement proves significant when it is compared against the feasibility cases which demand the use of Kriging models. In this sense, the combination of RBF and penalty method accelerates the convergence, a fact associated with both the aggressive character of the penalty method and the constraint model training cost reduction.



(a) Convergence of the airfoil design problem.



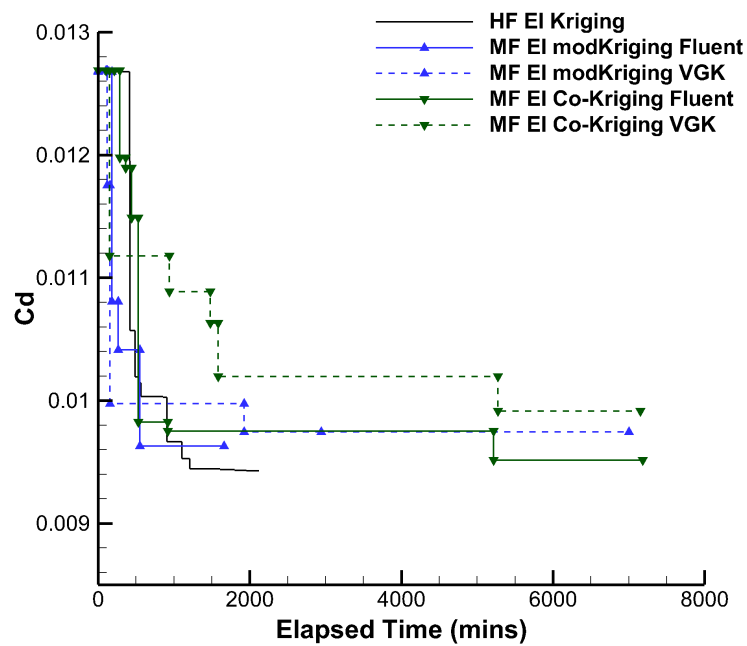
(b) Convergence of the airfoil design problem assuming costs similar to multidisciplinary optimisation.

Figure 5.14: Convergence comparison between two metamodeling approaches for the estimation of the constraint function. In this, VGK was used as the low fidelity tool. Results from the penalty method are plotted.

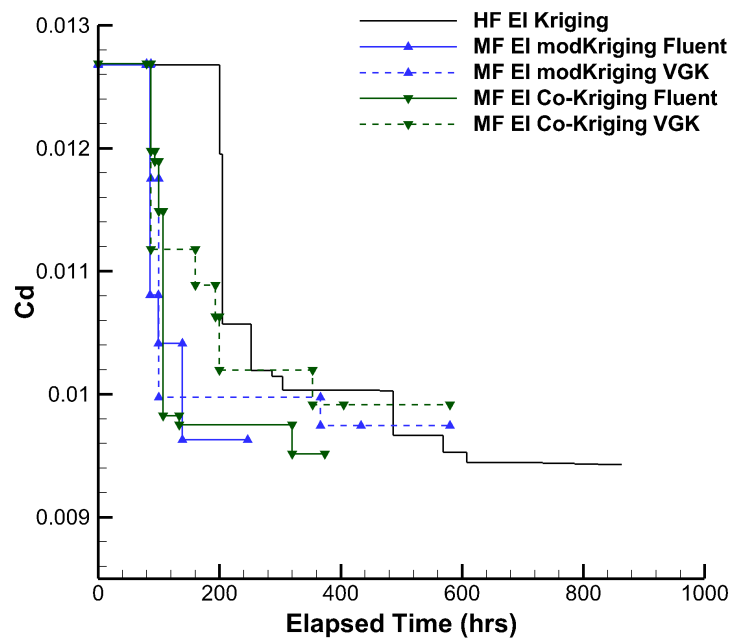
The effect of the LF tool cannot be evaluated in a definitive manner by these results. As shown in Fig.5.15, fluent partially converged simulations prove to be more robust compared to a reduced physics model like VGK when the conservative feasibility method is being used. However, with the use of the more aggressive penalty method (shown in Fig.5.16), the different LF tool options do not show a clear trend regarding their associated convergence rates. Further work and discussion on the effect of the LF tool, especially in the context of design space exploration, is presented in the next section.

Overall, the most significant outcome that can be claimed with confidence from the above, is the superiority of the multifidelity approach over traditional single fidelity EI method. This is particularly the case when analysis models of high computational cost are involved in the optimisation process. The design improvements attained by the HF method cannot be surpassed by the MF ones. However, the drag decrease achieved by the MF EI modKriging method is consistently within 5% from the HF one, requiring significantly reduced computational resources.

The optimum geometries displayed in Fig.5.17, share similarities to the unconstrained case. The local optimum configuration associated with the ALPSO driven optimisation is a supercritical design with slightly higher camber than the unconstrained case, to account for lifting constraints. As in the unconstrained case, the HF/MF EI methods explore the constrained space more efficiently, leading to similar configurations characterized by lower thickness, slight camber and aft reflex. Evidently, the difference between the HF and MF optimum configurations lie in the lower section. The comparison of the pressure distribution of these airfoils underline the high sensitivity of the flow characteristics to small changes in the geometry. Notice how the HF and the MF modKriging configurations share an almost identical upper surface but the lower surface is different as it originates from different camber distribution. The increased LE camber and thickness of the MF modKriging configuration leads to a higher suction, causing a shock. Another shock is formed slightly downstream, where the critical C_p is met. This is not the case however for the HF configuration which by having a slightly different camber distribution, features a single shock.

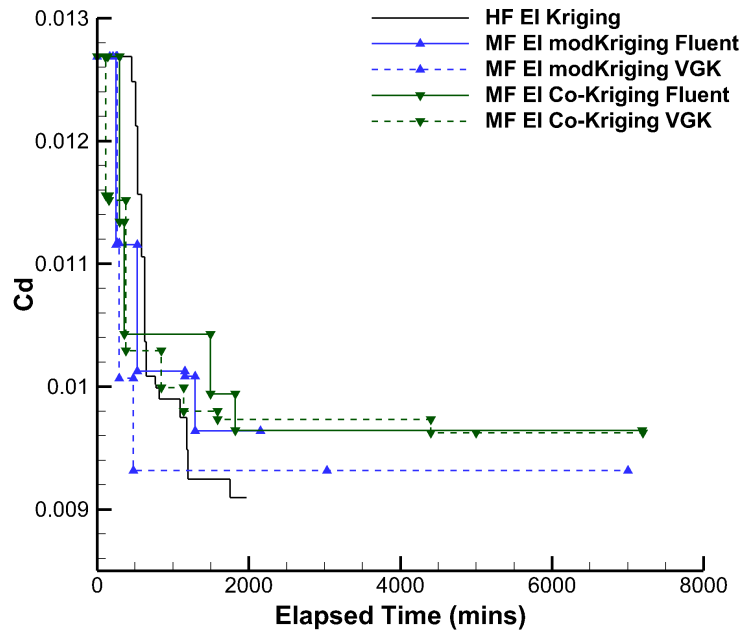


(a) Convergence of the airfoil design problem.

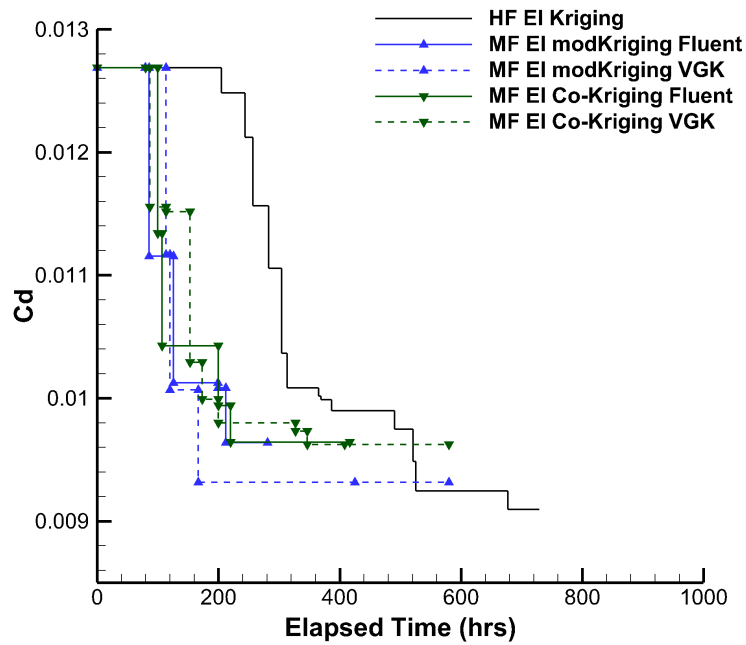


(b) Convergence of the airfoil design problem assuming costs similar to multidisciplinary optimisation.

Figure 5.15: Convergence comparison between two low fidelity analysis tool possibilities. Results are based on the feasibility method.



(a) Convergence of the airfoil design problem.



(b) Convergence of the airfoil design problem assuming costs similar to multidisciplinary optimisation.

Figure 5.16: Convergence comparison between two low fidelity analysis tool possibilities. Results are based on the penalty method.

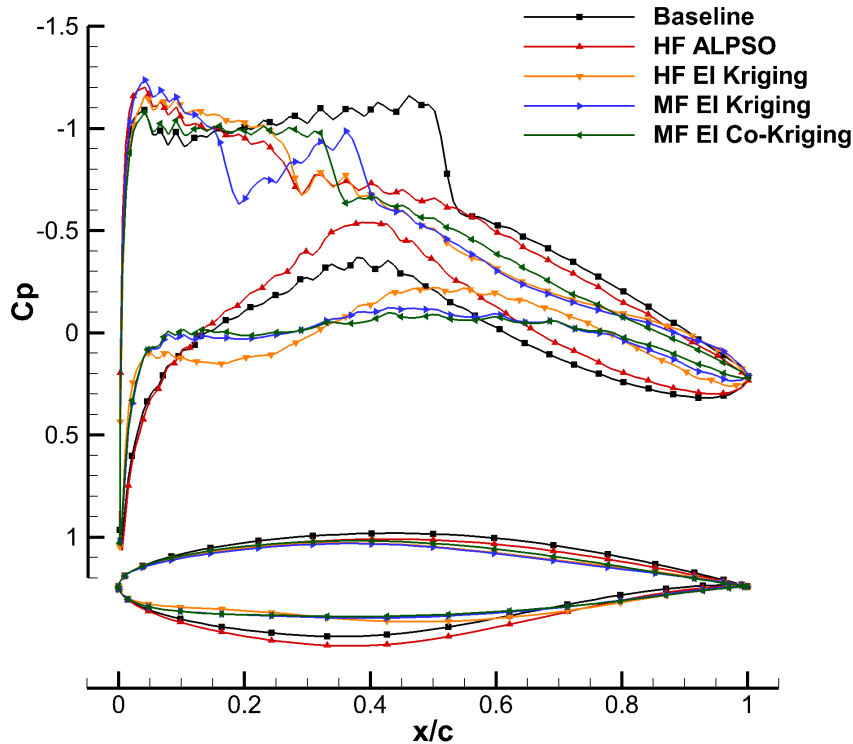


Figure 5.17: Comparison of the resulting geometries and corresponding C_p distributions in the constrained case.

5.3.3 Multiobjective Optimisation

Comparison of EI infill Sampling Methodologies

Before proceeding to the results of the multiobjective formulation of the airfoil design problem, it should be defined which formulation of the infill sampling process is being used. For this, a comparison of the standard methodology of EI for improving the pareto front (see [88] and Eq.3.3.24), against our parallel infill EI methodology of section 3.3.7 is performed.

The methods are compared in Fig.5.18 in terms of their respective pareto front results, for a defined computational budget. Since the only difference between the methods is found in the suboptimisation process, the sampling, surrogate training and infill analyses costs are identical. Therefore, the comparison is based on the number of high fidelity infill analyses⁴.

⁴The suboptimisation problem of EI maximisation is and EI pareto front generation is solved by ALPSO and MOPSO algorithms respectively. For this dimensionality, the observed difference between the two in terms of elapsed time was negligible.

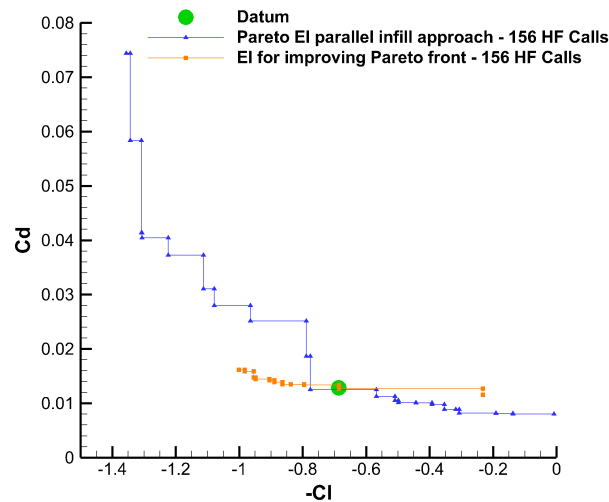


Figure 5.18: Comparison of the multiobjective formulations of expected improvement as presented in section 3.4.7.

The standard infill methodology can locate highly efficient tradeoff points in the mid C_l region — close to the datum point. In the low and high C_l objective space however, it is evident that this EI formulation does not exhibit the desired exploration characteristics. On the other hand, the proposed parallel formulation develops a wide Pareto front of efficient configurations especially in the low C_l region. This is an expected result as the standard "EI for improving the Pareto Front" method is designed to achieve just that, find new dominating designs. This does not necessarily mean that the new designs will be associated with an extended design or objective space exploration, rather than just being dominant over the previous ones. As such, a more balanced exploitation/exploration behaviour is observed. In our newly proposed approach however, the points used for infill sampling are explicitly selected to be the ones which are not only promising but also diverse in terms of objective function value. Since the main application of the methodology described in Chapter 3 requires efficient conceptual design (and objective) space exploration, all multiobjective applications demonstrated will be using our suggested suboptimisation process. Another significant advantage of our method is its inherent characteristic to provide multiple infill points, in this case it is set to three. Therefore, since these points are analysed in parallel, the effective computational cost is only a third of that of the standard method. Having established the behaviour of both approaches, it should be stated that there is the potential for a hybrid methodology using these two in sequence. Within such a concept, the proposed parallel infill can be initially used to satisfy exploration requirements followed by the other method after a "wide-enough" has been developed. This will provide a more local refinement, improving the performance of the wide Pareto front points.

Parallel EI Infill

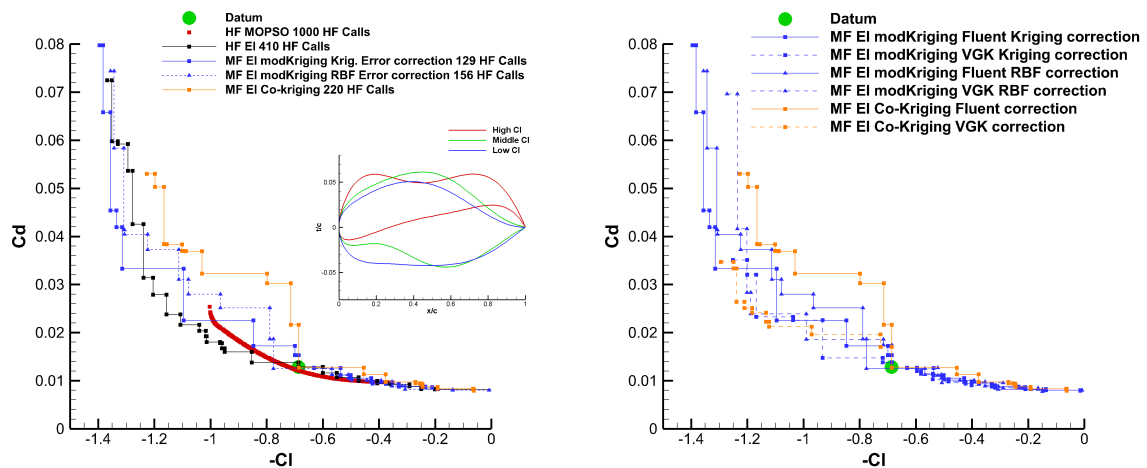
The MO formulation of this aero shape optimisation problem, solves the suboptimisation problem explicitly, providing a pareto front of possible infill points. The direct HF analysis based optimisation steered by MOPSO, quickly creates a dense front. However, later in the optimisation process no further improvements were observed and similarly to the respective single objective cases, this approach is stuck to a final plateau. Furthermore, the pareto front is quite narrow compared to the HF and MF cases which is an important factor to consider, as the main drive behind an MO formulation is to explore various decision solutions — especially in the low C_l , C_d regime. Nevertheless, it could provide slightly better designs in the moderate C_l region than the HF and MF approach. Both the HF and our proposed MF modKriging method however, showed better exploration attributes leading to more diverse designs. Apart from this benefit, our approach also improved the designs in high and low C_l regions with less than half of the cost of MOPSO case. In the C_l 0.7 – 1.2 region, the MF pareto front was coarser than the HF one, with inferior OF values. In higher C_l cases though, the C_d values were significantly lower than the ones resulting from the HF case. The improvement in the computational cost (reduction to half of the original elapsed time), further supports the use of the MF method. The Co-Kriging based MF method could not lead to a wide pareto front, with the high C_l region being especially limited. This is mostly apparent in designs with higher C_l than that of the datum, since the lower C_l region featured results similar to our MF modKriging based method. As a general trend, VGK narrows the pareto front, especially in high C_l values as the physical conditions including strong shocks and separated flow make the tool inaccurate. This is a direct result of the design space region associated with highly cambered unconventional configurations (see Fig.5.19.a). It is observed regardless of the method and the error correction model. The MO suboptimisation tries to explore the design space in a wide area of potential solutions, examining the possibility of thick and cambered airfoils. However, this is a region in which VGK is not robust nor accurate, and since the LF tool is failing, no information is provided to the surrogate model. One would argue that the design for which VGK fails are not promising and as such no need for exploration in this design space region is necessary. This might be the case in many of the design points. However, even inefficient configurations provide necessary information back to the surrogate model so that the optimisation is steered towards the efficient geometries. If the LF tool fails to provide any output then the extend and accuracy of both the surrogate model and the error correction model suffers. As a consequence, the suboptimisation process is prevented from exploring the promising regions. Therefore, such a LF tool cannot support reliable design space exploration in the conceptual design process. In such cases, a HF SBO method is more robust in providing a wider pareto front and should be preferred. Nevertheless, it is evident that the narrow pareto front is associated with superior OF values when the VGK is used, with the effect being more pronounced in the case of the Co-Kriging based method.

By comparing the corresponding values of the pareto front (see Fig.5.19) to the final results from the single objective cases, one can understand that the cost increase does not allow neither optimiser to reach global optimality for all pareto front points — at least in

our predefined computational resources. This however was not the purpose of the presented methodology. Following this cost efficient exploration of the conceptual design space, the engineer can use the pareto configurations for further local fine-tuning tradeoff studies depending on the needs of the design.

Table 5.4: Multiobjective case - Methodologies examined

Nr.	OF Model	LF Tool	Error Model	HF Calls/El. time (mins)
1	-	-	-	1000 / 8000
2	Kriging	-	-	410 / 8000
3	modKriging	Fluent	Kriging	129 / 4961
4	modKriging	Fluent	RBF	156 / 4388
5	modKriging	VGK	Kriging	227 / 7711
6	modKriging	VGK	RBF	170 / 7129
7	Co-Kriging	Fluent	-	220 / 7000
8	Co-Kriging	VGK	-	370 / 7199



(a) Comparison of the various methods, with partially converged analyses as an LF tool.

(b) Effect of the LF tool and the error correction model.

Figure 5.19: Pareto front comparison of the CFD based, HF EI, MF EI modKriging and MF EI Co-Kriging methods, and their sensitivity to the LF tool and the error correction model (where applicable).

5.4 Summary

Following the demonstration of the methodology in analytical problems, this chapter presented an industrially relevant application. The transonic airfoil design problem was formulated as an unconstrained, constrained and multiobjective optimisation study using the RAE2822 configuration as the baseline airfoil. Free form deformation parameterisation

was used to describe the deformation of the geometry using eight control points spread uniformly across the chord. Since each control point was associated with both X and Y displacements, the problem was described by 16 design variables. The low fidelity analyses were performed with both the VGK tool and the concept of partially converged RANS simulations of two different stages. Thus, the effect of the low fidelity tool inaccuracy and inability to follow the high fidelity trends could also be examined. For the high fidelity calls, RANS simulations were used. The framework was compared against ALPSO optimiser calling high fidelity CFD analyses directly, a high fidelity expected improvement and a multifidelity (Co-Kriging-based) expected improvement method. The unconstrained test case demonstrated the superior exploration attributes of the surrogate based optimisation methods over the gradient free approach which was also more computationally expensive. Both the high fidelity and multifidelity methods showed similar final results but the multifidelity framework required almost 30% of the computational budget. A similar trend was observed in the constrained problem, with the multifidelity approach providing designs slightly inferior to the high fidelity ones, but with significantly lower elapsed time costs. The constraint handling mechanism also showed an impact on the convergence behaviour. The penalty method was more aggressive, locating superior designs but only late in the optimisation study. The feasibility method on the other hand was more conservative, providing feasible designs with higher consistency but falling short in terms of final performance. In the multiobjective problem, the proposed multiobjective infill strategy was compared against the standard multiobjective expected improvement infill strategy for pareto improvement, demonstrating its objective space exploration superiority. The proposed multiobjective framework was compared against an inhouse implementation of the MOPSO algorithm calling directly high fidelity CFD analyses, as well as the standard high fidelity multiobjective expected improvement (with our proposed infill strategy). The multifidelity methodology displayed similar objective space exploration characteristics with the high fidelity one but with reduced costs. When VGK was used as a low fidelity tool, these exploration attributes were reduced, but the tradeoff configurations associated with the middle region of the pareto front were improved.

Comparison Between Trust Region and Expected Improvement Methods

Pride makes for a good servant but a bad boss...

Uncle Jesse

IN the initial stages of the design, perhaps the most important attribute an optimisation tool might offer to the designer, would be to provide information, thus acting as a very efficient trade study tool. As outlined in Chapter 3, to take full advantage of its elements and provide insight to support decision making, a conceptual/preliminary optimisation methodology should use a multiobjective (MO) formulation. Equally important is the reliability and design trends consistency in order to properly drive the design in these stages.

Although MO optimisation methods have been used in the aerospace industry [214, 215], tools based solely on gradient free MO optimisers might lead to very high computational expenses [216]. In response to that, there has been an effort to reduce the cost by using surrogate modelling techniques. Their effect is profound when metamodels substitute expensive [217] or challenging analyses. Their use is not limited in decreasing the computational requirements associated with high fidelity (HF) analysis but to guide the design [218] as well, as in Surrogate Based Optimisation (SBO) problems. Typical applications of metamodeling based methods involve aerospace applications [92, 128] like airfoil design [97]. Effort to develop more sophisticated metamodeling techniques focus on the accuracy and flexibility [84, 98] of the models.

To satisfy the needs for computational efficiency as well as provision of design-related information, a research methodology such as the one described in this work requires continuous evaluation to provide feedback to the researcher. In this sense, the methodology suggested by the author is compared against a similar multifidelity (MF) surrogate based approach developed by J. Demange of the same research group.

The latter is a trust region (TR) based framework [200] that uses a metamodel to correct the low fidelity (LF) aerodynamic solver steering the method to high fidelity optimality. In contrast to the methodology proposed in the present PhD work which aims in the efficient global exploration of the design space in the conceptual stage, the trust region method developed by Dr. Demange focuses on the exploitation of the information provided by the surrogates to perform local improvements. The TR method does not require gradients information [219, 220] nor an initial sampling. Both methods use their respective multiobjective formulation, employing our inhouse implementation of the multiobjective particle swarm optimisation (MOPSO) algorithm [139] and a Multiobjective Tabu Search [145, 147] (MOTS) framework. The aim of this comparison is to display the appropriateness of each approach and their dependency to the problem under consideration [221]. To further assess these methods, we also compare them against a gradient free method, a high fidelity-only SBO method using the expected improvement (EI) criterion and a MF EI method using Co-Kriging to handle the MF data. Two common industrial aerodynamic design problems are being used as test cases: the first design problem involves take-off performance maximisation, formulated as a $C_{l_{\max}}$ and lift-over-drag ratio maximisations, of the Garter high lift three elements configuration [222]. This is a problem involving six design variables and a challenging aerodynamic analysis. The second design scenario resembles a typical transonic airfoil design for cruising conditions, based on the RAE2822 airfoil [213] presented in the previous chapter. Here, C_l and C_d are used as objectives.

6.1 Surrogate Based Optimisation Methodology

6.1.1 Trust Region

The trust region method to be described was developed by my colleague J. Demange as a part of his PhD work. Dr. Demange is acknowledged for his contribution on this chapter by sharing the details of his method as well as his results in order to make the comparison of the two methodologies possible.

In Demange's method, the fundamental optimisation problem of Eq.6.1.1 is solved by a derivative-free trust region method presented by Conn et al. [219]. Instead of directly optimising directly the high-fidelity (HF) problem, an approximation model y of the HF function is used. At any iteration k , the following subproblem is solved under a trust region δ_k :

$$\min_{\mathbf{x} \in \delta_k} \hat{y}_k(\mathbf{x}). \quad (6.1.1)$$

The trust region can be considered as a hypersphere centered on the initial point of the subproblem but in Demange et al. [199], a second definition based on the number of improvements of the corrected model is used. The model $\hat{y}_k : \mathbb{T}_k \rightarrow \mathbb{R}^l$ is defined by Eq.6.1.2 at iteration k . It is formed by the sum of a Kriging surrogate model e_k approximating the

error of the LF function based on Eq.3.3.2, and the LF function f_{LF} itself.

$$\hat{y}_k(\mathbf{x}) = f_{LF}(\mathbf{x}) + e_k(\mathbf{x}) \quad (6.1.2)$$

It was shown by Demange [200] that an RBF or Kriging model is not sufficient to achieve a pareto front as wide as the one resulting from an optimisation acting directly on the HF function. Therefore, a Co-Kriging model is preferred when more than $2(n + 1)$ high-fidelity points are available for training. In this case, equation Eq.6.1.2 is replaced for Eq.6.1.3:

$$\hat{y}_k(\mathbf{x}) = m_k(\mathbf{x}) \quad (6.1.3)$$

with $m_k(\mathbf{x})$ being the Co-Kriging model, implemented according to Forrester et al [88]. Since this model is an extension of Kriging to include multiple levels of fidelity, it uses both HF and LF data. It no longer predicts the error, but directly the corrected function. To solve the subproblem of Eq.6.1.1, the Multiobjective Tabu Search [145, 147] (MOTS) optimiser is used. This is a MO version of the tabu search algorithm described in section 2.8.1. A summary of Demange's method is presented in the flowchart 6.1.

Ratio of Improvement and Trust Region Management

The ratio of improvements $\rho_k = [\rho_k^{(1)}, \rho_k^{(2)}, \dots, \rho_k^{(l)}]$ is calculated for each point provided by the suboptimiser and each objective as follows:

$$\rho_k^{(i)} = \frac{f_{HF}^{(i)}(\mathbf{x}_k) - f_{HF}^{(i)}(\mathbf{x}_s)}{m_k^{(i)}(\mathbf{x}_k) - m_k^{(i)}(\mathbf{x}_s)}, \quad i \in [1, \dots, l]. \quad (6.1.4)$$

Each point of suboptimisation's pareto front is analysed using the HF tool and the optimisation pareto front is updated accordingly. The ratio of improvement is extended to include multiple objectives as follows:

- For each candidate point $p_k = [f_{HF}^{(1)}(\mathbf{x}_k), \dots, f_{HF}^{(l)}(\mathbf{x}_k)]$ in the objective space,
 - If the number of objectives with a ratio of improvement greater than ρ_{bad} is higher or equal to the trigger n_f , the point p_k is marked as *moderate*.
 - If the number of objectives with a ratio of improvement strictly greater than ρ_{good} is higher or equal to the trigger n_f , the point p_k is marked as *good*.
 - Otherwise, the point is marked as *bad*.
- If the number of points p_k marked as:

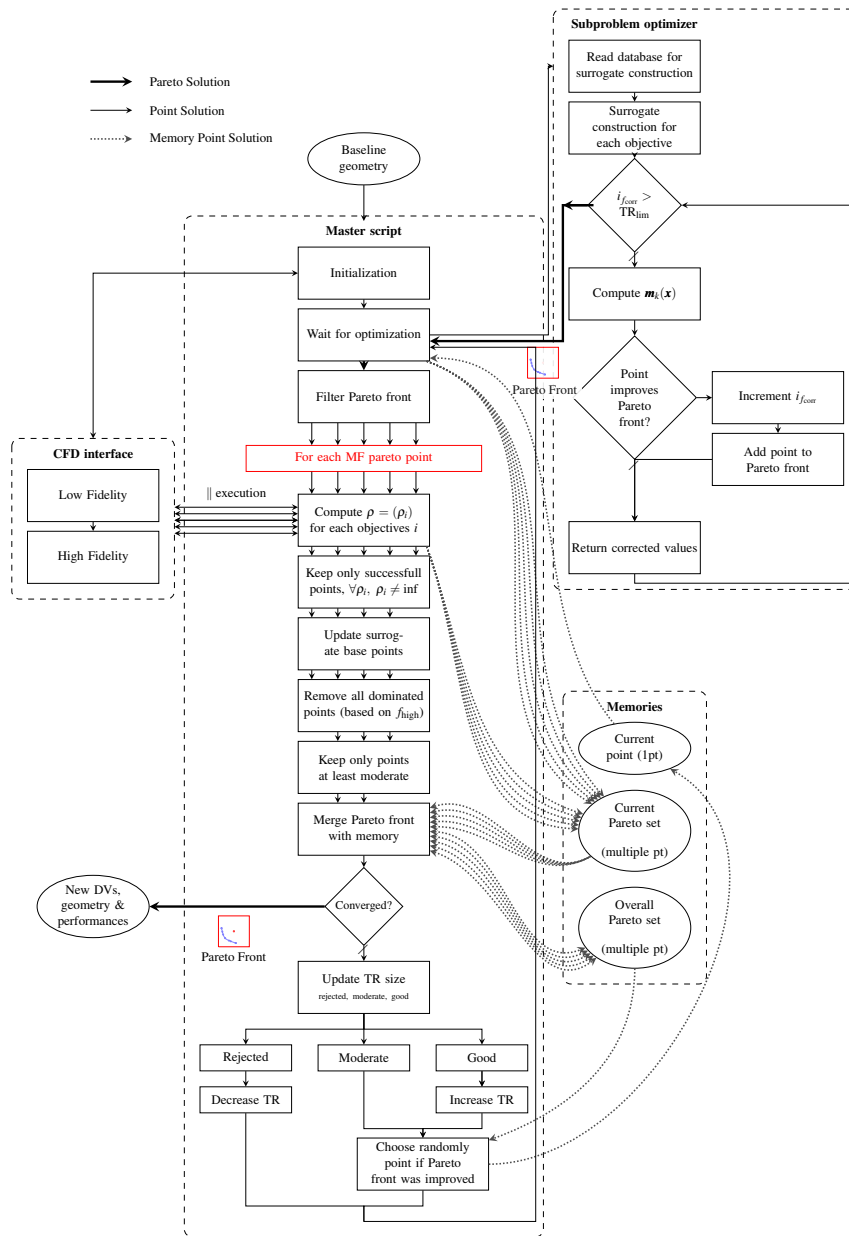


Figure 6.1: Multiobjective multifidelity trust region optimisation framework [200]

- *Moderate* is greater than the trigger n_p , the overall iteration is considered *moderate*.
- *Good* is greater than the trigger n_p , the overall iteration is considered *good*.
- Otherwise the iteration is considered *bad*.

The trust region is then increased or shrunk by γ_s according to the status of the current iteration as in Eq.6.1.5:

$$\delta_{k+1} = \begin{cases} \delta_k - \gamma_s & |\{p_{\text{moderate}}\}| < n_p & \text{(bad prediction)} \\ \delta_k & |\{p_{\text{moderate}}\}| \geq n_p & \text{(moderate prediction)} \\ \delta_k + \gamma_e & |\{p_{\text{good}}\}| \geq n_p & \text{(good prediction).} \end{cases} \quad (6.1.5)$$

The current pareto front is then merged with the overall one and the total pareto points number is calculated. If at least one point improves the pareto front, the new starting point is chosen from the overall pareto front. This selection is biased towards low-density parts of the pareto front, to promote objective space exploration. The Euclidean distances between each consecutive point from the pareto front are used as weighting factors for the selection. If no point improves the pareto front, the suboptimisation is restarted from the same point but with the corrected function now being more accurate.

6.1.2 Hypervolume Indicator

Pareto front plots are effective in showing a method's design space exploration efficiency for a given number of CFD calls. However, they lack information regarding the evolution of the pareto front during these infill analyses. The hypervolume indicator [223] aims at providing such information. It represents the hyper-volume (surface for 2 objectives) objective space dominated by the pareto front and bounded by a reference point provided by the user. Depending on this reference point location, the indicator reflects the importance to the number of points forming the pareto front (diversity) and its pareto-optimality, or to the extreme points of the pareto front.

Fig.6.2 describes the hypervolume indicator. The normalised front consists of the red points which are pareto equivalent. The point of reference used is slightly less optimal than the nadir point. Therefore, information from the most extreme points is used and the volume is then computed based on the coloured area. The process of selecting the reference point [223] $\mathbf{r}_p = (\mathbf{r}_1, \mathbf{r}_2)$ among m_p pareto points is summarised in Eq.6.1.6.

$$\begin{aligned} |\mathbf{r}_1| = |\mathbf{r}_2| > 2 & \quad \text{extremes points favoured} \\ |\mathbf{r}_1| = |\mathbf{r}_2| \in \left[1 + \frac{\sqrt{2}}{m_p - 1}, 1 + \sqrt{2}\right] & \quad \text{diversity favoured} \end{aligned} \quad (6.1.6)$$

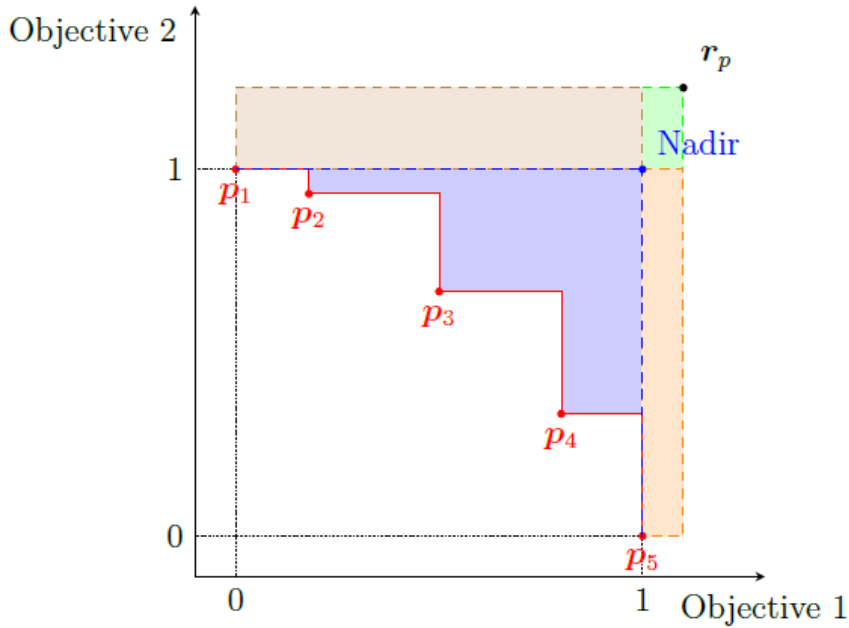


Figure 6.2: Hypervolume definition from a normalised Pareto Front and a reference point \mathbf{r}_p .

In order to compare multiple pareto fronts based on the concept of the hypervolume indicator, *contribution rate* has to be introduced. For n_p Pareto fronts (PF_1, \dots, PF_{n_p}) the procedure is formulated as follows:

1. All the pareto fronts are combined into a single dominant *surrogate Pareto Front*, PF_s which is containing only the non-dominated points.
2. For each front, only the intersection between PF_i and PF_s : $PF'_i = PF_i \cap PF_s$ are kept.
3. The surrogate Pareto front and the PF'_i are normalised.
4. The hypervolume indicator is calculated for each PF'_i and PF_s , relative to the same reference point \mathbf{r}_p .
5. The contribution rate c_r is computed for each PF'_i according to Eq.6.1.7.

$$c_r = \frac{I_h(PF'_i)}{I_{hs}}. \quad (6.1.7)$$

As this ratio approaches the value of 1, the Pareto front approaches *surrogate Pareto Front*.

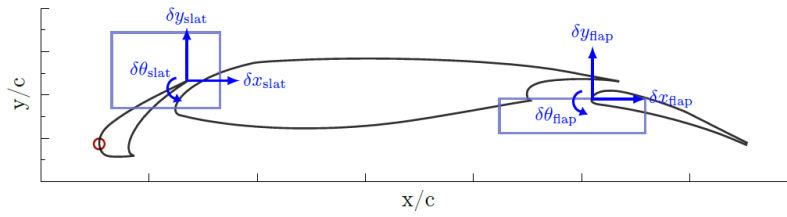


Figure 6.3: GARTEUR configuration

Parameters	Notation	Value
Reynolds number	Re	$4.10 \cdot 10^6$
Mach number	M	0.20
Fixed Angle Of Attack	$\alpha_{Cl_{max}}$	24 [deg]
Trigger for bad prediction	ρ_{bad}	0.0
Trigger for good prediction	ρ_{good}	0.0
Trust region shrink value	γ_s	2
Trust region expansion value	γ_e	2
Number of objectives required	n_f	1
Number of points required	n_p	2
Initial trust region size	δ_0	6

Table 6.1: High-Lift optimisation parameters

6.2 Garteur High-Lift Configuration

6.2.1 Problem Formulation and Geometry Parameterisation

The Garteur configuration is a 2D multielement airfoil composed of a single-slotted slat and a flap. The design variables of this test case are the slat and flap positions and deflection angles with a positive orientation shown in Fig. 6.3. The optimisation problem aims in trimming their position and their respective deflection angles in order to maximize takeoff performance. The flow conditions [222] are shown in Table 6.1 and the optimisation is performed at fixed angle of attack taken as the angle of attack at maximum lift $\alpha_{Cl_{max}}$.

High-lift devices are used during takeoff and landing, when both lift and drag generated are critical [224]. In addition to obvious lift considerations during takeoff and climb, drag should also be taken into account to fulfil these requirements. Similarly, drag has the significant effect of intentionally slowing the aircraft down when reaching the ground. The optimisation is considering both competing objectives. As such, a multiobjective formulation is used to obtain a pareto front solution instead of a single compromise optimum. In

this way, the objectives are formulated as in Eq.6.2.1 [225].

$$f^{(1)} = -\frac{C_l}{C_{l_{\text{datum}}}}, \quad f^{(2)} = \frac{C_d}{C_{d_{\text{datum}}}} \quad (6.2.1)$$

6.2.2 Aerodynamic Analysis

High Fidelity Tool

As in the study of Chapter 5, Fluent [226] is being used as the HF tool since it is considered as the most accurate tool available for this analysis. The mesh is generated with Icemcfd [227] and mesh regeneration is preferred over mesh deformation due to the large movements of the slat and flap as well as the low cost of generating the mesh. The robust meshing of this configuration took into account that the boundary layer must be accurately resolved to correctly predict the complex features involved in high-lift conditions. As in the typical practice within the aerospace industry, Reynolds Averaged Navier Stokes (RANS) simulations are being used [228] in conjunction with with Spalart-Allmaras turbulence model [214]. Second order Upwind discretisation scheme is used only after the first 500 iterations as the simulation starts with a first order scheme to ensure stability. The flow is considered converged when residuals fall below 10^{-5} , or when 2000 iterations are exceeded¹. Since this strict convergence cannot always be achieved, especially in these high lift conditions in which flow separates forming vortical structures, the lift and drag coefficients are averaged over the last 100 iterations. Validation of this model against wind tunnel data was performed by Demange et al. [199], and a typical evaluation cost in the machine used (GRID - 8 CPUs parallel processing) ranges between 10 to 20 minutes.

Low Fidelity Tool

As a LF tool, the coupled viscid-inviscid MSES [229] software provided by Professor Drela, MIT is used. In this, the Euler equations are coupled with a multiequation integral formulation and the coupling is being performed with a Newton solver. The software can handle the wakes from each element and can also predict separation and the aerodynamic coefficients quite accurately even near maximum lift [230] conditions. Each point evaluation typically requires up to two minutes. As similarly observed from the use of VGK in the RAE2822 test case, inefficient designs suggested by the optimisation procedure might diverge. This is observed in the coupling procedure, amplified by the quality of the discretisation used for the Euler solver. The information reduction due to divergence occurring in non-promising regions of the design space, is negative in a way similar to the findings of Chapter 5.

¹In some cases, this allow a fully converged flow but it is sufficient in capturing most of the flow physics.

6.3 Results

The multifidelity trust region (MF TR) and multifidelity expected improvement (MF EI) methodologies are compared against a high fidelity expected improvement approach and a gradient free optimisation, which directly calls only high fidelity analyses. For the latter, the Tabu Search optimiser is used in the Garteur case and our inhouse implementation of MOPSO is used in the RAE case.

6.3.1 Garteur case

Fig.6.4, 6.5 show the hypervolume indicators convergence, introduced in section 6.1.2, as well as the Pareto front after about 125 HF CFD calls for each method². The Tabu Search optimiser, acting directly on the HF analyses, finds good compromise points in a few iterations. However, as it can be seen from Fig.6.4 the Pareto front is narrow since TS first works locally and then extends its Pareto front. In the following iterations the front becomes wider, as implied by the hypervolume indicator convergence. This, however, requires many more HF calls.

Following a brief initial sampling (six high-fidelity and 18 low-fidelity), MF EI is very quick to discover the Pareto front thanks to the problem low dimensionality. In the initial iterations, with the design space not explored extensively, the explorative attributes of the method lead to a high infill success rate, as it is easy to find even slight improvements throughout the whole design space. However, after only 40 CFD calls the method seems to converge and no further improvement occurs. This is again a direct result of the method's behavior: with pareto points already identified, the — now multimodal EI suboptimisation problem — becomes more challenging and the method keeps exploring the design space for new design trends to find improvements. It is important to note that the LF tool is robust in specific design space locations, but when used as part of an explorative optimiser, its lack of global robustness complicates the task. The lack of pure exploitation and local search near the current pareto points, combined with the LF tool's inability to converge in the entire extend of the design space, leads to this early convergence. The former is an inherent attribute of the methodology, but the latter is a problem already observed in other applications of this method [200], and it is briefly discussed below.

It is important to discuss the effect that a LF tool has on the convergence of exploration-oriented MF methodologies, especially in the presence of a wide design space. The general effect of MSES is not beneficial for the widening of the pareto front. This is mostly observed in extreme operational regions like high C_l regions, that include interactions between wakes and large flow separation, complicating the coupling procedure between Euler inviscid and viscous boundary layer solutions. Hence, the initial global sampling does not provide information on an extensive design space region, and the MF EI method fails to

²Depending on optimiser implementation.

exploit its exploration attributes. As such, the use of a tool which is not robust in the whole design space is not appropriate for design space exploration even in the conceptual design stage, especially if the engineer is interested in finding novel design trends. In such cases, using information from a more mature stage provided by higher fidelity tools is preferable and a HF SBO method is definitely superior. Nevertheless, in regions where MSES is robust and accurate, the MF optimisation process is more efficient: it provides a more optimal pareto front. Following this, it is not a complete surprise that MF TR provides, to a small extent, a denser and wider pareto front. The MF TR pareto front convergence is initially slower due to the lack of sampling which limits the source of information MSES. The LF tool provides useful design trends but a couple of iterations are required before these are translated to dominant points. These uncorrected inaccuracies restrict the MF TR to the same convergence behaviour as the HF Tabu Search method. Nevertheless, the convergence is consistent and similar to what the HF Tabu Search performs, but with a quicker pareto front development. MF TR is able to locate design points which are better than the ones discovered by HF EI, in the whole range of its pareto front. Furthermore, it exhibits a slightly wider pareto front, especially in the low drag region. The superiority of the MF TR hypervolume indicator, compared to the TS only on HF, is explained by the extended objective space exploration. Despite this, the points predicted by TS only on HF in the mid C_l regime are dominating the respective ones from all other methods. MF EI provides an improvement over the results from the rest of the methods in the high C_l region. In lower lift design points, its performance is similar to MF TR, while it is being inferior in the lowest C_l objective space. Despite this fact, the use of MF data in the EI method can be considered as beneficial, since only one MF EI pareto point is dominated by HF EI. The drawback of the former though is the reduced number of pareto front points.

The above conclusions are better supported by a parallel coordinate plot [231], shown in Fig. 6.6 and the actual configurations displayed in Fig.6.7. These show the difference in the design variable values and design trends behind each methods' pareto points. As previously, the pareto front points are displayed at the same number of HF calls. The following information can be extracted:

- A qualitatively consistent slat movement is observed: all methods identify the importance of moving the slat forwards and down to increase wake interaction from slat to the main airfoil element.
- Discrepancies in slat angle: there is moderate movement from all methods but MF EI tends to deflect the slat as much as possible for increasing the lift. There is also an agreement in the low drag region, with lower slat deflection due to lower flap deflection.
- Low drag points have different arrangement compared to the datum: they use a lower flap position with a reduced deflection: less energy is extracted, with flap deflection being less affected from the main element to keep flap boundary layer attached.
- Only the MF methods explore the optimal design space extensively, due to the quick identification and exploitation of the importance of flap deflection. With this variable

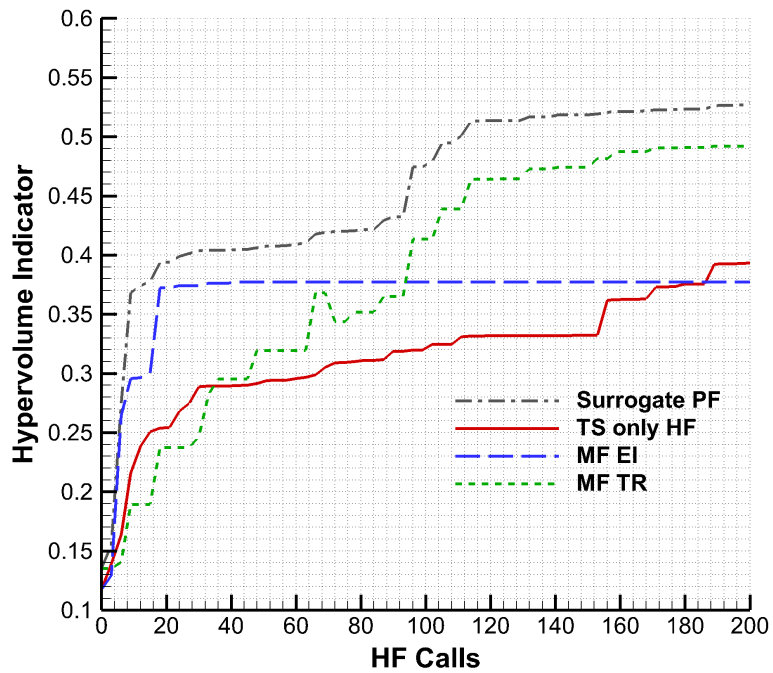


Figure 6.4: Hypervolume indicator convergence and Pareto front after 125 CFD calls for the Garteur case.

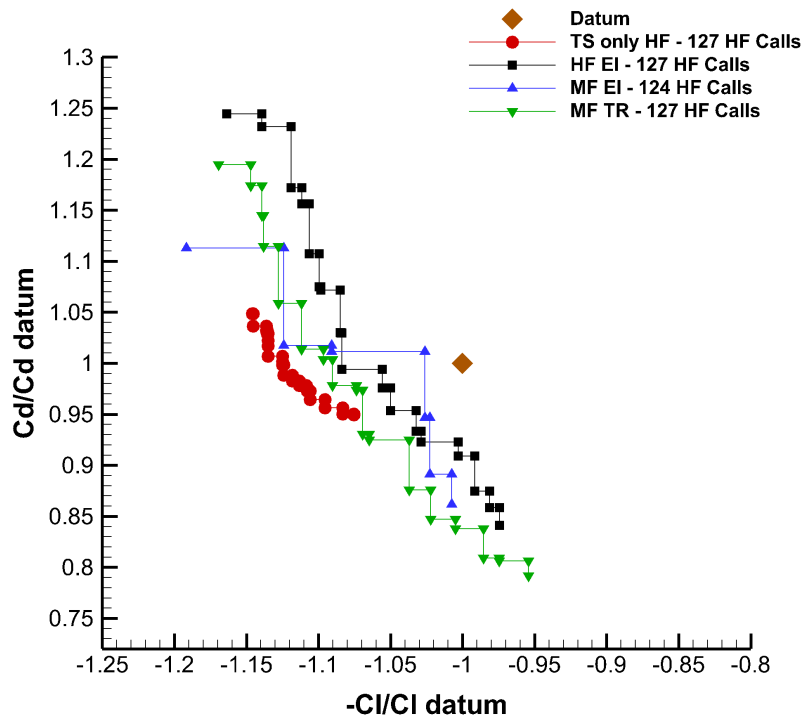


Figure 6.5: Pareto Front for the GARTUER airfoil optimisation case after 14-127 HF calls.

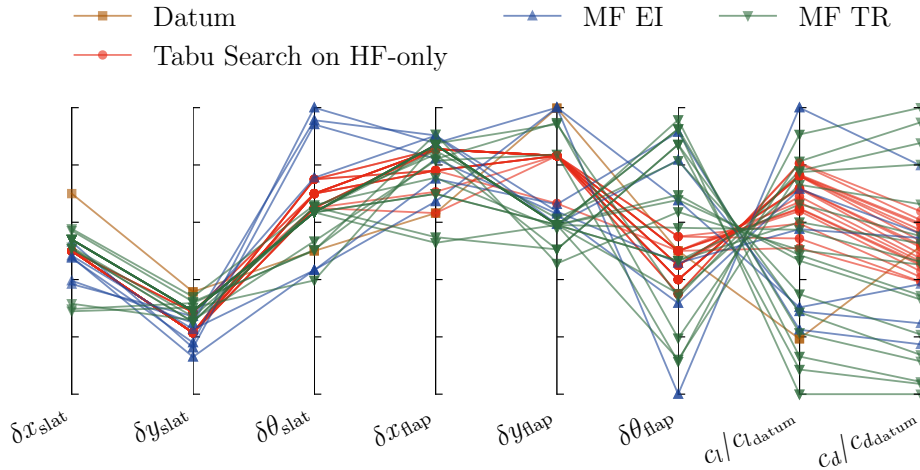


Figure 6.6: Parallel-coordinate plot for the Garteur case pareto points after 125 CFD calls.

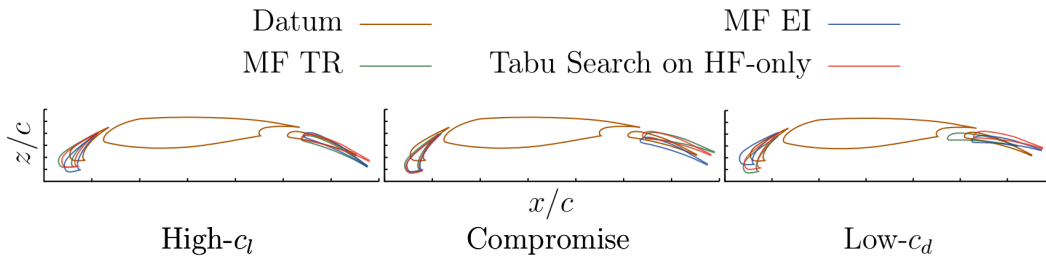


Figure 6.7: Garteur configurations resulting from all optimisation methodologies.

being the most dominant, MF EI uses the maximum allowed deflection to get maximum lift.

- The HF and MF methods' points tend to follow the same arrangement. Therefore, the discrepancies from the MSES LF tool are well corrected. MF approaches are quicker in finding promising regions. TS only on HF is the most efficient method at exploiting, that is to find the best solutions in the vicinity of datum point.

To conclude this comparison performed on the Garteur case, the TS only on HF is efficient in exploiting locally near the datum, but requires more HF calls than the rest of the methods to expand the pareto front. The HF EI explores the design space, but lacks exploitation and its points are dominated by the other methods. The MF TR has a behaviour very similar to HF EI, but shows a quicker pareto front advancement. The MF EI approach has fewer pareto points than all the other cases, but exploits the high-lift mechanisms better due to its initial full design space exploration. The design changes of the SBO methods are consistent with the direct gradient free optimisation. As for the MF methods, the LF tool inaccuracies have only a minimum effect in the final pareto front values.

6.3.2 RAE2822 case

As shown in Fig.6.8, in the initial HF infill calls MF TR develops a pareto front faster. However, following the end of the initial sampling MF EI quickly takes advantage of the surrogate, creating its respective pareto front. Following this, the hypervolume indicators show that MF EI dominates MF TR. An investigation of the pareto front reveals that this domination originates from the high C_l region.

By comparing the MF TR to the MF EI approach in terms of final pareto front as shown in Fig.6.9, it is evident that both methods exhibit similar objective space exploration as they both provide a wide pareto front. The objective function values are also similar in the mid and low C_l regions. Although in higher C_l values MF TR outperforms MF EI in a narrow region, MF EI shows an improved performance in the high C_l objective space.

The use of variable fidelity tools within the EI method is also assessed by comparing the HF EI method against MF EI method. There is a definite correlation between HF EI and MF EI pareto front as the corresponding values are very close across the whole pareto front. This shows that the LF tool provides correct design trends in a wide design space range. Therefore, the error correction is not only accurate, but also efficient as the quick RBF correction is sufficient in steering towards HF optimality. However, the computational cost between the three SBO methods is similar, with only a slight exploration improvement observed in the MF EI case. Hence, it can be concluded that there is not much benefit associated with using MF SBO methods for this design scenario.

The direct optimisation that uses our MOPSO implementation develops a dense but narrow pareto front. This is important since the purpose of a MO formulation is to explore different design possibilities in a wide objective regime. Although not shown here, no significant improvements are observed in the pareto front width or domination at later stages of the optimisation: the swarm does not find new pareto dominant points. MOPSO HF results are almost completely dominated by the MF and HF EI ones. Nevertheless, in the tradeoff region, some designs identified by MOPSO are superior to the ones from HF EI and MF EI. MF TR however is mainly dominated in MOPSO high lift anchor point region albeit MF TR pareto front extends more in the high lift region. Overall, SBO increases the design space exploration for a similar cost.

An example of the pareto front airfoil shapes is given in Fig. 6.10. Despite the similar pareto points between MF EI and HF EI showing proximity on the objective space, the respective shapes are distinctively different, exploring different points in the design space. However, MF TR and MOPSO approaches are more similar: the former methods are global whereas the latter ones are more local. Therefore, MF TR and HF MOPSO dominate in area close to datum (in design space) since they perform exploitation towards a local optimum but HF EI and MF EI explore configurations different from datum. By specifically examining the high C_l shapes, it is evident that these are very different from the datum, requiring global exploration to locate them. The MF EI method achieves high lift from its

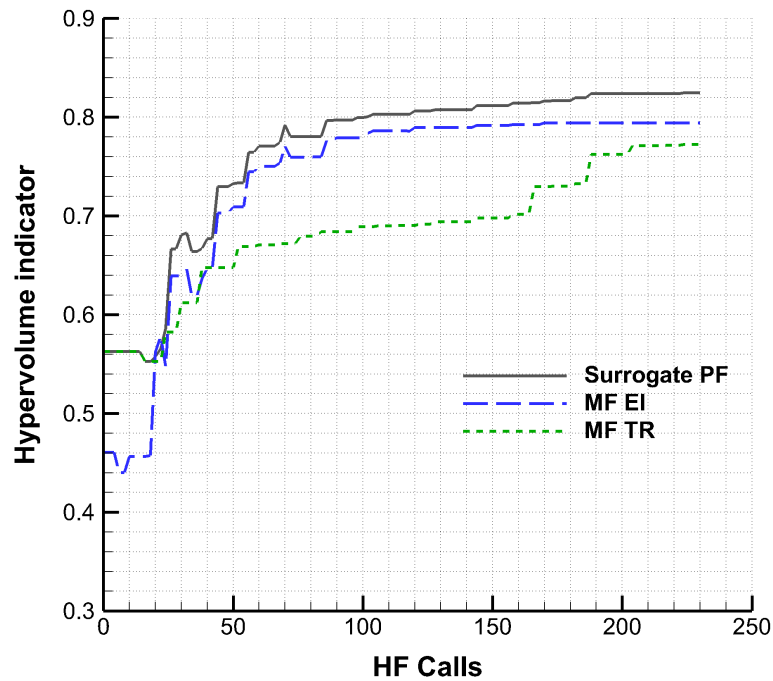


Figure 6.8: Hypervolume indicator convergence after 125 CFD calls for the RAE case.

aft camber as shown in Fig. 6.10. At the same time it is significantly thinner than the one designed by the MF TR approach in order to compensate for the wave introduced due to the achieved lift. In the compromise region all geometries display a big thickness reduction with the exception of the airfoil resulting from MOPSO, since it is only slightly thinner (mainly from the upper surface) than the datum while maintaining the original RAE2822 shape. The same is not true for the configurations by the MF TR and MF EI approaches which introduce a positive camber in the before the mid chord area. Evidently, the MF TR methodology retains the supercritical shape while producing the necessary lift through an aft camber design. A corresponding configuration is also defined by MF EI with its distinctive characteristic being the absence of an aft camber and an earlier thickening than the one by MF TR. The low drag MF designs both feature an inverse aft camber, with the MF TR being thinner and displaying a positive camber downstream of the LE area. It is evident that these designs are shaped as they are because of the positive angle of attack used in this optimisation problem (they minimise drag by reducing their thickness and creating zero lift). For an angle of attack of zero they would obviously produce negative lift.

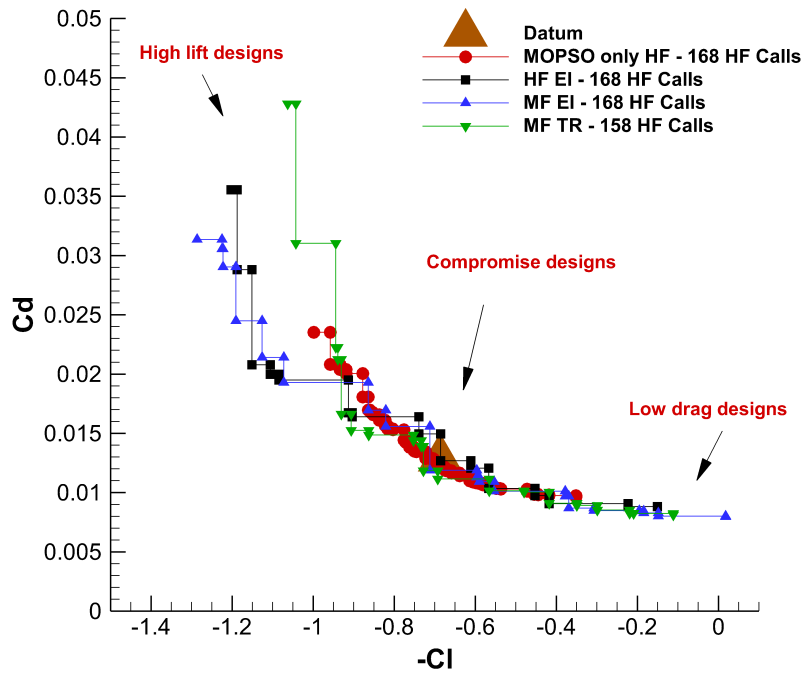


Figure 6.9: Pareto front after 125 CFD calls for the RAE case.

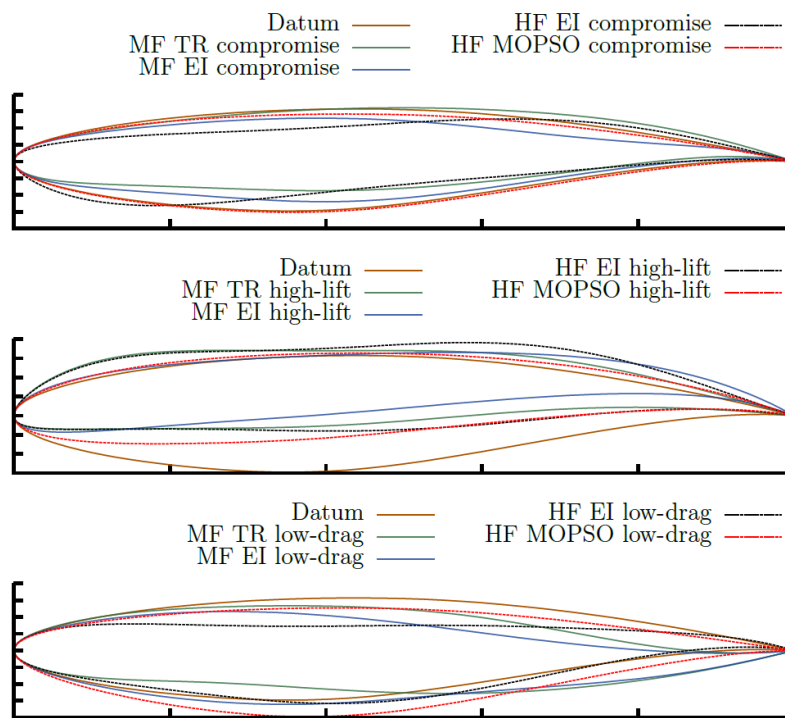


Figure 6.10: Three representative Pareto front shapes for the MF TR and MF EI methods.

6.4 Summary

This chapter presented the comparative study between an exploitation based multifidelity trust region framework developed by J.Demange against the more exploration-focused multifidelity expected improvement methodology developed during this PhD work — presented in Chapter 3. Both methods were also compared against benchmark gradient free optimisation tools such as Tabu Search and the Multi Objective Particle Swarm Optimisation. The study used a hypervolume indicator to assist the assessment of the pareto front convergence in two test cases: a high lift design case using the Garteur three elements airfoil, and an airfoil shape design problem for cruise conditions, involving the RAE2822 aerofoil also used in Chapter 5. It was observed that the gradient free methods, in spite of being reasonably efficient in improving the datum, cannot provide a wide pareto front for the same computational cost as the other surrogate based methods. Contrariwise, the trust region method provides a wide pareto front, dominating the expected improvement method in the mid lift region, which is closer to the datum point. In the high lift regime, for which more extensive exploration is required, the expected improvement method provides dominant results. The latter takes advantage of the initial sampling, by quickly finding global design point improvements and extending the pareto front. However, its exploration attribute, combined with the robustness characteristics of the low fidelity tool can lead to an early convergence plateau and to more sparse pareto points than the other methods. The high fidelity expected improvement method showed similar cost requirements to the multifidelity one, but proved to be more robust in creating a dense and wide pareto front. The trust region method showed similar pareto front characteristics but it was associated with a faster pareto front development. A parallel coordinates analysis and a resulting shape comparison showed consistency between the methods, with the multifidelity approaches identifying better the physical mechanism in increasing the lift.

Industrial Multidisciplinary Design Optimisation Application

*Knowledge will give you power, but
character respect.*

Bruce Lee

MATURITY in the aerodynamic design of conventional configurations has been achieved over the past decades to a level where performance is currently reaching a plateau. With essentially no room for ground-breaking improvements, steps forward are achieved by small and slow disciplinary improvements. It is still a common industrial practice to use a leading discipline based on which the rest of the disciplines will be designed. This approach not only reduces the subsystems' efficiency (due to the dominant discipline constraints) but the performance of the overall system as well. To attain new levels of design performance, redefining and improving the synergy between the disciplines is required.

There is a definite improvement when a global merit is guiding the design with the subsystems under parallel development. A typical example is the superiority of aerostructural wing design [164] over aerodynamic wing design. Therefore, one can argue that the supporting optimisation studies during the design process should always involve multidisciplinary interaction.

The development of multidisciplinary studies raises the additional considerations discussed in section 2.10. Depending on the MDO formulation [158], interdisciplinary communication is different. However, in most cases a multidisciplinary analysis (MDA) cannot be avoided, which for aerostructural optimisation translates to a specific case of an FSI problem.

This work uses the loosely coupled formulation in which different solvers are used for each discipline. Each disciplinary analysis involves its own computational domain and the

grid in the disciplinary interface is non-matching. This problem is tackled within the pre-processing stage, by setting up an RBF-based loads-displacement mapping closed loop. The other significant requirement arising by the aerostructural analysis is the robust grid deformation. Again, an RBF-based method similar to the one in [179] is used. Further details regarding the application of these methods in the context of the aerostructural analysis are provided in section 7.2.7.

When converged, the MDA provides the global quantities to be used as constraints or objective functions, typically involving drag and weight. These can be superimposed into a single objective using weighting parameters as in the work of Leoviriyakit [232] where a typical transonic wing configuration was optimised using both inviscid and viscous aerodynamic calculations and a simplified weight model, and can be also based on the Breguet equation for range maximisation, as by Martins et al. [233]. Stress constraints are mostly associated with high g maneuvers or fatigue and are usually formed into Kreis-selmeier–Steinhauser (KS) functions.

The effect of structural considerations in an optimisation study is profound in the work by Kenway [234] and Liem [217]. Optimising a typical transport configuration resulted to inward loads shifting to allow lighter structural designs. This is the core of MDO's superiority over aerodynamic shape optimisation justifying the extensive research work that has been performed on MDO [184–189].

Most recent design studies are using a single objective under many design parameters which relates to an advanced design stage. However, an MDO design problem increases the extent and multimodality of the design space as a direct result of using more design variables and interdisciplinary interaction creating new design trends. Subsequently, to get the maximum from an MDO study it is preferable to apply it at an early stage where the engineer can identify a set of promising and diverse designs. Following this, multiple parallel detailed optimisation studies can be launched. Therefore, this work aims in demonstrating the benefits of performing a multidisciplinary optimisation study as a part of an early stage design.

The Common Research Model (CRM) [235], is used as a wing design application [236], a wing model specifically developed to approximate the design and physical features of a typical conventional configuration transport wing. Before presenting the optimisation problem formulation and the numerical setup of the aerodynamic and structural models, some fundamental considerations on the wingbox structure elements are discussed.

7.1 Wingbox Structure and Structural Considerations

7.1.1 Loads and Structural Design Conditions

The structural components of system (e.g. wingbox) are designed based on well defined criteria and conditions. The loads assessment is responsible for identifying these critical operating conditions for each of the structural components as well as the corresponding aerodynamic loads. This has to be performed in the early stage of the design but with reasonably high accuracy.

Typical high load cases involve different maneuver conditions, gusts, landing scenarios etc, which of course depend on the mission and specifications of each aircraft and define the ultimate loads considered. Based on these loads the structural elements are sized or the structural philosophy is developed. The additional loads associated with such conditions are usually represented by a load factor, as in the case of V-n diagrams.

Critical loading conditions are in the order of hundreds even when only the wing structure is considered. Of course, for the needs of a current optimisation study only a very limited set of conditions can be considered for the structural constraints due to the high computational cost. Therefore, in the context of multidisciplinary optimisation, the discipline of loads typically reduces to defining a single maneuver condition and respective load factor, and projecting the aerodynamic forces in the structural numerical model.

In this sense, this work neglects high load cases associated with gusts which include dynamic phenomena, or any other scenario leading to a local increase of loads like landings. Instead, a simple generic maneuver of 2.5g — corresponding to a high bank angle turn or steep pitch-up maneuver — is considered as the limit load of the wing. The corresponding ultimate load is defined by introducing a safety factor of 1.5, a value commonly used in the aerospace industry.

Since wing design and optimisation is examined in an aeroelastic perspective, it is interesting to mention how the effects of aeroelasticity affect the loads. In non-swept wings, airloads are affected by structural deflection through torsional loads locally changing the angle of attack. In swept wings, there is also a contribution of bending loads through the torsion-bending coupling. The bending-induced deflections tend to decrease the bending moment since the resulting lift distribution experiences a shift inwards, towards the root.

7.1.2 Material Considerations for Typical Wingbox Configurations

Given the conditions and the loads that function as design specifications, the structural design is performed. This does not only include the wingbox topology and the element sizing

however; it also includes the selection of materials for each of the structural components.

Each component on a wingbox structure is subject to specific loads and as such the materials used can differ depending on their behaviour on the given conditions. Apart from the loading examples of the previous section, even the operational temperature can have an effect on the design. As such, temperature can be also used as a material selection criterion¹, next to other considerations like static strength, fatigue resistance, crack growth characteristics, corrosion etc.

In this work, flutter as well as fatigue are not explicitly taken into account. Therefore, the material to be used in the structural model is selected based mostly on its static tensile strength. However, fatigue considerations are still implicitly included in the material selection process and the effect of fatigue — as well as buckling — is still being qualitatively discussed in the context of the structural model. Criteria like stress concentration and crack propagation are neglected both in terms of material selection and constraints, since they are associated with local design which is beyond the scope of this work. The same holds for other detailed structural elements like bolts and joints.

Based on the criteria discussed earlier, the material being used for such structural applications belong in the family of aluminum alloys. High tensile strength applications favour the use of the 7XXX alloy series, which however generally lack corrosion and fatigue resistance. An improvement is achieved with the 7010 and 7050 alloys which sacrifice some of the tensile strength for a more balanced structural behaviour. Some typical material selections for aerospace applications are provided in Fig7.1.

Ideally, although fatigue is not being considered as a constraint, a material with reasonable fatigue resistance should be used in the structural model in order to provide results of realistic value. The structural model had to use a single material, and three possibilities were considered:

- 2024-T3, appropriate for components under fatigue.
- 7050-T7451, high tensile strength with balanced fatigue resistance properties.
- 7075-T651, high tensile strength especially under compression.

Out of these, the 7050-T7451 alloy was considered as the most representative for this generic application, and therefore it was used in the structural model.

¹As an example, titanium alloys are preferred over aluminum alloys in high temperature applications

Material	Recommended Application
2024-T3, T42, T351, T81	Use for high strength tension application; has best fracture toughness and slow crack growth rate and good fatigue life. -T42 has lower strength than -T3. Thick plate has low short transverse properties and low stress corrosion resistance. Use -T81 for high temperature applications.
2224-T3 2324-T3	8% improvement strength over 2024-T3; fatigue and toughness better than 2024-T3.
7075-T6, T651, T 7351	Has higher strength than 2024, lower fracture toughness, use for tension applications where fatigue is not critical. Thick plate has low short transverse properties and low stress corrosion resistance (-T6). -T7351 has excellent stress corrosion resistance and better fracture toughness.
7079-T6	Similar to 7075 but has better thick section (> 3 in) properties than 7075. Fracture toughness, between 7075 and 2024. Thick plate has low stress corrosion resistance.
7150-T6	11% improvement strength over 7075-T6. Fatigue and toughness better than 7075-T6.
7178-T6, T651	Use for compression application. Has higher strength than 7075, lower fracture toughness and fatigue life.
Aluminum-Lithium	Compared to conventional aluminum alloys: 10% lighter, 10% stiffer, and superior fatigue performance.
PM Aluminum	Compared to conventional aluminum alloys: Higher strength, good fatigue life, good toughness, higher temperature capability and superior corrosion resistance.

Figure 7.1: Materials traditionally used in aeronautical applications [237].

7.1.3 Structural Elements

The structural design traditionally refers to the minimisation of the structural weight given the external dimensions, fuel volume requirements — and in this case the defined material — through the sizing of the structural elements and the design of the structural topology. This approach corresponds to the aerodynamically dominant design in which the structural design is constrained by the aerodynamic shape requirements. In the present multidisciplinary application however, the structure is designed simultaneously with the aerodynamic shape². Nevertheless, the goal remains the same; and that is to minimise the structural weight so that the payload can be increased or the required power can be decreased. For a given load scenario and material, this is achieved by a design that features the highest stress allowed [237].

A conventional wingbox configuration involves:

- Longitudinal reinforcing members: Spar caps/stringers/stiffeners. They carry tensile

²The traditional structural design process is perhaps closer to the ASO-based multidisciplinary optimisation, since in the latter, a structural sizing is taking place given a defined wingbox shape provided by the global variables. However, the distinction between the two is that the global variables are driven by structural considerations as well, since weight remains still one of the objective functions.

loads, compressive loads, bending moments and secondary bending moments³. Spar caps are designed to have high secondary moment of inertia.

- Longitudinal reinforcing members: Spar webs. They provide the platform onto which the stiffeners are placed. They carry shear stresses, especially near the neutral axis. A secondary importance of their implicit stiffening action is that the deformation of the aerodynamic shape due to large deflections near the LE region is avoided. A large number of shear webs and spar caps reduces the stresses on the ribs and the stiffening elements are more efficient. However, this conflicts with typical fuel tank requirements.
- Skins: They carry loads in their planes and are subject to tension in the upper surface and compression in the lower surface. Torsional shear stresses are also carried by skins. The buckling resistance of the skins depend on the spacing between the ribs and the longitudinal stiffeners which effectively increase their thickness. Near the wingtip, the number of stringers is decreased, reducing the local effective thickness as well. As mentioned in the problem formulation section, stiffeners are not explicitly present in the form of spar caps in the structural model used. As such, the skin thickness of the model is increased to emulate this exact effect of the skin/stiffener assembly.
- Transverse members: Ribs. They provide stiffness and strength in their plane alone, transferring the airloads to the spars. Their spacing controls the aerodynamic shape as well as the axial loads in the skins. This property is not being used in the context of the optimisation studies, since defining rib spacing as a design variable would significantly increase the dimensionality of the problem.

Since the spar caps and the skin elements are responsible for approximately half of the structural weight of the wingbox, their design is critical for the success of the whole structural design. As far as the present work is concerned, this underlines the importance of the sizing of the skin panels effective thickness. This is especially apparent when the ASO architectures is being used, in which case the sizing process is being efficiently handled in a disciplinary level.

The aforementioned structural elements are illustrated in Fig.7.2.

³The upper stringers are stressed by bending and compression simultaneously. Since these are beam columns of high length-to-width ratio, they are subject to buckling and secondary bending moments are introduced. Buckling is in fact a driving criterion especially in areas near fuel tanks.

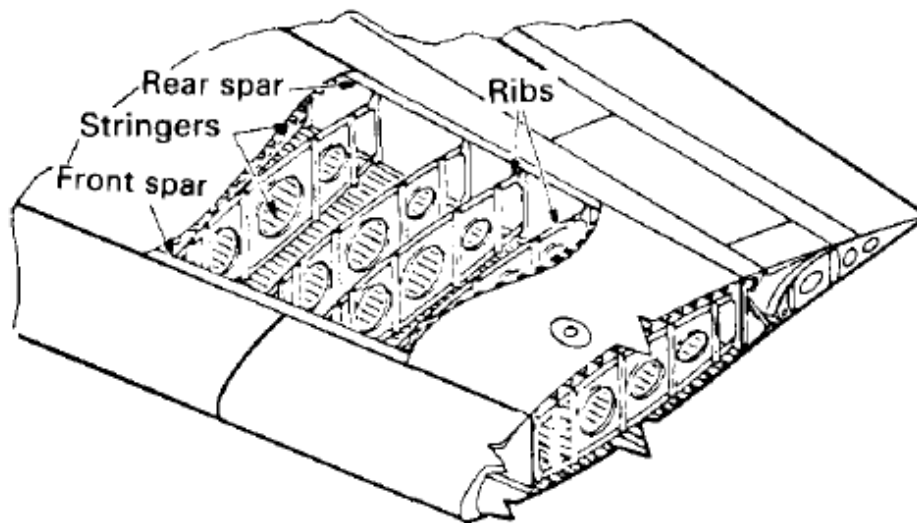


Figure 7.2: Wingbox structural elements [237].

7.2 Common Research Model

7.2.1 Problem Description

The CRM configuration was developed to satisfy the needs of a general benchmark configuration for CFD validation purposes [235]. Therefore, it represents the current typical supercritical transonic wing of a widebody commercial transport aircraft and its design allows reasonably good aerodynamic performance. It features an aspect ratio of 9, with a leading edge sweep angle of 35° . Following contemporary operating conditions, it was designed for cruise on $M = 0.85$. The model used in the present work is an up-scaling of the wind tunnel model, approximating real transport aircraft wing dimensions⁴.

The outer mold line (OML) corresponds to a cruising (1g) shape and not the jig shape. However, in lieu of an actual jig shape CRM model, both the OML and the structural model are used as jig shape models.

⁴In this study, the clean wing is considered with no fuselage and engine nacelles.

Table 7.2: CRM V.15 Wing characteristics

Parameter	Value
Span	52.64m
Projected Area	167.95m ²
MAC	3.19m
Spars	2
Ribs	42
Range	17185km ^a
Wingbox Str. mass	31000kg

Table 7.1: Physical conditions for CRM case

Condition	Value
Mach Number	0.85
Reynolds number	2x10 ⁷
Pressure	23842 Pa
Temperature	220. K

^aThis range corresponds to the clean wing. The respective range of the full CRM configuration is 13000km.

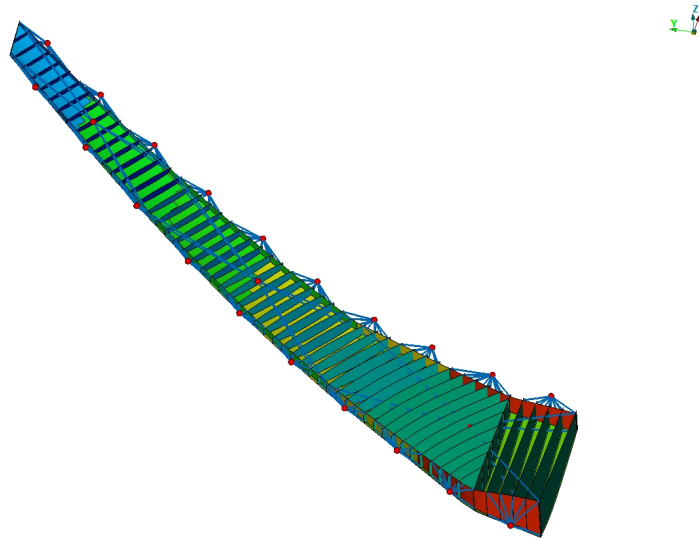


Figure 7.3: CRM structural configuration. CONM2 masses represent fuel and high lift systems' masses, connected with the structure with RBE3 elements. For clarity, shear webs are omitted.

For the structural analysis, we are using the NASA CRM V.15 wingbox model⁵. This structural model has been designed based on the aerodynamic CRM model and it features contemporary structural design elements found in a corresponding wingbox structure. Particularly, this model uses CBARs as implicit chord-spaced stiffeners and shear-webs instead of the mid-chord spar (found in V.12) which reduces the computational cost. Furthermore, this implicit stiffening has been shown to suppress local natural modes. In lieu of explicit stiffeners like stringers in the geometrical description of this model, the thickness of the skin has been increased to provide an effective structural area acting as a longitudinal stiff-

⁵commonresearchmodel.larc.nasa.gov/files/2014/02/CRM_wingboxFEM_description_1.pdf

ener for bending loads. Apart from stress relieving, this prevents excessive displacements⁶.

The effect of slat and flap activation systems' mass have been included by CONM2 lump masses connected with RBE3 interpolation elements attached to the front and rear spar cap elements respectively. Additional masses due to fuel have been similarly included using CONM2 elements. Three CONM2 elements have been used in the center of gravity of each fuel tank, as shown in Fig.7.3.b

Since the fuselage is not included in this wing design study, in order for the necessary cruise trim conditions to be imposed, a fixed fuselage, empennage and additional systems' weight had to be used along with the corresponding payload weight. The total take-off weight of the aircraft is calculated as follows:

$$W_{TO} = W_{w, str} + W_{fuel} + W_r \quad (7.2.1)$$

Here, W_r is the total weight that does not include fuel and wing's structural weight. It is based on statistical relations and the total number of passengers and it is considered fixed. $W_{w, str}$ corresponds to the weight of the structural components of the wing — provided by the NASTRAN code — and W_{fuel} is the weight of the fuel stored within the wingbox, used to complete the designed range. Evidently, the structural weight is dependent on the design point. This is also true for the fuel weight, since fuel mass is calculated based on the internal volume of the wingbox, which is dependent on the global design variables.

This weight estimation approach is hybrid, using Class I methods for the fuselage and the rest of the aircraft systems which are not included in the design optimisation problem. The structural weight of the wingbox is estimated by the FEM model and as such it is a Class III weight estimation approach [193].

7.2.2 Parameterisation Strategy

Conceptual stage studies typically examine the effect of small groups of well defined and influential aerodynamic parameters like sweep and twist, with some level of shape design being inserted usually by inverse airfoil design. In such an integrated design though, to which cruise trim is provided directly from wing shape and planform characteristics, the shape design has a role more important than simply maximizing the aerodynamic performance. It directly affects the structural design and its efficiency through secondary moment of inertia effects. To accomplish the above with minimum cost, in this study a combination of shape parameterisation using Free Form Deformation (FFD) [7] is used, accompanied by a twist and a sweep variable. These parameters are believed to be sufficient for an extensive and efficient conceptual aerostructural design study without prohibitively increasing

⁶This also accelerates the convergence of the multidisciplinary analysis loop.

the dimensionality of the problem. The bounds are also wide enough to satisfy typical conceptual design exploration requirements⁷. It should be noted that such a parameterisation approach requires care to make sure the grid is robust to geometrical changes. Since in this implementation FFD acts directly on the nodal description of the geometry, no further parameterisation steps are required to provide a ready-for-analysis computational model.

Table 7.3: Design variables

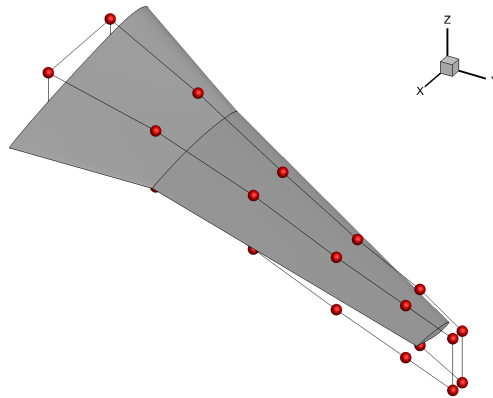
Parameter	Count	Lower bound	Upper bound
Shape variables	20	-1 m	1 m
Spar thickness	3	4 mm	21.1 mm
Rib thickness	4	0.5 mm	7 mm
Skin thickness	3	4.5 mm	19.5 mm
Sweep	1	33.5°	36.5°
Twist	1	-10°	10°
Angle of attack	1	2.8°	4°

The FFD control points act directly on the grid nodes. This approach is robust and efficient as it also allows for the deformation of the volume mesh during the iterative aerostructural analysis. These function as the global design variables, altering the Outer Mold Line (OML) and the wingbox shape at the same time⁸. Sweep and twist are controlled by a group of control points moving concurrently. The angle of attack is being used as an aerodynamic design variable and its role is to trim the configuration in cruise, since the changes in aerodynamic and structural design, influence the total lift and weight of the wing. Its presence is not necessary as trim could be achieved by the rest of the variables. However, this would lead to an inferior design since changes in the shape in order to meet lift constraints are also translated to shock intensity increase. On the other hand, the effect of the angle of attack on the lift is dominant and essentially linear. It is therefore preferable to separate the two functions with distinct variables. Structural parameters include the thickness of the wingbox elements: spars, shear-webs, ribs and skin [206]. Since this is a conceptual study, each one of these variables is not associated with a single structural element thickness. The structural elements are grouped, with a subset of thickness variables representing each group. As such, in the MDF formulation the six skin panels of the upper and lower surfaces are associated with three variables, the ribs' thickness is described by four variables, while three variables were used for the spars' and shear webs' thickness. An element thickness not defined by a variable is provided by an interpolation between the neighbouring thickness definitions⁹. A comprehensive overview of the described aerodynamic and structural model parameterisation is provided in Fig.7.4.

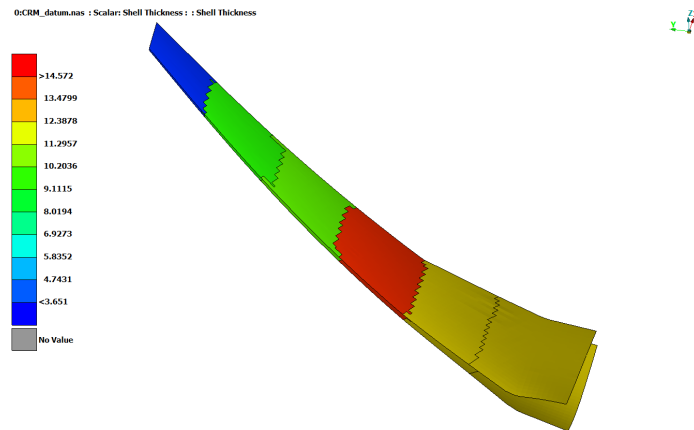
⁷With the extension of sweep which is limited to three degrees to avoid bad quality or invalid grids.

⁸The bounds of the shape design variables represent the maximum X or Z displacement of any FFD control point, relative to the local chord.

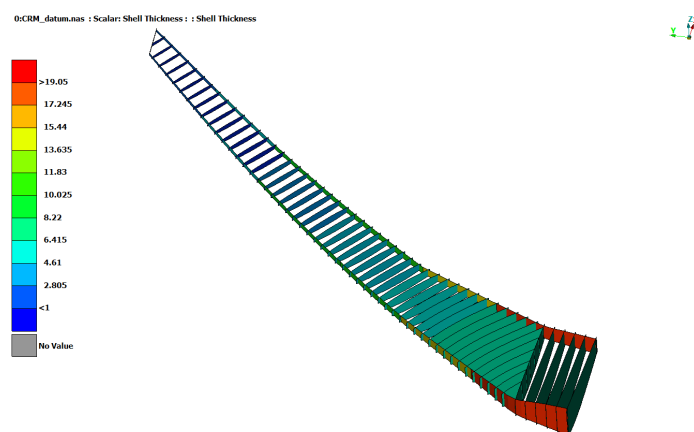
⁹In this ASO formulation case, this interpolation is avoided as the efficient structural sizing allows a slightly more detailed structural elements thickness design.



(a) FFD control points deforming the OML and the wingbox.



(b) CRM skin thickness variables and datum design thickness.



(c) CRM spar and ribs thickness variables and datum design thickness.

Figure 7.4: CRM aerodynamics and structural parameterisation. Thickness is in mm.

7.2.3 Design Constraints

As already mentioned, for the optimisation procedure on CRM to provide useful engineering feedback, it should be constrained to satisfy trim in cruising conditions. In this sense, the trim constraints take the following inequality form.

$$\frac{|L(\mathbf{x}) - W_{TO}(\mathbf{x})|}{W_{TO}(\mathbf{x})} \leq \epsilon \quad (7.2.2)$$

$$C_{Mcg}(\mathbf{x}) \leq \epsilon \quad (7.2.3)$$

where C_{Mcg} is the moment coefficient around the center of gravity of the wing and the tolerance is set to $\epsilon = 0.05$. In order for the use of C_{Mcg} in the optimisation to be meaningful so that the final wing design would be operational, the empennage is also required. This is of course because the horizontal stabiliser trims the C_{Mcg} of the full configuration¹⁰. The fuselage and the empennage are not available in use in this study. Therefore, the wing configuration is optimised as an isolated aircraft system — without considering the effect that the interaction between the wing, the fuselage and the empennage would have in the final wing design and in the longitudinal trim. As such, including a strict tolerance for this constraint is not relevant and therefore the constraint is omitted.

Another constraint considered in this optimisation problem is range. This is estimated based on the aerodynamic performance as well as the weight characteristics of each design. As such, apart from the structural weight it is dependent on the available fuel tank volume inside the wingbox, which is sensitive to the global design variables. In this way, an implicit fuel tank volume constraint is introduced, as the wingbox should be large enough to carry the fuel required for a 7000nm/13000km mission. The mass of the fuel m_f is directly calculated for every new developed design, and it is embedded in the structural model using CONM2 lump masses connected to spar and rib elements through RBE3 elements. Three lump masses were used for three fuel tanks along the semi-span.

The Range (R) is calculated using Breguet equation,

$$R(\mathbf{x}, m_f(\mathbf{x})) = \frac{V}{g} \frac{L}{SFC D} \ln\left(\frac{W_i}{W_f}\right) \quad (7.2.4)$$

where V is the flight speed, SFC is the thrust-specific fuel consumption, W_i is the initial and W_f is the final weight.

¹⁰The presence of the empennage and the fuselage also affects the aerodynamic characteristics of the wing, altering the C_{Mcg} value.

To avoid a too stiff or too flexible wing design¹¹, the first bending mode frequency is also constrained. For this modal analysis, the Nastran SOL103 is used. The use of this modal constraint also ensures that the structural design will not be too local during the optimisation process, since the eigenvalues are properties that depend on the whole structural wing design.

To secure structural integrity in limit loads, each wing configuration is tested to a stress analysis corresponding to a 2.5g maneuver. When using the maximum Von-Mises stress as the constraint, the resulting structural design would be local. To avoid this, while keeping the structural constraints number to the minimum of one, the KS function [238] was used in the MDF formulation case. In this, each constraint value g associated with each structural element, takes the form:

$$g_i(\mathbf{x}) = SF * \frac{\sigma_i}{\sigma_y} - 1 \geq 0 \quad (7.2.5)$$

where σ_i is the Von-Mises stress of the i^{th} element, and σ_y is the yield stress of the material, which is Aluminium 7050-T7451, with $\sigma_y = 469MPa$. SF is the safety factory, set to 1.5.

As mentioned earlier, inequality constraints are enforced during the suboptimisation process to steer the method towards feasible infill sampling points. In this case, when the feasibility method is used, the suboptimisation process becomes,

$$\mathbf{x}_1^*, \mathbf{x}_2^*, \dots, \mathbf{x}_n^* = \arg \left(\max_{\mathbf{x} \in \mathbb{D}} (PF_R \times PF_{trim} \times PF_{stress} \times PF_{mode} \times EI_{CD}) \right. \\ \left. v.s \max_{\mathbf{x} \in \mathbb{D}} (PF_R \times PF_{trim} \times PF_{stress} \times PF_{mode} \times EI_W) \right) \quad (7.2.6)$$

where the probability of feasibility for an inequality constraint problem of $g(\mathbf{x}) \leq g_c$ is expressed as,

$$PF(\mathbf{x}) = \frac{1}{2} \left(1 + erf \left(\frac{g_c - g(\mathbf{x})}{\hat{\sigma}(\mathbf{x}) \sqrt{2}} \right) \right) \quad (7.2.7)$$

The constraints are summarised in Table.7.4.

7.2.4 Aerodynamic Analysis

The CFD analyses are performed using the commercial solver ANSYS Fluent [208], providing the global aerodynamic coefficients. Two different numerical models have been set

¹¹In the case of a too flexible wing, a nonlinear structural analysis is required.

Table 7.4: Constraints

Constraint	Value
Range	$\geq R_{datum}$
Trim in Cruise	-
KS	≤ 1
1 st bending mode	$1 \leq f \leq 2Hz$

up in order to cover the requirements of this MF optimisation study. These feature different physics solved, grids used and convergence tolerance. For both cases, the final result is averaged using values from the last 50 iterations. This minimises noise induced from limited oscillation present in the converged solution.

Low Fidelity Tool

The LF analyses neglect the effect of viscosity using specifically developed grids, mostly aiming in the the minimisation of computational expenses. To reduce computational costs even more, the concept of partial convergence [111] is employed. In this, following an a priori investigation of the convergence [213] of the LF analysis of random points, a maximum number of iterations is set. All LF simulations executed during the optimisation are stopped once this predefined number of iterations is reached. As a result, the error bounds of the LF analyses are known.

High Fidelity Tool

In the HF CFD analysis, RANS equations are used solved by a Roe-FDS scheme [239] and *S-A* [210] to model turbulence effects. All equations are discretised with a 2nd order upwind scheme. These details are summarised in Table.7.5. The computational grid used for this model was selected following a grid convergence study [209] illustrated in Figs.7.5, ?? described below.

The mesh generated is hybrid, using a structured O-grid subdomain ensuring the required near wall resolution, while the outer volume uses tetra elements, as displayed in Fig.7.7. Four grid levels of successive refinement were examined starting from $y^+ = 10$, to a grid all well within the $y^+ = 1$. In a similar fashion, two inviscid grids were examined for the LF analysis, involving 10 and 15 structured layers respectively. For the HF analysis, the level 2 grid was selected as the most appropriate for the purposes of this optimisation, showing a satisfying resolution of the physics involved as well as grid converged aerodynamic coefficients. For the LF analysis, the coarsest grid was chosen for its low cost and insignificant accuracy penalty.

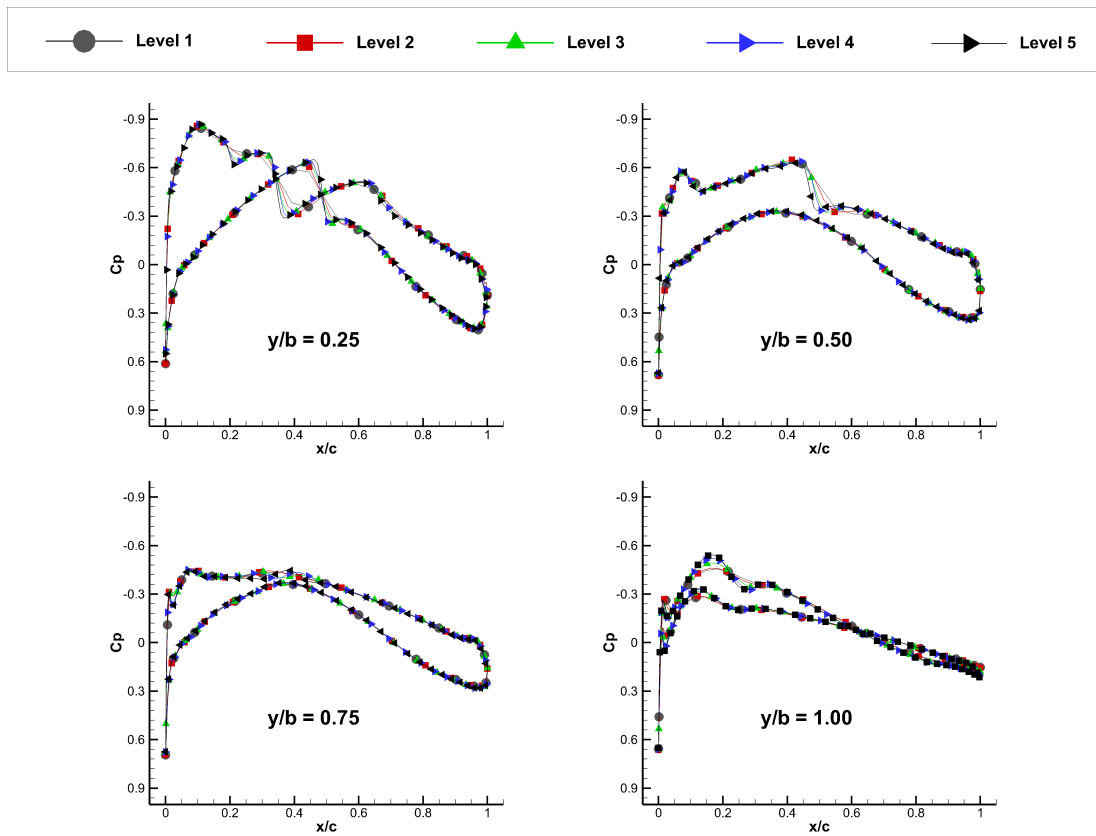


Figure 7.5: Cp distribution grid convergence study for the HF analysis.

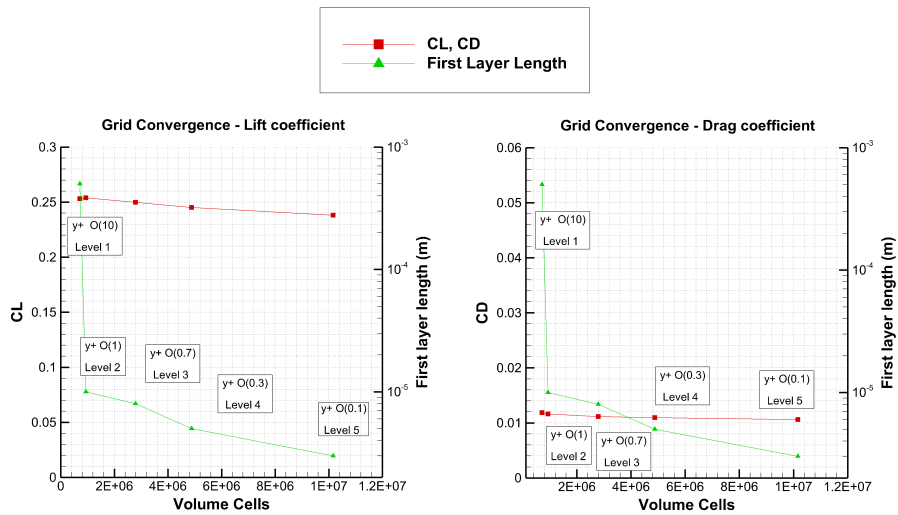


Figure 7.6: Global aerodynamic coefficients grid convergence study for the HF analysis.

To demonstrate the difference between the LF and HF solution, the two pressure distributions (corresponding to the EULER and RANS analysis respectively) are provided in

Fig.7.8. It is evident that in the inner mid part of the wing, the two methods predict similar physical field. The location of the shock in the upper part of the wing near the root is almost identical for both cases, while in the middle of the wing it is located only slightly downwind of the one predicted by RANS, followed by a pressure fluctuation. In the same part of the as expected, the inviscid solution also underestimates the pressure losses. However, in the outer portion of the wing the models differ greatly. The inviscid analysis consistently predicts a more gradual pressure drop in the upper section of the wing — especially very close to the wingtip. As a result, the shock location is identified significantly further downstream of the one estimated by the RANS analysis. Furthermore, the effect of the increased geometric washout near the tip is pronounced in the inviscid solution. The upper LE section is a stagnation area from which the flow accelerates until the shock occurs in $x/c \approx 0.85$. In the lower side conversely, a sudden suction is predicted until the mid-chord location.

This behaviour suggests an underestimation in the drag force predicted by the LF tool as well as wrong loads distribution in the outer part of the wing, effectively acting as loads alleviation. Therefore, in the design space particularly associated with high geometric twist or/and low bending and torsional stiffness, the LF analysis is expected to provide increasingly false data.

Table 7.5: HF analysis numerical model details

Parameter	Type
Scheme	Roe-FDS
Discretisation	2 nd order Upwind
Courant Number	10 - 20
Turbulence model	<i>S</i> – <i>A</i>

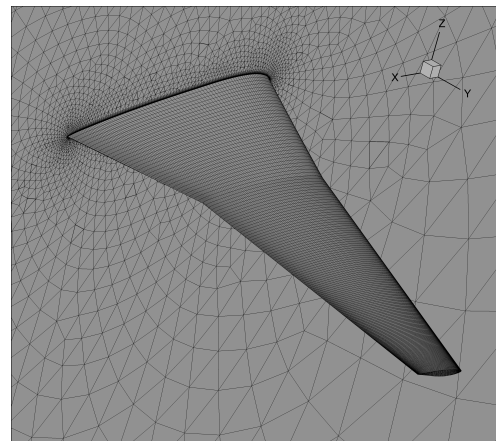


Figure 7.7: High fidelity aerodynamic surface grid. O-type grid layers are used for boundary layer resolution.

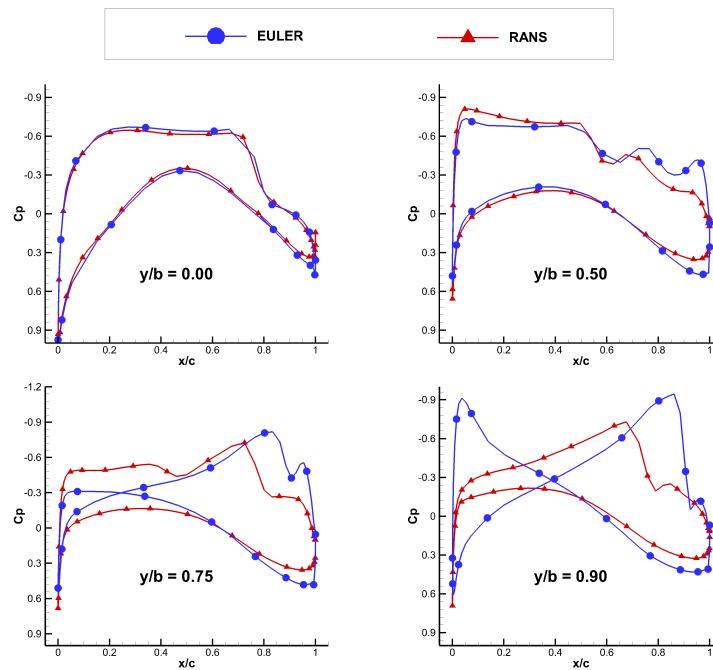


Figure 7.8: Comparison between low fidelity (EULER) and high fidelity (RANS) solution in terms of pressure distribution.

7.2.5 Multidisciplinary Feasible Architecture Formulation

As discussed in Chapter 2 and 3, MDF is perhaps the simplest of the MDO architectures both in terms of development as well as implementation either in a computational environment or even in a physical organisation as a design plan. As such, following the pattern used in Chapter 4 for the Sellar MDO problem, MDF is used as the basis of the MDO implementation studies of the developed optimisation methodology. Following again the XDSM approach of describing multidisciplinary processes, the aerostructural optimisation is presented in full detail in Fig.7.9.

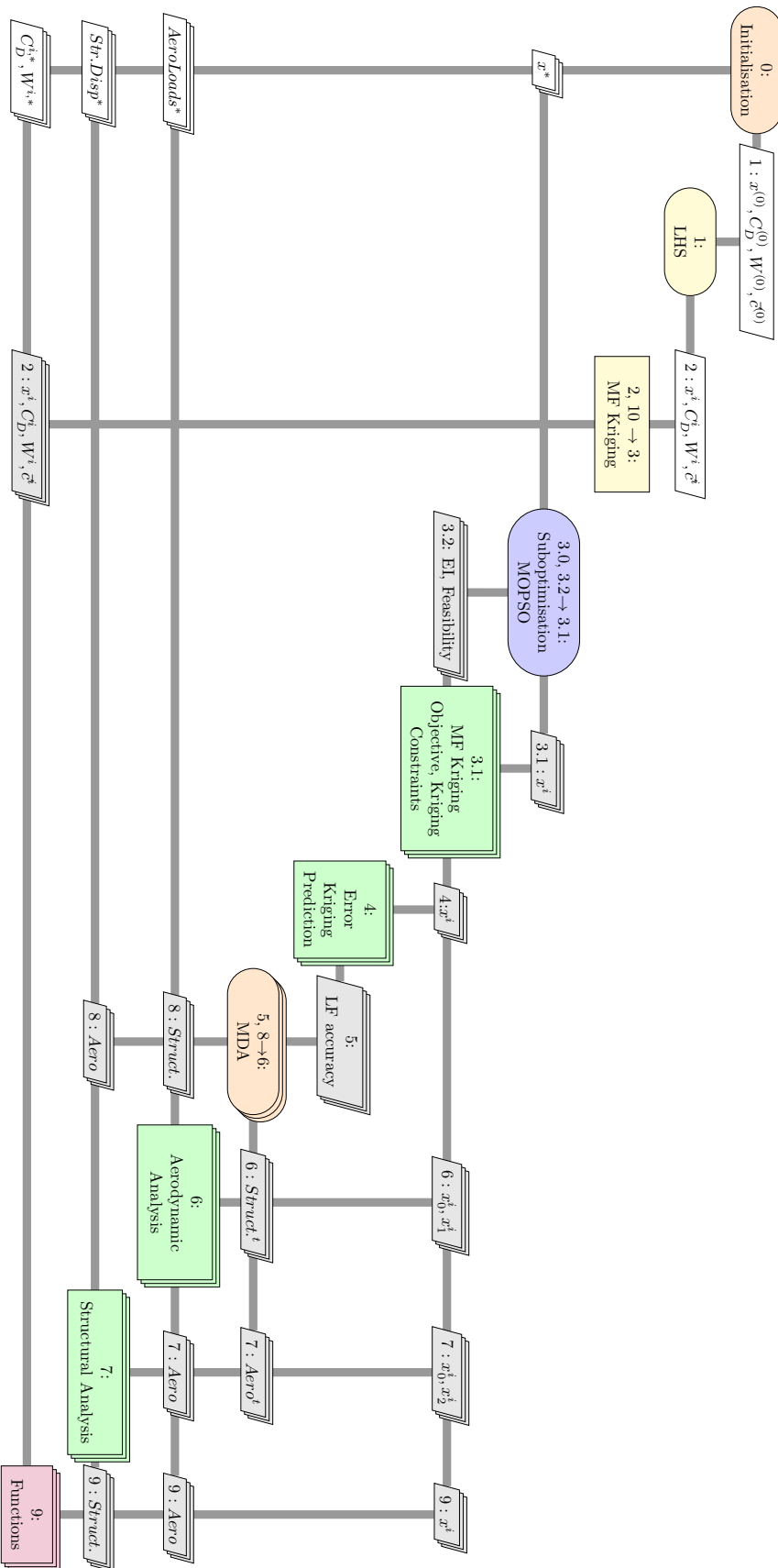


Figure 7.9: XDSM flowchart for MDF formulation of CRM aerostructural optimisation.

The procedure is fairly straightforward: All the elements of the optimisation methodology described in Chapter 3 are present (sampling, metamodel training, suboptimisation, infill sampling etc.). The optimisation framework now simply guides a multidisciplinary process contained within the MDA loop. This uses a Gauss-Seidel loop between the aerodynamics and structures until aerodynamic coefficient convergence is achieved.

Structural Analysis

For the structural analysis, MSC. Nastran is being used. Since the aspect ratio is not high, a linear static analysis (SOL 101) is considered accurate enough for the purposes of this study. The analysis provides the stress distribution at the nodes, used to formulate the stress constraints in form of KS functions. Furthermore, it allows the calculation of the structural weight of the wing similarly to how it has been used in the work by Dababneh [193]. Apart from an objective function itself, it is necessary in order for the trimming constraint functions to be evaluated. Under this plan, the cost of a structural and weight analysis is significantly lower than that of the LF aerodynamic analysis. Therefore, there would be no significant benefits in defining a lower fidelity structural analysis, due to poor load balancing reasons. In fact, using a wingbox analysis improves the accuracy of the LF aerostructural infill analyses, also making the weight metamodel — and the design space exploration — more efficient. Another side benefit is that there is no additional structural design parameterisation requirements for the LF structural configuration. Similarly to the aerodynamic MF analyses, a single parameterisation can be used. As such, the problem of mapping a set of design variables (corresponding to LF structural analysis) to another set (corresponding to HF structural analysis) is non-existing.

7.2.6 Asymmetric Subspace Optimisation Architecture Formulation

The ASO architecture is well suited to problems where there is poor load balancing between the disciplines. In this case, the structural analysis is significantly cheaper than any of the aerodynamic analyses used in this work. Therefore, such a formulation is a promising route towards more efficient aerostructural design exploration. The key elements behind this expected efficiency improvement are:

- Better load balancing. Performing a disciplinary optimisation on the structures maximises the information required to design this discipline, without significant cost increase.
- Reduction of the complexity of the system level optimisation problem. The surrogate based optimisation framework acting in the system level is more efficient due to the reduced dimensionality. The initial sampling costs, the metamodel training costs, as well as the suboptimisation exploration costs are reduced.

- The problem of structural optimisation — in this case *structural sizing* — is efficiently handled by specifically developed tools. In particular, the structural sizing is performed by a dedicated and well validated Nastran SOL200 process that uses gradient based methods, converging to a local optimum in a few iterations even for complex sizing problems.
- The structural integrity constraint is handled directly within the disciplinary optimisation process. Hence, a surrogate model for the KS function is no longer required, decreasing the training costs even more.
- Improvement of the synergy between aerodynamic and structures. Given a more effective way to design the wingbox structure, the expected weight decrease is more significant. Implicitly, the aerodynamic performance is improved since the lift required to support the aircraft weight is also decreased, minimising the wave and induced drag components.

The procedure followed by ASO architecture to tackle this aerostructural design problem is described in the XDSM diagram of Fig.7.10. The process is similar to MDF, with the — easy to implement — change of a structural analysis, to a structural sizing.

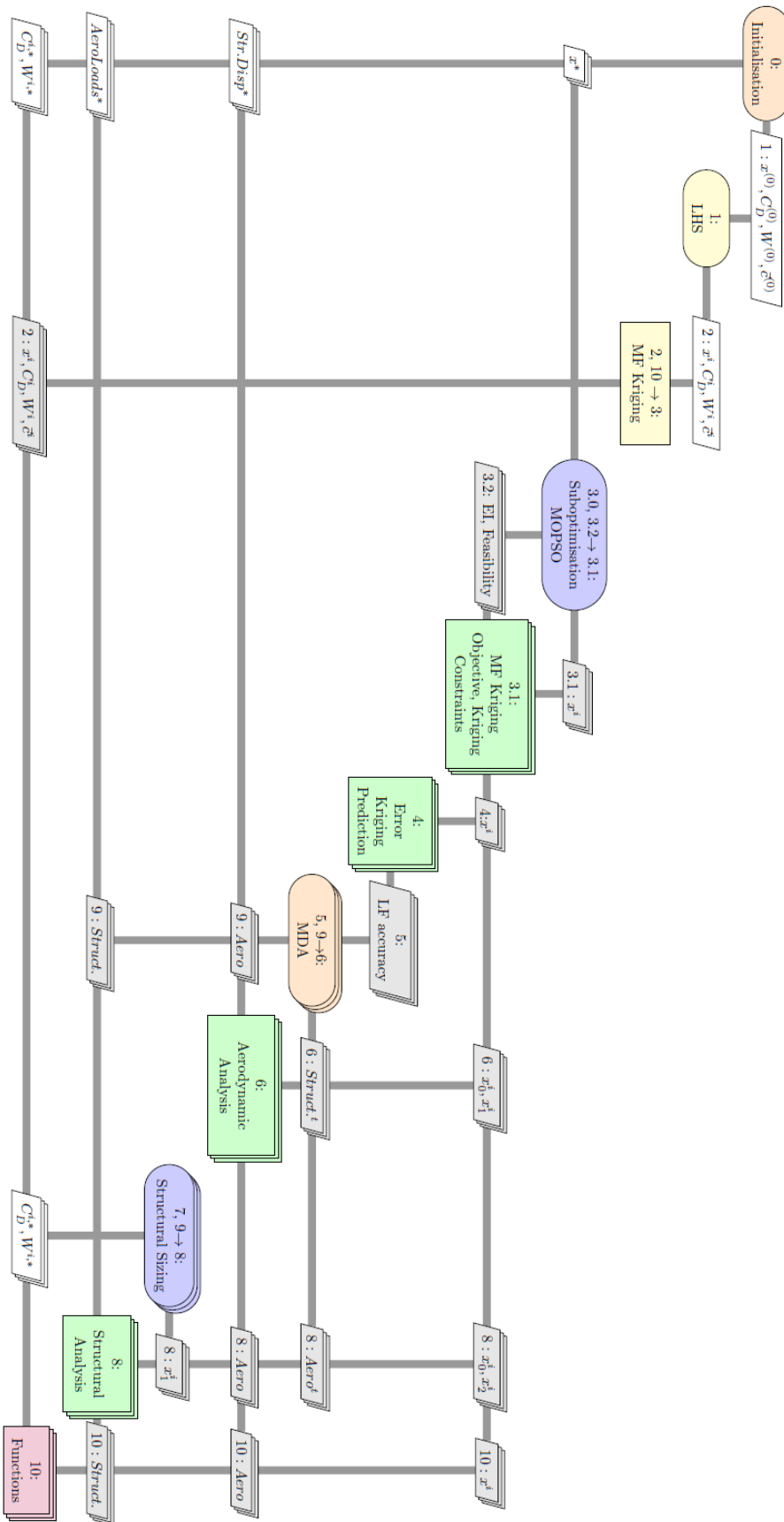


Figure 7.10: XDSM flowchart for ASO formulation of CRM aerostructural optimisation.

Structural Sizing

The structural sizing is the disciplinary optimisation process for which the structural parameters, are the local variables. Therefore, the purpose of the structural sizing is to minimise the weight of the structure with respect to the local design variables, that is the thickness of the structural elements. The global variables associated with the wingbox design are constant during this stage and are driven by the system level optimiser. The process is described as:

$$\begin{aligned} \min_{\mathbf{x}_{str} \in \mathbb{S}} W_{str}(\mathbf{x}_{str}) \\ \text{subject to } \sigma \geq \sigma_y/1.5 \end{aligned} \quad (7.2.8)$$

In Eq.7.2.8, \mathbb{S} is the structural design space where $\mathbb{S} \subset \mathbb{D}$, where \mathbb{D} is the design space of both the global and structural variables. The Von-Mises stresses σ should be lower than the yield stress σ_y divided by the safety factor, under a loading corresponding to a 2.5g.

The above procedure is performed by an efficient and dedicated Nastran SOL200 process. Therefore, given a specific wingbox shape design (defined by the global variables) the structural weight is minimised by the appropriate thickness definition of the structural model shell elements. The SOL200 procedure is using gradient based methods (see Chapter 2) as described in the work of Dababneh [240] and increasing the number of structural variables does not affect the problem formulation in a negative way; the sizing process remains cheaper than a aerodynamic analysis. Hence, the structural design variables are increased. Each variable now corresponds to a different structural element shell thickness and the structural variables grouping described in the MDF formulation is discarded.

A Note on High Loads Maneuver Structural Analysis

The high-g maneuver loading employed by the structural analysis used within the SOL200 sizing, is simply simulated by using a load factor of 2.5 in the preprocessing stage. More specifically, the aerodynamic loads of the current Gauss-Seidel iteration are multiplied by the factor 2.5¹².

A limitation of the present work is that an aerostructural loop is not performed for the high loading conditions as done for the cruising loads. That is, following the structural sizing which results to a deformed wing shape, no additional aerodynamic analyses are performed to update the loads that would correspond to the high loading maneuver. The

¹²This is only one of the possible ways of simulating a high maneuver. Another approach would be to perform an aerodynamic analysis with an angle of attack value that would correspond to a total lift of 2.5 times the cruising lift. This would be consistent with the load factor requirement. However, it would of course provide a different loads distribution than the method used in this work since the latter is based on cruising load distribution conditions simply multiplied by the load factor. Although a topic rarely discussed in the literature, it is of great importance as it has great impact in the optimisation process.

same limitation holds of course for the MDF formulation, in which a simple additional aerostructural Gauss-Seidel loop would have been performed using the maneuver loads, following the aerostructural Gauss-Seidel loop based on cruising loads. The most accurate method to treat these structural constraints would be to use an additional aerostructural loop under the maneuver loads which would result from a high angle of attack aerodynamic analysis.

However, this approach essentially doubles the effective analysis cost of this MDO problem which for the given computational resources and PhD timeframe would prove prohibitive. Nevertheless, it should be noted that such an accurate constraint function analysis is expected to increase the inwards shifting of the aerodynamic loads during the high g conditions due to structural deformation as a means of loads alleviation. Exploiting this constraints information, the optimisation would be expected to lead towards a design which during cruising conditions would feature an aerodynamic load distribution closer to the elliptic one.

7.2.7 Aerostructural loop: Mapping the Aero Loads and Structural Displacements

The interdisciplinary communication between the aerodynamic and structural grid topologies in this loosely coupled analysis is being carried out with python scripts acting through the CAE software ANSA [241]. These scripts guide the mapping of the aerodynamic loads from the aerodynamic grid to the structural one. This load transfer is split into two stages; mapping the pressure loads corresponding to the wingbox skin and mapping the rest of the loads, associated with aerodynamic surfaces for which no structural elements are present, such as the Leading Edge (LE) and Trailing Edge (TE) region. The pressure distribution is interpolated between the two sets of grids using an RBF based method [178]. For the LE and TE surfaces, the pressure loads are integrated so that a single resultant force acting on the respective center of pressure is defined out of each surface. This force is connected with the corresponding structural beam elements using RBE3 elements. For better accuracy, the LE and TE surfaces are discretised into three subsurfaces each associated with its own forces and RBE3 elements, as shown in Fig.7.11.

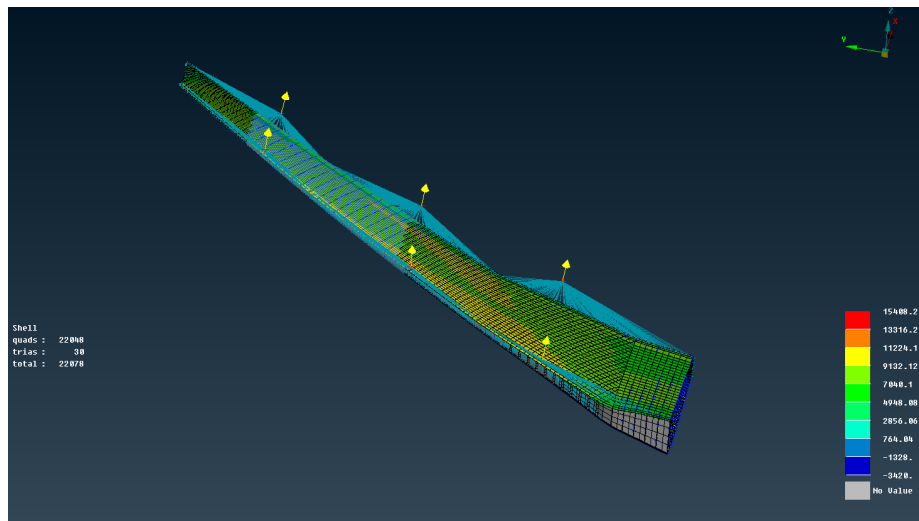


Figure 7.11: Aerodynamic loads mapping on the CRM datum. Pressure loads are interpolated with RBF functions while the forces generated near non-structural surfaces (LE/TE) are transferred to the beams using RBE3 elements.

During every MDA loop iteration, the structural displacements of the skin nodes should be transferred to the nodes of the aerodynamic surface mesh. In this loosely coupled approach, these displacements are mapped directly on the jig shape aerodynamic model. This is because the structural deformation is defined in an absolute manner, as a difference between the aerodynamically loaded and the jig shape [206]. The node displacements are passed to the aerodynamic surface nodes using RBF functions similar to Rendall and Allend's unified method [179]. Following the deformation of the aerodynamic surface, the aerodynamic volume mesh should also be deformed. This is performed again using an RBF method like the one described in the work by A. de Boer et al. [47].

7.3 Multidisciplinary Feasible Architecture Results

7.3.1 Sensitivity in Constraint Models

The MF EI methodology is very effective in exploring the design space and finding dominant designs. A concurrent drag and wingbox structural weight minimisation is achieved in the first iterations, directly after the sampling process, since the effect of the global variables and the disciplinary ones (structural element thickness) to the objective functions is significant. However, the existence of the constraints — primarily Range and cruising constraints — complicates the problem, making the convergence sensitive to the accuracy of the respective surrogate models as it is discussed. The modal constraint is satisfied almost everywhere in the design space, while the structural integrity constraint is smooth, allowing

a reasonably accurate surrogate model prediction¹³. Therefore, both of these constraints are satisfied in every infill design point even when cheap RBF models are used for them. However, the same is not true for cruising and range constraints which are very challenging. Range is used as a more "design-related" alternative to an internal volume constraint as it includes the effect of fuel weight, structural weight and the aero performance of the design at the same time. The dependency on these quantities make range highly nonlinear and multimodal, creating "islands of feasibility" within the design space. In a similar fashion, the cruising constraint space is filled with sparse regions of feasibility.

A scheme with inherent exploration attributes requires a number of iterations before feasible and promising solutions are identified in a high dimensional space. This problem is only intensified by the dependency on the surrogate models, which for a given computational budget cannot be sufficiently accurate. The initial iterations only improve the accuracy of the surrogates near the, already identified from sampling, feasible space boundaries. Securing a pareto front convergence becomes even more challenging when the penalty method is used to handle the constraints¹⁴, especially when it is based on RBF models. The high dimensionality of this problem makes cheap RBF models generally inaccurate, with the trim of shape parameters of the function and function correction, θ and θ_e respectively, critical for the success of the optimisation process. When θ and θ_e become lower than a certain value, the models are so flat that information from the sparse sampling is diffused in the extrapolating regions of the design space. This creates fictitious promising points, steering the suboptimisation process into false sampling points in the bounds. This prevents the improvement of the knowledge of the actual promising design space regions, stalling the optimisation process completely.

In an exploitation based approach however, such as a trust region based framework [200], the whole process is initiated from the area near the datum point in which the constraint is satisfied, and its value is known locally, even cheap RBF models could be used. Therefore, the convergence of the problem simply follows the objective function reduction path until the constraint boundary is reached. However, such an approach would not satisfy the exploration requirements specified for conceptual design studies, set prior to the development of our methodology as well as requiring a prohibitive number of LF analyses.

Another factor having an impact on the observed problem of satisfying these constraints is the correlation between them, through lift and structural weight. Low drag and low weight configurations are identified through the appropriate values of the global variables (shape parameters) which have a significant impact on these quantities¹⁵. This translates to a reduction of the wing's thickness/volume which reduces both drag and structural weight at the same time (for given wingbox structural elements' thickness). However, this also

¹³Of course in a high dimensional SBO problem, where computational costs constraint the number of the available training data, by "accurate" we mean that the metamodels predict the correct trends.

¹⁴For more information on the convergence behaviour of penalty and feasibility methods, see Kontogiannis et al. [213].

¹⁵The shape parameters have a direct effect in wave drag as well as the structural weight since they control the size of the wingbox elements (but not their thickness).

results to a decrease of the internal volume and the corresponding fuel mass. As such, a higher aerodynamic efficiency is required to maintain the constrained value of Range. Given a lower drag value however, whether or not the L/D value will increase depends on the decrease of weight as well, since lift is trying to match the aircraft gross weight through the cruising condition constraint $L = W$. Therefore, improving the $L = W$ constraint surrogate model accuracy is critical before the range constraint is satisfied. In the failure of satisfying this constraint in the infill sampling, as in the case of penalty methods in Fig.7.13, the optimisation is steered to very low weight configurations which are easy to locate. However, due to low $L = W$ model accuracy, lift is almost always lower than the aircraft weight and as a result, L/D is reduced leading to non-satisfying range performance.

To tackle the above challenges, it is necessary to use the feasibility method to satisfy the constraints, as it has proven to be more conservative. Furthermore, equally important is the fact that in this method, Kriging has to be used to model for the constraints. As explained earlier, the process is sensitive to θ_e , and as such Kriging is also preferred for modelling of the LF tool error for all objective functions and constraints. This has proven to be an efficient way to deal with the problem of the fictitious promising points in the extrapolating region. The additional computational cost requirements for training these Kriging models is fully justified by the optimisation convergence gains. Furthermore, since the points to which LF error is defined is only a small subset of the LF training points set, the respective training costs are very small compared to the training costs of the LF function estimators.

7.3.2 Pareto Front Results

The feasibility method, being a more conservative approach, leads to feasible infill points which of course have significantly higher structural weight values than the infeasible ones predicted by the penalty method — not showing here for clarity reasons.

The obvious solution to the problem described, would be to use a single objective formulation with Range as an objective function. Although an efficient approach, this does not provide the objective space exploration desired for a conceptual study to which this is aiming. This is achieved by a multiobjective formulation. We require a wide solutions spectrum to provide high fidelity information for various design directions early in the design space. As such, the various design possibilities are known to the engineer for given performance requirements. Fig.7.12, shows the design directions in this MO problem and the qualitative effect on the range.

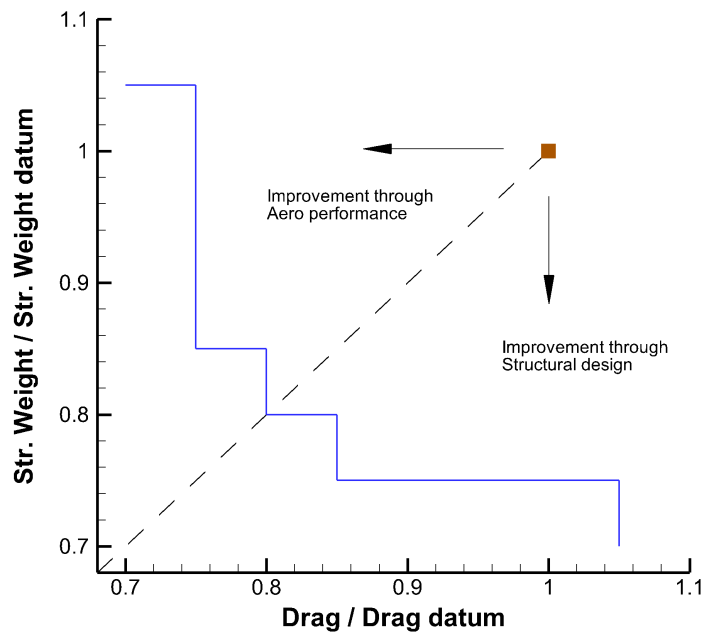


Figure 7.12: The satisfaction of the range constraint can be achieved through a more efficient aerodynamic design, a more efficient structural design or a tradeoff between both.

In Fig.7.13, it is shown that points that dominate the datum do not necessarily translate into a range increase. The inverse can be also true. Pareto front points can even lead to reduction of range. This shows how the problem can be tailored to the design needs. High aerodynamic performance configuration with poor structural design — and the inverse — do not provide a unique range performance trend. This is a direct result and demonstration of the increased effect that L/D has on range, based on Breguet equation. The impact of the structural weight is lower, and a significant increase of the fuel tank volume with concurrent thickness element reduction should be achieved to provide similar range values¹⁶.

¹⁶The comparison between the impact of aerodynamic performance and structural weight is also observable through a parallel coordinates analysis that has been observed. Here it is omitted, as the dimensionality and the number of design points make visualisation very difficult.

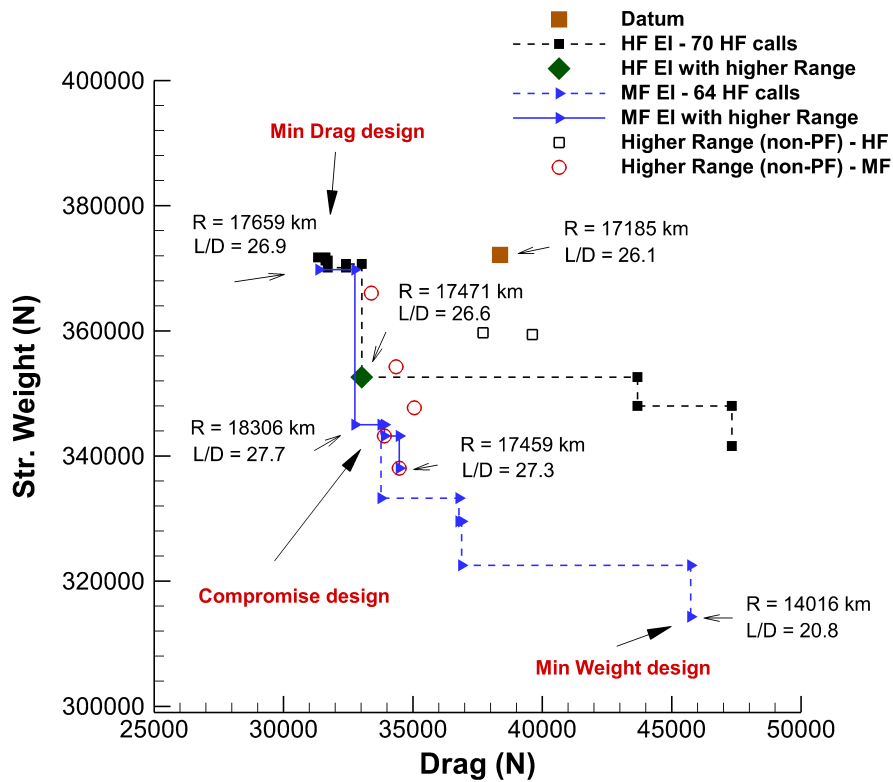


Figure 7.13: Pareto front comparison between the HF and the MF methods, using "feasibility" to handle the constraints for the MDF formulation. Balance is required between aerodynamic and structural performance. A very efficient structural design leading to low aerodynamic performance will not improve range. Aerodynamic efficiency is more important in that aspect. Even dominated points can provide higher range than high drag pareto points.

Following the observations above, a pareto front composed of drag and structural weight objectives can be generated even through a single objective setup, via range optimisation. However, the exploration associated with such an optimisation formulation is limited and does not cover our needs.

Comparing the MF EI method with the established HF EI approach, it is fairly evident that the former is much more efficient in all aspects. It provides a pareto front that dominates the HF one both in terms of value as well as in terms of exploration, with similar computational costs. The hypervolume convergence study shown in Fig.7.14 verifies the superiority of the MF method throughout the whole optimisation process. An interesting observation is that the new configurations are associated with slightly higher structural weight than the ones from MF EI. Despite the drag and weight improvement compared to datum, the L/D decrease of these points — combined with decreased fuel mass — lead to the decrease of the range. Out of the points that do increase the range, a single dominant point is identified. The conclusion that can be drawn by this comparison is that by not augmenting our data by using cheap LF analyses, a lot of useful information is lost. Therefore,

extra HF calls are required to recover it, increasing the final computational expenses to attain similar results. Finally, it should be clearly stated that the reason behind the success of the MF method is the ability of the LF tool to follow the trends of the HF one. As such, the cheap LF data are efficiently exploited, providing information that would otherwise require costly HF analyses.

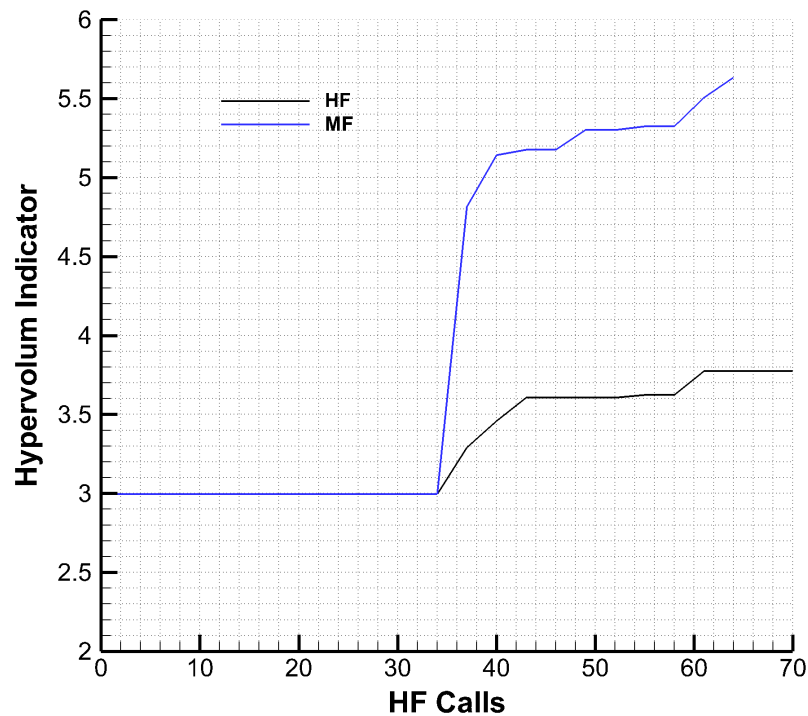
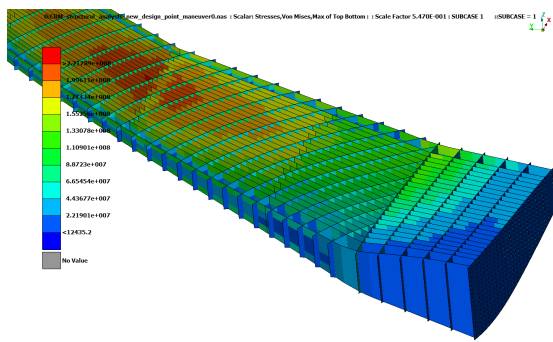


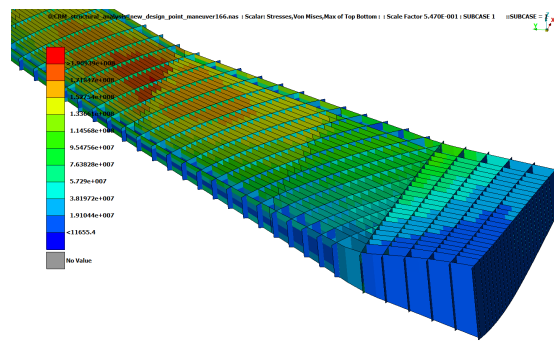
Figure 7.14: Comparison of the HF and MF pareto front convergence via the hypervolume indicator for the MDF formulation.

Despite these encouraging results, the effect of constraints in actual industrial practice should not be neglected. In particular, equality constraints — in the form of $L = W$ — are challenging to satisfy and the accepted tolerance strongly depends on the design stage. In this work, all the presented results were of course within the predefined tolerance, with constraint being satisfied by the optimisation framework. However, some were satisfying the equality constraint more accurately than others. There is a consequent effect on the objective function values as follows: a configuration that has $L < W$ is more likely to have less drag than another for which $L = W$, despite both being accepted as feasible cases in the scope of the study¹⁷. The design engineer applying any optimisation tool — not just this one of course — should be well aware of this potentially deceiving area, define the

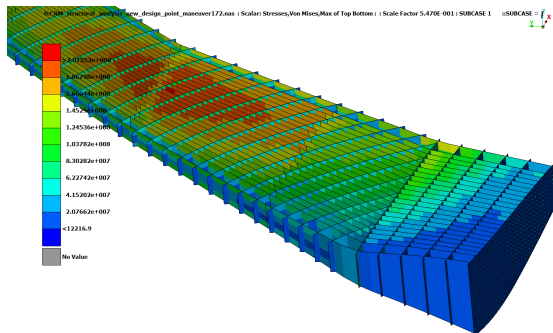
¹⁷This has been also observed in the ASO formulation results where the structural weight is decreased by the structural sizing process.



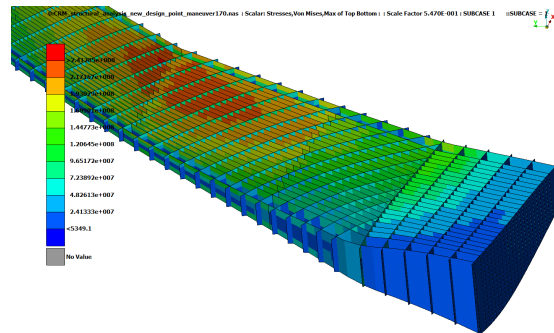
(a) Datum, max Von Mises stress: 221 MPa



(b) Minimum Drag design, max Von Mises stress: 190 MPa



(c) Compromise design, max Von Mises stress: 207 MPa



(d) Minimum Weight design, max Von Mises stress: 241 MPa

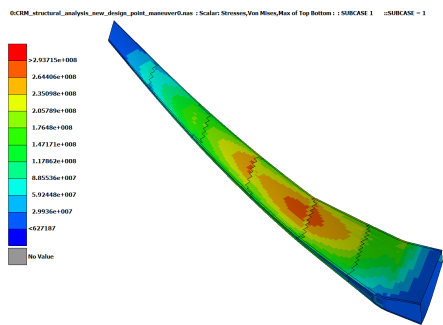
Figure 7.15: Maximum Von Mises stress in the rib-shear webs assembly during high g maneuvers, MDF formulation.

tolerance according to his needs and of course always be careful while interpreting the results, using his own physical understanding and experience.

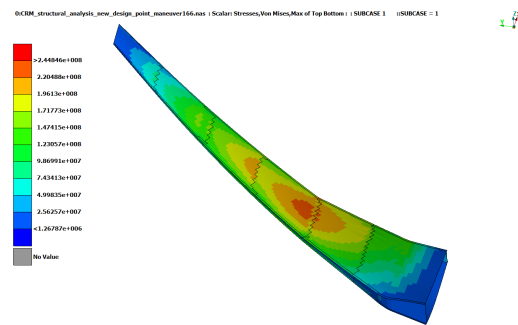
7.3.3 Physical interpretation

The physics behind the structural and aerodynamic performance of the MF resulting configurations, can provide information to the engineers, to support further design stages. The stiffness of the wing is qualitatively provided through contour plots of vertical displacements from the high loading maneuver. Von Mises stresses distributions are displayed in Figs.7.15,7.16 providing a visualisation of how the structural elements take the loads. They also imply a qualitative view on the structural design performance which is very much dependent on local section moments of inertia, which in turn is partly dependent on the airfoil thickness distribution. The latter, which also affects the total mass of the fuel, is more clearly shown in Fig.7.20 in which the airfoil shapes of the various wing designs are compared in different locations across the span.

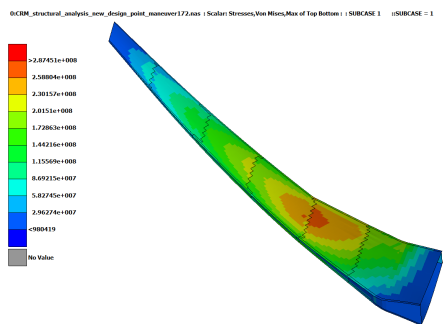
In Fig.7.15.b, it is shown that the minimum drag design is associated with lower stresses



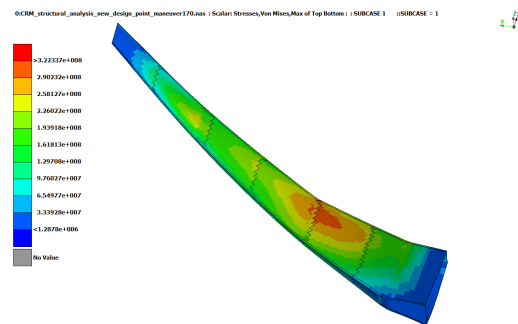
(a) Datum, max Von Mises stress: 293 MPa



(b) Minimum Drag design, max Von Mises stress: 244 MPa



(c) Compromise design, max Von Mises stress: 287 MPa



(d) Minimum Weight design, max Von Mises stress: 322 MPa

Figure 7.16: Maximum Von Mises stress in the skins assembly during high g maneuvers, MDF formulation.

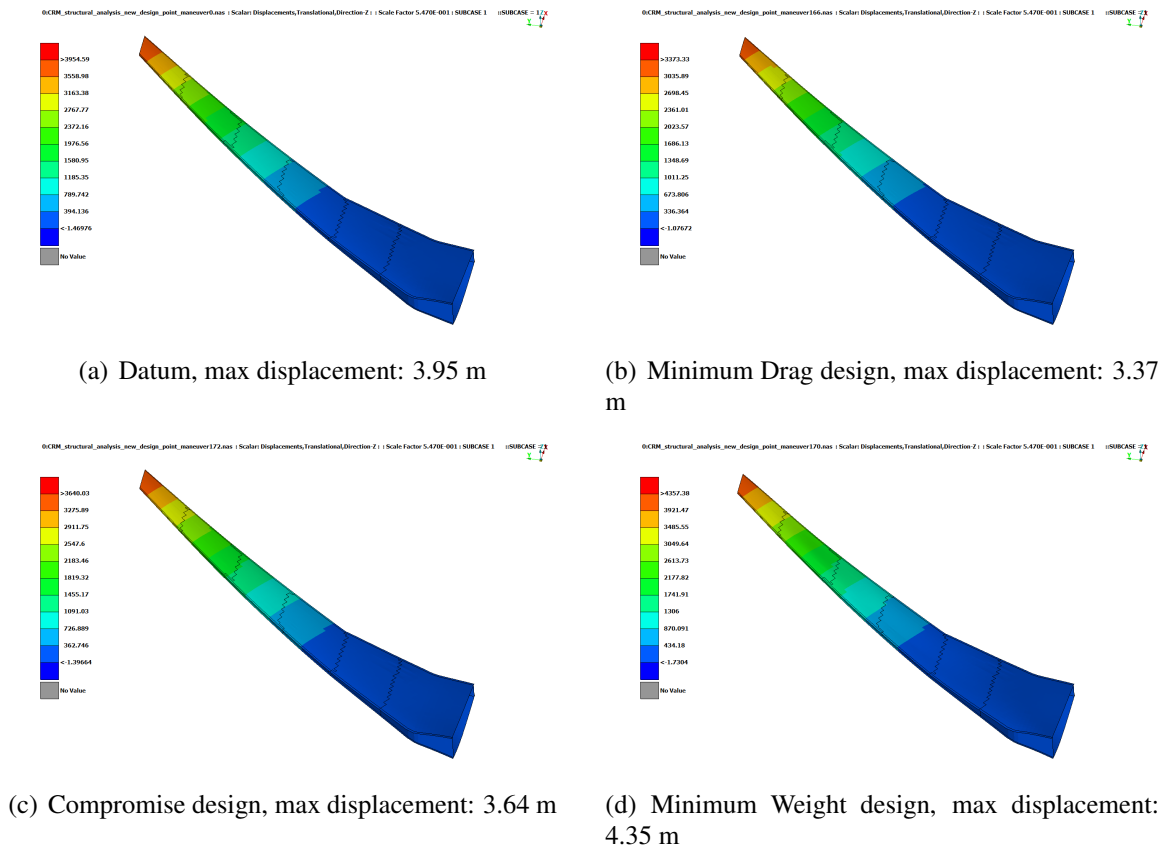


Figure 7.17: Maximum vertical displacements during high g maneuvers, MDF formulation.

as well. This shows how the internal structure is far from optimum. It is the heaviest one, due to this over-conservative design which is also apparent in Fig.7.18.b and Table 7.6, through the increased thickness of its structural elements. This also leads to a more stiff design as shown in Fig.7.17.b, which is also an important factor into keeping aerodynamic efficiency high. The minimum weight design on the other hand, displays an opposite design direction. It features the highest stresses, showing how the structural integrity constraints were efficiently exploited for this design. A reduction of the skin thickness is shown in Fig.7.18.d. This design approach provides the most flexible out of the pareto front wings, reaching a tip vertical displacement of $4.35m$. This is translated to an inferior aerodynamic performance. The compromise configuration offers a mean between the two design approaches. It is slightly stiffer than the datum, with the maximum stress and displacements being decreased compared to it. This structural deformation reduction — in conjunction with a moderately improved aerodynamic shape — is the foundation behind the superiority of its the aerodynamic performance and range increase.

Following the contours of skin thickness distribution in Fig.7.18, all the element thickness values are provided in Table 7.6. It can be observed how as a general trend the thickness is reduced towards the wingtip¹⁸ since the bending moment is increased towards the

¹⁸Variable groups "1" correspond to the root while variable groups "6"/"7" correspond to the tip.

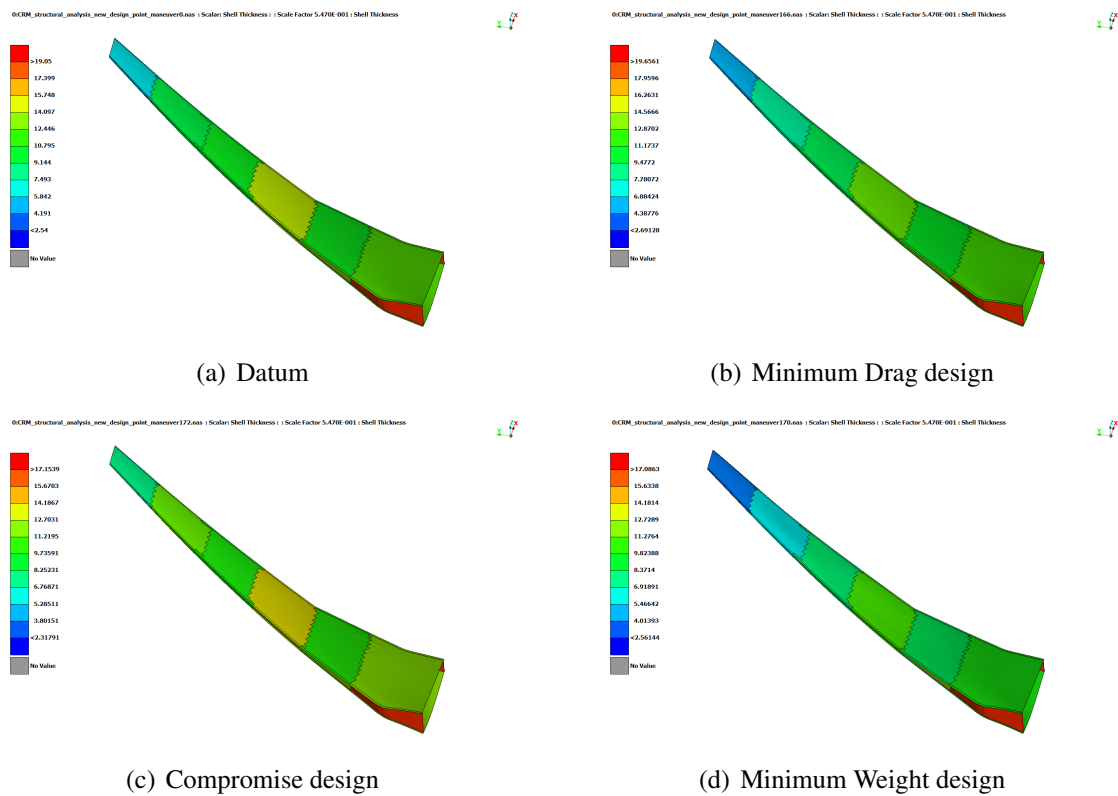


Figure 7.18: Skin thickness distribution, MDF formulation.

wing root. Therefore, in order to keep the stresses almost constant (close to their maximum allowed value), an increase in the structural element thickness increases the second moment of inertia of the structural cross section for the given geometry and topology (given wingbox design). What is of interest is also the existence of a region near the yehudi break (group 2 and 3) in which the structural thickness is maximised. It is in fact this region where the structural loading is maximised and not the wing root area, leading to the aforementioned increase in thickness. This is only apparent in the skin thickness however, since the internal structural elements (ribs, spars, shear webs) all decrease their thickness consistently towards the tip.

Table 7.6: Shell Elements Thickness (mm) - MDF Architecture

	Datum	Min Drag	Tradeoff	Min Weight
Upper Skin 1	12.5	12.57	12.15	9.94
Upper Skin 2	10.5	10.55	10.21	8.35
Upper Skin 3	14.5	13.22	13.93	11.03
Upper Skin 4	10.44	9.51	10.03	7.94
Upper Skin 5	9.5	8.14	11.52	5.91
Upper Skin 6	6.175	5.29	7.49	3.84
Lower Skin 1	12.5	12.57	12.15	9.94
Lower Skin 2	10.5	10.55	10.21	8.35
Lower Skin 3	14.5	13.22	13.93	11.03
Lower Skin 4	10.44	9.51	10.03	7.94
Lower Skin 5	9.5	8.14	11.52	5.91
Lower Skin 6	6.175	5.29	7.49	3.84
Rib 1	6.35	6.37	6.32	5.73
Rib 2	5.33	5.35	5.31	4.81
Rib 3	4.57	4.47	4.31	3.96
Rib 4	3.29	3.22	3.1	2.85
Rib 5	2.54	2.51	2.34	2.29
Rib 6	1.65	1.63	1.52	1.49
Rib 7	1	1.13	1.19	0.92
Spars/Shear Webs 1	19.05	19.65	17.15	17.08
Spars/Shear Webs 2	15.24	15.72	13.72	13.66
Spars/Shear Webs 3	10.27	10.15	10.15	9.95
Spars/Shear Webs 4	9.52	9.41	9.41	9.22
Spars/Shear Webs 5	5.08	5.38	4.63	5.12
Spars/Shear Webs 6	2.54	2.69	2.31	2.56

Fig.7.19 provides an insight on the aerodynamic behaviour of these configurations. It is evident that the minimum drag design as well as the compromise design, improve their aerodynamic efficiency by reducing the effect of wave drag. With the exception of the mid-span region which is not efficiently designed, other areas of the wing clearly show that the strong shock found in the upper surface of the datum design is attenuated. This is achieved by a better design of the LE section of the airfoils, as also shown in Fig.7.20. As such, the pressure in the suction region is decreased in a more gradual way as it should in a transonic design, with the sudden pressure recovery Δp decreasing even when the shock occurs earlier. It also comes as no surprise that the lower section is altered towards the TE, which is another focus of the traditional supercritical airfoil design. The different vertical as well as torsional displacements are evident here as well. For completeness, it should be stated that the different thickness distribution, apart from its impact on local bending and torsional stiffness of the wing (through moment of inertia), of course affects the fuel tank volume as well. Despite the availability of such information, this cannot be properly visualised here however, since the spar web positions and a three dimensional representation is preferred.

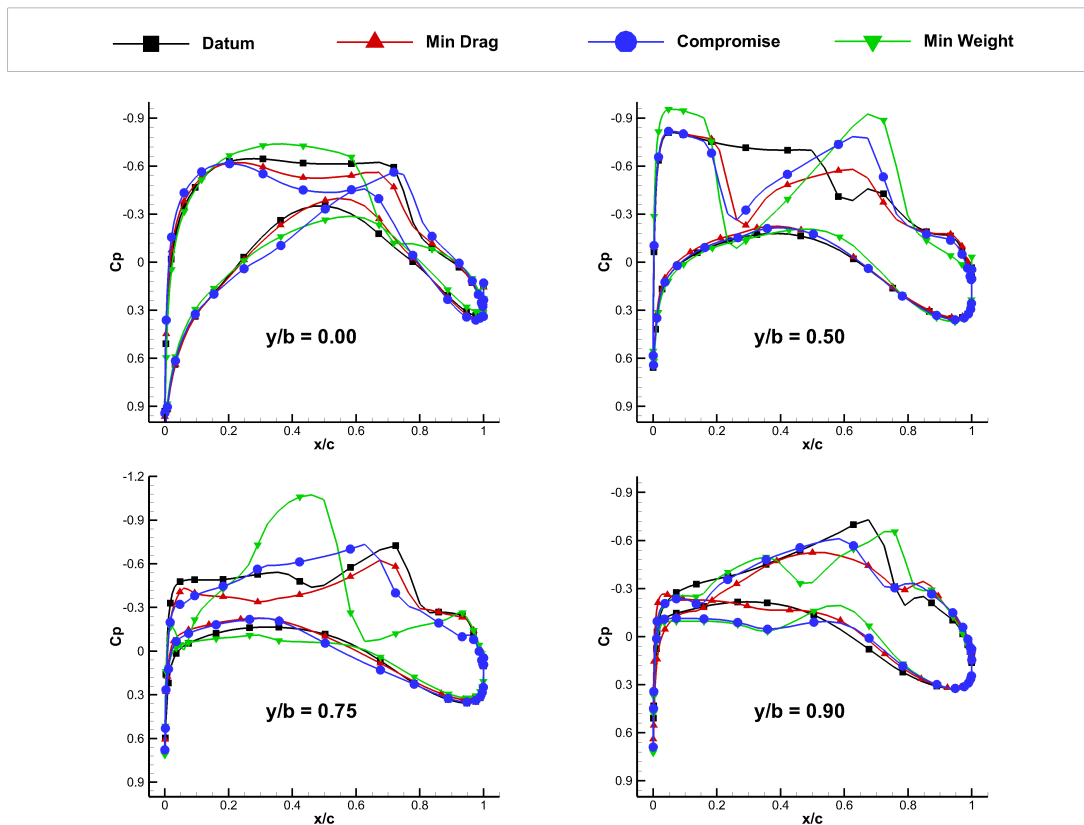


Figure 7.19: Pressure distribution of the datum, minimum drag, minimum weight and compromise design in different locations across the span, MDF formulation.

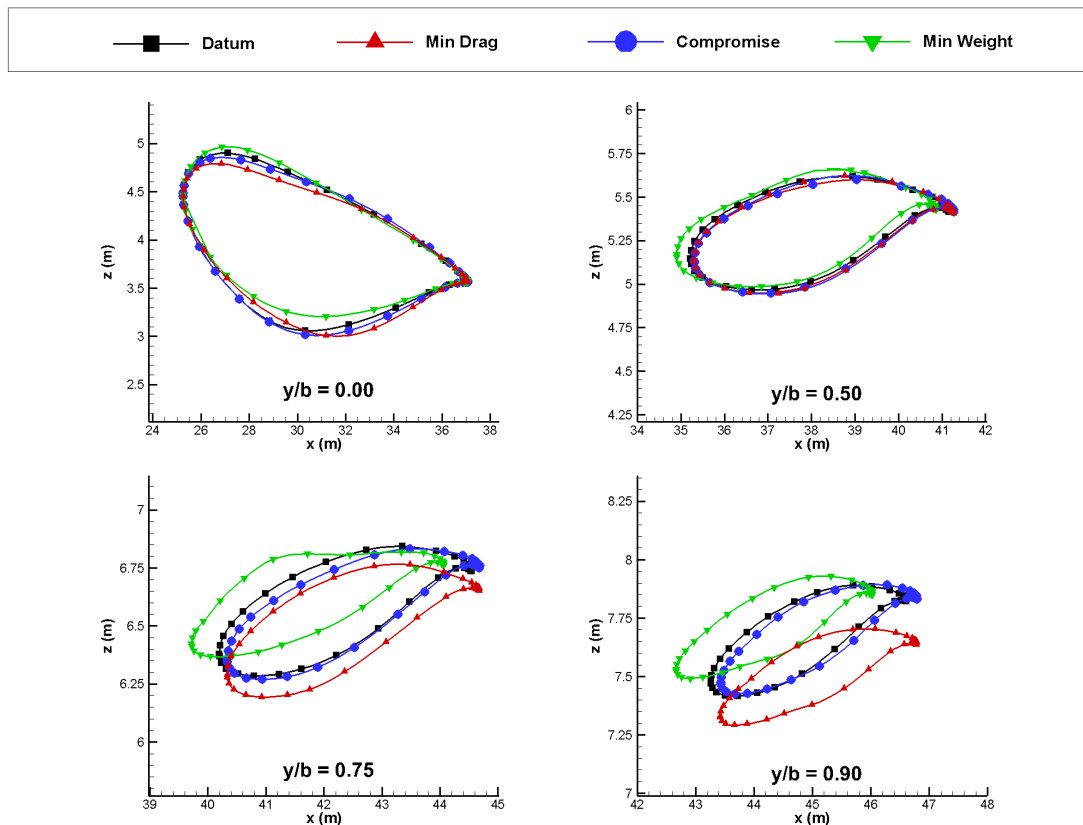


Figure 7.20: Wing sections of the datum, minimum drag, minimum weight and compromise design in different locations across the span, MDF formulation.

The changes in (jig) sweep for all configurations (datum, minimum drag, compromise, minimum weight) are listed in Fig.7.21. This figure also provides information regarding the pressure distribution for all planforms, complimentary to what has been described in Fig.7.19. Despite the limited bounds of the sweep variable, it is evident that the compromise and minimum drag designs tend to slightly increase the sweep in favour of aerodynamic efficiency. On the other hand, the minimum weight design almost minimises the sweep-related variable.

By the above analysis it was evident that the performance of each discipline correlates to the other and only when a good synergy is identified the performance can be further improved. In this MO MDO study, efficient design space exploration provided a pareto set of designs. The fact that the optimum performance, in terms of range in this case, was achieved by the compromise point and not by any disciplinary optimum point was not a surprise. It clearly shows and supports the necessity of MDO studies for more efficient future aircraft.

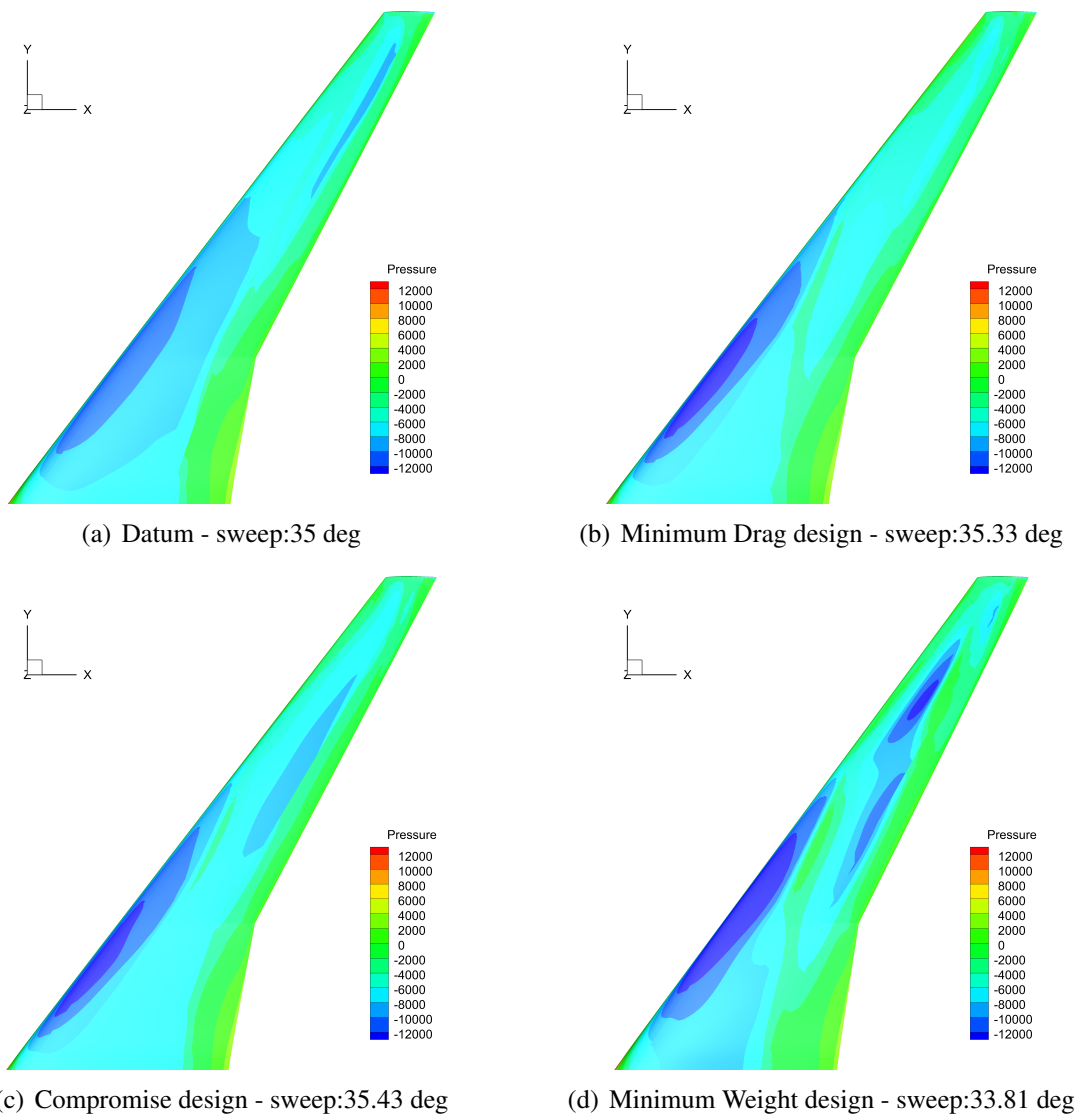


Figure 7.21: Pressure distributions - Planform view and sweep angle, MDF formulation.

7.4 Asymmetric Subspace Optimisation Architecture Results

With the potential benefits of this particular architecture described in Chapter 2 as well as in section 7.2.6, evidently the step to follow an MDF-based aerostructural design should be an ASO-based one. This provides not only an opportunity to assess how the optimisation framework performs in the system level of a distributed architecture-based industrial aerostructural problem, but also how the problem itself adapts to this MDO formulation. This section follows a structure similar to the MDF-one. The final pareto front results for a given computational budget are presented, focusing on the comparison between an HF and an MF-based framework. The results are also discussed in a physics basis for three different design directions: minimum drag, compromise and minimum weight design.

7.4.1 Pareto Front Results

Similarly to the MDF case in which the RBF-based penalty method failed, the problem's constraints were handled with the Feasibility method which requires the more accurate — but more expensive — MF modKriging models instead. However, the reduced dimensionality of the system level in the ASO formulation triggered the idea that the RBF-based error correction would be efficient, as it was proven to be in the less complicated test cases. This could potentially provide cost savings over the Kriging-based error correction which in the MDF case was necessary since RBF was not accurate enough.

Unfortunately, despite the successful predictions of the design trends which lead to efficient designs, the RBF error correction model could not accurately approximate the constraints of the problem. Particularly, the cruising constraint ($L = W$) was almost never satisfied during the optimisation process. A part of the problem does not only lie to the limited accuracy of RBF models, but also to the challenging nature of this constraint specifically within the ASO formulation.

It should be reminded that structural weight is sensitive to the structural sizing, that is, it is significantly dependent to the local variables. Therefore, with the surrogate models being trained in the system level, the effect of the local variables is not directly implemented in them and the metamodels lose sensitivity to the structural variables. The cruising constraint metamodel predictor y correlates $L - W$ with the global variables (wingbox design), $y : y(W_{str}) = y(W_{str}(x_0))$. However, a part of the physical mechanism responsible for the structural weight value is expressed by the local variables, $y : y(W_{str}) = y(W_{str}(x_0, x_{str}))$. The *lack of the explicit* description of the effect that the local variables have in the constraint metamodel, raises an *implicit mapping* between the global and the local variables when estimating the cruising condition. This is because a global variables set corresponds to a local one in a deterministic way, through the gradient based structural sizing process. That is,

$x_0 \rightarrow x_{str}$; which makes the model $y : y(W_{str}) = y(W_{str}(x_0(x_{str})))$. To put it more simply¹⁹, the constraint metamodel only sees the effect of the structural variables implicitly and not directly because local variables are not used in the training process. As shown from their results in Fig.7.22 however, the Kriging-based error correction and the HF EI method were more successful in handling this challenging situation.

The same figure also provides a comparison between the HF and MF expected improvement approaches within the ASO formulation. While having a similar computational cost, the pareto front designs of the MF method dominate most of the ones predicted by the HF approach. The latter has an advantage over the MF approach in the low weight objective space. Also, in a manner consistent to all the cases examined so far, it succeeds in providing more pareto points. Nevertheless, the extent of both pareto fronts are very similar, with MF dominating in the low drag objective space. What is also of interest is how both methods propose configurations of similar structural weight. This suggests the existence of (at least) three strong local minima in the structural weight design space, forming three (at least) efficient design trends.

Interestingly, a reduction in the aerodynamic performance is observed when moving from the HF set towards the dominant points of the MF pareto front. This shows that interdisciplinary synergy is achieved through disciplinary tradeoff; pareto front sets are generated when none of the conflicting disciplines is optimised. This implicitly stresses the importance of an efficient structural design which should not be overlooked in favour of aerodynamics. It is evident that once again — as in the MDF case — the maximum performance in terms of range occurs in the tradeoff pareto point, which helps to underline the importance of multidisciplinary interactions-driven design processes²⁰. Also, since the range achieved by the MF and the HF tradeoff point are almost identical, the effect of interdisciplinary synergy on the design trends is once again obvious. The MF design achieves the same range performance, but with a lower drag value resulting from lower lift requirements, which in turn are the result of a slightly lower structural weight.

However, the fact that the maximum feasible range is not a found in any of the pareto points — as in the MDF case — indicates that a parametric study and applications of other potential objective functions would be very useful for the design engineer, depending on his needs. In addition to this however, it shows the great effect that the wingbox design has on the range, through fuel tank design. Perhaps it is not explicitly referred in this PhD thesis, but this MDO study is in reality a case of three disciplines. While the aerodynamic surface and the structural wingbox are designed by the global variables in the system level, the fuel systems discipline is provided with a fuel tank design (tank volume) — which clearly affects the objective functions.

¹⁹This was indeed quite complicated.

²⁰Implicitly, a range optimisation is a tradeoff between aerodynamics and structures.

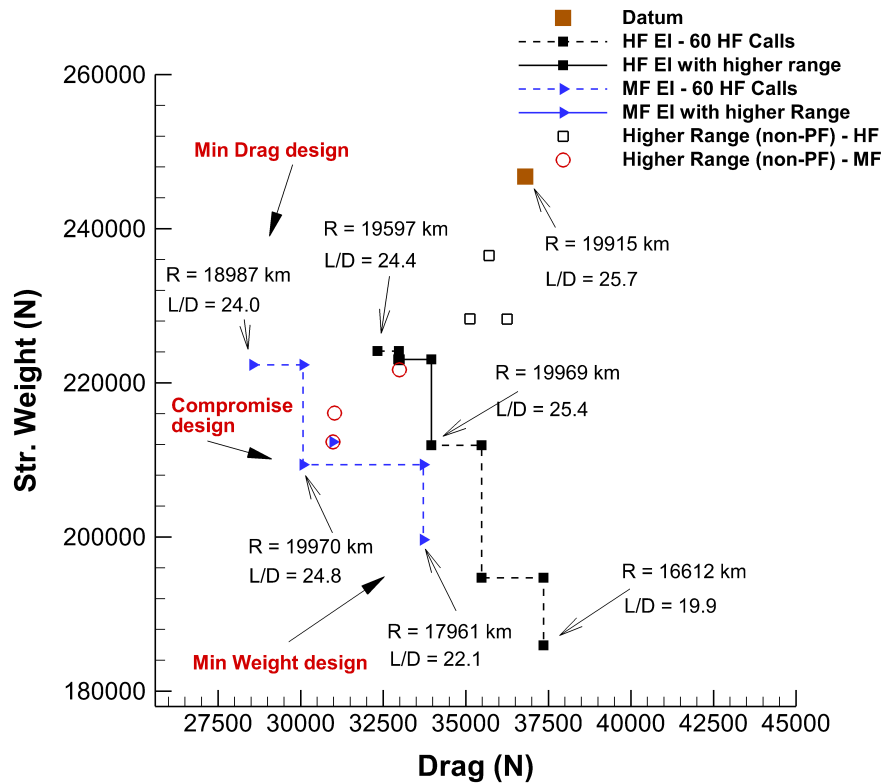


Figure 7.22: Pareto front comparison between the HF and the MF methods, using "feasibility" to handle the constraints for the ASO formulation. As in MDF, a tradeoff is required between aerodynamics and structures to achieve range performance.

The MF method shows a lack of robustness and consistency in terms of being completely superior to the HF one, especially in such complicated multiobjective problems. This non-definite performance against the HF SBO approach was also observed in the RAE2822/GARTEUR applications, when the work progressed from the single objective to multiobjective cases. Therefore, the hypervolume indicator is once again employed in order to provide information regarding the evolution of the HF and MF pareto fronts. This is shown in Fig.7.23.

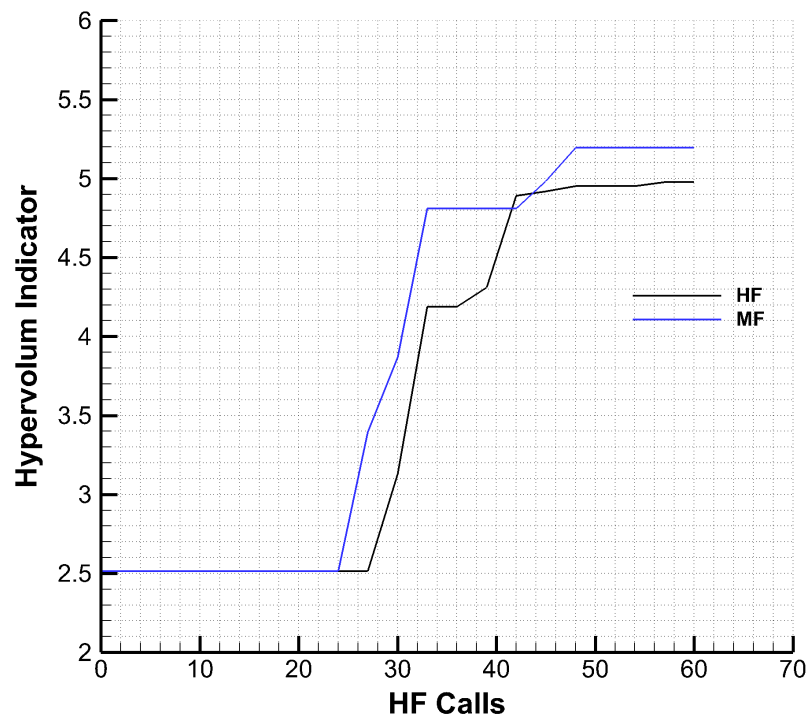


Figure 7.23: Comparison of the HF and MF pareto front convergence via the hypervolume indicator for the ASO formulation.

Evidently, the MF method shows superior characteristics over the HF one in the beginning of the optimisation process. Such an attribute was also observed in the single objective applications of the RAE2822 test case. Another common characteristic with these test cases is that the MF approach features convergence plateaus which are more extended than the ones of the HF method. The plateaus towards the end of the optimisation process suggest that the HF EI could be more efficient following that point on in the process. As such, the benefits of an MF methodology have been conclusively proven only in the early stage of the process. Such an observation is consistent with the typical design process workflow, which uses LF tools early in the design and HF tools afterwards.

As a final note in this section, the cost of the LF tool should not be neglected as a consideration when assessing any MF methodologies. In this particular case, the cost of the LF analysis never exceeded a 1/3 of the HF one, and the exploitation of performing LF and HF analyses on parallel allowed an almost identical elapsed time cost between the HF and the MF approach. However, if the need for LF data is increased, such a MF methodology will gradually become more expensive compared to an HF one. Finally, considering that the LF tool used in this work is accurate and robust (being an Euler CFD/SOL101-SOL200 analysis loop), only a tool of similar accuracy and robustness but of lower cost would be able to improve the presented results in terms of multifidelity efficiency.

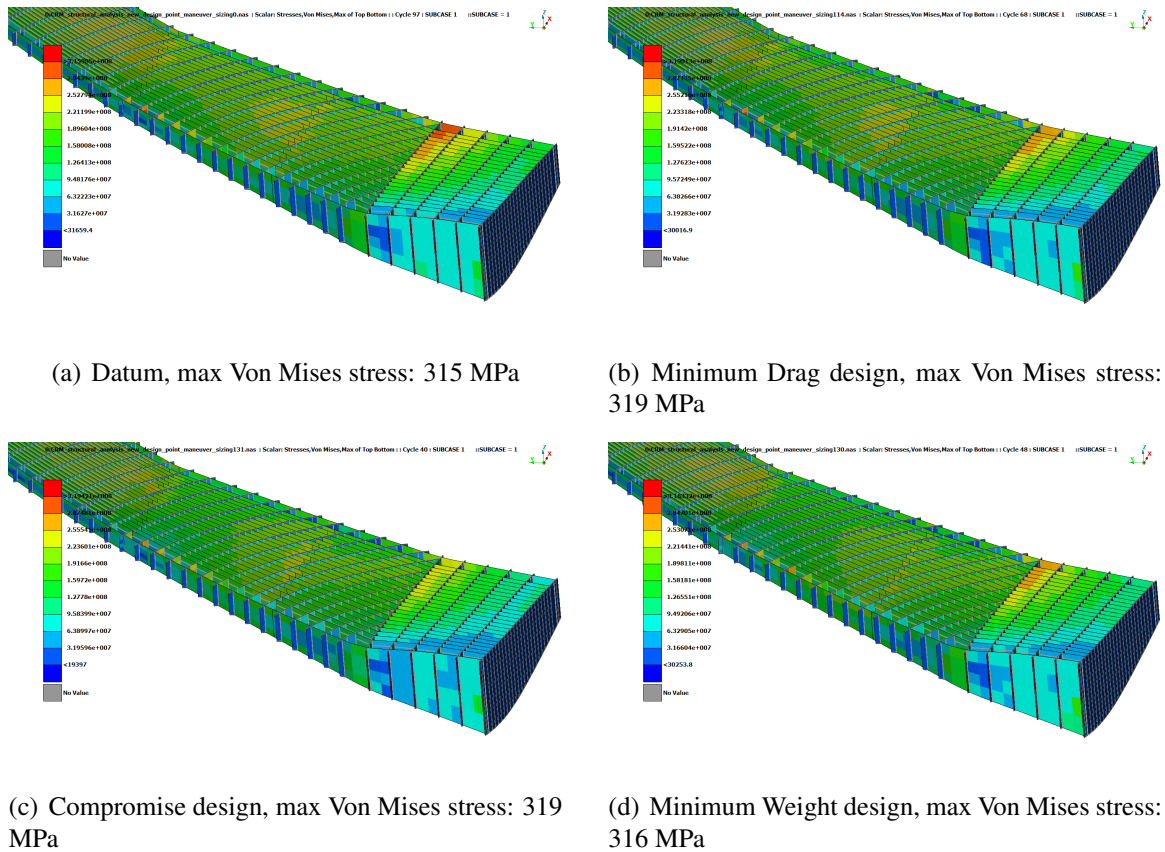
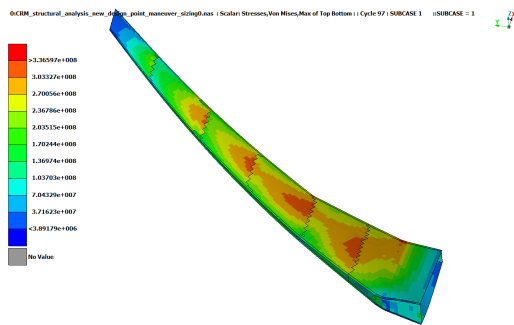


Figure 7.24: Maximum Von Mises stress in the rib-shear webs assembly during high g maneuvers, ASO formulation.

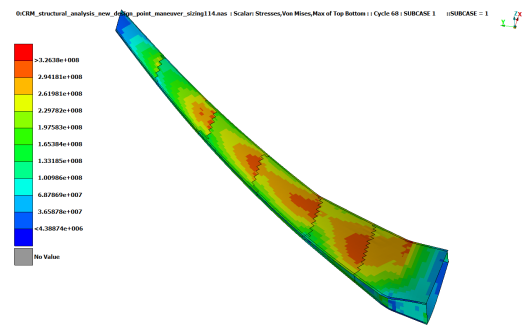
7.4.2 Physical Interpretation

As for the MDF architecture, the physical and design characteristics of the pareto configurations are discussed since they represent to the information that would be exploited by the design engineers. Therefore, the structural stiffness and the structural design efficiency of the minimum drag, compromise and minimum weight design are examined based on the vertical displacements and Von Mises stress distribution respectively.

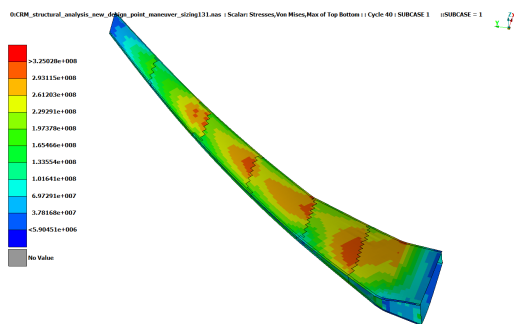
Figs.7.24,7.25 display the Von Mises stresses in the structural elements of the datum and pareto configurations. Since in ASO each aerodynamic analysis (loads calculation) is followed by a structural sizing, then for each wingbox design — controlled by the global variables — the structural design is optimised. The structural design is most efficient when it leads to the maximum allowed stress that provides the minimum structural weight [237]. Consequently, it is evident that in ASO where the elements are sized, the maximum stress is common to all wingbox designs regardless of the corresponding design direction (be it minimum drag or minimum weight). Contrariwise to the MDF cases, this maximum stress is constant throughout the skin and is of course the maximum yield stress allowed based on the defined safety factor, showing the efficiency of the structural sizing process.



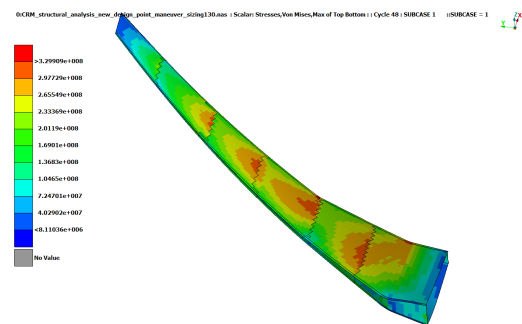
(a) Datum, max Von Mises stress: 315 MPa



(b) Minimum Drag design, max Von Mises stress: 319 MPa



(c) Compromise design, max Von Mises stress: 319 MPa



(d) Minimum Weight design, max Von Mises stress: 316 MPa

Figure 7.25: Maximum Von Mises stress in the skins assembly during high g maneuvers, ASO formulation.

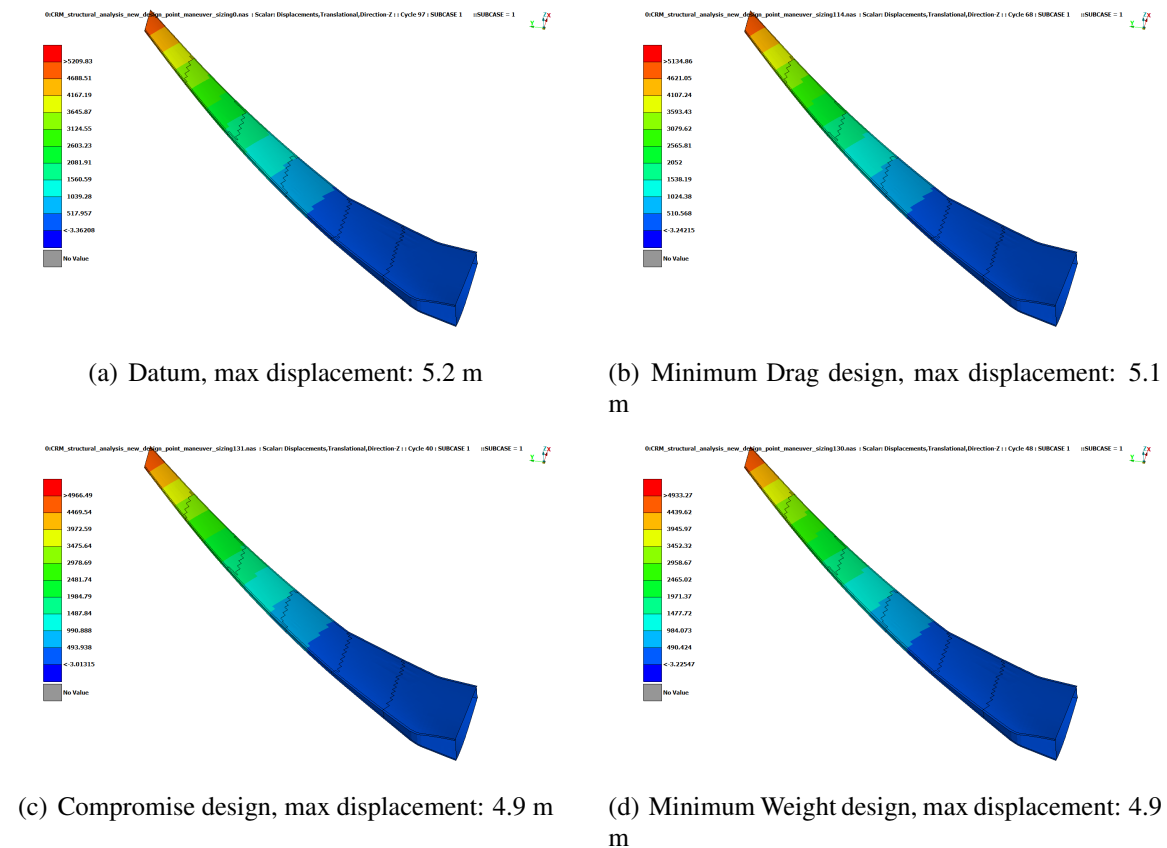


Figure 7.26: Maximum vertical displacements during high g maneuvers, ASO formulation.

The stiffness characteristics of the wingbox configuration is dependent to an extent on the thickness of the structural elements. Therefore, since structural thickness is optimised for all the configurations, the vertical displacements during a 2.5g maneuver are similar in all the design approaches (as shown in Fig.7.26). This is in direct comparison with the MDF-based results where the structural thickness design was not as efficient for all the pareto configurations — with this structural optimisation inefficiency contributing to the design being either aerodynamics or structural oriented. That is, the "design philosophy" was not completely de-associated from local structural variables.

With the ASO formulation involving a higher structural sizing efficiency, all design directions have the minimum allowed structural element thickness and the design direction is now mainly a result of the global variables²¹, that is the system level optimiser. These control the Outer Mold Line (aerodynamic performance) and the wingbox shape (fuel tanks volume and structural mass)²².

²¹Of course the local variables have an effect as well since the potential of thickness/weight reduction during the structural sizing is not constant throughout the system level design space.

²²In reality, the local variables (structural element thickness) also affect the fuel tank volume, but this is neglected since within SOL200 shell elements are not associated with a physical volume. Nevertheless, the volume difference is not significant.

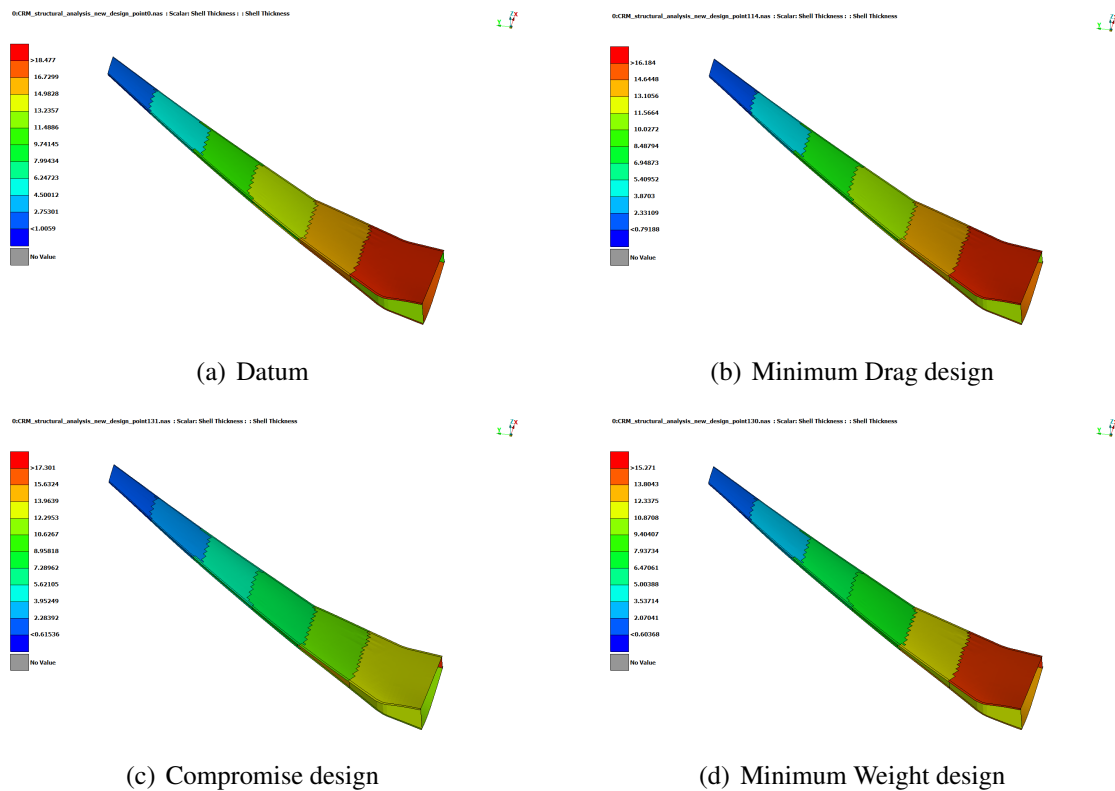


Figure 7.27: Skin thickness distribution, ASO formulation.

A factor which implicitly helps to reduce the structural weight in ASO formulated problems is the dimensionality increase of the structural disciplinary optimisation. The use of a dedicated gradient based optimisation like SOL200 allows a more detailed description of the structural sizing problem. Therefore, higher weight savings can be achieved without important adverse effects like cost increase.

Fig.7.27 and table 7.7, report the thickness of all structural elements of each pareto configuration. The same observations on the thickness reduction towards the tip as well as the local thickness increase near the yehudi break are drawn; similarly to the MDF case. Again, the yehudi break is the most critical region, guiding the structural sizing process to slightly higher local thickness values than in the actual wing root. Interestingly enough, the skin panel elements are designed thicker in the ASO than in the MDF formulation. Since the structural sizing is undoubtedly more efficient than the MDF structural design, it is not hard to follow the physical reasoning behind this. The way the structural problem is formulated (as described early in this chapter), the skin panels function implicitly as spar caps as well, providing "effective spar cap area". Therefore, the second moment of inertia is maximised, in order for the Von Mises stress constraints to be met. In turn, not critical regions like shear webs that are closer to the neutral axis, are significantly thinner. The same also holds for the ribs, which do not have to be as thick as the skin and the front/rear spars — the latter (skins and front/rear spars) also taking the torsional loads. This detailed and more effective structural design is the key advantage of the ASO over the MDF formulation.

Table 7.7: Shell Elements Thickness (mm) - ASO Architecture

	Datum	Min Drag	Tradeoff	Min Weight
Upper Skin 1	18.47	16.18	13.24	15.02
Upper Skin 2	15.82	13.94	11.06	11.97
Upper Skin 3	13.66	11.36	7.41	7.70
Upper Skin 4	10.78	8.61	5.75	6.72
Upper Skin 5	5.34	4.10	2.63	3.26
Upper Skin 6	2.19	1.50	1.50	1.50
Lower Skin 1	17.45	14.80	11.91	13.20
Lower Skin 2	17.24	15.35	11.98	13.27
Lower Skin 3	14.23	11.83	7.69	8.12
Lower Skin 4	11.18	9.04	6.03	7.01
Lower Skin 5	5.63	4.31	2.65	3.53
Lower Skin 6	1.00	0.79	0.61	0.60
Rib 1	3.30	3.19	2.97	2.87
Rib 2	5.15	5.39	5.54	5.74
Rib 3	6.37	4.81	1.50	2.71
Rib 4	3.80	1.96	1.50	1.50
Rib 5	1.26	0.89	0.62	0.65
Rib 6	0.66	0.58	0.50	0.50
Rib 7	0.71	0.50	1.24	0.58
Front Spar 1	12.87	11.61	12.83	11.49
Front Spar 2	16.49	13.06	14.47	11.15
Front Spar 3	10.10	9.44	9.45	8.09
Front Spar 4	9.33	8.49	9.00	6.12
Front Spar 5	6.65	3.49	2.50	2.99
Front Spar 6	1.50	1.60	1.71	1.76
Rear Spar 1	11.01	11.16	17.30	15.27
Rear Spar 2	11.57	6.09	5.58	7.60
Rear Spar 3	10.41	9.67	11.30	10.43
Rear Spar 4	9.55	8.94	3.60	3.08
Rear Spar 5	4.02	3.71	2.63	3.26
Rear Spar 6	2.23	2.33	1.82	1.65
Shear Webs 1	5.79	6.42	7.42	5.50
Shear Webs 2	6.20	5.50	6.19	6.56
Shear Webs 3	5.50	5.50	5.50	5.50
Shear Webs 4	3.68	3.79	3.67	2.71
Shear Webs 5	2.50	2.50	2.50	2.50
Shear Webs 6	1.53	1.50	1.50	1.50

Figs.7.28,7.29 display the aerodynamic characteristics of the pareto configurations. As in the MDF case, efficiency in transonic shape design is primarily the result of trimming the upper surface so that suction peak is slowly achieved, reducing wave drag losses. The lower (pressure side) is similar for all the configurations, corresponding to typical supercritical shape which is maintained especially towards the outer part of the span. In fact, as it can be seen from Figs.7.28.d,7.29.d, any aerodynamic performance inefficiencies such as the strong suction peak in the lower section (particularly in the compromise and minimum weight designs), are due to the structural deformation (especially torsional) which increases the washout accelerating the flow locally in the lower leading edge section and not the airfoil shape itself. The torsional deformation of the ASO formulation (7.29.d) is higher than the MDF-based one (7.20.d), which follows the previous discussion on how the MDF configurations were stiffer than the ASO ones. It is also evident, that even the minimum weight configuration has a reasonably efficient airfoil shape (something not observed in the MDF formulation), with the resulting C_p distribution not involving strong shock waves. Furthermore, the decrease of the system level dimensionality associated with ASO, proved beneficial for the aerodynamics discipline, with the surrogate based framework now being more efficient in designing the aerodynamic surfaces. All the configurations offer a similar upper section — particularly near the root which is less affected by structural displacements (7.29.a) — as the optimisation framework has identified the main drag reduction mechanism. The pressure is decreased gradually until it reaches the critical C_p value followed by a shock wave of reduced intensity. This is not the case however for the compromise and minimum weight design which still experience strong shocks in the inner span. Nevertheless, the outer span is more efficiently designed, with the compromise configuration sharing an almost identical upper section C_p distribution with the minimum drag configuration.

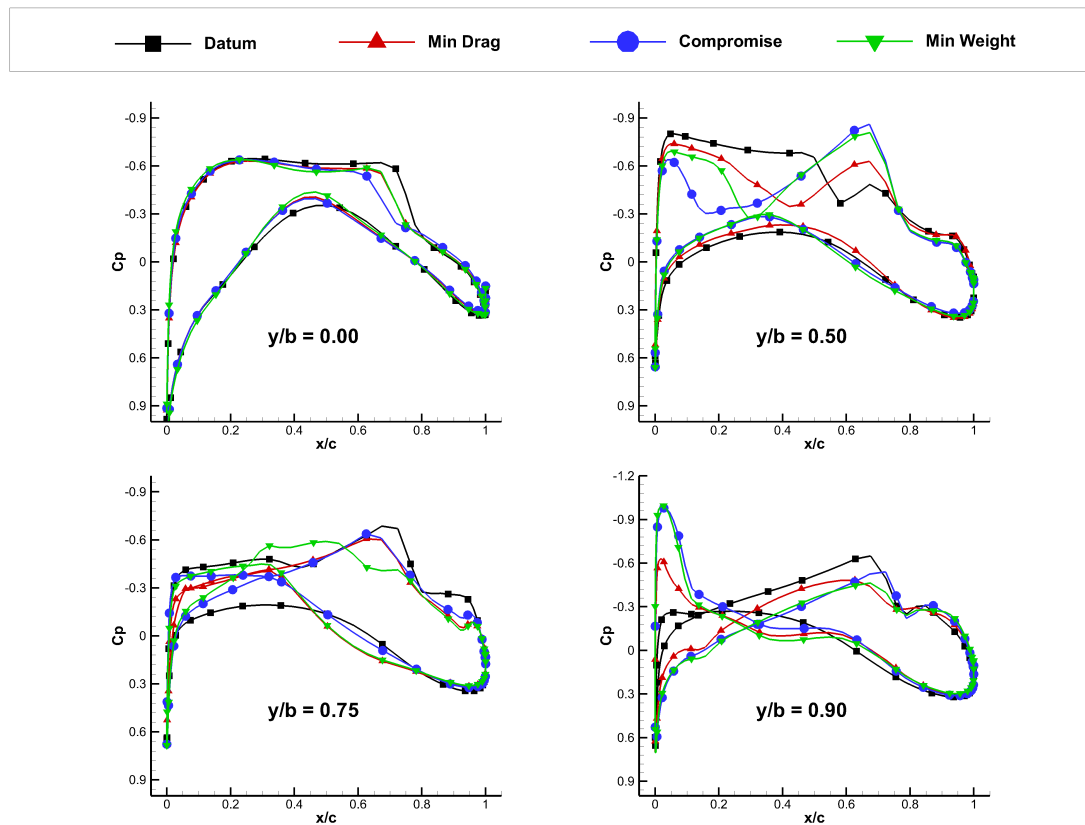


Figure 7.28: Pressure distribution of the datum, minimum drag, minimum weight and compromise design in different locations across the span, ASO formulation.

Despite the configurations being structurally sized on a 2.5g maneuver and displaying similar vertical displacements in these conditions, their corresponding bending deformations during cruising conditions are different. The trend observed under cruise loading is the same as the one observed in the MDF formulation, in which the minimum drag configuration was the stiffest with the minimum weight design experiencing the maximum displacements. This suggests that the structural behaviour in conditions far from the ones for which the structures were sized, is dependent more on the global variables than the local ones (wingbox rather than elements' thickness). If formulated in optimisation terms, the above states that the global variables (through system level) are exploring the multiobjective problem, while the local variables are important for the satisfaction of the (structural) constraints. This is why during the cruise conditions that provide the objective function values, the proposed system level optimisation framework behaves as expected and described in Chapters 3-6, confirming its multiobjective exploration attributes (as in the MDF case).

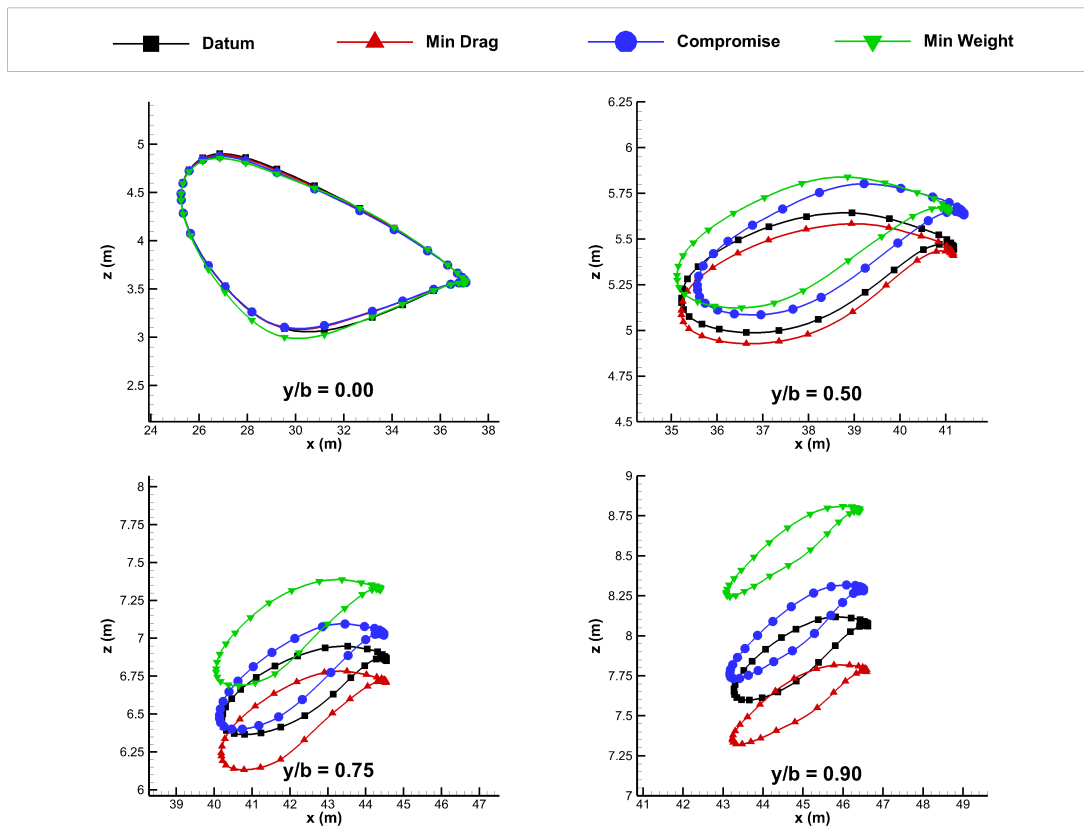


Figure 7.29: Wing sections of the datum, minimum drag, minimum weight and compromise design in different locations across the span, ASO formulation.

Similarly to the MDF case, the (jig) sweep for all configurations (datum, minimum drag, compromise, minimum weight) are provided in Fig.7.30, accompanied by surface pressure distribution. In this particular formulation case — being characterised by the limited number of system level variables — the sweep in all pareto front configurations is almost identical to the one in the datum design. That is particularly true in the minimum drag and compromise design, with the minimum weight configuration once showing the lowest sweep angle.

7.5 Comparison between the Formulations

Although implicitly compared in the previous section, it is helpful to provide further and more direct comparison between the results of the MDF and ASO formulated problems. This involves the comparison of the pareto fronts generated, as well as some further physical insight in the form of the lift distribution.

Regarding the pareto fronts generated by the two architectures, a lack in terms of objec-

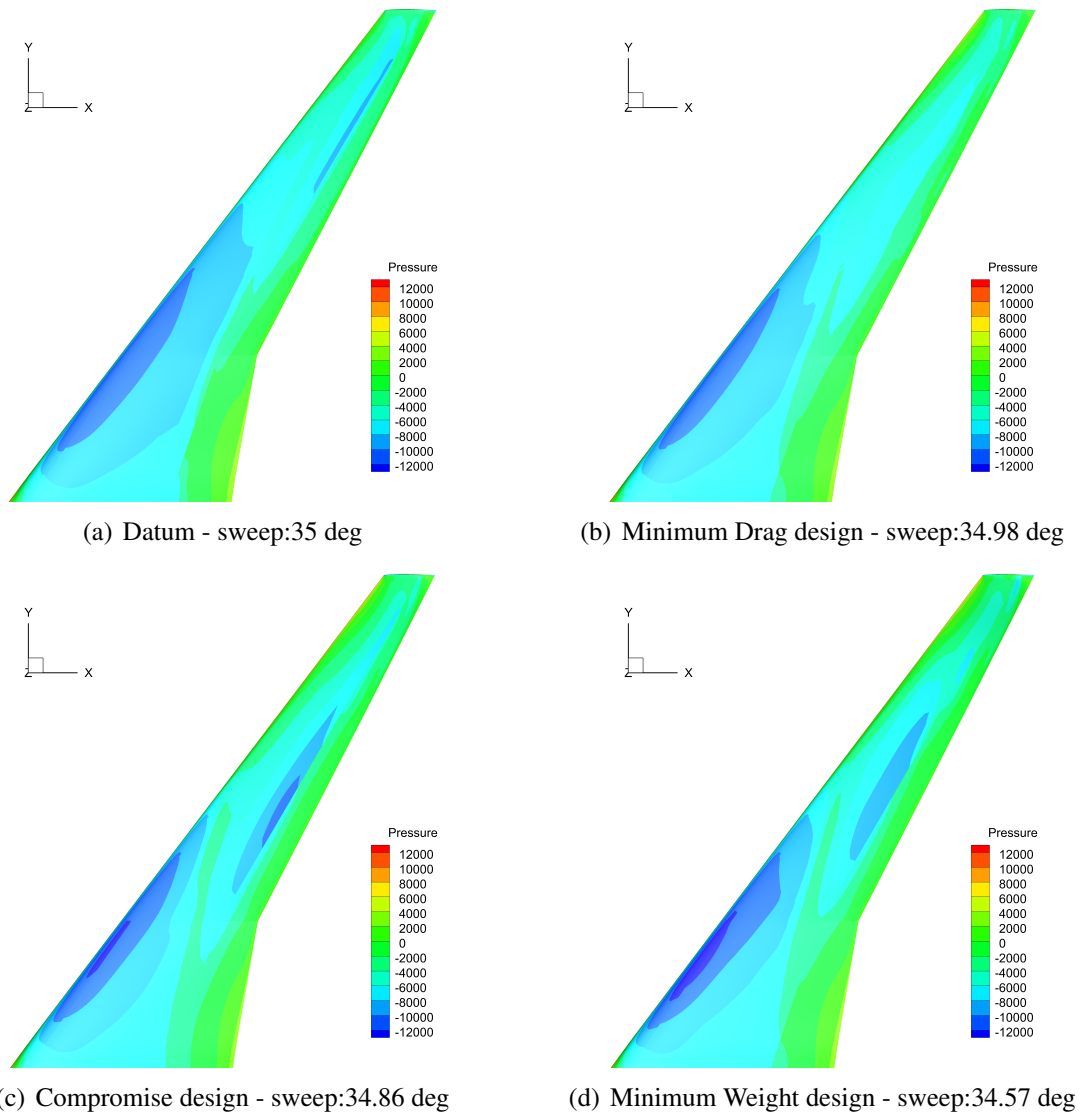


Figure 7.30: Pressure distributions - Planform view and sweep angle, ASO formulation.

tive space exploration is evident in the ASO architecture. This objective space exploration reduction was observed in the ASO formulation case in Fig.7.22 for both the HF and the MF formulation. It is attributed to two factors associated with the MDO architecture²³: Firstly, the global variable design space is reduced, with the objective space extent being consequently decreased. However, more significant is the effect of the structural sizing. The drastic weight reduction leads to drag savings through beneficial interdisciplinary coupling, which was not exploited in its full potential with the MDF formulation due to the higher dimensionality — which deteriorates the quality of the surrogate models. Therefore, the narrower pareto front is a result of a more efficient optimisation formulation. The pareto front convergence characteristics of the ASO case is qualitatively similar to that of the MDF, but displaying a greater improvement with respect to its initial value. This is a result of the reduced dimensionality of the system level in the case of the ASO, making the metamodels more efficient, while requiring fewer HF analyses during the initial sampling. It should be noted that since their datum points are not identical (because of the structural sizing acting also in the datum in the ASO formulation), the curves should be compared only in a qualitative manner — the actual hypervolume indicator values (shown in Fig.7.32) being incomparable.

Nevertheless, from Fig.7.31 it is fairly obvious that ASO dominates over MDF in terms of final values and range performance. What is more interesting however is to take a more careful look to reveal some details and reasons behind this. First of all, the significant improvement of ASO over MDF is the structural weight reduction due to the structural sizing. Furthermore, a small drag decrease is observed in the pareto set of the ASO formulation. This is the result of the reduced dimensionality of the system level optimisation problem which allows the surrogate based framework to minimise drag more efficiently. More importantly however, it is due to the interdisciplinary effect between aerodynamics and structures. With the significant decrease of the weight — through the efficient disciplinary optimisation — and the cruise constraint $L = W$, the required lift is decreased as well. As a result, the drag generated is also reduced, since lower lift requirements allow for decreased wave drag (and induced drag as well)²⁴. It should be mentioned though, that the drag reduction is not sufficient to maintain the same level of L/D as in the MDF cases. An MDO architecture that would involve aerodynamics disciplinary optimisation might be able to maintain or even improve L/D levels. Nevertheless, despite the decrease in aerodynamic efficiency the range is increased due to the structure weight reduction (see Breguet equation in Eq.7.2.4). Typical range increase is in the range of 6% – 14% between analogous pareto points. This shows the importance of interdisciplinary synergies for an efficient aircraft design. In addition, the significance of MDO is supported by the fact that in the ASO results (as in the MDF results), the highest range is achieved by a tradeoff design. This underlines the findings of the respective literature — as well as this work's — that to maximise aircraft performance, the design should not be driven simply by optimising one

²³Of course, the multifidelity formulation as well as the surrogate based optimisation plan being an explorative one are also contributing, as discussed in previous chapters. However, here the effect of the architecture alone is discussed.

²⁴Remember however that airfoil lift is only a part of wave drag "sources", the other being of course the shape and thickness of the airfoil, controlled by the global variables.

discipline but by appropriate synergy mechanisms between the disciplines.

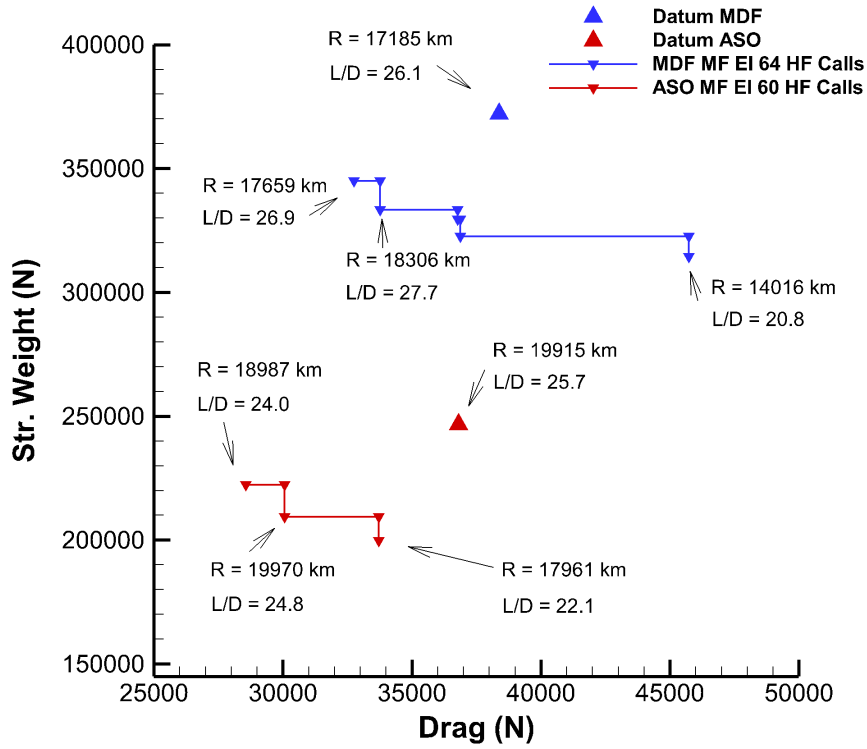


Figure 7.31: Comparison between the pareto front generated using the MDF and the ASO formulation.

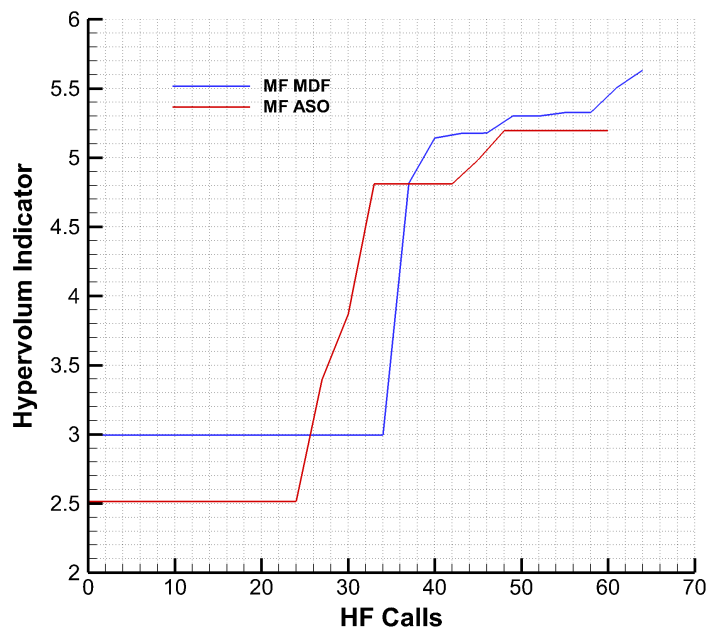


Figure 7.32: Comparison between the convergence of pareto front generated using the MDF and the ASO formulation using the hypervolume indicator.

Another way to view the multidisciplinary design approach and compare it against the "conventional" aerodynamics-led approach is through spanwise lift distribution. In this view, the elliptic lift distribution is compared against the distribution used by the tradeoff design of each MDO approach²⁵. The findings are in agreement with the conclusions of other researchers [3], since the MDO-based configurations do not use an elliptic lift distribution. In fact, the trend of inwards loads shifting is apparent. Shifting the aerodynamic loads towards the root allows for a more efficient (lighter) structural design. As shown by various researchers, as well as in this work (Figs.7.13,7.22), the efficiency of the complete aircraft system (e.g. range) is maximised when both disciplines interact beneficially and not when one of these is optimised. In this sense, the MDF/ASO lift distributions do not correspond to an aerodynamic optimum, but the structural gains which they allow (as explained above) make the overall design superior. In terms of comparison between the two formulations, it was somewhat expected that ASO — being a more structure-focused and structurally efficient approach — would point more to this inward load shifting MDO design direction than MDF. The system level guides the multidisciplinary process in such inner span loaded designs, so that the disciplinary optimisation (structural sizing) can maximise the structure weight reduction, a fact that eventually leads to the superiority of ASO proposed configurations over the MDF ones.

²⁵The lift distributions are normalised with the maximum sectional lift of each case. Therefore, any consideration or assumptions based on the cases' total lift should not be made as the distribution is provided in Fig.7.33 only for a qualitative comparison. Furthermore, the total lift differs between the two MDO cases because of the different aircraft weight.

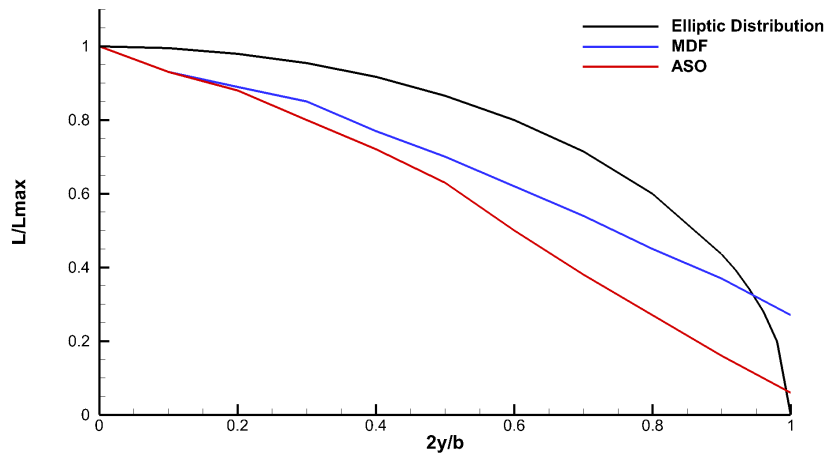


Figure 7.33: Comparison between the normalised lift distribution resulting from the MDF and ASO formulations and that of the aerodynamic optimum.

7.6 Summary

Representing a typical complex and costly industrial wing design application, the Common Research Model was used as the multidisciplinary design test case of this chapter. The purpose of this test case was two-fold: to demonstrate how an effective methodology like the proposed can be applied for aerostructural design in the conceptual to preliminary stage and also to assess its performance within an multidisciplinary feasible and an asymmetric subspace optimisation architectures. The problem proved to be very sensitive in the satisfaction of the challenging range and especially cruising constraints, with cheap radial basis functions models used with a penalty method not being accurate enough to tackle the problem. The use of our more expensive but conservative feasibility constraint handling approach was required as well as the use of a Kriging error correction model. The results highlight the necessity of interdisciplinary studies and the advantage of multifidelity tools especially in the early stage of the optimisation process. Unfortunately, the results cannot provide a conclusive proof as to whether or not the benefits of the multifidelity formulation overcome the ones of the — less complicated — high fidelity formulation. The major drawbacks include the sensitivity of the method's performance in the low fidelity tool itself, the seemingly superiority of the high fidelity results in the stages that would follow this optimisation process and the reduced robustness, since the method fails to be consistently superior in all the test cases examined. Following the study of the impact of the multidisciplinary formulation, the asymmetric subspace optimisation architecture was found to be a noteworthy improvement over the multidisciplinary feasible approach in every aspect. This was due to the increased efficiency of the — lower dimensionality — system level optimisation, as well as the significant structural weight reductions achieved through the structural sizing disciplinary optimisation process.

Conclusions and Future Work

*There is no trap so deadly as the trap
you set for yourself.*

Raymond Chandler

EVENTUALLY, the work being conducted is summarised and compared against the aims and objectives of the thesis as well as the contributions to knowledge as originally presented in Chapter 1. It also provides a comprehensive summary of the findings of this research, demonstrating its success in covering the research questions. Finally, some applications and ideas for further development in the field are suggested. These are concepts relating to the core of this work that are not implemented in this methodology but would provide interesting research directions.

8.1 Summary

Following the increasing demand for air travel and the subsequent fuel emissions increase, strict international environmental regulations and goals have been set highlighting the need for novel and more efficient aircraft configurations.

Such new design approaches of course have to be supported by reliable and efficient design tools. One of the novel ways to get a step-like design improvement is multidisciplinary design. In particular, designing an aircraft wing using no leading discipline — traditionally aerodynamics served that role — but using a coupling of all the disciplines involved and their interaction, has shown to attain a better overall performance.

Supporting research needs for a new generation of tools for multidisciplinary design, *this work suggested an optimisation methodology specifically developed for such multi-*

disciplinary applications. More specifically, an effort was put to provide an *algorithm computationally efficient in the conceptual design stage since this is associated with the development of the much needed novel configurations.* Furthermore, early development stages provide more design freedom so that *advantage of the interdisciplinary synergies can be taken.*

Therefore, the optimisation methodology specifications set in the beginning of the PhD involved:

- Design space exploration attributes appropriate for the conceptual stage
- Maximisation of design feedback to support decision making
- Appropriate multidisciplinary formulation
- Computational efficiency for problems associated with expensive analysis

The above specifications were treated using the following concepts:

Design exploration and cost reduction through surrogate based optimisation: The expected improvement surrogate based optimisation plan which balances global exploration and exploitation has been used to guide the optimisation process within the methodology developed. This approach requires an estimation of the mean squared error of the surrogate model, which can be provided in gaussian-based metamodels. As such, Kriging was used.

Cost reduction through multifidelity approach: The reduction of computational cost was further achieved by using multifidelity data to train the surrogate model. In particular, since in its standard formulation the ordinary Kriging method cannot exploit data of variable fidelity, it was decided that it had to be modified accordingly. Co-Kriging was not used as it was evident from early on in the research that it would be too costly in realistic industrial applications that involve more objective and constraint functions, also scaling badly with dimensionality. As a result, a lot of research effort during this PhD thesis was put into modifying the ordinary Kriging into a multifidelity version of it. This was achieved by using a gaussian kernel-based Radial Basis Functions or a Kriging error correction metamodel, also correcting the formulation of the mean squared error, necessary for the surrogate based optimisation plan.

Maximise design feedback through multiobjective formulation: This optimisation methodology was formulated in a way that can handle multiobjective problems, so that the maximum amount of information is provided to the engineer to support decision making. The infill sampling criterion was specifically defined to reduce cost arising from expensive analysis problems, by promoting parallel infill sampling analyses and the use of the estimate of the low fidelity tool error.

Multidisciplinary design optimisation: Ultimately, the developed methodology was implemented in multidisciplinary architectures, providing an all-inclusive numerical framework for complex multidisciplinary conceptual design optimisation studies.

The challenges met during the development of this tool were tackled by a step by step development, validation and assessment of the methodology. In other words, the objectives described in Chapter 1 (reproduced here in italics), were satisfied through the following:

- *Use a surrogate based optimisation plan to reduce the analysis-related computational costs, taking advantage of the low dimensionality of the conceptual design studies.*

This was supported by the use of 1D, 2D and variable dimensionality test functions which allowed the development and assessment of the surrogate based optimisation plan and the quantification of the cost reductions.

- *Develop a multifidelity method to further decrease computational costs while still providing high fidelity results that correspond to a preliminary design stage.*

The multifidelity plan was developed and tested in multifidelity variations of these test cases, providing an initial estimate of the cost reduction to be expected.

- *Evaluate the effect of the low fidelity analysis tool in the convergence and cost attributes of the developed optimisation methodology.*

The effect of the low fidelity tool approach and its respective error, as well as the constraint handling method used were evaluated in an industrially relevant airfoil design problem.

- *Adjust the methodology into a multiobjective formulation so that it can be used for design problems that involve conflicting objectives.*

- *Assess and improve the methodology using a series of analytical and aerospace-related test cases.*

The efficiency of the multiobjective formulation of the developed methodology was assessed in aerodynamic design problems, with the tool being ultimately exploited in a multiobjective wing aerostructural design study.

- *Embed the method within a greater multidisciplinary design and optimisation formulation and demonstrate the capabilities of the complete multidisciplinary optimisation methodology in the aerostructural design of a transonic wing configuration.*

- *Compare and assess the use of different multidisciplinary architectures that are suitable for aerostructural optimisation.*

The aerostructural design of a transonic wing configuration (common research model) was used as a demonstrator of the methodology's capabilities in tackling expensive problems as well as being effectively combined with state of the art multidisciplinary

architectures. The efficiency of these architectures specifically for aerostructural design problems was also examined. In particular, the multidisciplinary feasible and asymmetric subspace optimisation formulations were used.

8.2 Conclusions

The satisfaction of the original aim and objectives of this PhD work through the above described methodology and development process, led to a series of conclusions and thoughts regarding the scientific topics involved, as well as the attributes of the methodology in particular. These are probably best described and understood when classified in categories. Additionally, for the reader's convenience they follow the course of the objectives, displaying how the goal of the PhD has been achieved: a robust and computationally efficient multidisciplinary design tool has been developed, able to provide a set of design directions to support early stage decision making towards a new generation of aircraft.

8.2.1 Surrogate Modelling for Multifidelity Optimisation

The modification of the ordinary Kriging model was visually assessed in 1D and 2D cases to ensure that its behaviour was the one originally intended prior to its development. Indeed, these test cases show that the modification of the ordinary Kriging into its multifidelity version succeeds in improving the design space representation in the presence of two levels of fidelity (see section 4.1.1 and 4.1.2). The local minimum regions associated with the low fidelity tool in the Branin test function were not present in the modified Kriging's represent of the design space. The latter could provide a close approximation of the high fidelity design space (see Fig. 4.3 and 4.4).

As discussed in detail in Chapter 3, a modification of the mean squared error and the expected improvement formulation had to be performed, to accommodate multifidelity data when used with modified Kriging. It was achieved that low fidelity points were no longer associated with zero expected improvement. The optimisation framework could now visit areas near low fidelity data, which in cases might prove to be regions of improvements.

The performance of the modified Kriging was assessed using a series of comparisons against its equivalent, Co-Kriging. In the scalable Rosenbrock problem, the modified Kriging was proven more robust than Co-Kriging. It showed better improvements and the ability to handle problems of higher dimension than Co-Kriging which failed in cases involving more than eight design variables. The simple unconstrained aerodynamic design problem revealed that Co-Kriging was by 3.1% more effective in terms of final results. However, this approach was significantly more expensive, as well as not efficient in more complicated and realistic problems like the constrained and multiobjective design cases. In these cases,

the developed modified Kriging was superior both in terms of objective function reduction, by 8.4% and pareto front exploration, as well as cost. Cost savings become significant when the number of required surrogate model increases, as in multiobjective or constrained cases. Especially when a radial basis function model is used instead of Kriging as an error correction model in the modified Kriging, the cost improvements are even larger. In these cases, the cost of the modified Kriging is only marginally higher than that of an ordinary Kriging but significantly lower than that of Co-Kriging. Overall, it can be concluded that even for problems involving 16 design variables, the error correction was more efficient when an radial basis function was used instead of kriging model — if the error space is smooth — making modified Kriging superior to Co-Kriging.

8.2.2 Multifidelity Tools in Surrogate Based Optimisation Formulation

The performance of the multifidelity approach against the equivalent high fidelity optimisation methodology was evaluated in all of the examined test cases. Simple — in terms of dimensionality — test cases like the Branin and the Sellar function showed that equal function value reduction can be attained, but with a decrease in the required number of high fidelity analyses. Similar trends were observed in the aerodynamic design test cases. In the unconstrained formulation, the multifidelity and high fidelity methods shared results of almost equal aerodynamic performance, with the proposed multifidelity approach achieving a reduction of 70% in computational expenses. This pattern was also observed in the constrained case with a slightly more moderate cost gains of 50%. In most of the multiobjective aerodynamic design cases (see Chapter 5 and 6), the multifidelity formulation attained similar objective space exploration capabilities with the high fidelity approach, but requiring a reduced computational budget. The overall gain when using a multifidelity method is analogous to the analysis cost and was found to be dependent on the complexity of the problem and whether or not a multiobjective formulation was used. Computational cost reductions were significant in the unconstrained cases, but were decreased in complicated multiobjective problems, particularly in aerodynamic shape design.

Despite all the different cases examined throughout this PhD thesis, unfortunately there is yet to be a conclusive proof that the multifidelity is a universally superior to a high fidelity approach, especially without the compromise of the quality of the final results in problems of industrial complexity. It was seen that the multifidelity approach can indeed provide design improvements earlier in the optimisation study, but the final results are not always superior to the ones of the high fidelity approach, as the method did not provide consistent results in all of the test cases examined in this PhD thesis. Furthermore, a superiority of the method is secured only when the low fidelity tool is cheap, robust and can consistently predict the trend of the high fidelity tool throughout the design space. If such conditions are not secured, then the multifidelity approach might provide inferior results since even if the cost is similar, the pareto front can also be less dense.

Following this, the effect of the cost and accuracy of the low fidelity tool was investigated. As such, two different low fidelity tools based on partially converged RANS simulations were used as this allowed control over their cost, accuracy and induced randomness. Furthermore, a reduced physics tool (VGK) was also employed to assess the effect of cost and consistency of the low fidelity analysis. It was observed that even when a bad low fidelity tool is used — that is one that does not share trends similar to the high fidelity tool — the methodology could still locate design improvements. However, the deliberate randomness introduced in the form of a completely unconverged RANS simulation was reducing the efficiency of the multifidelity optimisation. The error space was no longer smooth and more high fidelity calls were required to correct the error prediction model. On the other hand, both partially converged RANS and VGK low fidelity analysis cases were following the trends of the high fidelity tool in a consistent manner. This was the foundation of the success of the multifidelity approach.

Furthermore, the importance of the accuracy scope of a low fidelity tool was also revealed, especially in multiobjective design and objective space exploration studies. VGK being a reduced physics tool offers a narrow operational range and as such when its limits are exceeded the error correction process becomes more challenging. This translated to a reduction in the exploration capabilities of the multiobjective multifidelity framework.

Finally, regarding the use of a surrogate based approach in general, it is evident that it has its own application limitations, the most profound being its use in the conceptual stage where the design is represented by the few and dominant design variables. Even in this conceptual stage however, the need for consistent low fidelity and high fidelity tools might prove to be too restricting for practical situations. What is more, the multifidelity approach raises the issue of securing consistent geometry parameterisation (or defining a potential mapping between a low fidelity parameterisation and a high fidelity parameterisation) so that the same set of design variables is kept. This might be easier towards the end of the conceptual stage and even early preliminary stage, where the low and high fidelity analysis might share more similarities than it does very early in the conceptual stage¹.

8.2.3 Multiobjective Formulation

The multiobjective exploration attributes of the developed methodology were assessed by a comparison against benchmark multiobjective gradient free optimisers and the currently standard multiobjective expected improvement infill strategy. In the aerodynamic design problems, the methodology was compared against our inhouse implementation of the multiobjective particle swarm optimisation and the multiobjective tabu search optimiser. Evidently, the high fidelity and multifidelity methodologies were superior to both gradient free optimisers in terms of objective space exploration as well as optimum values especially in the case of the multiobjective particle swarm optimiser. A significant reduction on compu-

¹As we progress in the design stage, the analysis tools increase their complexity and fidelity.

tational costs was also achieved. Similar observations were made by the comparison of the proposed multiobjective infill method against the current multiobjective expected improvement approach of section 3.3.7. The developed method could provide a wider pareto front in a lower computation budget.

8.2.4 Surrogate Based Optimisation Plan

The success of the expected improvement surrogate based optimisation plan to provide design space exploration as required for conceptual design, was partly evaluated by a direct comparison against the trust region surrogate based optimisation plan. No hard conclusions could be withdrawn as the results were case-dependent. As a trend however, it was found that in lower dimensionality cases and in the mid-lift region of the pareto front, the trust region performed better than the expected improvement approach. The latter however was dominant in the high lift area especially in the higher dimensionality problem. This suggest it indeed performs a more extended design space exploration than trust region but suffers in locally exploiting design information.

8.2.5 Handling Constraints

Regarding the methods used to tackle the constraints, the proposed methodology was tested with both the general method of hard penalties, as well as the probability of feasibility which is limited to surrogate based optimisation frameworks. The penalty method offered a reduction in the training costs of the constraint functions metamodels since only the constraint value prediction was required and cheap radial basis functions could be used. However, cost savings came in the expense of accuracy. The penalty method was not effective into steering the optimisation process towards feasible designs during its initial stages, partly because of its nature and partly because of the cheaper metamodels. Nevertheless, the final results — when feasible — were superior to the ones provided by the feasibility method. The latter demanded the use of Kriging models, which made the constraint approximation more expensive but also more accurate. This was reflected in the convergence history, with design improvements being almost always feasible. Robustness in terms of feasibility success is also an inherent result of the formulation of the method which seeks for a tradeoff between improvement and feasibility. Penalty method led to infill points for which the predicted constraints were always active. Therefore, it was proved more dependent on the accuracy of the constraint model but were more suitable for an aggressive optimisation in which only the final result is of use. If feasible designs have to be ensured during the process, the feasibility method is recommended.

To complete this section of conclusions regarding the handling of the constraints, some more general thoughts on the constraints satisfaction should also be provided. The multifidelity surrogate model-based framework proposed, also affects the satisfaction of con-

straints in the context of the design stage of their application. If the constraints are not considered as "hard constraints" but allow a tolerance, then an optimisation method can provide useful information to support the design even if a subset of the suggested configurations are — within a tolerance — infeasible. This forms yet an additional argument supporting the application of the methodology to conceptual and early preliminary stage design. In such stages the constraints are not yet hard; what is more important is extracting design information through the optimisation study.

8.2.6 Multidisciplinary Architectures

The formulation of the optimisation tool is complete when the methodology is implemented in a multidisciplinary optimisation architecture. This was initially performed in the Sellar test function, followed by the industrially relevant complex transonic wing aerostructural design problem. The purpose of these investigations was to demonstrate the performance of the method in a multidisciplinary environment and compare two different architectures.

Multidisciplinary Feasible Formulation

The datum wing design was significantly improved both in terms of aerodynamic and structural performance using the multidisciplinary feasible architecture. An increase on the range of the initial design was achieved by an efficient aerodynamic, structural design or a tradeoff between the two. What was of interest was that pareto points did not necessarily led to an increase on the range and the inverse. Depending on the fuel capacity of a wingbox design — described by global variables — a "bad" aerostructural design might display a wider range than a "good" aerostructural design with a small internal wingbox volume. This underlined the necessity of the range constraints defined in the problem, with the ultimate aim being the development of efficient long range aircraft of lower fuel consumption.

Interdisciplinary synergies were easily identified through the multiobjective formulation of this design study. Hence, efficient designs were either supported on aerodynamic, structural performance or their compromise. As expected, aerodynamically inclined designs (with minimum drag) were more rigid, while more flexible designs featured higher stresses as a result of the efficient structural design minimising their weight.

The multifidelity approach proved to be more efficient than the high fidelity one with its results being superior for a given computational budget. The improvement over the high fidelity formulation was greater than the one earlier observed in the less expensive aerodynamic design problems. Such a behaviour was expected however because — for a given smoothness of error space — multifidelity optimisation increases analysis cost savings with the increase of analysis cost.

Asymmetric Subspace Optimisation Formulation

The asymmetric subspace optimisation architecture was selected for examination as it is a very promising formulation particularly for aerostructural problems. This is due to the poor load balancing between the aerodynamic analysis and the structural analysis in the multidisciplinary feasibility approach. The structural sizing is very efficient in reducing the structural weight of the wing through the disciplinary optimisation involving the structural element thickness as local variables.

The conclusions drawn regarding the pareto front results were similar to the multidisciplinary feasible case summarised above. Furthermore, a significant weight reduction was achieved through the structural sizing process. The design of the structural elements was very efficient since the maximum allowed Von Mises stress was observed in almost the entire structural model for all the pareto configurations. Similarly, all pareto designs had — essentially — the same vertical displacement under a 2.5g maneuver. During cruise conditions, which were responsible for the objective function values, the same trend as in the multidisciplinary feasible formulation was observed: the minimum drag design was the stiffest with the minimum weight one displaying the maximum vertical displacement. As in the multidisciplinary feasible architecture, the maximum range was achieved by a tradeoff configuration, highlighting the necessity of interdisciplinary coupling and compromises.

8.2.7 Multidisciplinary Architecture Comparison

The Sellar function offered a computationally inexpensive comparison between the multidisciplinary feasible and the asymmetric subspace optimisation architectures. Evidently, the decoupling of the optimisation process benefited the overall convergence rate, due to a dimensionality reduction in each optimisation level. However, it was stressed that this is strongly dependent on the analysis cost of the discipline under disciplinary optimisation.

This fact was verified in the aerostructural case in which both the cost and results of the asymmetric subspace optimisation were clearly improved over the ones from the multidisciplinary feasible architecture. Since a structural analysis was significantly cheaper than an aerodynamic analysis, a structural optimisation — especially by a dedicated and well developed gradient based optimisation tool — would not greatly increase the cost of a multidisciplinary analysis. The superiority of the asymmetric subspace optimisation formulation was then based on the reduction of the system level dimensionality, having a positive effect particularly in surrogate based optimisation methodologies.

8.2.8 Summary of conclusions

The above sections provided a description of the conclusions based on each scientific topic investigated or used in this work. Following the same order as above, a brief bullet-point list for quick reference is provided:

- The multifidelity Kriging modification provided a robust approximation of the high fidelity design space, avoiding the representation of low fidelity optimality regions.
- The multifidelity modification of the mean squared error of the multifidelity Kriging model was successful in restoring a non-zero expected improvement value in low fidelity data.
- The multifidelity Kriging modification was computationally cheaper as well as more effective in terms of final results than Co-Kriging for all complex test cases.
- The multifidelity approach was efficient when the low fidelity tool was cheap, robust and able to follow the trends of the high fidelity one through the entire design space.
- The multifidelity approach-related gains were reduced as case complexity increased, especially in multiobjective problems.
- Surrogate based multiobjective optimisation led to significantly wider pareto sets than gradient free multiobjective algorithms, but not as dense.
- The trust region surrogate based optimisation plan was superior to the expected improvement approach in low dimensionality problems, but the opposite was found in high dimensionality cases where the expected improvement also performed a wider design space exploration.
- The penalty method for handling constraints was aggressive and more effective in terms of final results compared to feasibility method, which in turn — being more conservative — featured a higher constraint satisfaction ratio.
- The aerostructural optimisation of the common research model showcased the multidisciplinary design optimisation gains through interdisciplinary synergy, particularly in the tradeoff pareto design.
- The aerodynamic loads of the multidisciplinary optimised design were shifted inwards compared to the theoretical aerodynamic optimum, especially when the asymmetric subspace optimisation formulation was used.
- The asymmetric subspace optimisation architecture was superior to the multidisciplinary feasible formulation in all aspects like cost and performance.

8.3 Future Work

8.3.1 Dimensionality Reduction

Given that the proposed methodology involves Kriging models which have to be trained, information on the significance of a design variable is available with no additional cost through the values of the smoothness parameters. Thus, the smoothness parameters of the objective function and constraint models can form a criterion to decide whether the respective design variables are important for the optimisation or if they can be dropped to reduce cost and improve the final results.

8.3.2 Kriging Training Frequency

Since the training of the Kriging models is an expensive process, a set of criteria may be exploited to define the frequency of the hypertuning procedure. For instance, Kriging may be trained only after high fidelity infill sampling analyses.

8.3.3 Concept for Hybrid Algorithm - 1

Surrogate based optimisation formulations like the one suggested in this work can be efficient in exploring a low dimensionality design space, guiding the process towards a global optimality region. Contrariwise, gradient based methods may be very efficient in high dimensionality cases (detailed design) but can only guarantee a local fine-tuning. Therefore, a hybrid method able to exploit the best of both worlds will be very effective. A hybrid surrogate based optimisation-gradient based framework to achieve a rapid global convergence can be developed as follows: A coarse initial space filling sampling will provide coarse design space subregions. In each subregion, a local surrogate can be used in conjunction with a local trust region approach. Then, an adjoint-based method can perform the suboptimisation process with the trust radius as a constraint for the line search step. Furthermore, the surrogate accuracy may be enhanced by the use of the derivatives (potentially even including derivatives from the hessian approximation) which are already computed. Hence, several deterministic local optimisation procedures are executed in parallel.

Each dimension of the discretised regions should be in the order of $1/N$ (where N is the number of design variables). This concept, although improving the global search characteristics of both trust region and adjoint-based optimisation cannot guarantee global convergence. An advantage of this however is that it also allows multiobjective optimisation based on local subregion pareto dominance, as well as the incorporation of a multifidelity approach within trust region. The concept is displayed in Fig.8.1.

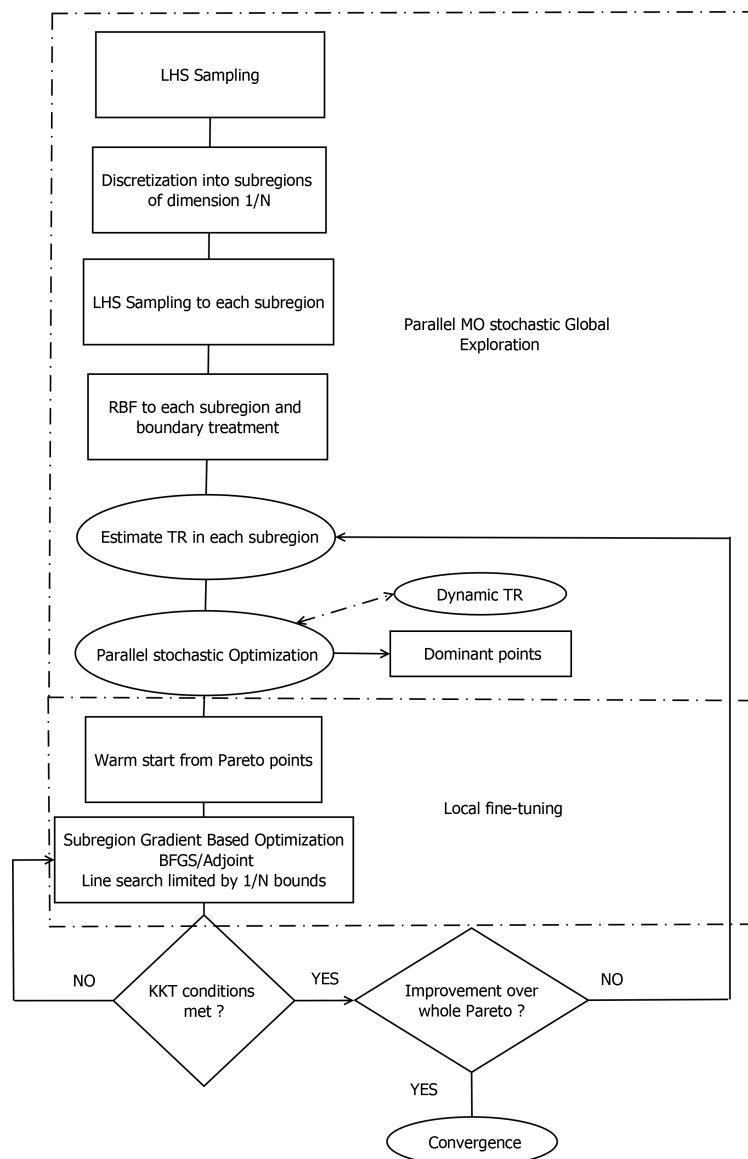


Figure 8.1: Brief overview of hybrid algorithm 1.

8.3.4 Concept for Hybrid Algorithm - 2

Since the developed framework focused in the efficient exploration of the design space, it is only natural that it can be followed by a more local approach. More specifically, the resulting pareto front can simply provide the starting points for a series of parallel more detailed local gradient based optimisation procedures.

8.3.5 Multipoint Optimisation

A topic of great significance in the optimisation field is uncertainty and robustness; that is how can an optimisation process guarantee that the final result has a satisfying off-design performance. Robustness considerations in optimisation may be taken into account through multipoint optimisation. Typically, this is done by running parallel analyses of the additional conditions and performing a weighted summation for the objective function. This is similar to superimposing multiple objectives into a single weighted objective. Hence, multipoint optimisation can be performed as a multiobjective optimisation to produce a pareto front of an objective space with dimensions equal to the conditions under consideration.

8.3.6 Mesh Deformation

A problem that frequently arises in optimisation problems that involve aerodynamic analyses — especially in exploration formulations — is the bad quality of the deformed mesh. A procedure that could alleviate this problem is the following. Before the start of an optimisation process, a mesh validation study may be performed in space filling points of the design space. A series of mesh deformation cases will then be compared to their mesh regeneration equivalent. In cases where a tolerance is surpassed, the mesh deformation would not be considered successful and the corresponding design space area will be reported (a surrogate model of the tolerance can be even created). Therefore, if during the optimisation an infill point close to that area has to be examined, the mesh will not be deformed but will be regenerated. It is an approach loosely similar to how the error correction model is used to decide whether an infill point will use a low or high fidelity analysis in the present work.

8.3.7 Low Fidelity Tool for Aerostructural Optimisation

Throughout this work, it was evident that the success of the multifidelity approach strongly depends on the low fidelity tool characteristics. In particular, the aerostructural analysis of Chapter 7 involved a low fidelity tool that featured the same physics as the high fidelity one with only the computational cost being lower. It is of high interest to examine how a cheaper reduced physics aerostructural tool — like the one from [242] — would affect the convergence of the aerostructural optimisation described in Chapter 7. The expected effect would be observed in total elapsed time costs, high fidelity calls required as well as pareto front characteristics. The challenge in using such reduced physics tools in an aerostructural problem is the necessity of design variables that correspond to both low and high fidelity analysis tools. For instance vortex lattice methods and beam models do not explicitly include thickness distribution and geometrical descriptions as the tools described in Chapter 7 do. A mapping from a set of "low" to "high fidelity design variables" might be necessary.

8.3.8 Bi-Level Multidisciplinary Formulation for Aerostructural Optimisation

Following the success of the asymmetric subspace optimisation architecture, due to its efficient splitting of the optimisation process, a question is raised on the potential effect caused by including an aerodynamic disciplinary optimisation [243]. Of course this should be efficient enough to promote good load balancing. In an opposite case, a Bi-Level formulation may be used for low fidelity points and an asymmetric subspace optimisation architecture for the high fidelity one, since it includes an aerodynamic analysis and not aerodynamic disciplinary optimisation. A particular test case for this would be the analytical one introduced by Sobieski et al. [162].

8.3.9 Alternative Cruising Constraints Formulation in Asymmetric Subspace Optimisation

Following the difficulty faced by the metamodels to faithfully represent the cruising constraints ($L = W$) in the asymmetric subspace optimisation architecture — due to the structural sizing — an alternative method could make the process more efficient. A simple solution while handling this constraint in the system level, would be to include information about the structural (local) variables during the training of the surrogate model; hence creating a hybrid architecture. Alternatively, the ideal solution would be to develop a structural disciplinary suboptimisation procedure (structural sizing) that can handle cruising conditions as well, in the same way it handles the structural integrity considerations. This would have the additional benefit of dropping one surrogate model, thus saving its costs.

8.3.10 Additional Work on the Common Research Model

Since the range uses information from both the aerodynamics and structural discipline, it can be considered as a form of composite multiobjective and multidisciplinary function, in fact being commonly used in this way by researchers [244]. A direct comparison of such a single objective optimisation process against the multiobjective problem provided in Chapter 7 would reveal interesting information regarding the final design characteristics, function values and computational cost.

In addition to this problem formulation, a multiobjective problem of interest and practical use would be the one involving the range and operational/manufacturing cost as the objective functions, with the addition of a total fuel mass limitation as a constraint. Using the drag and the weight as objective functions indeed provided distinctive engineering design directions, however it might be of similar industrial interest to provide a pareto set suggestions based on predicted performance (summarised by range calculations) and

financial estimations.

Bibliography

- [1] "Future of the airline industry 2035" , *ATA's Industry Affairs Committee (IAC)*
- [2] "Flightpath 2050 Europe's Vision for Aviation" , *Directorate-General for Research and Innovation/Directorate General for Mobility and Transport, Report of the High Level Group on Aviation Research*
- [3] Alonso, J.J., and Stanford University MDO Lab, "Multidisciplinary Design Optimization" , *Lecture notes, Stanford University, 2012*
- [4] Sobester, A., Forrester, A.I.J., "Aircraft Aerodynamic Design: Geometry and Optimization" *ISBN 978-0-470-66257-1, John Wiley & Sons Ltd, 2015*
- [5] D., Salomon, "Curves and Surfaces for Computer Graphics", *ISBN 978-0-387-28452-1, Springer, New York, NY, 2006*
- [6] J., Ferguson, "Multivariable curve interpolation" , *Journal of the Association for Computing Machinery, Vol. 11, No. 2, 1964, pp. 221–228*
- [7] Sederberg, T.W., Parry, S.R., "Free-Form Deformation of Solid Geometric Models" , *Association for Computing Machinery, Vol. 20, No. 2, 1986, pp. 151-160, doi:10.1145/15922.15903*
- [8] Lyu, Z., Martins, J.R.R.A., "Aerodynamic Design Optimization Studies of a Blended-Wing-Body Aircraft" , *43rd AIAA Fluid Dynamics Conference and Exhibit, San Diego, California, 24–27 June 2013, AIAA Paper 2013-2586, doi:10.2514/1.C032491*
- [9] Yamazaki, W., Mouton, S., Carrier, G., "Efficient Design Optimisation by Physics-Based Direct Manipulation Free-Form Deformation" , *AIAA paper 2008-5953, Sep. 2008, doi:10.2514/6.2008-5953*
- [10] Samareh, J.A., "Geometry and Grid/Mesh Generation Issues for CFD and CSM Shape Optimisation" , *Optimisation and Engineering, Vol. 6, No. 1, 2005, pp. 21-32, doi:10.1023/B:OPTE.0000048535.08259.a8*
- [11] Coquillart, S., "Extended Free-Form Deformation: A sculpturing Tool for 3D Geometric Modelling" , *Computer Graphics, Vol. 24, No. 4, 1990, pp. 187 - 196, doi:10.1145/97879.97900*

- [12] Hsu, W.M., Hughes, J.F., Kaufman, H., "Direct Manipulation of Free-Form Deformations" , *Computer Graphics*, Vol. 26, No. 2, 1992, pp. 177 - 184, doi:10.1145/133994.134036
- [13] Lamousin, H.J., Waggenspack, W.N., "NURBS-Based Free-Form Deformations" , *IEEE Computer Graphics and Applications*, Vol. 14, No. 6, 1994, pp. 95-108, doi:10.1109/38.329096
- [14] Samareh, J.A., "Aerodynamic Shape Optimisation based on Free-Form Deformation" , *10th AIAA/ISSMO Multidisciplinary Analysis and Optimization Conference*, 30 August - 1 September 2004, AIAA Paper 2004-4630, doi:10.2514/6.2004-4630
- [15] Kulfan, B.M., Bussoletti, J.E., "'Fundamental' Parametric Geometry Representations for Aircraft Component Shapes" , , *11th AIAA/ISSMO Multidisciplinary Analysis and Optimization Conference: The Modeling and Simulation Frontier for Multidisciplinary Design Optimization* 6 - 8 September 2006, AIAA Paper 2006-6948
- [16] Kulfan, B.M., "Universal parametric geometry representation method" , *Journal of Aircraft*, Vol. 45, No. 1, 2008, pp. 142-158, doi:10.2514/1.29958
- [17] Kulfan, B.M., "Modification of CST airfoil representation methodology" , *unpublished note*, <http://brendakulfan.com/docs/CST8.pdf>, Accessed: 7 September 2015
- [18] Samareh, J.A., "Survey of Shape Parameterization Techniques for High-Fidelity Multidisciplinary Design Optimization" , *AIAA Journal*, Vol. 39, No. 5, 2001, pp. 877-884, doi:10.2514/2.1391
- [19] Antunes, A.P., Azevedo, J.A.L.F., Silva, R.G.D., "A Framework for Aerodynamic Optimisation Based On Genetic Algorithms" , *47th AIAA Aerospace Sciences Meeting including The New Horizons Forum and Aerospace Exposition* 5 - 8 January 2009, AIAA Paper 2009-1094, doi:10.2514/6.2009-1094
- [20] Castonguay, P., Nadarajah, S., "Effect of Shape Parameterisation on Aerodynamic Shape Optimisation" , *45th AIAA aerospace sciences meeting, Reno, Nevada, 2007*, AIAA Paper 2007-3837, AIAA Paper 2007-59, 2007
- [21] Mousavi, A., Castonguay, P., and Nadarajah, S.K., "Survey of Shape Parameterisation Techniques and Its Effect on Three-dimensional Aerodynamic Shape Optimisation" , *8th AIAA Computational Fluid Dynamics Conference, Fluid Dynamics and Co-located Conferences*, Miami, Florida, 25 - 28 June 2007, AIAA Paper 2007-3837, doi:10.2514/6.2007-3837
- [22] Sripawadkul, V., Padulo, M., "A Comparison of Aerofoil Shape Parameterisation Techniques for Early Design Optimisation" , *13th AIAA/ISSMO Multidisciplinary Analysis Optimization Conference, Multidisciplinary Analysis Optimization Conferences*, Fort Worth, Texas, 10 -15 September 2010, AIAA Paper 2010-9050, doi:10.2514/6.2010-9050

- [23] Wu, H.-Y., Yang, S., Liu, F., "Comparison of Three Geometric Representations of Aerofoils for Aerodynamic Optimisation" , *16th AIAA Computational Fluid Dynamics Conference, Fluid Dynamics and Co-located Conferences, Orlando, Florida, AIAA Paper 2003-4095*, doi:10.2514/6.2003-4095
- [24] Samareh, J.A., "A Novel Shape Parameterization Approach" , *NASA/TM 1999 209116, NASA Langley Research Center, Hampton, VA 23681*
- [25] Ronzheimer, A., "Prospects of Geometry Parameterisation based on Freeform Deformation in MDO" , *ERCOFTAC 2006: Design Optimisation: Methods and Applications, pp. 1-10, International Conference Las Palmas de Gran Canaria, Spain, ISBN 84-85650-12-3*
- [26] Thomson, J.F., "Handbook of grid generation" , *ISBN 0849326877*
- [27] Samareh, J.A., "Grid Generation for Multidisciplinary Design and Optimization of an Aerospace Vehicle – Issues and Challenges" , *Technical Report, NASA Langley Research Center, Hampton, VA, United States, January, 2000*
- [28] Gaitonde, A.L., Fiddes, S.P., "Three-Dimensional Moving Mesh Method for the Calculation of Unsteady Transonic Flows" , *Aeronautical Journal, Vol. 99, No. 984, 1995, pp. 150-160*, doi:10.1017/S0001924000027135
- [29] Soni, B.K., "Two and Three-Dimensional Grid Generation Internal Flow Applications" , *7th Computational Physics Conference, Meeting Paper Archive, Cincinnati, OH, AIAA Paper, 85-1526, 1985*, doi: 10.2514/6.1985-1526
- [30] Jones, W.T., Samareh, J.A., "A Grid Generation System for Multidisciplinary Design Optimization" , *Surface Modeling, Grid Generation, and Related Issues in Computational Fluid Dynamic (CFD) Solutions, Lewis Research Center, NASA, pp. 657-667, 1995*
- [31] Hartwich, P.M., Agrawal S., "Method for perturbing Multiblock Patched Grids in Aeroelastic and Design Optimization Applications" , *13th Computational Fluid Dynamics Conference, Fluid Dynamics and Co-located Conferences, AIAA Paper 97-2038, 1997*, doi: 10.2514/6.1997-2038
- [32] Le Moigne, A., "A discrete Navier-Stokes adjoint method for aerodynamic optimization of Blended Wing-Body configurations" , *Ph.D. thesis, Cranfield University, 2002*
- [33] Kenway, G.K.W., Kennedy, G.J., Martins, J.R.R.A., "A CAD-Free Approach to High Fidelity Aerostructural Optimization" , *13th AIAA/ISSMO Multidisciplinary Analysis Optimization Conference, Fort Worth, Texas, 10 -15 September 2010, AIAA 2010-9231, 2010*, doi:10.2514/6.2010-9231
- [34] Botkin, M.E., "Three-Dimensional Shape Optimization Using Fully Automatic Mesh Generation" , *AIAA Journal, Vol. 30, No. 5, 1992, pp. 1932-1934*, doi:10.2514/3.11162

- [35] Farhat, C., Lin, T.Y., "Structure-attached corotational fluid grid for transient aeroelastic computations" , *AIAA Journal*, Vol. 31, No. 5, 1993, pp. 597-599, doi: 10.2514/3.11371
- [36] Batina, J.T., "Unsteady Euler airfoil solutions using unstructured dynamic meshes" , *AIAA Journal*, Vol. 28, No. 8, 1990, pp. 1381-1388, doi: 10.2514/3.25229
- [37] Palmerio, B., "An attraction-repulsion mesh adaptation model for flow solution on unstructured grids" , *Comput Fluids*, Vol. 23, No. 3, 1994, pp. 457-506, doi: 10.1016/0045-7930(94)90015-9
- [38] Farhat, C., Degand, C., Koobus, B., Lesoinne, M., "Torsional springs for two-dimensional dynamic unstructured fluid meshes" , *Computer Methods in Applied Mechanics and Engineering*, Vol. 45, No. 1-4, 1998, pp. 163-231, doi: 10.1016/S0045-7825(98)00016-4
- [39] Degand, C., Farhat, C., "A three-dimensional torsional spring analogy method for unstructured dynamic meshes" , *Computers and Structures*, Vol. 80, No. 3-4, 2002, pp. 305-316, doi: 10.1016/S0045-7949(02)00002-0
- [40] Murayama, M., Nakahashi, K., Matsushima, K., "Unstructured Dynamic Mesh for Large Movement and Deformation" , *40th AIAA Aerospace Sciences Meeting and Exhibit, Aerospace Sciences Meetings, Reno, Nevada, AIAA 2002-0122*, 2002, doi: 10.2514/6.2002-122
- [41] Xia, H., Qin, N., "Detached-eddy simulation for synthetic jets with moving boundaries" , *Modern Physics Letters B*, Vol. 19, 2005, pp. 1429-1434, doi: 10.1142/S0217984905009584
- [42] Nielsen, E.J., Anderson, W.K., "Recent improvements in aerodynamic design optimisation on unstructured meshes" , *AIAA Journal*, Vol. 40, No. 6, 2002, pp. 1155-1163, doi: 10.2514/2.1765
- [43] Dwight, R.P., "Robust Mesh Deformation using the Linear Elasticity Equations" , *Computational Fluid Dynamics 2006*, H. Deconinck and E. Dick, eds. Springer Berlin Heidelberg, 2006, pp. 401-406, doi: 10.1007/978-3-540-92779-262
- [44] Crumpton, P.I., Giles, M.B., "Implicit Time-Accurate Solutions on Unstructured Dynamic Grids" , *International Journal for Numerical Methods in Fluids*, Vol. 25, No. 11, 1997, pp. 1285-1300, doi: 10.1002/(SICI)1097-0363(19971215)25:11<1285::AID-FLD607>3.0.CO;2-M
- [45] Liu, X.Q., Qin, N., Xia, H., "Fast dynamic grid deformation based on Delaunay graph mapping" , *Journal of Computational Physics*, Vol. 211, No. 2, 2006, pp. 405-423, doi: 10.1016/j.jcp.2005.05.025
- [46] Beckert, A., Wendland, H., "Multivariate interpolation for fluid-structure-interaction problems using radial basis functions" , *Aerospace Science and Technology*, Vol. 5, No. 2, 2001, pp. 125-134, doi: 10.1016/S1270-9638(00)01087-7

- [47] de Boer, A., van der Schoot, M.S., Bijl, H., "Mesh deformation based on radial basis function interpolation" , *Computers and Structures*, Vol. 85, 2007, pp. 784-795, doi: 10.1016/j.compstruc.2007.01.013
- [48] Sacks, J., Welch, W.J., Mitchell, T.J., and Wynn, H.P., "Design and Analysis of computer experiments" , , *Statistical Science*, Vol. 4 No. 4, 1989, pp. 409-423
- [49] I.M. Sobol, "On the systematic search in a hypercube" , *SIAM Journal of Numerical Analysis*, Vol. 16, No. 5, 1979, pp. 790-793, doi:10.1137/0716058
- [50] Fang, K-T, Lin, D.K.J., Winker, P., and Zhang, Y., "Uniform Design: Theory and Application" , *Technometrics*, Vol. 42, No. 3, 2000, pp. 237-248, doi: 10.2307/1271079
- [51] Tang, A., "Orthogonal Array-Based Latin Hypercubes" , *Journal of the American Statistical Association*, Vol. 88, No. 424, 1993, doi: 10.2307/2291282
- [52] Liem, R.P., Mader, C.A., Martins, J.R.R.A., "Surrogate Models and Mixtures of Experts in Aerodynamic Performance Prediction for Mission Analysis" , *Aerospace Science and Technology*, Vol. 43, 2015, pp. 126-151, doi:10.1016/j.ast.2015.02.019
- [53] J.H. Halton, "On the efficiency of certain quasi-random sequences of points in evaluating multi-dimensional integral" , *Numerische Mathematik*, Vol. 2, No. 1, 1960, pp. 84-90
- [54] Halton, J., "Algorithm 247: Radical-inverse quasi-random point sequence", , *ACM*, Vol. 7, No. 12, pp. 701-702, 1964, doi:10.1145/355588.365104
- [55] Nair, P. B., Choudhury, A., Keane, A.J., "Bayesian Surrogate Modeling of Deterministic Simulation Codes for Probabilistic Analysis", , 19th *AIAA Applied Aerodynamics Conference, Fluid Dynamics and Co-located Conferences*, Seattle, Washington, AIAA-2001-1676, doi:10.2514/6.2001-1676
- [56] Sasena, M., Goovaerts, P., Papalambros, P., and Reed, M., "Adaptive experimental design applied to an ergonomics testing procedure" , , *ASME 2002 International Design Engineering Technical Conferences and Computers and Information in Engineering Conference*, Vol. 2, 28th *Design Automation Conference*, Montreal, Quebec, September 29 – October 2, doi: 10.1115/DETC2002/DAC-34091
- [57] Keane, A.J., Nair, P.B, "Computational Approaches for Aerospace Design: The Pursuit of Excellence" , ISBN-13 978-0-470-85540-9, *John Wiley & Sons Ltd*, 2005
- [58] McKay, M.D., Beckman, R.J., Conover W.J., "Hypercube sampling, A comparison of three Methods for selecting values of input variables in the analysis of output from a computer code" , *Technometrics*, Vol. 21, No. 2, 1979, pp. 239-245, doi: 10.2307/1268522
- [59] Johnson, M.E., Moore, L.M., Ylvisaker, D., "Minimax and maximin distance designs" , *Journal of Statistical Planning and Inference*, Vol. 26, No. 2, 1990, pp. 131-148, doi:10.1016/0378-3758(90)90122-B

- [60] Morris, M.D., Mitchell, T.J., "Exploratory designs for computational experiments" , *Journal of Statistical Planning and Inference*, Vol. 43, 1995. pp. 381-402, doi:10.1016/0378-3758(94)00035-T
- [61] Currin, C., Mitchell, T., Morris, M., Ylvisaker, D., "Bayesian Prediction of Deterministic Functions With applications to the design and analysis of computer experiments" , *Journal of the American Statistical Association*, Vol. 86, No. 416, 1991, pp. 953-963, doi: 10.2307/2290511
- [62] Simpson, T.W., Lin, D.K.J., Chen, W., "Sampling strategies for computer experiments: design and analysis" , *International Journal of Reliability and Applications*, Vol. 2, 2001, pp. 209-240
- [63] Kleijnen, J.P.C., "Statistical Tools for Simulation Practitioners" , *Marcel Dekker, NY*, 1987
- [64] Morris, M.D., "Factorial Sampling for Preliminary Computational experiments" , *Technometrics*, Vol. 33, No. 3, 1991, pp. 161-174, 1991, doi: 10.2307/1269043
- [65] Campolongo, F., Cariboni, J., Saltelli, A., "An effective screening design for sensitivity analysis of large models" , *Environmental Modelling & Software*, Vol. 22, 2007, pp. 1509-1518, doi: 10.1016/j.envsoft.2006.10.004
- [66] Andres, T.H., Hajas, W.C., "Using iterated fractional factorial design to screen parameters in sensitivity analysis of a probabilistic risk assessment model" , *Joint international Conference on Mathematical Methods and Supercomputing in Nuclear Applications*, ed. Kusters, Stein, and Werner, 2, pp. 328-337
- [67] Elster, C., Neumaier, A., "Screening by Conference Designs" , *Biometrika*, Vol. 82, No. 3, 1995, pp. 589-602, doi: 10.2307/2337536
- [68] Jacoby, J.E., Harrison, S., "Multi-variable experimentation and simulation models" , *Naval Research Logistics Quarterly*, Vol. 9, 1962, pp. 121-136, doi: 10.1002/nav.3800090206
- [69] Bettonvil, B., Kleijnen, J.P.C., "Searching for important factors in simulation models with many factors: Sequential bifurcation" , *European Journal of Operation Research*, 1996, pp. 1080-194, doi: 10.1016/S0377-2217(96)00156-7
- [70] Campolongo, F., Kleijnen J., and Andres, T., "Screening methods in sensitivity analysis" , *Mathematical and statistical methods for sensitivity analysis of model output*, ed. A. Saltelli and K. Chan. Chichester, England: Wiley, 2000
- [71] Schonlau, M., Welch, W.J., "Screening the Input Variables to a Computer Model Via Analysis of Variance and Visualization" , *Screening Methods for Experimentation in Industry, Drug Discovery, and Genetics*, Editors: A. Dean, S. Lewis, ISBN:978-0-387-28013-4

- [72] Goldsman, D., Nelson, B.L., "Statistical Screening, Selection, and Multiple Comparison Procedures in Computer Simulations" , *Proceedings of the 1998 Winter Simulation Conference D.J. Medeiros, E.F. Watson, J.S. Carson and M.S. Manivannan, eds.*
- [73] Kleijnen, J.P.C., "Review of random and group-screening designs" , *Communications in statistics: Part A: Theory and methods, Vol. 16, No. 10, 1987, pp. 2885-2900, doi: 10.1080/03610928708829548*
- [74] Trocine, L., Malone, L.C., "Finding important independent variables through screening designs: A comparison of methods" , *Proceedings of the 2000 Winter Simulation Conference, J.A. Joines, R.R. Barton, B. Kang, and P.A. Fishwick, eds., doi: 10.1109/WSC.2000.899789*
- [75] Constantine, P.G., Dow, E., Wang, Q., "Active subspace methods in theory and practice: Applications to Kriging surfaces" , *Society for Industrial and applied Mathematics, Journal on Scientific. Computing, Vol. 36, No. 4, A1500–A152, doi: 10.1137/130916138*
- [76] Lukaczyk, T.W., Constantine, P., Palacios, F., Alonso, J.J., "Active Subspaces for Shape Optimization" , *10th AIAA Multidisciplinary Design Optimization Conference, AIAA SciTech Forum, AIAA 2014-1171, doi: 10.2514/6.2014-1171*
- [77] Grey, Z.J., Constantine, G., "Active Subspaces of Airfoil Shape Parameterizations" , *10th AIAA/ASCE/AHS/ASC Structures, Structural Dynamics, and Materials Conference, AIAA SciTech Forum, Grapevine, Texas, 9 - 13 January 2017, AIAA Paper 2017-0507, doi: 10.2514/6.2017-0507*
- [78] Schmit, L.A., Farshi, B., "Some Approximation Concepts for Structural Synthesis" , *AIAA Journal, Vol. 12, No. 5, 1974, pp. 692-699, doi: 10.2514/3.49321*
- [79] Balabanov, V.O., Giunta, A.A., Golovidov, O., Grossman, B., Mason, W.H., Watson, L.T. and Haftka, R.T., "Reasonable design space approach to response surface approximation" , *Journal of Aircraft, Vol. 36, 1999, pp. 308–315, doi:10.2514/2.2438*
- [80] Kim, C., Wang, S., Choi, K.K., "Efficient response surface modeling by using moving least squares method and sensitivity" , *AIAA Journal, Vol. 43, No. 11, 2005, pp. 2404-2411, doi: 10.2514/1.12366*
- [81] Franke, R., "Scattered data interpolation: tests of some methods" , *Mathematics of Computation, Vol. 38, No. 157, 1982, pp. 181–200*
- [82] Wang, B.P., "Parameter optimization in multiquadric response surface approximations" , *Struct Multidisc Optim Vol. 26, No. 3-4, 2004, pp. 219–223, doi:10.1007/s00158-003-0341-4*
- [83] van Keulen, F., Vervenne, K., "Gradient-enhanced response surface building" , *Structural and Multidisciplinary Optimization, Vol. 27, No. 5, 2004, pp. 337-351*

- [84] Mullur, A.A., Messac, A., "Extended Radial Basis Functions: More flexible and Effective Metamodelling" , *AIAA Journal*, Vol. 43, No. 6, 2005, pp. 1306-1315. doi: 10.2514/1.11292
- [85] Mongillo, M., "Choosing Basis Functions and Shape Parameters for Radial Basis Function Methods" , *Society for Industrial and applied Mathematics, SIAM Undergraduate Research Online (SIURO)*, Vol. 4, doi:10.1137/11S010840
- [86] Fornberg, B., Larsson, E., and Flyer, N., "Stable Computations with Gaussian Radial Basis Functions" , *Society for Industrial and applied Mathematics, Journal on Scientific Computing*, Vol. 33, No. 2, pp. 869–892, doi: 10.1137/09076756X
- [87] Vapnik, V., "Statistical Learning Theory" , *John Wiley & Sons*, 1998
- [88] Forrester, A.I.J., Sobester, A., and Keane, A.J., "Engineering Design via Surrogate Modelling: A Practical Guide" , *John Wiley & Sons*, ISBN 978-0-470-06068-1, 2008
- [89] Wackernagel, H., "Multivariate Geostatistics: An Introduction with Applications" , 3rd ed. *Heidelberg: Springer, Berlin*, 2003
- [90] Joseph, V.R., Hung, Y., and Sudjianto, A., "Blind Kriging: a new method for developing metamodelling" , *ASME, Journal of Mechanical Design*, Vol. 130, No. 3, 2008, doi: 10.1115/1.2829873
- [91] Martin, J.D., Simpson, T.W., "A study On the Use Of Kriging models to approximate deterministic computer models" , *ASME 2003 Design Engineering Technical Conferences and Computers and Information in Engineering Conference Chicago, Illinois USA, 2 - 6 September*, pp. 567-576, 2003, doi: 0.1115/DETC2003/DAC-48762
- [92] Simpson, T.W., Mauery, T.M., Korte, J.J., and Mistree, F. "Kriging models for global approximation in simulation-based multidisciplinary design optimization" , *AIAA Journal*, Vol. 39, No. 12, 2001, pp. 2233-2241, doi: 10.2514/2.1234
- [93] Toal, D.J.J., Bressloff, N.W., and Keane, A.J., "Kriging Hyperparameter Tuning Strategies" , *AIAA Journal*, Vol. 46, No. 5, 2008, pp. 1240-1352, doi:10.2514/1.34822
- [94] Jin, R., Chen, W., and Simpson, T.W., "Comparative studies of metamodelling techniques under multiple modeling criteria" , *Structural and Multidisciplinary Optimization*, Vol. 23, No. 1, 2001, pp. 1-13, doi: 10.1007/s00158-001-0160-4
- [95] Haftka, R.T., "Combining global and local approximations" , *AIAA Journal*, Vol. 29, No. 9, 1991, pp. 1523–1525, doi:10.2514/3.10768
- [96] Kirsch, U., "Reduced basis approximation of structural displacements for optimal design" , *AIAA Journal*, Vol. 29, No. 10, 1991, pp. 1751–1758, doi:10.2514/3.10799
- [97] LeGresley, P.A., Alonso, J.J., "Airfoil design optimization using reduced order models based on proper orthogonal decomposition" , *Fluids 2000 Conference and Exhibit, Fluid Dynamics and Co-located Conferences, Denver, Colorado, 2000*, AIAA Paper 2000-2545

- [98] Jacobs, R.A., Jordan, M.I., Nowlan, S.J., and Hinton, G.E., "Adaptive Mixtures of Local Experts" , *Journal Neural Computation*, Vol. 3, No. 1, 1991, pp. 79–87, doi:10.1162/neco.1991.3.1.79
- [99] Masoudnia, S., Ebrahimpour, R., "Mixture of experts: a literature survey" , *Artificial Intelligence Review*, Vol. 42, No. 2, 2014, pp 275–293, doi:10.1007/s10462-012-9338-y
- [100] Tang, B., Heywood, M.I., and Shepherd, M., "Input partitioning to mixture of experts" , *Proceedings of the 2002 International Joint Conference on Neural Networks*, Vol. 1, IEEE, 2002, pp. 227–232, doi: 10.1109/IJCNN.2002.1005474
- [101] Meckesheimer, M., Booker, A.J., Barton, R.R., and Simpson, T.W., "Computationally Inexpensive Metamodel Assessment Strategies" , *AIAA Journal*, Vol. 40, No. 10, 2002, pp. 2053-2060, doi: 10.2514/2.1538
- [102] Jones, D.R., Schonlau, M., and Welch, W.J., "Efficient Global Optimization of Expensive Black-Box Functions" , *Journal of Global Optimization*, Vol. 13, No. 4, 1998. pp. 455–498, doi:10.1023/A:1008306431147
- [103] Alexandrov, N.M., Dennis, J.E., Lewis, R.M., and Torczon, V., "A trust region framework for managing the use of approximation models in optimization" , *Structural Optimization*, Vol. 15, 1998, pp. 16-23, doi:10.1007/BF01197433
- [104] Jones, D.R., "A Taxonomy of Global Optimization Methods Based on Response Surfaces" , *Journal of Global Optimization*, Vol. 21, No. 4, 2001, pp. 345–383, doi:10.1023/A:1012771025575
- [105] Dennis Jr., J.E., and Schnabel, R.B., "Numerical Methods for Unconstrained Optimization and Nonlinear Equations" , *Prentice-Hall, Englewood Cliffs, NJ, 1983*, doi: 10.1137/1.9781611971200
- [106] Alexandrov, N.M., Lewis, R.M., Gumbert, C.R., Green, L.L., and Newman, P.A., "Approximation and Model Management in Aerodynamic Optimization with Variable-Fidelity models" , *Journal of Aircraft* Vol. 38, No. 6, 2001, pp. 1093-1101, doi:10.2514/2.2877
- [107] Forrester, A.I.J., Keane, A.J., "Recent Advances in Surrogate Based Optimization" , *Progress in Aerospace Sciences*, Vol. 45, No. 1-3, 2009, pp. 50–79, doi:10.1016/j.paerosci.2008.11.001
- [108] Jarrett, J.P., Ghisu, T., "An Approach to Multi-Fidelity Optimization of Aeroengine Compression Systems" , *12th AIAA Aviation Technology, Integration, and Operations (ATIO) Conference and 14th AIAA/ISSM, Indianapolis, Indiana, 17-19 September 2012, AIAA Paper 2012-5634*, doi:10.2514/6.2012-5634
- [109] Choi, S., Alonso, J.J., Kroo, I.M., and Wintzer. M., "Multifidelity Design Optimization of Low-Boom Supersonic Jets" , *Journal of Aircraft*, Vol. 45, No. 1, 2008, pp. 106-118, doi: 10.2514/1.28948

- [110] Chung, H.S. , Alonso, J.J., "Design of a Low-Boom Supersonic Business Jet Using Cokriging Approximation Models" , 9th AIAA/ISSMO Symposium on Multidisciplinary Analysis and Optimization, Atlanta, Georgia, 2002, AIAA 2002-5598, doi: 10.2514/6.2002-5598
- [111] Forrester, A.I.J., Bressloff, N.W., Keane, A.J., "Optimization using Surrogate Models and Partially Converged Computational Fluid Dynamics Simulations" , *Proceedings of the Royal Society A: Mathematical, Physical and Engineering Sciences*, Vol. 462, No. 2071, 2006, pp. 2177-2204, doi:10.1098/rspa.2006.1679
- [112] Nelson, A., Alonso, J.J., Pulliam, T.H., "Multi-Fidelity Aerodynamic Optimization using Treed Meta-Models" , 25th AIAA Applied Aerodynamics Conference, Miami, Florida, 25 - 28 June 2007, AIAA 2007-4057, doi: 10.2514/6.2007-4057
- [113] Bandler, J.W., Biernacki, R.M., Chen, S.H., Grobelny, P.A., and Hemmers, R.H., "Space mapping technique for electromagnetic optimization" , *IEEE Transactions on Microwave Theory and Techniques*, Vol. 42, No. 12, 1994, pp. 2536–2544, doi:10.1109/22.339794
- [114] Bandler, J., Cheng, Q., Dakrouy, S., Mohamed, A., Bakr, M. and Madsen, K., "Space Mapping: the state of the art" , *IEEE Transactions on Microwave Theory and Techniques*, Vol. 52, No. 1, 2004, pp. 337-361, doi:10.1109/TMTT.2003.820904
- [115] Bandler, J.W., Biernacki, R.M., Chen, S.H., Hemmers, R.H., and Madsen, K. "Electromagnetic optimization exploiting aggressive space mapping" , *IEEE Transactions on Microwave Theory and Techniques*, Vol. 43, No. 12, 1995, pp. 2874–2882
- [116] Bakr, M.H., Bandler, J.W., Biernacki, R.M., Chen, S.H., and Madsen, K., "A trust region aggressive space mapping algorithm for EM optimization" , *IEEE Transactions on Microwave Theory and Techniques*, Vol. 46, No. 12, 1998, pp. 2412–2425, doi: 10.1109/22.739229
- [117] Bandler, J.W., Ismail, M.A., Rayas-Sanchez, J.E., and Zhang, Q.J., "Neuromodeling of microwave circuits exploiting space mapping technology" , *IEEE Transactions on Microwave Theory and Techniques*, Vol. 47, No. 12, 1999, pp. 2417–2427, doi: 10.1109/22.808989
- [118] Forrester, A.I.J., Sobester, A., Keane, A.J., "Multi-fidelity optimization via surrogate modelling" , *Proceedings of the Royal Aeronautic Society*, Vol. 463, No. 2088, 2007, pp. 3251-3269, doi:10.1098/rspa.2007.1900
- [119] Chung, H.S. , Alonso, J.J., "Using Gradients to Construct Cokriging Approximation Models for High-Dimensional Design Optimization Problems" , 40th AIAA Aerospace Sciences Meeting and Exhibit, Reno, Nevada, 2002, AIAA 2002–0317, doi: 10.2514/6.2002-317
- [120] Edwards, A., "An introduction to linear regression and correlation" , *A series of books in psychology*, W.H. Freeman and Comp., San Francisco, 1976, ISBN-10: 0716705613

- [121] Rajnarayan, D., Haas A., and Kroo, I., "A Multifidelity Gradient-Free Optimization Method and Application to Aerodynamic Design" , *12th AIAA/ISSMO Multidisciplinary Analysis and Optimization Conference, Victoria, British Columbia, 10 - 12 September 2008*, AIAA 2008-6020, doi: 10.2514/6.2008-6020
- [122] Hinton, G.E., Nowlan, S.J., "How learning can guide evolution" , *Complex Systems, Vol. 1, pp. 495-502, 1987*
- [123] Zoutendijk, G., "Methods of Feasible Directions: A study in linear and nonlinear programming" , *Elsevier, Amsterdam, 1960*
- [124] Fiacco, A.V., McCormick, G.P., "Nonlinear Programming: Sequential Unconstrained Minimization Techniques" , *Classics in Applied Mathematics series, 1990 ISBN: 978-0-89871-254-4*
- [125] Nocedal, J., Wright, S.J., "Numerical Optimization" , *Springer series in Operational Research, Springer, ISBN 0-387-98793-2, 2006*
- [126] Boggs, P.T., Tolle, J.W., "A strategy for global convergence in a sequential quadratic programming algorithm" , *SIAM Journal of Numerical Analysis, Vol. 26, No. 3 1989, pp. 600–623*
- [127] Nash, S.G., Sofer, A., "Linear and Nonlinear Programming" , *McGraw-Hill, ISBN-10: 007046065, 1996*
- [128] Parr, J.M, Keane, A.J., Forrester, A.I.J., and Holden, C.M.E., "Infill sampling criteria for surrogate-based optimization with constraint handling Engineering Optimization" , *Engineering Optimization, Vol. 44, No. 10, 2012, pp. 1147-1166, doi: 10.1080/0305215X.2011.637556*
- [129] Marler, R.T., Aurora, J.S., "Survey of multi-objective optimization methods for engineering" , *Structural and Multidisciplinary Optimization, Vol. 26, No. 6, 2004. pp. 369-395, doi:10.1007/s00158-003-0368-6*
- [130] Drela, M., "Pros & Cons of Airfoil Optimization" , *Frontiers of Computational Fluid Dynamics 1998, edited by D. A. Caughey and M. M. Hafez, World Scientific, Singapore, 1998, pp. 363-381, doi: 10.1142/9789812815774_019*
- [131] Huyse, L., Lewis, R.M., "Aerodynamic Shape Optimization of Two-dimensional Airfoils Under Uncertain Conditions" , *NASA CR–2001–210648, Jan. 2001, Also ICASE Report No. 2001-1*
- [132] Mastroddi, F., Gemma, S., "Analysis of Pareto frontiers for multidisciplinary design optimization of aircraft" , *Aerospace Science and Technology, Vol. 28, No. 1, 2013, pp. 40-55, doi: 10.1016/j.ast.2012.10.003*
- [133] Nemec, M., Ziing, D.W., Pulliam, T.H., "Multi-Point and Multi-Objective Aerodynamic Shape Optimization" , *AIAA Journal, Vol. 42, No. 6, 2004, pp. 1057-1065, doi: 10.2514/1.10415*

- [134] Toal D.J.J., Keane, A.J., "Efficient Multipoint Aerodynamic Design Optimization Via Cokriging" , *Journal of Aircraft*, Vol. 48, No. 5, 2011, pp. 1685-1695. doi:10.2514/1.C031342
- [135] Tan, K.C., Khor, E.F., and Lee, T.H., "Multiobjective Evolutionary Algorithms and Applications" , *Springer*; ISBN-1852338369, 2005
- [136] Chiong, R., Weise, T., and Michalewicz, Z., "Variants of Evolutionary Algorithms for Real-World Applications" , *Springer*, ISBN 978-3-642-23423-1, 2012
- [137] Antoine, N.E., "Aircraft optimization for minimal environmental impact" , *PhD thesis*, Stanford, 2004
- [138] Eberhart, R.C., Kennedy, J.A., "New optimizer using particle swarm theory" , *The 6th international symposium on Micro Machine and Human Science*, pp. 39-43, Nagoya, Japan, 1995
- [139] Alvarez-Benitez, J.E., Everson, R.M., and Fieldsend J.E., "A MOPSO Algorithm Based Exclusively on Pareto Dominance Concepts" , *International Conference on Evolutionary Multi-Criterion Optimization EMO 2005: Evolutionary Multi-Criterion Optimization*, Vol. 3410, 2005. pp. 459-473, doi:10.1007/978-3-540-31880-4_32
- [140] Durillo, J.J., Garcia-Nieto, J., Nebro, A.J., Coello, C.A., Luna, F., and Alba, E., "Multi-Objective Particle Swarm Optimizers: An Experimental Comparison" , *International Conference on Evolutionary Multi-Criterion Optimization EMO 2009: Evolutionary Multi-Criterion Optimization*, Vol. 5467, pp. 495-509, *Proceedings*, doi:10.1007/978-3-642-01020-0_39
- [141] Nelder, J.A., Mead, R., "Simplex method for function minimization" , *Computer Journal*, Vol. 7, No. 4, 1965, pp. 308 - 313, doi:10.1093/comjnl/7.4.308
- [142] Glover, F., "Tabu Search (Part I)" , *ORSA Journal on Computing*, Vol. 1, No. 3, 1989, pp. 190-206, doi:10.1287/ijoc.1.3.190
- [143] Glover, F. , "Tabu Search (Part II)" , *ORSA Journal on Computing*, Vol. 2, No. 1, 1990, pp. 4-32, doi:10.1287/ijoc.2.1.4
- [144] Hooke, R., Jeeves, T.A., "Direct Search Solution of Numerical and Statistical Problems" , *Journal for the Association of Computing Machinery*, Vol. 8, No. 2, 1961, pp. 212-229
- [145] Glover, F., Laguna, M., "Tabu Search" , *Technical report*, Kluwer Academic Publishers, Boston, MA, 1997
- [146] Connor, A.M., Tilley, D.G., "A Tabu Search method for the optimisation of fluid power circuits" , *IMechE Journal of Systems and Control*, Vol. 212, No. 5, 1998, pp. 373-381, 1998, doi: 10.1243/0959651981539541

- [147] Jaeggi, D.M., Parks, G.T., Kipouros, T., and Clarkson, P.J., "The development of a multi-objective Tabu Search algorithm for continuous optimisation problems" , *European Journal of Operational Research*, Vol. 185, No. 3, pp. 1192–1212, 2008, doi: 10.1016/j.ejor.2006.06.048
- [148] Trapani, G. Kipouros, T., Savill, M., "The Design of Multi-Element Airfoils Through Multi-Objective Optimization Techniques" , *Computer Modelling in Engineering and Sciences*, Vol. 88, No. 2, 2012, pp. 107-140, doi: 10.3970/cmcs.2012.088.107
- [149] Le Tallec, P., Laporte, E., "Numerical Methods in Sensitivity Analysis and Optimization" , ISBN 978-1-4612-0069-7, 2002, doi:10.1007/978-1-4612-0069-7
- [150] Martins, J.R.R.A., Sturdza, P., and Alonso, J.J., "The Complex-Step Derivative Approximation" , *ACM Transactions on Mathematical Software*, Vol. 29, No. 3, 2003, pp. 245-262, doi:10.1145/838250.838251
- [151] Lyu, Z., Kenway, G.K.W., Paige, C., Martins, J.R.R.A., "Automatic Differentiation Adjoint of the RANS equations with a Turbulence Model" , 21st AIAA Computational Fluid Dynamics Conference, Fluid Dynamics and Co-located Conferences, San Diego, California, AIAA 2013-2581 doi: 10.2514/6.2013-2581
- [152] Giannakoglou, K.C., Papadimitriou, D.I., "Adjoint Methods for Shape Optimization" , *Optimization and Computational Fluid Dynamics*, Editors: D. Thevenin, G. Janiga, ISBN 978-3-540-72152-9, 2008, doi:10.1007/978-3-540-72153-64
- [153] Mader, C.A., Martins, J.R.R.A., Alonso, J.J., van der Weide, E., "ADjoint: An Approach for the rapid development of discrete adjoint solvers" , *AIAA Journal*, Vol. 46, No. 4, 2008, pp. 863-873, doi: 10.2514/1.29123
- [154] Cramer, E.J., Dennis Jr., J.E., Frank, P.D., Lewis, R.M., and Shubin, G.R., "Problem Formulation for Multidisciplinary Optimization" , *SIAM Journal on Optimization*, Vol. 4, No. 4, 1994, pp. 754-776, doi:10.1137/0804044
- [155] Haftka, R.T., "Simultaneous Analysis and Design" , *AIAA Journal*, Vol. 23, No. 7, 1985, pp. 1099-1103, doi:10.2514/3.9043
- [156] Kennedy, G.J., Martins, J.R.R.A., "Parallel solution methods for aerostructural analysis and design optimization" , 13th AIAA/ISSMO Multidisciplinary Analysis Optimization Conference 13 - 15 September 2010, Fort Worth, Texas AIAA Paper 2010-9308, doi:10.2514/6.2010-9308
- [157] Lambe, A.B., Martins, J.R.R.A., "Extensions to the Design Structure Matrix for the Description of Multidisciplinary Design, Analysis, and Optimization Processes" , *Structural and Multidisciplinary Optimization*, Vol. 46, No. 2, 2012, pp. 273-284, doi:10.1007/s00158-012-0763-y
- [158] Martins, J.R.R.A., Lambe, A.B., "Multidisciplinary Design Optimization: A Survey of Architectures" , *AIAA Journal*, Vol. 51, No. 9, 2013, pp. 2049-2075, doi: 10.2514/1.J051895

- [159] Bloebaum, C.L., Hajela, P., and Sobieszczanski-Sobieski, J., "Non-Hierarchical System Decomposition in Structural Optimization" , *Engineering Optimization*, Vol. 19, No. 3, 1992, pp. 171-186, doi:10.1080/03052159208941227
- [160] Sellar, R.S., Batill, S.M., and J.E. Renaud, "Response Surface Based, Concurrent Subspace Optimization for Multidisciplinary System Design" , *34th Aerospace Sciences Meeting and Exhibit, Reno, Nevada, 15 - 18 January, 1996*, AIAA Paper 96-0714, doi:10.2514/6.1996-714
- [161] Huang, C.-H., Galuski, J., and C.L. Bloebaum, "Multi-Objective Pareto Concurrent Subspace Optimization for Multidisciplinary Design" , *AIAA Journal*, Vol. 45, No. 8, 2007, pp. 1894-1906, doi:10.2514/1.19972
- [162] Sobieszczanski-Sobieski, J., Agte, J.S., and Sandusky Jr, R.R., "Bilevel Integrated System Synthesis" , *AIAA Journal*, Vol. 38, No. 1, 2000, pp. 164-172, doi:10.2514/2.937
- [163] Sobieszczanski-Sobieski, J., Altus, T.D., Phillips, M., and Sandusky Jr., R.R., "Bilevel Integrated System Synthesis for Concurrent and Distributed Processing" , *AIAA Journal*, Vol. 41, No. 10, 2003, pp. 1996-2003, doi:10.2514/2.1889
- [164] Chittick, I.R., Martins, J.R.R.A., "An asymmetric suboptimization approach to aerostructural optimization" , *Optimization and Engineering*, Vol. 10, No. 1, 2009, pp. 133-152, doi: 10.1007/s11081-008-9046-2
- [165] Braun, R.D., Gage, P., Kroo, I.M., and Sobieski, I.P., "Implementation and Performance Issues in Collaborative Optimization" , *6th AIAA, NASA, and ISSMO Symposium on Multidisciplinary Analysis and Optimization, Bellevue, WA, 4 - 6 September, 1996*, doi:10.2514/6.1996-4017
- [166] Haftka, R.T., Watson, L.T., "Multidisciplinary Design Optimization with Quasiseparable Subsystems" , *Optimization and Engineering*, Vol. 6, No. 1, 2005, pp. 9-20, doi:10.1023/B:OPTE.0000048534.58121.93
- [167] Tosserams, S., Etman, L.F.P., and Rooda, J.E., "Augmented Lagrangian Coordination for Distributed Optimal Design in MDO" , *International Journal for Numerical Methods in Engineering*, Vol. 73, No. 13, 2008, pp. 1885-1910, doi:10.1002/nme.2158
- [168] Depince, P., Guedas, B., Picard, J., "Multidisciplinary and multiobjective optimization: Comparison of several methods" , *7th World Congress on Structural and Multidisciplinary Optimization, Seoul, South Korea, 2007*
- [169] Perez, R.E., Liu H.H.T., and Behdinan, K., "Evaluation of Multidisciplinary Optimization Approaches for Aircraft Conceptual Design" , *10th AIAA/ISSMO Multidisciplinary Analysis and Optimization Conference, 30 August - 1 September 2004, Albany, New York, AIAA Paper 2004-4537*, doi: 10.2514/6.2004-4537

- [170] de Boer, A., van Zuijlen, A.H., Bijl, H., "Review of coupling methods for non-matching meshes" , *Computer Methods in Applied Mechanics and Engineering*, Vol. 196, No. 8, 2007, pp. 1515-1525, doi: 10.1016/j.cma.2006.03.017
- [171] Thevenza, P., Blu, T., Unser, M., "Interpolation revisited" , *IEE Trans, Med. Imaging* Vol. 19, No. 7, 2000, pp. 739-758, doi: 10.1109/42.875199
- [172] Farhat, C., Lesoinne, M., Tallec, P., "Load and motion transfer algorithms for fluid/structure interaction problems with non-matching discrete interfaces: Momentum and energy conservation, optimal discretization and application to aeroelasticity" , *Computer Methods in Applied Mechanics and Engineering*, Vol. 157, No. 1-2, 1998, pp. 95-114, doi: 10.1016/S0045-7825(97)00216-8
- [173] Cebal, J.R., Lohner, R., "Conservative load projection and tracking for fluid-structure problems" , *AIAA Journal* Vol. 35, No. 4, 1997, pp. 687-692, doi: 10.2514/2.158
- [174] Loehner, R., Yang, C., Cebal, J., Baum, J.D., Luo, H., Pelessone, D., Charman, C., "Fluid-structure interaction using a loose coupling algorithm and adaptive unstructured grids" , 29th AIAA, *Fluid Dynamics Conference, Fluid Dynamics and Co-located Conferences*, Albuquerque, NM, 1995, AIAA Paper 98-2419, doi: 10.2514/6.1998-2419
- [175] Brown, S.A., "Displacement Extrapolation for CFD+CSM Aeroelastic Analysis" , 38th *Structures, Structural Dynamics, and Materials Conference, Structures, Structural Dynamics, and Materials and Co-located Conferences*, Kissimmee, Florida, 1997, AIAA Paper 1997-1090, doi: 10.2514/6.1997-1090
- [176] Smith, M.J., Cesnik, C.E.S., Hodges, D.H., "Evaluation of some data transfer algorithms for noncontiguous meshes" , *Journal of Aerospace Engineering*, Vol. 13, No. 2, 2000, pp. 52-58, doi: 10.1061/(ASCE)0893-1321(2000)13:2(52)
- [177] Smith, M.J., Hodges, D.H., Cesnik, C.E.S., "Evaluation of computational algorithms suitable for fluid-structure interactions" , *Journal of Aircraft*, Vol. 37, No. 2, 2000, pp. 282-294, doi: 10.2514/2.2592
- [178] Beckert, A., Wendland, H., "Multivariate interpolation for fluid-structure-interaction using radial basis functions" , *Aerospace Science and Technology*, Vol. 5, No. 2, 2001, pp. 125-134, doi: 10.1016/S1270-9638(00)01087-7
- [179] Rendall, T.C.S., Allen, C.B., "Unified fluid-structure interpolation and mesh motion using radial basis functions" , *International Journal for Numerical Methods in Engineering*, Vol. 74, 2008, pp. 1519-1559, doi: 10.1002/nme.2219
- [180] Goura, G., "Time Marching Analysis of Flutter using Computational Fluid Dynamics" , *PhD thesis, University of Glasgow*, 2001

- [181] Chen, P. Jadic, I., "Interfacing of fluid and structural models via innovative structural boundary element method" , *AIAA Journal*, Vol. 36, No. 2, 1998, pp. 282–287, doi: 10.2514/2.7513
- [182] Samareh, J.A., "Discrete Data Transfer Technique for Fluid–Structure Interaction" , *18th AIAA Computational Fluid Dynamics Conference Miami, Florida, 25 - 28 June 2007*, AIAA 2007-4309, doi: 10.2514/6.2007-4309
- [183] Guruswamy, G.P., "A review of numerical fluids/structures interface methods for computations using high-fidelity equations" , *Computers and Structures*, Vol. 80, No. 1, 2002, pp. 31–41, doi: 10.1016/S0045-7949(01)00164-X
- [184] Wunderlich, T.F., "Multidisciplinary wing optimization of commercial aircraft with consideration of static aeroelasticity" , *CEAS Aeronautical Journal*, Vol. 6, No. 3, 2015, pp. 407–427, doi: 10.1007/s13272-015-151-6
- [185] Liu, Q., Jrad, M., Mulani, S.B. and Kapania, R.K., "Integrated Global Wing and Local Panel Optimization of Aircraft Wing" , *56th AIAA/ASCE/AHS/ASC Structural Dynamics, and Materials Conference, AIAA 2015-0137*, 2015, doi: 10.2514/6.2015-0137
- [186] Doyle, S., Robinson, J., Ho1, V., Ogawa, G. and Baker, M., "Aeroelastic Optimization of Wing Structure Using Curvilinear Spars, Ribs (SpaRibs)" , *58th AIAA/ASCE/AHS/ASC Structures, Structural Dynamics, and Materials Conference, AIAA 2017-1303*, 2017, doi: 10.2514/1.C032249
- [187] Bach, T., "Automated sizing of a composite wing for the usage within a multidisciplinary process" , *Aircraft Engineering and Aerospace Technology*, Vol. 88 No. 2, 2016, pp.303-310, doi: 10.1108/AEAT-02-2015-0057
- [188] Kennedy, G.J., Kenway, G.W., Martins, J.R.R.A., "High Aspect Ratio Wing Design: Optimal Aerostructural Tradeoffs for the Next Generation of Materials" , *52nd Aerospace Sciences Meeting, AIAA SciTech Forum, 2014*, AIAA 2014-0596, doi: 10.2514/6.2014-0596
- [189] Anhalt, C., Monner, H.P., Breitbach, E., "Interdisciplinary Wing Design – Structural Aspects" , *03WAC-29, German Aerospace Center (DLR), Institute of Structural Mechanics*, doi: 10.4271/2003-01-3026
- [190] Drela, M., "Integrated simulation model for preliminary aerodynamic, structural and control-law design of aircraft" , *40th Structural Dynamics, and Materials and Co-located Conferences, 12-15 April, 1999, St. Louis, Montana*, AIAA 99-1394, doi: 10.2514/6.1999-1394
- [191] Drela, M., "Method for simultaneous wing aerodynamic and structural load prediction" , *Journal of Aircraft*, Vol. 27, No. 8, 1990, pp. 692-699, doi: 10.2514/3.25342

- [192] Howcroft, C., Cook, R., Calderon, D., Lambert, L., Castellani, M., Cooper, J.E., Lowenberg, M.H., Neild S.A., and Coetzey, E., "Aeroelastic Modelling of Highly Flexible Wings" , 15th *Dynamics Specialists Conference, AIAA SciTech, 4-8 January 2016, San Diego, California, AIAA 2016-1798, doi: 10.2514/6.2016-1798*
- [193] Dababneh, O., Kayran, A., "Design, analysis and optimization of thin walled semi-monocoque wing structures using different structural idealization in the preliminary design phase" , *International Journal of Structural Integrity, Vol. 5, No. 3, 2014, pp.214-226, doi: 10.1108/IJSI-12-2013-0050*
- [194] Elham, A., La Rocca, G., van Tooren., "Development and implementation of an advanced, design-sensitice method for wing weight estimation" , *Aerospace Science and Technology, Vol. 29, No. 1, 2013, pp. 100-113, doi: 10.1016/j.ast.2013.01.012*
- [195] Elham, A., van Tooren, M.J.L., "Toward Wing Aerostructural Optimization Using Simultaneous Analysis and Design Strategy" , 58th *AIAA/ASCE/AHS/ASC Structures, Structural Dynamics, and Materials Conference, AIAA SciTech Forum 9 - 13 January 2017, Grapevine, Texas, AIAA Paper 2017-0802, doi: 10.2514/6.2017-0802*
- [196] Clarkson, P.J., Simons, C., and Eckert, C., "Predicting Change propagation in complex design" , *Journal of Mechanical Design, Vol. 126, No. 5, 2004. pp. 788-797, doi:10.1115/1.1765117*
- [197] Nadarajah, S., and Jameson A., "A Comparison of the Continuous and Discrete Adjoint Approach to Automatic Aerodynamic Optimization" , 38th *AIAA Aerospace Sciences Meeting and Exhibit, Reno, Nevada, 2000, AIAA 2000-0667, doi:10.2514/6.2000-667*
- [198] Kennedy, M.C., O'Hagan, A., "Predicting the output from complex computer code when fast approximations are available" , *Biometrika Vol. 87, No. 1, 2000, pp. 1-13, doi:10.1093/biomet/87.1.1*
- [199] Demange, J., Savill A.M., and Kipouros, T., "Multifidelity Optimization for High-Lift Airfoils" , 54th *AIAA Aerospace Sciences Meeting, AIAA Scitech Forum, San Diego, California, 2016, AIAA Paper 2016-0557, doi:10.2514/6.2016-0557*
- [200] Demange, J., Savill, A.M., and Kipouros, T., "A Multifidelity Multiobjective Optimization Framework for High-Lift Airfoils" , *AIAA AVIATION Forum, 17th AIAA ISSMO Multidisciplinary Analysis and Optimization Conference, Washington, DC, 2016, Paper AIAA 2016-3367, doi: 10.2514/6.2016-3367*
- [201] Jarrett, J.P., Ghisu, T., "Balancing Configuration and Refinement in the Design of Two-Spool Multistage Compression Systems" , *ASME Journal of Turbomachinery, Vol. 137, No. 9, 2015, doi: 10.1115/1.4030051*
- [202] Leifsson, L., Koziel, S., "Multi-fidelity design optimization of transonic airfoils using physics-based surrogate modeling and shape-preserving response prediction" , *Journal of Computational Science, Vol. 1, No. 1, 2010, pp. 98-106, doi:10.1016/j.procs.2010.04.146*

- [203] Perez, R.E., Janses, P.W., and Martins, J.R.R.A., "pyOpt: a Python-based object-oriented framework for nonlinear constrained optimization" , *Structural and Multidisciplinary Optimization*, Vol. 45, No. 1, 2012, pp. 101-118, doi:10.1007/s00158-011-0666-3
- [204] Rosenbrock, H.H., "An automatic method for finding the greatest or least value of a function" , *The Computer Journal*, Vol. 3, No. 3, 1960, pp. 175–184, ISSN 0010-4620, doi:10.1093/comjnl/3.3.175
- [205] Shang Y.W., Qiu Y.H., "A Note on the Extended Rosenbrock Function" , *Evolutionary Computation*, Vol. 14, No. 1, 2006, pp.119-126, 10.1162/evco.2006.14.1.119
- [206] Kontogiannis, S.G., Savill, M.A., and Kipouros, T., "Multiobjective aerosturctural optimization for efficient transport wing conceptual design" , 59th AIAA/ASCE/AH-S/ASC Structures, Structural Dynamics, and Materials Conference, AIAA SciTech Forum, Kissimmee, Florida, 2018, AIAA Paper 2018-0104, doi:/10.2514/6.2018-0104
- [207] Tedford, N.P., Martins, J.R.R.A., "Benchmarking multidisciplinary design optimization algorithms" , *Optimization and Engineering*, Vol. 11, No. 1, 2010, pp.159-183, doi:10.1007/s11081-009-9082-6
- [208] ANSYS FLuent 14.5, "User's Manual" , ANSYS Inc
- [209] Roache, P.J., "Verification and validation in computational science and engineering" , *Hermosa*, 1998, ISBN 0913478083, 9780913478080
- [210] Wilcox, D.C., "Turbulence modeling for CFD" , *La Cãnada, Calif. : DCW Industries, c2006; 3rd ed., ISBN-10: 1928729088*
- [211] Mitchell, D.J., "VGK method for two-dimensional aerofoil sections, Part 1: principles and results" , *ESDU 96029, Issued October 1996 with Amendments A and B, April 2004, ISBN: 9780856799938*
- [212] Garabedian, P.R., Korn, D.G., "Analysis of transonic aerofoils" , *Communications on Pure and Applied Mathematics*, Vol. 24, 1971, pp. 841-851, doi: 10.1002/cpa.3160240608
- [213] Kontogiannis, S.G., Savill, M.A., and Kipouros, T., "A Multi-Objective Multi-Fidelity framework for global optimization" , 58th AIAA/ASCE/AHS/ASC Structures, Structural Dynamics, and Materials Conference, AIAA SciTech Forum, Grapevine, Texas, 2017, AIAA Paper 2017-0136, doi:10.2514/6.2017-0136
- [214] Wild, J., "Multi-objective constrained optimisation in aerodynamic design of high-lift systems" , *International Journal of Computational Fluid Dynamics*, Vol. 22, No. 3, 2008, pp. 153-168, doi: 10.1080/10618560701868420
- [215] Ali, N., Behdinan, K., "Optimal geometrical design of aircraft using genetic algorithms" , *Article in Transactions - Canadian Society for mechanical Engineering*, Vol. 26, No. 4, 2003, pp. 373-388, doi: 10.1139/tcsme-2002-0022

- [216] Hilbert, R., Janiga, G., Baron, R., and Thevenin, D., "Multi-objective shape optimization of a heat exchanger using parallel genetic algorithms" , *International Journal of Heat and Mass Transfer*, Vol. 49, No. 15-16, 2006, pp. 2567-2577, doi: 10.1016/j.ijheatmasstransfer.2005.12.015
- [217] Liem, R.P., Kenway, G.K.W., Martins, J.R.R.A., "Multimission Aircraft Fuel-Burn Minimization via Multipoint Aerostructural Optimization" , *AIAA Journal*, Vol. 53, No. 1, 2015, pp. 104-122, doi:10.2514/1.J052940
- [218] Kipouros, T., Molinary, M., Dawes, W.N., Parks, G.T., Savill, M., and Jenkins, K.W., "An investigation of the potential for enhancing the computational turbomachinery design cycle using surrogate models and high performance parallelisation" , *GT2007-28106, Proceedings of ASME Turbo Expo 2007 Power for Land, Sea and Air*, Vol. 6, 2007, pp. 1415-1424, doi:10.1115/GT2007-28106
- [219] Conn, A. R., Scheinberg, K., and Vicente, L. N., "Global Convergence of General Derivative-Free Trust-Region Algorithms to First and Second-Order Critical Points" , *SIAM Journal on Optimization*, Vol. 20, No. 1, 2009, pp.387-415, doi: 10.1137/060673424
- [220] March, A. and Willcox, K., "Provably Convergent Multifidelity Optimization Algorithm Not Requiring High-Fidelity Derivatives" *AIAA Journal*, Vol. 50, No. 5, 2012, pp.1079-1089, doi: 10.2514/1.J051125
- [221] Kontogiannis, S.G., Demange, J., Savill, M.A., and Kipouros, T., "A comparison study of two multifidelity methods for aerodynamic optimization" , 59th *AIAA/ASCE/AHS/ASC Structures, Structural Dynamics, and Materials Conference, AIAA SciTech Forum, Kissimmee, Florida, 2018, AIAA Paper 2018-0415*, doi: 10.2514/6.2018-0415
- [222] Thibert, J.J., "The Garteur High Lift Research Programme" *High Lift System Aerodynamics, AGARD CP-515, Sept. 1991*, pp. 16-1 - 16-21
- [223] Cao, Y., Smucker, B.J., and Robinson, T.J., "On using the hypervolume indicator to compare pareto fronts: Applications to multi-criteria optimal experimental design" , *Journal of Statistical Planning and Inference*, Vol. 160, 2015, pp. 60-74, doi: 10.1016/j.jspi.2014.12.004
- [224] Flaig, A. and Hilbig, R., "High-Lift Design for Large Civil Aircraft", , *High Lift System Aerodynamics AGARD CP-515, Sept. 1991*, pp.31-1 31-12
- [225] Trapani, G., "The Design of High-Lift Aircraft Configurations through Multi-Objective Optimisation" , *Ph.D. thesis, Cranfield University, March 2014*.
- [226] "ANSYS, Fluent 14.5" , *User's Manual, Lebanon, 2013*.
- [227] "ANSYS, ICEM CFD 14.5" , *User's Manual, Lebanon, 2013*.

- [228] Rumsey, C.L. and Ying, S.X., "Prediction of High Lift: Review of Present CFD Capability" *Progress in Aerospace Sciences*, Vol. 38, No. 2, 2002, pp.145-180, doi: 10.1016/S0376-0421(02)00003-9
- [229] Drela, M., "Newton Solution of Coupled Viscous/Inviscid Multi-element airfoil Flows" , 21st *Fluid Dynamics, Plasma Dynamics and Lasers Conference, Fluid Dynamics and Co-located Conferences*, Seattle, Washington, doi: 10.2514/6.1990-1470 AIAA-90-1470
- [230] van Dam, C.P., "The Aerodynamic Design of Multi-Element High-Lift Systems for Transport Airplanes" *Progress in Aerospace Sciences*, Vol. 38, No. 2, 2002, pp.101-144
- [231] Inselberg, A. and Dimsdale, B., "Parallel Coordinates" *Human-Machine Interactive Systems*, Springer, 1991, pp. 199-233, doi: 10.1016/S0376-0421(02)00002-7
- [232] Leoviriyakit, K., "Wing Planform Optimization via an adjoint method" , *PhD thesis*, Stanford, 2005
- [233] Martins, J., Alonso, J., and Reuther, J., "High-Fidelity Aerostructural Design Optimization of a Supersonic Business Jet" , *Journal of Aircraft*, Vol. 41, No. 3, 2004, pp. 523-530, doi: 10.2514/1.11478
- [234] Kenway, G.K.W., Martins, J.R.R.A., "Multipoint High-Fidelity Aerostructural Optimization of a Transport Aircraft Configuration" , *Journal of Aircraft*, Vol. 51, No. 1, 2014, pp. 144-160, doi: 10.2514/1.C032150
- [235] Vassberg, J., Dehaan, M., Rivers, M. and Wahls, R., "Development of a Common Research Model for Applied CFD Validation Studies" , 26th *AIAA Applied Aerodynamics Conference, Guidance, Navigation, and Control and Co-located Conferences*, 18-21 August 2008, AIAA Paper 2008-6919, doi:10.2514/6.2008-6919
- [236] Lyu, Z., Kenway, G.K.W., Martins, J.R.R.A., "RANS-based ASO of the CRM wing" , *AIAA Journal*, Vol. 53, No. 4 ,2015, pp. 968-985, doi: 10.2514/1.J053318
- [237] Niu, M. C., "Airframe Structural Design" , *Hong Kong Conmilit Press limited*, 1988, ISBN: 962712804X
- [238] Kreisselmeier, G., Steinhauser, R., "Systematic Control Design by Optimizing a Vector Performance Index" , *IFAC Proceedings Volumes*, Vol. 12, No. 7, 1979, pp. 113-117, doi:10.1016/S1474-6670(17)65584
- [239] Roe, P.L., "Approximate riemann solvers, parameter vectors and difference schemes" , *Journal of Computational Physics*, Vol. 43, No. 2, 1981, pp. 357-372, doi:10.1016/0021-9991(81)90128-5
- [240] O. Dababneh, "Multidisciplinary Design Optimisation for Aircraft Wing Mass Estimation" , *PhD Thesis*, Cranfield University, April 2016

- [241] "ANSA v17.1.0 Theory guide" , *Beta CAE Systems*, 2016
- [242] Portapas, V., Yusuf, S.Y., Lone, M.M., and Coetzee, E., "Modelling Framework for Handling Qualities Analysis of Flexible Aircraft" , *AIAA Modeling and Simulation Technologies Conference, AIAA SciTech Forum, Grapevine Texas, 2017, AIAA 2017-0577, doi: 10.2514/6.2017-0577*
- [243] Gazaix, A., Gallard, F., Gachelin, V., Druot, T., Grihon, S., Ambert, V., Guenot, D., Lafage, R., Vanaret, C., Pauwels, B., Bartoli, N., Lefebvre, T., Sarouille, P., Desfachelles, N., Brezillon, J., Hamadi, M. and Gurol, S. , "Towards the Industrialization of New MDO Methodologies and Tools for Aircraft Design" , *18th AIAA/ISSMO Multidisciplinary Analysis and Optimization Conference, AIAA AVIATION Forum, Denver, Colorado, 2017, AIAA Paper 2017-3149, doi:10.2514/6.2017-3149*
- [244] Liem, R.P., Mader, C.A., Lee, E. and Martins, J.R.R.A., "Aerostructural design optimization of a 100-passenger regional jet with surrogate-based mission analysis" , *13th Aviation Technology, Integration, and Operations Conference, AIAA AVIATION Forum, Los Angeles, California, 2013, AIAA Paper 2013-4372, doi:10.2514/6.2013-4372*
- [245] Khurana, M.S., Winarto, H., Sinha, A.K., "Aerofoil Geometry Parameterisation through Shape Optimizer and Computational Fluid Dynamics" , *AIAA paper 2008-295, Jan. 2008, doi:10.2514/6.2008-295*
- [246] Martins, J.R.R.A., Alonso, J.J., and Reuther, J.J., "A coupled-adjoint sensitivity analysis method for high-fidelity aero-structural design" , *Optimization and Engineering, Vol. 6, No. 1, 2005, Page 33-62, doi:10.1023/B:OPTE.0000048536.47956.62*
- [247] Marriage, C.J., Martins, J.R.R.A., "Reconfigurable Semi-Analytic Sensitivity Methods and MDO Architectures within the π MDO Framework" , *12th AIAA/ISSMO Multidisciplinary Analysis and Optimization Conference, 10 - 12 September 2008, Victoria, British Columbia, Canada, AIAA Paper 2008-5956*
- [248] Sobieszczanski-Sobieski, J., "Sensitivity of Complex, Internally Coupled Systems" , *AIAA Journal, Vol. 28, No. 1, 1990, pp. 153-160, doi:10.2514/3.10366*
- [249] Brown, N.F., Olds, J.R., "Evaluation of Multidisciplinary Optimization Techniques Applied to a Reusable Launch Vehicle" , *Journal of Spacecraft and Rockets, Vol. 43, No. 6, 2006, pp. 1289-1300, doi:10.2514/1.16577*
- [250] Sturdza, P., "An Aerodynamic Design Method For Supersonic Natural Laminar Flow Aircraft" , *PhD thesis, Stanford, 2004, 3781-2004*
- [251] Makinen, R.A.E., Periaux, J., and Toivanen, J., "Multidisciplinary shape optimization in aerodynamics and electromagnetics using genetic algorithms" , *International Journal for Numerical Methods in Fluids, Vol. 30, No. 2, 1999, pp. 149-159, doi:10.1002/(SICI)1097-0363(19990530)30:2<149::AID-FLD829>3.0.CO;2-B*

-
- [252] Reist, T.A., Ziing, D.W., "Aerodynamic Shape Optimization of a BWB regional transport for a short range mission" , 31st *AIAA Applied Aerodynamics Conference, San Diego, 24-27 June 2013, AIAA 2013-2414, doi: 10.2514/6.2013-2414*
- [253] Mader, C.A., Martins, J.R.R.A., "Stability-Constrained Aerodynamic Shape Optimization of Flying Wings" , *AIAA Journal, Vol. 50, No. 5, 2013, pp. 1431-1449, doi:10.2514/1.C031956*
- [254] Mader, C.A., Martins, J.R.R.A., "Computing Stability Derivatives and Their Gradients for Aerodynamic Shape Optimization" , *AIAA Journal, Vol. 52, No. 11, 2014, pp. 2533-2546, doi: 10.2514/1.J052922*

Appendix

A. List of Conference Papers

- Kontogiannis, S.G., Savill, M.A., and Kipouros, T., "A Multi-Objective Multi-Fidelity framework for global optimization" 58th AIAA/ASCE/AHS/ASC Structures, Structural Dynamics, and Materials Conference, AIAA SciTech Forum, 2017, AIAA Paper 2017-0136, doi:10.2514/6.2017-0136
- Kontogiannis, S.G., Demange, J., Savill, M.A., and Kipouros, T., "A comparison study of two multifidelity methods for aerodynamic optimization", 2018 AIAA/ASCE/AHS/ASC Structures, Structural Dynamics, and Materials Conference, AIAA SciTech Forum, 2018, AIAA 2018-0415, doi:10.2514/6.2018-0415
- Kontogiannis, S.G., Savill, M. A., and Kipouros, T., "Multiobjective aerostructural optimization for efficient transport wing conceptual design", 2018 AIAA/ASCE/AHS/ASC Structures, Structural Dynamics, and Materials Conference, AIAA SciTech Forum, 2018, AIAA 2018-0104, doi:10.2514/6.2018-0104
- Kontogiannis, S.G., Savill, M.A., and Kipouros, T., "Global Multiobjective optimization of a long range BWB configuration", 2018 AIAA Aviation Forum, AIAA under submission

B. Posters

Airbus PhD Day 2016

Getafe, 20th October 2016

Airbus PhD day 2016

Rapid Multidisciplinary Design Optimization

Student name : Spyridon Kontogiannis

Supervisors: Prof. M. Savill, Dr. T. Kipourou (Cranfield University)
T. Engelbrecht (AIRBUS)

WHAT IS YOUR PhD ABOUT?

A LONG TIME LATER ...

METHODOLOGY AIMS & REQUIREMENTS

- Accelerate the Optimization Process
- Surrogate Modelling
- Multi-Fidelity Analysis
- Support Decision Making
- Multi-Objective Formulation
- Global-High Fidelity Optimality
- Design Space Exploration
- Consider Multidisciplinary Interactions
- Multi-Disciplinary Architecture based

THE WHOLE PROCESS IS QUITE SIMPLE IT LOOKS LIKE THIS ...

THIS IS THE TEST CASE I AM WORKING ON THIS PERIOD ...

RAE 2822 Test Case

Angle of Attack: 2.31 deg
Mach: 0.725
Re: 6.5 million

Objectives

- Assess surrogate models & training process
- Develop & test fine-tune constraint handling
- Examine convergence rate in terms of elapsed time

Findings

- Sufficient Design Space Exploration to provide design solutions
- HF Surrogate Based Optimization (SB O) more efficient than CFD Based
- Modified MF approach finds almost High Fidelity Optimum
- MF Well suited for preliminary design
- Physically sensible result: Reflexed airfoil featuring weakened shock
- Low Fidelity tool should capture the trend of the objective
- Multi Fidelity formulation gains to be apparent in heavy analyses cases

HMM... IS IT ANY GOOD?

Case	Number of HF calls for almost HF optimality	Total Cost (cases)	HF cost (cases)	LF cost (cases)	Total Cost (times)
CFD Based	100	400	300	-	30000
SB O	10	40	300	10	3000
Modified MF	7 (+21 LF calls)	42	300	10	2310

THIS IS NOT MDO!

WELL... YES... BUT... THE OPTIMIZATION PROCESS IS COMPLETELY READY!

NOW IT JUST NEEDS AN MDO!

Handling MDO

- Developed Multi-Objective framework controls an optimization case that uses Multi-Disciplinary Analysis

- Interaction between Aerodynamics, Structures & Weight estimation within a closed iterative loop

- Acceleration of convergence by optimization of cheap disciplines within each analysis sub-iteration

WELL... YES... BUT... THE OPTIMIZATION PROCESS IS COMPLETELY READY!

SO, WHAT'S THE PLAN FOR THE FUTURE?

LET'S SEE...

Future Work

- Reduce dimensionality by screening/active subspace methods
- 3D Test Case High Aspect Ratio Wing geometries
 - Employ torsional spring grid deformation
- Development of an Aeroelastic Multi-Disciplinary Analysis
 - LF analysis: Panel method/Beam model
 - HF analysis: RANS CFD/Wing-box model

A. J. J. Forrester, A. Sobester, and A. J. Keen, "Engineering Design via Surrogate Modelling: A Practical Guide", John Wiley & Sons, ISBN 978-1-119-95058-2, 2016

J.R.R.A. Martins, A.R. Lambe, "Multidisciplinary Design Optimization: A Survey of Architectures", AIAA Journal, Vol. 51, No. 9, Pages: 2049-2075, 2013

Figure 8.2: Poster from Airbus PhD Day 2016.

Airbus PhD Day 2017


Bristol, 6th September 2017


Airbus PhD day 2017

Rapid Multidisciplinary Design Optimisation

Student name : Spyros Kontogiannis

Supervisors: M. A. Savill, T. Kipourou, T. Engelbrecht





HEY RAPID MDO?

WELL, FOR STARTERS, MDO IS MORE EFFICIENT THAN SEQUENTIAL OPTIMISATION, EXPLORES INTERDISCIPLINARY INTERACTIONS AND LEADS TO SUPERIOR DESIGNS

THEY RAPID MDO?

WELL, IT'S SIMPLE ACTUALLY... AFTER A MULTIFIDELTY (MF) SEARCHING I TRAIN AN MF KRIGING TO SEARCH FOR THE POINTS WITH THE MAX EXPECTED IMPROVEMENT. THEN, I RUN AN MDA OR AN ASD LOOP FOR THESE POINTS.

Sequential

MDO

...YOU DON'T SAY...!

SON, YOU TALK TOO MUCH.

HOW WILL YOU ACHIEVE ALL THESE?

SAME BLACK-BOX METHODOLOGY ADAPTS TO DIFFERENT MDO ARCHITECTURES

THE WHY (YOU NEED IT) & THE HOW MY METHOD

- MDO IS BETTER THAN SEQUENTIAL OPT. (FACT) METHOD SUPPORTS DECISION MAKING (NOT JUST OPTIMISATION)
- ACCELERATES MDO PROCESS & IMPROVES RELIABILITY OF CONCEPTUAL STAGE
- MULTIFIDELTY & SURROGATE TOOLS REDUCE COSTS (VERY EFFICIENT WHEN FEW DOMINANT VARIABLES A.K.A. CONCEPTUAL DESIGN)
- EFFICIENT EXPLORATION
- MULTI-OBJECTIVE TRADEOFF INFORMATION
- ADAPTABLE TO INDUSTRY NEEDS & TOOLS

RAE 2822 Lift Coefficient - Comparison of Methods

I ALSO CHECK HOW THE METHOD PERFORMS FOR MORE DESIGN VARIABLES I USED THE ROSENBRUCK FUNCTION HERE

Dimension Scaling behaviour - Rosenbrock function

RAE 2822 Airfoil Case in Unconstrained and Multiobjective Formulation

HERE'S A BUNCH OF FIGURES FROM MY RECENT RESULTS

RAE 2822 Unconstrained - Comparison of Methods

RAE 2822 Multiobjective - Comparison of Methods

YEAH, OK! BUT WHAT ABOUT MDO? WHAT ABOUT CONSTRAINTS? THIS IS THE INDUSTRY YOU KNOW!

DON'T WORRY! I'VE GOT TWO DIFFERENT CONSTRAINT HANDLING METHODS UP AND RUNNING!

(a) Probability of Feasibility (b) Penalty on EI

Seller Function - Comparison of Methods and Architectures

OK, SO... TO CONCLUDE...

A BWB GEOMETRY AND THE AEROSTRUCTURAL OPTIMISATION OF THE CRM WING

OK, SO... TO CONCLUDE...

- THE KRIGING MODIFICATION WORKS!
- THE METHOD IS MORE ACCURATE THAN TYPICAL LOW FIDELTY (LF) CONCEPTUAL STUDIES AS IT REACHES A HIGH FIDELTY OPTIMUM
- PROVIDES BALANCED EXPLORATION ATTRIBUTES
- IT IS FASTER THAN ANY HIGH FIDELTY (HF) GRADIENT FREE CODE (THAT VE TRIED.)
- REQUIRES LESS HF CALLS THAN THE HF EI METHOD IF THE LF ERROR TOOL IS SMOOTH
- IT EFFICIENTLY USES TWO CONSTRAINT HANDLING METHODS
- IT IS EXTENDED FOR DIFFERENT MDO ARCHITECTURES
- IT ADAPTS TO ANY INDUSTRIAL PRACTICE OR TOOL

AND HERE'S WHAT I AM WORKING ON THIS PERIOD...

AHH... THE FUTURE...

- PARAMETERISE BWB SHAPE OPTIMISATION
- PARAMETERISE AEROSTRUCTURAL PROCESS
- WRITE THESES
- WRITE PAPERS
- GET THE PHD
- GO HOLIDAYS (???)
- GET A JOB

* Variable Reliability Aerospace Design Integration Process Using Surrogates

[1] "An asymmetric suboptimization approach to aerostructural optimization", Chittick and Mortin, Structural and Multidisciplinary Optimization, 2008

[2] "A Multi-Objective Multi-Fidelity Framework for global optimization", S. G. Kontogiannis, T. Kipourou and A.M. Savill, 58th AIAA/ASCE/AHS/ASC Structures, Structural Dynamics, and Materials Conference

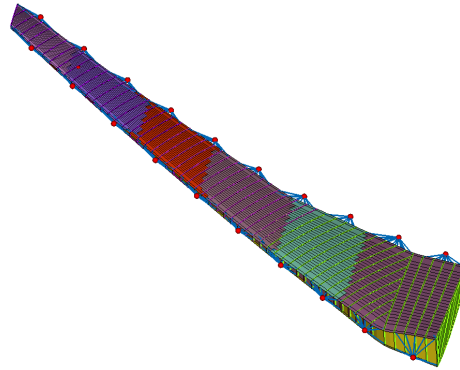
WORK & COMICS BY SPYROS KONTOGIANNIS

Figure 8.3: Poster from Airbus PhD Day 2017.

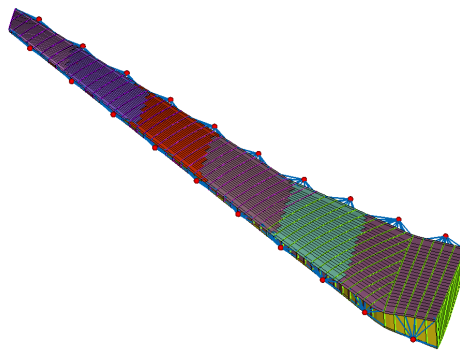
C. Modal Analysis of the Common Research Model

The aerostructural optimisation problem of Chapter 7 used the structural modes as a means to constraint the design of the wingbox to a not too flexible or too stiff configuration. This section provides qualitative examples of the typical first mode shape of the wingbox in the figures that follow

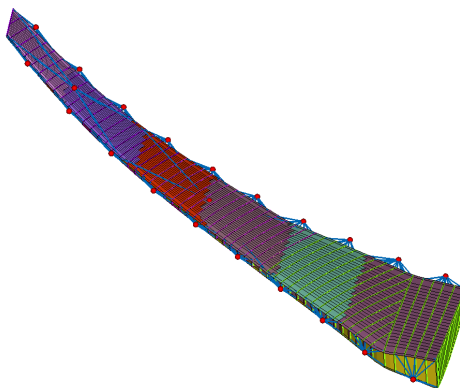
0:CRM_struct_modal0.nas : ORIGINAL STATE



(a) Non-excited state.

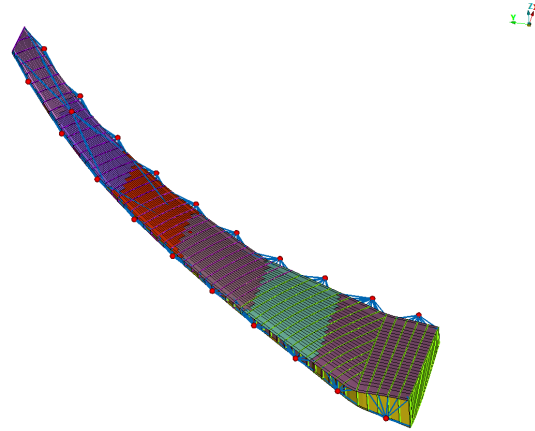


(b) Mode 1.

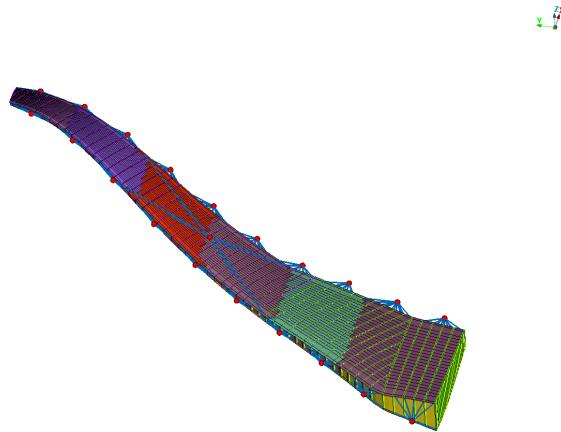


(c) Mode 2.

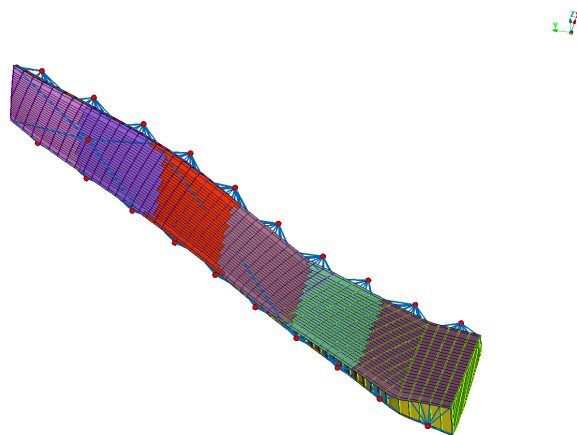
Figure 8.4: Modal shapes of datum common research model



(a) Mode 3.

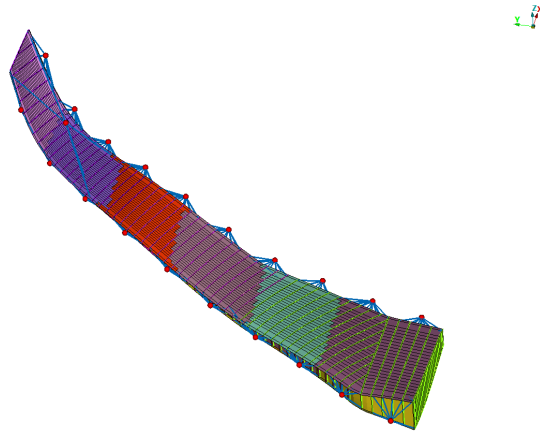


(b) Mode 4.

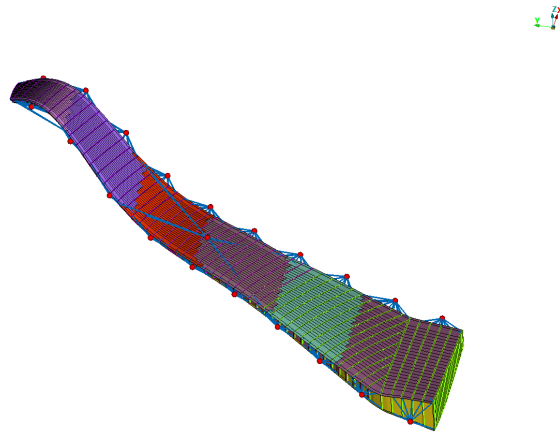


(c) Mode 5.

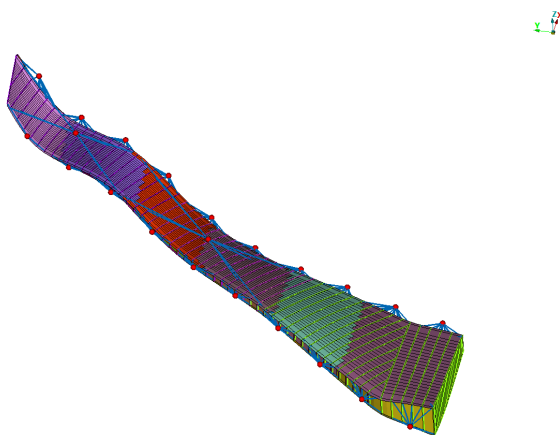
Figure 8.5: Modal shapes of datum common research model



(a) Mode 6.



(b) Mode 7.



(c) Mode 8.

Figure 8.6: Modal shapes of datum common research model

